AN EQUIVALENT UNIFORM DOSE-BASED CLASS SOLUTION FOR CERVICAL CANCER RADIOTHERAPY

BY

WILLIAM SHAW

Thesis submitted to comply with the requirements for the Ph.D. (Medical Physics) degree in the Faculty of Health Sciences at the University of the Free State

Promoter: Prof. William Ian Duncombe Rae

Co-Promoter: Prof. Markus Lothar Alber

Department of Medical Physics

June 2014

DECLARATION

AUTHOR: William Shaw

DEGREE: PhD

TITLE: An equivalent uniform dose-based class solution for cervical cancer radiotherapy

DATE OF DEPOSIT: 1 July 2014

I, William Shaw, certify that the thesis hereby submitted by me for the PhD (Medical Physics) degree at the University of the Free State, is my independent effort and had not previously been submitted for a degree at another University/faculty. I furthermore waive copyright of the thesis in favour of the University of the Free State.

Signature: William Shaw

Contents

Glossary 6

Abstract 9

Chapter 1: Introduction 11

1.1. Background 11

1.1.1. Cause and prevalence of cervical cancer 11

1.1.2. Radiotherapy treatment options 11

1.2. Recent improvements in treatment techniques 16

1.2.1. Improvements in EBRT 16

1.2.2. Improvements in brachytherapy 17

1.3. Adaptive radiotherapy 19

1.3.1. Motivation for EBRT dose adaptation to a tumour in a mobile organ surrounding 19

1.3.2. Image-guided adaptive radiotherapy 20

1.3.3. Motivation for BT dose adaptation to a tumour in a mobile organ surrounding 21

1.3.4. Image guided adaptive brachytherapy 23

1.4. Improvements in treatment outcome and late toxicity 24

1.4.1. Rational for dose escalation 24

1.4.2. Improvement in tumour control 24

1.4.3. Late toxicity 25

1.5. Uncertainties in treatment 29

1.5.1. Dosimetric Uncertainties 29

1.5.2. Contouring Uncertainties 31

1.5.3. Radiobiological Uncertainties 32

1.6. Aim 33

1.7. References 34

Chapter 2: On expedient properties of common biological score functions for multi-modality, adaptive and 4D dose optimization (Appendix I) 53

2.1. Introduction 53

2.2. Methods and Materials 54

2.2.1. Monte Carlo Simulation 57

2.2.2. Clinical Simulation 60

2.3. Results and discussion 61

2.3.1. Monte Carlo Simulation 61
2.3.2. Clinical Simulation 62
2.4. Conclusions 64
2.5. References 66
Chapter 3: A Solution for Brachytherapy Biologically Guided Dose Individualisation in the Treatment of Cervix Cancer (Appendix II) 68
3.1. Introduction 68
3.2. Methods and materials 69
3.2.1. Treatment and patient data 69
3.2.2. Conventional treatment planning 69
3.2.3. Biologically guided treatment planning 70
3.2.4. EUD calculation and biological parameters 71
3.2.5. Dose accumulation 72
3.3. Results 72
3.3.1. OAR D2cc and EUD 72
3.3.2. Point A and HR-CTV D90 73
3.4. Discussion 77
3.5. Conclusion 79
3.6. References 80
Chapter 4: Equivalence of Gyn GEC-ESTRO guidelines for image guided cervical brachytherapy with EUD-based dose prescription (Appendix III) 82
4.1. Introduction 82
4.2. Methods 83
4.2.1. Patient selection, imaging and contouring 83
4.2.2. Fractionation and dose evaluation parameters 84
4.2.3. Study 1: prescription constraints 85
4.2.4. Study 2: safety of EUD constraints in terms of GGE constraints 86
4.2.5. Study 3: comparison of GGE and CV planning strategies for the entire treatment 87
4.3. Results 87
4.3.1. Prescription constraints 87
4.3.2. Safety of EUD criteria in terms of GGE criteria 88
4.3.3. Comparison of GGE and CV planning strategies 91
4.4. Discussion 94

4.5. Conclusions 100
4.6. References 101
Chapter 5: Image Guided Adaptive Brachytherapy Dose Escalation for Cervix Cancer using Fractionation Compensation 106
5.1. Introduction 106
5.2. Methods and Materials 107
5.2.1. Contouring and dose constraints 108
5.2.3. Dose prescription and IGABT treatment planning 108
5.2.4. Choosing the optimal OAR dose per fraction 109
5.2.5. Dose planning criteria 112
5.2.6. Statistical analysis 112
5.3. Results 112
5.3.1. Effect of the number of fractions on fractionation compensation 112
5.3.2. Effectiveness of fractionation compensation when using EUD-based dose prescription 117
5.3.3. Verification of DVH parameter total dose computation against EUD 117
5.3.4. Effectiveness of total OAR dose compensation when per-fraction constraints can be violated 119
5.5. Discussion 120
5.6. Conclusion 124
5.7. References 125
Chapter 6: EUD-based off-line and on-line image guided adaptation in intensity modulated radiotherapy for cervical cancer 129
6.1. Introduction 129
6.2. Methods and Materials 130
6.2.1 Patient population and conventional treatment planning 130
6.2.2. Contouring 130
6.2.3. Imaging 131
6.2.4. Setup correction protocols 131
6.2.5. Treatment planning and margin evaluation 132
6.2.6. Setup variation simulation 133
6.2.7. Adaptive treatment simulation 134
6.3. Results 135
6.3.1. Imaging and setup deviations 135

6.3.2. EUD-based determination of the margin size 137
6.3.4. Effect of margin size on PTV and OAR dose 140
6.3.5. Adaptive treatment simulation 144
6.4. Discussion 150
6.4.1. Geometric and dosimetric margin assessment 151
6.4.2. Geographic and dosimetric adaptive treatment simulation 152
6.5. Conclusion 153
6.6. References 155
Chapter 7: Conclusion 158
7.1. Cumulative dose 158
7.2. Brachytherapy treatment planning 160
7.3. Fractionation compensation 161
7.4. Fast evaluation for adaptive radiotherapy 162
7.5. Future development 163
Summary 164
Opsomming 166
Acknowledgements 168
Appendixes 170

Glossary

ABS	- American Brachytherapy Society
Ant	– anterior
BED	- biological effective dose
BT	- brachytherapy
cc	- cubic centimetres
COMP	- fractionation compensation
CONST	- constant per-fraction constraints
CT	- computed tomography
CTV	- clinical target volume
CV	- comprehensive volume technique
DIR	- deformable image registration
DNA	- Deoxyribonucleic Acid
DVH	- dose volume histogram
DRR	- digitally reconstructed radiograph
Dx	– minimum dose in x% of the volume
D2cc	- most exposed 2cc of a volume of interest
EBRT	- external beam radiotherapy
eNAL	- extended no-action level
EPI	- electronic portal images
EQD2	- 2 Gy equivalent dose
ESTRO	- European SocieTy for Radiotherapy & Oncology
EUD	- equivalent uniform dose
Ex	- exhale
FIGO	- International Federation of Gynaecology and Obstetrics
GEC	- Groupe Européen de Curiethérapie
gEUD	- generalized equivalent uniform dose
GGE	- Gyn GEC-ESTRO
GI	- gastro-intestinal
GLOBOCAN	– Global Burden of Cancer Study
GTV	- gross tumour volume
GU	- gastro-urinary
Gyn GEC-ESTRO WG	- gynaecological Groupe Européen de Curiethérapie and the European SocieTy for Radiotherapy & Oncology working group
G2	- grade II or grade 2
G3	- grade III or grade 3
G4	- grade IV or grade 4

HDR	- high dose rate
HIV	- human immunodeficiency virus
HR-CTV	- High Risk CTV
hrHPV	- High-risk human papillomavirus
IARC	- International Agency for Research on Cancer
IC	- intracavitary
ICRU	- International Commission of Radiation Units
IDL	- Interactive Data Language
IGABT	- image guided adaptive brachytherapy
IGBT	- image guided brachytherapy
IGART	- image guided adaptive radiotherapy
Inf	– inferior
IS	- interstitial
IMAT	- intensity modulated arc therapy
IMRT	- intensity modulated radiotherapy
In	- inhale
IR-CTV	- Intermediate Risk CTV
L	- Left
Lat	– lateral
LCI	- left common iliac
LDR	- low dose rate
LEI	- left external iliac
LII	- left internal iliac
LKB	- Lyman-Kutcher-Burman
LQ	- linear quadratic
LRC	- late recto-sigmoid complications
MRI	- magnetic resonance imaging
NTCP	- normal tissue complication probability
OAR	- organ at risk
PDF	- probability density function
PDR	- pulsed dose rate
PET	- Positron Emission Tomography
Post	- posterior
PTV	- planning target volume
R	– Right
RAW	- uncorrected setup errors
RCI	- right common iliac
REI	- right external iliac

RII	- right internal iliac
RMC	- recto-sigmoid mucosal changes
rms	- root-mean-square
SAS	- Statistical Analysis Software
SCP	- setup correction protocol
SD	– standard deviation
SOI	- structure of interest
Sup	– superior
US	- ultrasound
VMAT	- volumetric modulated arc therapy
VOI	– volume of interest
Voxels	- volume elements
Vx	– Volume receiving x Gy dose
WG	- working group
2D	- 2 dimensional
3D	– 3 dimensional
4D	- four dimensional
#	- Fraction

Abstract

Cervix cancer radiotherapy treatment consists of external beam radiotherapy (EBRT) and brachytherapy (BT). Currently there exists no method to combine the dose of both modalities in a single dose value or dose distribution. This study derived a method to use the equivalent uniform dose (EUD) concept as a worst case dose estimate for both modalities, and the combination thereof.

The EUD was used as dose evaluation tool in clinical brachytherapy planning of 10 patients that received conservative organ at risk (OAR) toxicity avoidance treatment plans. OAR EUD dose constraints were also derived for brachytherapy treatment planning so as to be equivalent to the Gyn GEC-ESTRO guidelines for cervix cancer brachytherapy based on a population of 20 patients receiving 5 high-dose-rate image guided brachytherapy treatments each. Furthermore, a method to escalate tumour dose without increasing OAR dose was investigated using the EUD as a safeguard against OAR over-dosage and exploiting the effects of fractionation radiobiologically and by organ geometry variations. The EUD was also used as an external beam IMRT evaluation tool to calculate suitable planning target volume (PTV) margin sizes for treatment plan optimization and as a quick cumulative dose computation to enable on-line and off-line image guided adaptive radiotherapy (IGART).

This study utilizes the underlying mathematical properties of the EUD to act as a method for determining a worst case dose estimate for tumours and OARs. The method is accurate and reliable and easy to use. OAR dose constraints for brachytherapy treatment planning based on EUD prescription were derived and they compare well with existing Gyn GEC-ESTRO recommended methods and constraints. The safety of the EUD as a worst case dose estimate motivates the use thereof in fractionation compensation based treatment planning that strives to maximize OAR dose to a fixed constraint level and maximize tumour dose at no extra toxicity cost. The EUD derived external beam planning margins also corresponded well with the published margin recipes, but showed that margin recipes potentially overestimate the required margin size and that PTV dose levels could be reasonably lower in some cases compared to the CTV dose level and not lead to tumour under-dosage. The EUD is also an effective 4D dose evaluation and planning tool for IGART and can be used to ensure adequate total dose is delivered in a mobile and deforming tumour without overdosing the OARs. The quick and reliable application of this method is its biggest attribute.

The mathematical properties of the EUD open the possibility to determine a worst case estimate of cumulative dose in different treatment modalities and when they are used in combination. The application of this estimate can be extended to safe tumour dose

escalation in both image guided adaptive brachytherapy (IGABT) and IGART and their combination.

Key Words: Equivalent Uniform Dose, Cumulative Dose, Dose Volume Histogram, Treatment Planning, Organ at Risk, Tumour, Worst Case Scenario, IGABT, IGART

Chapter 1: Introduction

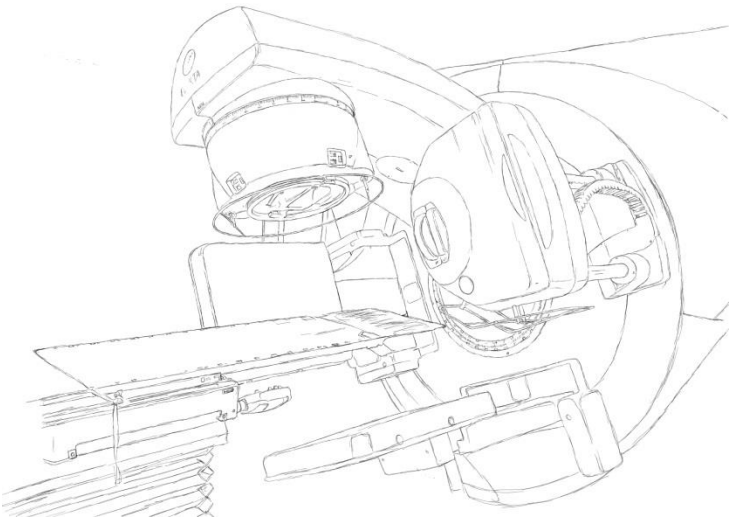

1.1. Background

1.1.1. Cause and prevalence of cervical cancer

According to the GLOBOCAN 2012 [1] worldwide estimations of incidence, mortality and prevalence, cervical cancer incidence was recorded as approximately 528 000 cases per year with a resultant 266 000 yearly deaths and a 5 year prevalence of 1547 000. This is the fourth most common cancer in women and the second most common cause of female cancer deaths and often affects young women. Quite alarmingly, the incidence is estimated at 445 000 (230 000 deaths, 51.7%) in less developed countries, while only 83 000 (35 000 deaths, 42.2%) in the more developed countries. The 2012 estimate showed that almost 9 out of 10 cervical cancer deaths occur in the less developed regions. Eastern, Middle and Southern Africa ranks amongst the highest numbers of incidence and have more than 50% mortality rates as a result of presentation only at an advanced stage.

It is well established that High-risk human papillomavirus (hrHPV) infection is a prerequisite for an actual rare outcome of development of cervical cancer. A workgroup of the International Agency for Research on Cancer (IARC) has confirmed that screening for cervical cancer by cytology examination of Pap smear cell samples will prevent death [2]. With early detection and decisive action, an 80% reduction in mortality is estimated via screening and vaccination. However, resource limited developing countries carry most of the burden of cervix cancer where screening and vaccination programs are limited, if at all existent. Many of these countries also have a poorly controlled human immunodeficiency virus (HIV) epidemic with high HIV prevalence, late diagnosis and incomplete access to timely treatment [3]. It can thus be expected that the effect of early detection and vaccination programs will not become evident within the next few decades, at least in the developing world.

1.1.2. Radiotherapy treatment options

Radiotherapy treatment of cervical cancer is one of the most essential components in obtaining tumour control and can be supplemented by concurrent chemotherapy.

Radiation treatment consists of a combination of external beam radiotherapy (EBRT) and brachytherapy (BT). To this day, standard EBRT is to deliver doses of 45-50 Gy via mostly four-field-box treatment techniques and in some clinics simultaneous integrated boosts have been applied to the primary tumour and uterus [4, 5], while larger fields deliver dose to the affected lymph drainage systems. Parametrial boosts of 10-15 Gy can also be given [6-8] in combination with midline shielding of the organs at risk (OARs), like the rectum and bladder, to reduce side effects of treatment while increasing systemic control [9].

It has been shown that the overall survival of patients treated with radiotherapy alone versus radio-chemotherapy is significantly lower at 5 year follow-up [10]. Higher disease free survival and lower local recurrence rates have also been evident, as well as reduced rates of distant metastatic and cause specific failure. Historically, such results have been obtained when radiotherapy was administered with standard EBRT techniques and an additional BT boost dose was given. EBRT could either have been based on 2 dimensional (2D) or 3D treatment planning, while BT treatment planning would be based on the use of 2D radiography imaging where prescription and reporting relied on dose points. These points are amongst others Point A, a hypothetical point representing the primary tumour and where the dose rate will vary least in different source configurations [11-13]. OAR dose points have also been used widely for reporting purposes [14]. Recently, there have been major advances in both EBRT and BT treatment techniques that have shown superior outcome compared to standard EBRT and BT. The improvements in BT contributions in tumour control alone is estimated to be at least equal and better than the recently reported impact of concurrent chemotherapy on tumour control [4, 15].

1.1.2.1. External beam radiotherapy

External beam radiotherapy is primarily used to reduce the primary tumour volume, irradiate microscopic infiltration of normal tissue outside the primary tumour and to irradiate nodal disease at the same time. The aim of radiotherapy treatment is similar to radical hysterectomy and lymphadenectomy, though these surgical techniques are usually only used in early stage disease and younger patients since radiotherapy has some associated late sequelae [16-18]. These late complications typically present in the form of proctitis, cystitis, vaginal stenosis and small and large bowel complications.

High energy photons (6 – 18 MV) are typically used for parallel opposed, four fields box and opposing parametrial boost fields and the dose prescription is normally to the International Commission of Radiation Units and Measurements (ICRU) reference point

[19]. Typical dose prescriptions range from 45 Gy in 25 fractions once daily to 50.4 Gy in 28 fractions, or 50 Gy in 25 fractions for advanced stage disease. Parametrial boosts to the nodes are usually left to the discretion of the treating physician. During the EBRT part of the treatment, patients with tumour regression of less than 20% usually have significantly worse progression free survival [20]. The tumour diameter and response during treatment are considered prognostic for overall survival and progression free survival and adequate EBRT dose is thus essential [21].

Nodal disease at the time of diagnosis is a predictor for development of distant failures and node negative patients have significantly higher 3 year progression free survival and overall survival than node positive patients, especially in early stage disease [20]. For the eradication of subclinical microscopic disease, Petereit and Pearcey [22] estimated that at least 52Gy should be delivered to such low risk volumes. Additionally, overall treatment time (EBRT + BT) also has a major impact of which treatment delivered in less than 60 days is more beneficial in terms of tumour control compared to longer or protracted treatment times. However, EBRT at these and higher dose levels have major associated risks of acute and late complications. Parametrial boosts to 55 and 60 Gy combined with BT may result in severe late toxicity (grade 3 or higher) in the event of shortened overall treatment time and concurrent chemotherapy if specific dose limiting techniques to normal tissue is not implemented [6].

Recently, intensity modulated radiotherapy (IMRT) and intensity modulated arc therapy (IMAT) have been investigated for nodal boosts and elective nodal irradiation as they have the capability to successfully reduce organ at risk (OAR) morbidity [23, 24]. IMRT produces steep dose gradients for gross tumour volume (GTV) boosts and OAR sparing, but it is not capable of producing the high dose region in the middle of the tumour that BT applications can achieve. BT boosts cannot be mimicked by EBRT boosts. Such EBRT attempts lead to far greater volumes of OARs receiving intermediate dose levels, resulting in specific endpoints of complications that can be avoided with BT [25-27]. When suitable doses at low incidence of acute and late complications are desired, IMRT and IMAT for whole pelvis irradiation are quite effective in combination with BT boosts. However, extreme caution should be taken in such highly conformal treatment procedures to ensure that the dose is conformed to the tumour volume and that it follows the regression pathways of the tumour and surrounding OAR geometrical and positional changes over time [28].

1.1.2.2. Brachytherapy

Brachytherapy allows the application of high radiation doses to tumour volumes while sparing normal tissues and OARs because of a rapid dose fall-off with distance from the radiation source and close treatment distances. Historic and 2D radiographic image treatment planning was performed with standard source loading patterns and traditional rectum and bladder points [14] have been used to limit the OAR dose below acceptable dose thresholds. These thresholds were in turn derived from OAR complication rates based on point doses recorded from standard source loading patterns [29-31]. Understandably, single dose points do not account for tumour and normal tissue anatomy and are simply not accurate to assess late OAR complications and tumour control, although some studies have provided useful information using them [32].

The important role of brachytherapy is to improve local control and maintain low normal tissue toxicity levels in addition to EBRT [29, 30]. In 2000, the American Brachytherapy Society (ABS) presented a guideline in which it was suggested that 80 – 90 Gy total dose (30 – 40 Gy by BT) be delivered in 4 to 6 fractions to point H (or point A) and the OAR ICRU points be kept below 80 Gy and 75 Gy for the bladder and rectum respectively [25]. These dose values are the 2Gy per fraction total dose equivalents calculated with the linear quadratic (LQ) model and α/βvalues of 10 Gy and 3Gy for the tumour and OARs respectively [33,34].

BT can be applied in various ways, and such guidelines were set up to produce equivalent treatments when different applicator configurations are used, intracavitary or interstitial BT or the combination of both is used, whether low dose rate (LDR), pulsed dose rate (PDR) or high dose rate (HDR) treatments are given. The versatility in the LQ model for various dose rates and tissue response allows the calculation of equivalent total doses for tumours and OARs, irrespective of the technique. Although these equivalent doses consider various fractionation dependent factors and tissue response parameters, some other treatment related variables, like the timing of chemotherapy administration, are disregarded [35]. This model considers tumour repopulation rates, incomplete repair of sub-lethal DNA damage and its conversion to lethal damage, as well as overall treatment time.

The limitations of the 2D treatment planning techniques are obvious due to the simplified consideration of tumour dose and possible gross under- or overestimation of OAR dose. Unfortunately the use of such dose points for prescribing and reporting population treatment outcomes has resulted in poor tumour control, especially in the case of advanced disease where local failure rates have been as high as 20-40% [9, 10, 36-39].

Differentiation between various treatment protocols is also obscured beneath the uncertainties of 2D planning [40]. The same applies to the point dose approach for assessing late morbidity in the OARs. The displacement in point A in multiple treatment fractions along with the ICRU isodose volume that exhibits significant variability with respect to height, width, thickness and volume, irrespective of the applicator used, has called for a revision of the guidelines set for intracavitary and interstitial brachytherapy [41-54]. The use of point A for dose reporting also loses all meaning when interstitial brachytherapy is performed [55].

More recent volumetric considerations based on 3D treatment plan evaluation demonstrated that dose to the most exposed 2cc of the rectum (D2cc) is a more reliable indicator of the actual dose in 2cc of the rectal wall and that this value can be used for reporting a high dose volume in the rectum. Similarly, the ICRU bladder dose point is not representative of the maximum dose to the bladder when making use of a liquid filled Foley-catheter [56]. In fact, the highest dose point constantly lies more superior to the ICRU defined dose point.

These limitations on prescriptions and dose reporting associated with dose points also resulted in variations in toxicity outcome. Variations in ICRU rectum and bladder dose points have been shown to be much larger than the variations found when planning according to DVH parameters of D2cc, for example [57]. The clinical significance of dosimetric findings from orthogonal film-based analysis has been shown to be inadequate for intracavitary cervix brachytherapy [58]. Point dose values of OARs inaccurately reflect heterogeneity of dose distributions within these organs and give no indication of volumes of tissue exposed to high doses. They are simply not reliable for treatment prescription and outcome correlation [48, 59-61]. Additionally, volumetric dose assessments of treatment planning performed on point A and 2D radiographs has shown that the 3D volume of the cervix tumour could not be covered optimally and that there are negative correlations between coverage and cervix size, while ICRU dose points do not necessarily correlate with DVH parameters used in 3D treatment planning [62]. Even the use of the LQ model could not derive better correlations between Point A biological effective doses (BEDs) and survival or pelvic control. Large literature reviews could also not produce significant dose response relationships between Point A BEDs and normal tissue complications and the lack of correlation is mostly attributable to the quality of treatment reporting, emphasizing the limitations of such points [22].

1.2. Recent improvements in treatment techniques

1.2.1. Improvements in EBRT

In order to reduce distant failures, dose in the range of 45 – 50 Gy to the effected nodes does not seem to be adequate [22]. Logsdon et al. [63], based on conformal EBRT treatment, estimated that the optimal ratio between tumour control and complications is achieved with doses of 45 – 50 Gy whole pelvic EBRT combined with BT. Doses larger than this increase the volume of normal tissues and OARs irradiated to dose levels at which faecal incontinence has been reported, namely >60 Gy [25]. Although opposing field parametrial boosts have been used extensively to cover these nodal areas, they are often associated with higher toxicity levels, as are extended field treatments [9, 6, 39, 64].

Since the advent of more conformal techniques like IMRT in the treatment of cervical cancer, evidence has been mounting that moderate and severe late morbidity can be reduced by 50% compared to conventional EBRT techniques by reducing the volume of normal tissue exposed to high doses. However, the introduction of image guided adaptive brachytherapy (IGABT) has had a significant effect, beyond that of concomitant chemotherapy and IMRT [4, 15], on local control rates as no EBRT technique has the capability to deliver such localized high doses to an internal tumour [26, 27, 65]. IMRT though, has a significant role in nodal boosts and is an effective way of reducing toxicity [4, 24]. Furthermore, the occurrence of distant metastases is linked to some degree to local and regional failures [15]. IGABT may play a dose escalating role to the primary tumour volume and subsequently reduce the incidence of local failures, while IMRT and chemotherapy address nodal disease. IMRT has been shown to reduce volumes of some normal organs that receive 90% of the prescribed dose by more than 20 – 30% compared to conformal EBRT [66].

As mentioned before, the greatest regression in tumour volume occurs during the EBRT component of treatment. If conformal techniques are used to boost nodal volumes, tracking of these volumetric changes can be performed either by probabilistic planning [67], treatment plan adaptation or re-planning [68], or optimal pre-treatment plan selection on a plan-of-the-day basis. These planning techniques ensure that tumour coverage is adequate while OARs moving in and out of the original planned high dose regions are taken into account in terms of dose limitation. With current 3D imaging techniques of computed tomography (CT) and magnetic resonance imaging (MRI) widely available, such adaptations are now implementable.

1.2.2. Improvements in brachytherapy

The poor local failures, especially for more advanced disease [20, 69-70, 5, 71], was one of the driving forces for progress in brachytherapy and was achieved by changing from the point dose concept to full 3D morphologic imaging. The use of CT, ultrasound (US) and most importantly MRI now allows accurate tumour and OAR contouring with full dose volume histogram (DVH) data available for treatment plan analysis and dose optimization. Particularly in MRI-based treatment planning, the GTV and clinical target volume (CTV) topographical changes can be considered during fractionated treatment of which the topography at the time of diagnosis and time of brachytherapy is most important. The greatest decrease in tumour volume occurs during EBRT, whereas tumour regression between the first and subsequent brachytherapy fractions are minor [72] if the brachytherapy treatment starts close to the end of the full treatment course. Substantial volumetric regression of 60 to 80% of the pre-therapeutic volume may occur during EBRT and concomitant chemotherapy [73, 74, 21]. Although these regression rates of response are considered prognostic for overall survival and progression free survival [21], brachytherapy dose should be adapted to these changing volumes to ensure that normal tissue dose constraints are obeyed to without losing conformance to the tumour volume itself [20], as is suggested in EBRT.

Since 1998, MRI-based 3D treatment planning was introduced which allow the individualization of dose distributions based on the patient's anatomical configuration at the time of treatment [75]. The GTV could be assessed at the time of diagnosis and BT so that a CTV volume could be adapted to the tumour configuration at the time of brachytherapy. The Groupe Européen de Curiethérapie (GEC) and the European SocieTy for Radiotherapy & Oncology (ESTRO) working group (Gyn GEC-ESTRO WG) presented guidelines that comprise of imaging and organ segmentation for individualized planning of every treatment fraction [76, 77].

The Gyn GEC-ESTRO WG I described basic concepts of 3D target definition required for 3D treatment planning, laying the foundation for the terminology required for a common language for prescription and reporting. They identified two CTVs: One derived from the use of point A and is the tumour extent (GTV) in 3D MRI imaging at the time of the start of BT. A dose of 80-90 Gy was required in the past to this CTV (or point A). The other made use of the ICRU [14] recommendations starting from the GTV at diagnosis for defining the CTV at the time of BT. The total dose prescribed to this CTV is 60Gy.

These two CTVs are known as:

High Risk CTV (HR-CTV) – has major risk of local recurrence. Treatment intent is to deliver a total dose as high as possible and appropriate to eradicate all residual microscopic tumour.

Intermediate Risk CTV (IR-CTV) – has a major risk of local recurrence in areas that correspond to initial macroscopic extent of disease with at most residual macroscopic disease at the time of BT. Treatment intent is to deliver a dose appropriate to cure significant microscopic disease in cervix cancer, which is 60 Gy.

The Gyn GEC-ESTRO WG II focused on 3D dose-volume parameters for cervix cancer brachytherapy, specifically DVH parameters for GTV, HR CTV, IR CTV and the OARs. The target doses are the minimum dose delivered to 90 and 100% of the respective CTVs: For example, D90 of the HR- and IR CTVs. In the case of OARs, the minimum dose in the most irradiated tissue volume was recommended for reporting: 0.1, 1, and 2 cm^3. A further two optional parameters of 5 and 10 cm^3 was also proposed. Similar to earlier methods of 2D treatment planning, the assumption is made that the full prescribed dose of EBRT is delivered in these volumes of interest. There are no differentiations made in the spatial location of these volumes within the 3D dose distribution during treatment fractions of EBRT and BT. The most irradiated OAR volumes are also regarded as contiguous volumes and outer walls are contoured since there seems to be negligible differences in the dose values when comparing the outer wall plus content with the wall only [48].

The LQ formalism is used when adding doses from BT and EBRT, as well as dose from subsequent fractions of the same modality. The dose values are reported as absorbed dose and converted to 2 Gy equivalent dose (EQD2) with this radiobiological model while considering differences in treatment dose rates as well [33,34]. This formalism allows systematic assessment within one patient, one centre and comparison between different centres with analysis of dose volume relations for GTV, CTV, and OARs. These technological advances in MRI-based brachytherapy and 3D dose-based treatment planning optimization to the HR-CTV can lead to high rates of local control in the range 80%-95% in small tumours, such as International Federation of Gynaecology and Obstetrics (FIGO) stage IB1 and small stage IIB [78]. However, the local control rate declines significantly for larger tumours, and especially for tumours with unfavourable topography in relation to the pear shape of the standard BT prescription isodose [70]. These 3D treatment planning techniques are however resource demanding.

1.3. Adaptive radiotherapy

1.3.1. Motivation for EBRT dose adaptation to a tumour in a mobile organ surrounding

Since most of the tumour shrinkage takes place during EBRT, any conformal treatment approach should consider the dramatic changes that may occur in tumour and OAR spatial position and geometry. The introduction of IMRT has primarily resulted in decreased gastrointestinal and haematological toxicities, and preliminary outcome studies have reported similar tumour control and survival with IMRT [79-81]. Because of the substantial organ motion in the pelvis, image-guided and adaptive radiotherapy has the potential to account for it and reduce possible over-dosage of normal tissues moving into the high dose region, thereby further enhancing the benefit of IMRT. So far we could not identify a significant impact in terms of primary tumour control with IMRT in a literature survey, although it is a useful option in post-surgery radiation [81]. IMRT has particular importance in elective nodal boosts [4], while OAR sparing is significantly better than conventional methods.

Sparing of normal tissue is of utmost importance for the delivery of full treatment schedules of concomitant chemotherapy because acute bowel and bone marrow side effects often prevent the completion thereof. IGART can significantly reduce the volume of irradiated bone marrow and it translates into clinical benefits [80, 82] while the dose to organs at risk are reduced with decreased morbidity as an end result [23, 24] with careful correlation of OAR spatial variations [82,83].

By means of image guided adaptive radiotherapy (IGART) the effects of inter- and intrafraction anatomic changes and their consequences can be considered to implement suitable planning target volume (PTV) margins to minimize geographical miss and for reliable dose accumulation [83–85, 68]. These anatomical and morphological changes require either an optimal frequency of imaging with subsequent re-planning, or methods that account for such changes in the planning optimization process [67, 86, 87]. The execution of the treatment requires initial treatment planning, imaging and patient positioning correction strategies that may be performed on-line or off-line. Furthermore, for IGART good image quality is mandatory for manual or automatic registration using on-line or off-line protocols and for the topographic assessment of both the target and OARs. These techniques are not available as standard practice packages yet, thus requiring long treatment times for re-contouring and re-planning. There is a high demand for faster methods and workflow, which may be provided in coverage probability planning that is performed pre-treatment, but may also require additional re-planning.

Image quality in the multiple imaging approach and re-planning should also contribute to an improved adaptation method and not create more uncertainties.

1.3.2. Image-guided adaptive radiotherapy

IGART has evolved intensely over the past few years [83]. Treatment individualization is based on the use of repetitive imaging of the treatment area with MRI and CT to adapt the treatment over the course of radiotherapy [68, 88]. Positron Emission Tomography (PET) has also been investigated for this purpose. Since IMRT and IMAT can be used to produce very steep dose margins, the choice of PTV margins to compensate for setup errors and organ motion is extremely important. Several studies have recently documented the extent of inter- and intrafraction motion for cervical cancer patients [68, 82-85].

In addition to the pelvic organs being extremely mobile and they bear significant geometrical changes during the treatment process, the setup variations encountered in day-to-day treatment of pelvic tumours should also be corrected or compensated for [89, 90]. The combination of these variations represent a significant challenge in conforming the prescribed dose to target volume with precision throughout the whole course of treatment, consisting of several treatment fractions that are to be delivered. The use of image guidance and immobilization techniques are vital for consistent patient set-up verification and dose adaptation. These geometrical variations are mostly addressed with suitable PTV margins that are often calculated for each individual institution, based on their positioning and immobilization technique. Margins of 5-7 mm have been deemed to be accurate for setup variations to account for systematic and random effects [91-93]. Furthermore, to account for the organ movement effects, these margins are increased to 1.5 up to 2.0 cm resulting in significant OAR volumes included in the PTV, unless repetitive imaging is used to direct the dose precisely to the target [94-95] in several sub-sections of the full treatment course.

Cone beam computed tomography imaging is commercially available nowadays and can be used to provide high quality images for adaptive radiotherapy strategies. Kilovoltage cone beam CT and megavoltage images are relatively fast to obtain with the patient in the treatment position. CT images unfortunately suffer from low soft-tissue contrast which makes clear identification of tumour and cervix difficult. MRI provides superior soft tissue discrimination within the pelvis compared to CT. The effectiveness of MRI in cervix treatment has been described in repetitive imaging studies to quantify inter- and intrafraction organ motion and determine non-isotropic margins around the gross tumour volume and the CTV [82, 83]. A proposal for a dedicated MR linac for IGRT has been

made [96] and online MR IGART of cervical cancer can be performed with such novel technologies [97] that would result in significant reduction of OAR volumes exposed to high doses.

Alternatively, these variations in patient anatomy and uncertainty in dose delivery can be addressed during the treatment planning optimization process with coverage probability optimization. This concept considers sequential patient image data and calculates the probability of organ movements and setup- and other treatment errors to improve the statistical description of variations for treatment planning. Using this information, dose distributions can be optimized to an individual's pre-treatment probabilistic geometries and uncertainties calculated from multiple organ instances using multiple images [67, 98].

1.3.3. Motivation for BT dose adaptation to a tumour in a mobile organ surrounding

It was mentioned in section 3.1. that most of the tumour regression occurs during week 3-4 of radiotherapy treatment. This point in time is where many treatment schedules start with brachytherapy boosts. To be able to apply high boost doses to the tumour, adaptation of the dose distribution to the regressing tumour will aid in the reduction of normal tissue dose through dwell position and dwell time optimization, applicator adaptation while conforming high dose regions to the tumour. This procedure unfortunately requires time and resource investments since treatment plan adaptation needs to be performed on a per-fraction basis for best results while imaging for this purpose is also required on a per-fraction basis.

As indicated by the Gyn GEC-ESTRO WG I target coverage can be improved by adapting the dose distribution to tumour response in brachytherapy treatment planning. IGABT does just this by allowing the dose to be adapted and escalated according to the individual tumour topography by dwell point optimization and eventual interstitial needle implantation [99-102]. Tan et al. [103] showed that IGABT resulted in significant improvement in local control without the risk of serious toxicity. Compared to the 2D treatment approach, they found that the dose to point A was less than what was recorded in the well-known Vienna Series [78], but due to their target dose conformance HR-CTV D90 doses were higher than the Vienna results. This is a clear indication that adaptive treatment planning is focussed on improving treatment outcome for the individual and has major advantages compared to past techniques that were more focussed on population based treatment protocols. In 2D-based BT point A is a poor surrogate for the evaluation of dose to a four dimensional (4D) target such as a

regressing cervical cancer [104]. A prerequisite for IGABT is an adaptive target concept that includes both space and time domains [76, 77]. This approach requires investment in personnel, time and equipment. Several investigations to curb these requirements have been performed; some with positive attributes to the standard technique while others have highlighted reasons for caution.

To reduce the resource load, Davidson et al. [57] investigated the possibility of utilizing the dose distribution from one 3D treatment plan for a second subsequent treatment and thus reducing the number of imaging fractions. The first insertion was done during the third or fourth week of EBRT (concurrently) and dose was prescribed to point A. They concluded that the changes in OAR geometry and position, as well as applicator positional changes may result in significant OAR dose increases and an unstable treatment method. Treatment plans should be tailored for each insertion to reflect current applicator and anatomical geometry. Other studies produced similar results [105-107].

Studies investigating internal movement between the acquisition of planning images and images taken at the time of treatment revealed that if the delay between them is long enough, significant changes may occur for individual patients [108]. In the light of severe late toxicity, pre-treatment images should thus be taken to confirm dosimetry before treatment, or the amount of time taken between applicator insertion and treatment should be minimized. OAR dose constraints may be violated for individuals even after dose optimization was performed on the first treatment fraction [107, 109, 110]. These results have serious consequences for treatments of which only selected few fractions include imaging and plan optimization, or where the HR-CTV dose objective cannot be reached without sometimes having to violate OAR dose constraints. Georg et al. [111] have established that rectal D2cc doses above 75Gy EQD2 is associated with an increase in the percentage of patients with higher rates of grade 2–4 late toxicity. Significant OAR movements that have been observed between BT fractions underline the importance of repetitive adaptive planning for each BT fraction [36, 105, 106, 108, 112, 109, 110, 99].

Previous clinical outcomes [78, 113, 114] have shown that a dose of more than 87 Gy is required to D90 of the HR-CTV to achieve local control rates of more than 90% in large volume disease. More recent studies have shown that a D90 of 91 Gy (EQD2) result in local control rates of 91% [4]. By use of image guided adaptive radiotherapy and, in particular IGABT, these doses are now deliverable and have the added advantage of a reduction in radiation-induced morbidity which largely improves the therapeutic ratio.

As to the use of IMRT as a single alternative to combined modality treatment in the boost of the primary tumour without brachytherapy applications, recent studies comparing advanced BT with IMRT conclude that it is not adequate to perform an IMRT boost alone [26, 27]. To achieve dose distributions of equal quality offered by IGABT, IMRT would lead to significant increases in the volume of normal tissue irradiated to toxically high doses.

The major advantage to be expected from IGABT seems to be that through more precise 3D assessment of organ related dose volume relationships, adverse side effects may become better predictable and therefore also avoidable for defined clinical situations. Current dose-response relationships of the tumour and normal tissues do not fully consider the effect of changing anatomy causing variations in dosimetry of the treatment plans with time progression. These variations cause uncertainties in the total cumulative dose that is absorbed in the different volumes. The consequences of these uncertainties may be unpredicted local recurrence and severe late toxicity, even when the initial treatment plans obeyed the dose constraints.

1.3.4. Image guided adaptive brachytherapy

Further improvement upon the recommendations by the Gyn GEC-ESTRO group included the evaluation of time trends of tumour regression that can be described by sequential imaging of the tumour. Other than the significant regression exhibited by fast responding tumours, more resistant tumours are prone to less regression [72]. These time trends add the fourth dimension to individualized treatment planning considering the residual tumour at the time of BT (HR-CTV) and initial tumour at diagnosis (IR-CTV). Dose adaptation to a changing tumour volume results in considerably higher tumour dose compared to historical methods of point based treatment planning or a single treatment plan applied over several treatment fractions [78, 115-117, 4, 15, 118, 65]. This means that IGABT has particular importance in locally advanced cervix cancer and can be extended to the adaptation of the applicators used for treatment. It must be stressed though that small tumours also require re-optimization [7].

IGABT significantly improves the therapeutic ratio by tumour dose escalation and OAR dose reduction [20, 78, 115-117, 119-121], leading to reduced severe toxicity rates [122]. Significantly reduced late morbidity and high rates of local control are ensured [4, 15]. Clinical outcomes have shown 15% improvement in survival and 50% reduction in late morbidity when combined with IMRT. While IGABT delivers a substantial portion of the total radiation dose compared to EBRT, it has a significant effect on overall survival, disease free survival, distant metastasis development and local control. With IGABT,

relatively low levels of grade I and II complication can be achieved (10-30%) along with the excellent local control [123]. Some isolated severe late toxicities do occur (grade 3 and 4) which can sometimes be correlated with other co-morbidities as well [8].

Since advanced stages of the disease still have worse local control and overall survival compared to early stage disease, the rational is to escalate the brachytherapy dose since it has had the largest influence on treatment outcome over the past few decades of development [4]. To achieve this goal without violating OAR dose constraints and increasing late morbidity, adaptation of the high dose volume to the tumour is required and at the same time avoiding small volumes of high doses to the OARs. Full utilization of a maximum number of treatment fractions in this respect could potentially improve the total tumour dose [124].

1.4. Improvements in treatment outcome and late toxicity

1.4.1. Rational for dose escalation

Distant metastases occurrence in cervix cancer has been linked to local and regional failures and dose to the HR-CTV is a significant predictor for such metastases, in particularly so for patients with advanced disease [15]. While chemotherapy plays an essential role in the management of systemic disease, local recurrences may induce distant metastases and they are usually the result of inadequate dose to the primary tumour. If the dose to the tumour volumes can be tailored and maximized to an individual patient's anatomical and morphological arrangement, such incidence of local failures can be reduced [125-127].Tumour regression has also been labelled as an early response indicator for local control and distant metastases development and can be used in the identification of patients requiring intensive systemic treatment. Patients with high tumour stage at diagnosis and positive lymph nodes are typically at high risk of developing distant metastasis. IGART can be extremely useful in combination with IGABT in this context since in general, better tumour control can be achieved if greater tumour doses can be delivered [128-130].

1.4.2. Improvement in tumour control

IGABT has shown dramatic increases in local control rates as well as overall survival [7, 78, 103, 131]. The early Vienna Group results [131] showed improved treatment outcome with optimized 3D treatment planning for patients with tumours larger than 5cm. These results emphasize the particular advantage that adaptive treatment planning has for the improvement of local control in advanced disease. Further dose escalation

can be achieved with the use of novel applicator designs to combine intracavitary and interstitial application of brachytherapy treatment at acceptable toxicity rates [99-101].

Dimopoulos et al. [102, 113, 114] have shown that local control rates in the order of 95% can be achieved when the HR-CTV D90 is 87 Gy or more. Other very high rates of local control, disease free survival and overall survival for intermediate term follow up have also been demonstrated [118]. Nomden et al. [20] saw a correlation between tumour stage and overall survival and progression free survival with better outcome in early stage disease. Tumours larger than 5cm tend to perform worse than smaller tumours. But, the later Vienna results [116] based on a large patient group showed that 3D conformal radiotherapy and concomitant chemotherapy, with the addition of IGABT with interstitial implantations in some cases of advanced disease, result in excellent local control rates in limited disease and slightly poorer results, though still very high, in advanced disease. Lindegaard et al. [4] found that a D90 of 90 Gy to the HR-CTV results in local control rates of 91% and overall survival improvement of about 15% compared to 2D based BT. Especially in the larger tumours, this effect is a result of the dose contribution from IGABT and not as much from chemotherapy. Similar results were found when D90 of 93 Gy was delivered with comparable local control, cancer specific- and overall survival [20, 116].

Several studies have now shown improved treatment outcome with IGBT [20, 116, 117, 119, 132, 133, 134]. The benefit of these techniques may differ between various institutes due to differences in treatment approaches, like treatment schedules, dose rates and applicator types. These dose levels are only achievable by way of sequential optimization to assure adequate normal tissue sparing. Care should be taken to ensure adequate tumour dose though, because too much reduction in OAR dose leads to decreased D90 and a loss in local control [117].

Post-operative IMRT boosts of cervical cancer patients may also achieve local control rates of 76% at 3 and 5 years follow-up, with progression free survival and overall survival being at 74% and 67% respectively [23]. CTV dose in these cases were 78.5 to 82 Gy EQD2 with no significant acute morbidity.

1.4.3. Late toxicity

Patients with tumours larger than 5 cm usually perform worse than with smaller tumours, especially if dose adaptation is not performed leading to the inclusion of large OAR volumes in close proximity of very high doses [20, 118]. In IGABT, moderate rates of treatment related morbidity are still evident and large reductions in major morbidity has been shown to be possible, like the late Vienna results revealed [116]. Moderate and

severe late morbidity can be reduced by 50% when IGABT and IGART are combined. Further reduction in toxicity is achievable with the combination of intracavitary and interstitial brachytherapy. This technique improves the DVH parameters in terms of tumour coverage and provides the opportunity of more normal tissue and OAR sparing at the same time. Consequently, this leads to better local control and a reduction of toxicity. However, even with the use of CT image guidance, late toxicity rates of up to 13% have been reported and typically include proctitis, small bowel obstructions, fistulas, and vulvovaginal toxicity [102].

In a recent study by Güth et al. [135] investigating the underreporting of severe late toxic reactions after chemo-radiotherapy it was found that total vaginal necrosis is an underreported but serious late complication after chemo-radiation and leads to considerable chronic morbidity [136]. 5 year toxicity rates have been reported for ≥grade 2 rectal complications of 20%, bladder of about 12%, small bowel of more than 6%, while grade 3 rectal ulcers and grade 4 recto-vaginal fistulas were also seen. But, the most common late toxicities are sometimes related to vaginal contracture and adhesion [137]. Chemo-radiotherapy is associated with a higher probability of developing vaginal severe late toxicity [138] and urologic severe late toxicity, compared to patients receiving only radiotherapy. Results from centres where the GEC ESTRO 3D adaptive brachytherapy guidelines have been implemented have led to a decrease in the overall incidence of late side effects, compared to traditional point A based treatment [4, 78, 116, 117, 139]. Adaptation to the target volume reduces dose to the OARs significantly [140], but this could lead to significantly higher or lower vaginal doses [141]. IGABT is capable of reducing vaginal morbidity to less than what has been reported in the past. However, mild to moderate vaginal morbidity is still pronounced with currently applied IGABT and it needs further attention and low incidence of serious vaginal side effects do occur [136].

A strong motivational factor for OAR dose reduction and accurate dose-effect prediction, as that older patients are more prone to severe late toxicities than younger patients, especially skeletal toxicities. Cancer survivors live longer than a few decades before and have higher occurrence of symptoms that appear at larger time intervals after treatment. These do not just include complications of the urinary and gastrointestinal tract, but also lymph oedema, sexual dysfunction and pelvic pain [142]. Possible deficiencies in the calculation of accumulated dose could also highlight discrepancies between late toxicities and lower dose levels [143], falsely motivating even lower dose constraints.

Unacceptably high toxicity rates were demonstrated in a study where the overall treatment time was limited to 7 weeks consisting of EBRT, BT and concomitant chemotherapy for locally advanced carcinoma of the cervix [64]. Depending on the tumour stage, 45 Gy EBRT and additional parametrial boosts were delivered to total doses of 55 to 65 Gy. Additional BT of 30 Gy in 5 fractions was delivered to point A. Bladder and rectal dose points were in the range of 60 Gy, while the vaginal surface dose was on average close to 130 Gy. Late toxicity rates were extremely high at 27.6% grade II, 17.2% grade III and 6.9% grade IV. This meant that 24.1% of patients experienced severe late toxicity. These included grade 4 ileal obstructions, grade 4 vaginal necrosis, and several grade 3 complications ranging from vaginal to intestinal toxicity. This particular study stressed the need for detailed 4D adaptive treatment planning. In addition, careful consideration of overall treatment time, timing of chemotherapy administration and more reliable ways of determining dose accumulation must be exercised.

Kim et al. [144] performed a prospective observational study to assess the value of dose-volumetric parameters predicting recto-sigmoid mucosal changes (RMC) and late recto-sigmoid complications (LRC). In contradiction to studies like Georg et al. [2009, 2012], they found 13 % late rectal bleeding rates when D2cc was < 70 Gy, 34.6% between 70 and 85 Gy, and 43% when > 85 Gy. Interestingly, they found that D5cc was a significant factor for predicting RMC ≥ score 3 and late rectal bleeding ≥ grade 2, while Georg et al. [111, 145, 146] found D2cc predictive and at other dose levels. Other authors could also not find any correlations between D2cc and D0.1cc of the OARs and the development of morbidity. Dose to these volumes were similar between the patients with no grade 3-5 morbidity and those that had it. Possible reasons for developing grade 3-4 gastrointestinal events might be bi-lateral nodal boosts and larger fields for extensive primary and nodal disease [117] and raises the question about the repeatability of dose accumulation using DVH parameters.

There are several studies that show deviations from the rectosigmoidoscopy studies of Georg et al. [111, 145]. Koom et al. [46] reported 45% of patients with grade 2 or higher telangiectasia at dose levels of 67 ± 9 Gy to D2cc of the rectum. Kang et al. [7] reported that 43% of their patients had late rectal bleeding, but 3D dose optimization reduced the incidence of severe late rectal bleeding. Importantly it should be considered that matching of the high dose volumes with locations of mucosal changes could be performed in some studies [111], while others could not make this match [144]. This stresses the inherent uncertainty in the calculation of accumulated dose via DVH parameters such as D2cc, but uncertainties are not necessarily limited to the use of

these parameters alone since co-morbidities and other less important factors should also be considered [20].

Toxicity with the use of IMRT as opposed to conventional whole-pelvic irradiation is lower than what is found in conventional techniques. IMRT leads to reduced acute grade 2 and grade 3 gastro-intestinal (GI) and gastro-urinary (GU) toxicity, while chronic GI toxicity is lower with IMRT [146]. In contrast, extended field conventional radiotherapy used to treat pelvic masses and para-aortic lymph nodes lead to substantial acute gastrointestinal toxicity and grade 3 hematologic toxicity [39]. An advantage of IMRT is that it has the capability to reduce protracted treatment duration by simultaneously integrated boost and lowering the incidence of acute toxicity, especially GI complications.

Late treatment related morbidity is one of the major concerns in curative radiotherapy, primarily because of its clinical aspects, but also due to its significant impact on the quality of life of cancer survivors [152-154]. Most late side effects are irreversible and some are progressive. A recent interesting study by Georg et al. [155] investigated the crude rates of later complications from radiotherapy treatment (ratio of the number patients who developed a complication and the total number treated), Actuarial incidence rates assessed by the Kaplan–Meier method describe the risk of developing a defined maximum grade side effect at least once within a certain time period and prevalence rates (percentage of patients suffering from late side effects at certain time points).

Rectal doses in this study were on average (± one standard deviation) 65 ± 11 Gy D2cc (median 65 Gy), 69 ± 13 Gy D1cc (median 68 Gy), 82 ± 33 Gy D0.1cc (median 77 Gy). These doses are reasonably low and few late effects are expected, especially since the D1cc and D0.1cc values are also towards the lower end of published results. Still, this patient population exhibited grade 1 + 2 rectal bleeding rates of 8% and 6 patients (almost 3%) with grade 3 + 4 rectal bleeding. The actuarial incidence rates for all rectal side effects of all grades were 16% at 3 years and 19% at 5 years follow up, but diminished to 9% and 2% prevalence at 3 and 5 years respectively.

Bladder doses were on average (± one standard deviation) 90 ± 19 Gy D2cc (median 86 Gy), 101 ± 27 Gy D1cc (median 94 Gy), 142 ± 66 Gy D0.1cc (median 118 Gy). Again, these doses correspond well with other published data and are not deemed to be in the high dose category. Of the late side effects, urinary incontinence was most prevalent at rates of 11.6% grade 1 + 2 and 5 patients (2.2%) grade 3. Increased urinary frequency was 4.9% for grade 1 + 2 and 2 patients (almost 1%) grade 4. Incidence rates for

bladder morbidity were 18 and 28% at 3 and 5 years respectively, while the prevalence rates were 18 and 21% respectively.

The fact that severe side effects are seen in these studies is somewhat cumbersome, especially since IGABT results in increased rates of long term survivors. This creates an opportunity for the manifestation of complications over long time periods such as the bladder with a later onset of complication and prolonged healing time compared to rectum. There is thus a requirement to improve the predictability of late complications by addressing amongst others, the accuracy of dose determination when EBRT and BT are combined and to use suitable constraint criteria for treatment planning.

Late grade 3 complications of more than 10% can be found even if adaptive brachytherapy is performed [156] and if the number of imaging fractions are reduced to reduce the workload for such procedures, substantial variations can occur in fractionated IGABT and Nesvacil et al. [157] showed that the impact of these variations are higher close to clinical threshold levels. They concluded that the treatment approach has to balance uncertainties for individual cases against the use of repetitive imaging, adaptive planning and dose delivery.

For the rectum, a dose volume effect has been reported by 2 groups indicating that a D2cc above 75 Gy results in significantly more late side effects, in particular rectal bleeding [111, 154, 158]. For bladder and sigmoid, little clinical evidence has been provided so far for any correlation. However, in the Vienna series [116] on IGABT, it is remarkable that in parallel to a dose escalation by 9 Gy to the HR-CTV (81-90 Gy) a decrease in side effects grade >3 was observed from 10% to 2% at 3 years taking into account certain dose volume constraints for rectum, sigmoid, and bladder in the second period with full implementation of IGABT.

1.5. Uncertainties in treatment

The uncertainties in source calibration and dose calculations fall outside the scope of this study. They are named here for completeness' sake. The same applies to applicator reconstruction and the effect they might have on the dose distribution as well as geometrical uncertainties of source positioning and image artefacts.

1.5.1. Dosimetric Uncertainties

Of critical importance in IGABT is the calculation of accumulated dose. Tanderup et al. [65] has pointed out that DVH parameter-based dose accumulation is one of the major limitations in the current methods of total dose determination. Current recommendations

are to perform dose accumulation across several fractions by DVH addition (''worst case scenario''). The result of this simplification may be potential overestimation of dose [77]. On the other hand the experience from EBRT toxicity outcome in, for example prostate treatment, could be considered helpful when relating both techniques to the Lyman-Kutcher-Burman (LKB) model [159-160] of normal tissue complication. Georg et al [145] have warned against the misinterpretation of prostate and cervix rectal doses that have substantially different characteristics as a result of the extreme dose gradients of cervix brachytherapy applications. Careful considerations of these differences and the added descriptions of dose-volume effects in the rectum that have been derived from experience with conformal therapy for prostate cancer [161-163], may allow reliable dose comparison and calculation from multiple fractions in future. This is of utmost importance in the addition of total dose from non-uniform IGART dose distributions and IGABT non-uniform dose distributions.

To account for these differences, the non-rigid nature of organ motion and deformation could be taken into account by the application of dose warping and deformable image registration (DIR) algorithms during the optimization process, or simply to calculate accumulated dose [164-168]. Such algorithms could help to address the uncertainties in dose-volume effect assessments since volume registration can be performed for voxels irradiated by EBRT and matched with the corresponding voxel irradiated with BT. Some recent tests were performed for the first time in cervix BT in which it was shown that simple bladder DVH parameter addition performs reasonably well compared to DIR [169-170]. Such tests have not been performed for any other organs. It was mentioned that simple characterization of the dose to an organ, by 1 or 2 points on the DVH is only appropriate if the shape of the histogram is similar to the curves used for determination of the dose constraints [65]. The loading patterns used clinically should preferably not be changed drastically from the ones used in determination of the constraints. They advocate to use standard loading patterns as the starting point of any dose optimization, and to keep as close as possible to the standard loading pattern while optimizing DVH parameters. So, overestimation of OAR dose based on worst case DVH addition is one probable outcome due to the current vagueness in dose accumulation, but this questions whether studies in which dose constraints were derived suffers from the same associated vagueness. There are off course other reasons, like patient population characteristic differences, that would also play a role.

The effect of large inter-fraction deformations typically found in the sigmoid colon and sometimes the rectum, warrants the use of more reliable techniques of dose accumulation [171]. Without these reliable techniques, inter- and intra-fraction motion may additionally be responsible for the delay in establishing dose response relationships

for sigmoid [146] and differences observed for rectal toxicity [20, 64, 145, 146]. This is also of particular importance in the combination of IMRT and BT which require more detailed analyses than conventional EBRT and BT. When midline shielding is performed the problem is especially challenging since it results in significant EBRT dose gradients in the BT region.

These algorithms are not yet commercially available. Current treatment planning systems do not have adequate functionality to perform dose accumulation over several fractions, nor for combined modality treatment and thus no integrated approach for EBRT and BT exists. Such inadequacies disregard the effects of geometrical variations and their subsequent impact on dose variations, and the same is true for dose accumulation between different treatment modalities. These limitations contribute to uncertainties in the assessment of dose-volume effects and radiobiological modelling. Even with the added benefits of image guidance for treatment planning and consideration of tumour regression and OAR geometrical variations, these limitations can only be overcome with algorithms that allow accurate determination of accumulated dose, or the determination of a reliable worst case estimate of accumulated dose. Combination of such algorithms with adaptive treatment planning and re-optimization of the dose distributions could potentially increase the credibility of dose-response relationships.

Since the applicators implanted into the tumour volume define the dwell positions for dose delivery, it is critically important that the relation of the applicators to the tumour and OARs be constant during the treatment. If daily imaging is performed, the reproducibility of the implantation is not that critical as dose optimization allows recovery of the required dose distribution to some extent. However, applicator displacements can take place between insertion of applicators and treatment delivery and/or during treatment itself. It is of major importance to reduce the time between implantation of applicators, imaging and treatment by as much as possible [108, 112]. Whilst the applicators might be stable during the treatment procedure, OARs can be prone to large spatial and geometrical variations which will consequently result in deviations of the delivered from the planned dose.

1.5.2. Contouring Uncertainties

As in any form of radiotherapy, contouring has a determinant role in the outcome of treatment and this is particularly true for the CTV in IGABT [131]. Uncertainties in the CTV contour have major impact in the BT component of radiotherapy because underestimation of the CTV volume will directly impact the actual HR-CTV D90 leading to

more probable local recurrences. The EBRT component is not as sensitive due to the shallower gradients in dose reduction outside the CTV, but motion and deformation should be compensated for. Use of MRI for CTV contouring is unmatched in BT and instrumental for retaining the reliability of the proposed DVH parameters [172]. Functional imaging techniques like PET and apparent diffusion-coefficients in MRI have also been investigated to refine tumour contouring. US may also play a supporting role, while CT is often used in centres with limited MR access. Such imaging techniques are extremely useful, but should be considered as calculated risks with respect to MRI as a gold standard.

Furthermore, uncertainties in the delineation of OARs are equally as important. Spatial and geometrical variations in OARs must be accounted for during the planning process. Fixed contours over several fractions or dose points do not reflect the true nature of dose accumulation, while organ motion results in the largest uncertainties in OAR dose. In addition, intra- and inter-fraction OAR and applicator changes may occur between imaging and treatment and over the full treatment course and contributes largely to the uncertainty in the accumulated dose.

Tanderup et al. [124] summarizes that physics uncertainties related to dosimetry and geometry are in general more limited as compared to the pronounced clinical uncertainties related to contouring and organ motion. Contouring is by far the largest contributor to uncertainties for targets, whereas organ motion has the largest impact on uncertainties in OARs.

1.5.3. Radiobiological Uncertainties

The validity of the LQ model has been questioned in the modelling of high doses per fraction in radiosurgery [173] while others strongly support the use of the model in determining iso-effective doses at large dose per fraction [174]. Standard parameters for the model have now been accepted by the Gyn GEC-ESTRO society and have provided clear comparative dose ranges between different institutes [76,77, 5, 78, 116-117, 119, 120-121]. There are some unexpected reports of α/β ratios for the rectum [175], but overall clinical outcome and reported EQD2 values correlate reasonably. Repair half-times are not very well known, which may have inadvertent consequences especially if a therapeutic gain is expected on the basis of an assumed difference in repair half-times between tumour and normal tissue.

Clearance of irreparably damaged tumour cells have been described by cell clearance constants derived from clinical studies [176, 177]. Similarly, loss of tumour control per day for prolonged treatments has also been described [149-150, 151]. The importance

of accelerated repopulation has also been shown and values for the onset of this effect have been expressed in days, while the loss in dose due to this effect has been well documented [178, 179]. Uncertainties in the exact values of these parameters are probably not that critical since they are mostly used for comparative purposes between different institutions. However, when they are used in the comparison of different treatment plans for an individual, their role diminishes as calculated doses will describe relative differences. The GEC-ESTRO and ABS recommendations are to use the LQ model to calculate the total dose in equivalent dose in 2-Gy fractions (EQD2) with the $\alpha/\beta = 10$ for tumours and 3 Gy for late responding OARs, while the repair half-time of 1.5 hours is acceptable in the case of LDR and PDR.

Brachytherapy treatment is completed in very few fractions compared to many in EBRT. This short BT component necessitates effective and calculated dose delivery in each of the BT fractions. When BT is limited to fewer fractions, the consequence might be that the radiobiological advantage of fractionation diminishes as less opportunity for optimization and adaptation of the dose can be performed, while more fractions put more strain on the resources available for BT treatment.

1.6. Aim

The aim of this study was to establish a suitable solution for dose accumulation in multimodality radiotherapy treatment of cervix cancer by way of the equivalent uniform dose (EUD). Once established, further objectives were to implement and verify treatment planning techniques based on EUD prescription and treatment evaluation for image guided adaptive brachytherapy and image guided adaptive radiotherapy. Additionally, fractionation effects in both modalities were exploited through biological optimization of treatment plans to escalate tumour dose.

1.7. References

1. http://globocan.iarc.fr/Pages/fact_sheets_cancer.aspx accessed 23-04-2014

2. International Agency for Research on Cancer (IARC). Globocan 2014. Cancer incidence, mortality and prevalence worldwide in 2012. Available at: http://www.iarc.fr/en/media-centre/pr/2013/pdfs/pr223_E.pdf. Accessed 23 April 2014.

3. Richter K, Dreyer G. Paradigm shift needed for cervical cancer: HPV infection is the real epidemic. S Afr Med J. 2013;103:290-292.

4. Lindegaard JC, Fokdal LU, Nielsen SK, Juul-Christensen J, Tanderup K. MRI-guided adaptive radiotherapy in locally advanced cervical cancer from a Nordic perspective. Acta Oncol 2013;52:1510-1519.

5. Jakobsen A. External radiation of cervix cancer with a concomitant boost. Int J Gynecol Cancer 2004;14(S1):11–12.

6. Martinez-Monge R, Gaztanaga M, Aramendia J, Cambeiro M, Arbea L, Espinos J, Aristu J, Jurado M. A Phase II trial of less than 7 weeks of concomitant Cisplatin-Paclitaxel chemo-radiation in locally advanced cervical cancer. Int J Gynecol Cancer 2010;20:133-140.

7. Kang H, Shin K, Park S, Kim J. 3D CT-based high-dose-rate brachytherapy for cervical cancer: clinical impact on late rectal bleeding and local control. Radiother Oncol 2010;97:507–513.

8. Tharavichitkul E, Chakrabandhu S, Wanwilairat S, Tippanya D, Nobnop W, Pukanhaphan N, Galalae RM, Chitapanarux I. Intermediate-term results of image-guided brachytherapy and high-technology external beam radiotherapy in cervical cancer: Chiang Mai University experience. Gynecol Oncol 2013;130:81-85.

9. Kato S, Ohno T, Thepamonkhol K, Chansilpa Y, Cao J, Xu X, et al. Long-term follow-up results of a multi-institutional phase 2 study of concurrent chemo-radiation therapy for locally advanced cervical cancer in East and Southeast Asia. Int J Radiat Oncol Biol Phys 2013;87:100-105.

10. Eifel P, Winter K, Morris M, Levenback C, Grigsby P, Cooper J, Rotman M, Gershenson D, Mutch D. Pelvic irradiation with concurrent chemotherapy versus pelvic and para-Aortic irradiation for high-risk cervical cancer: An update of Radiation Therapy Oncology Group Trial (RTOG) 90-01. J Clin Oncol 2004;22:872-880.

11. Paterson R. The treatment of malignant disease by radium and x-rays. Edward Arnold, London 1948.

12. Paterson R, Parker H. A dosage system for gamma ray therapy. Br J Radiol 1934;VII:592.

13. Lamarque P, Coliez R, Les cancers des organes génitaux de la femme. Electroradiothérapie, Delheim, L., Ed. (Masson, Paris), 1951.

14. ICRU. International Commission on Radiation Units and Measurements. ICRU report 38: Dose and volume specification for reporting intracavitary therapy in gynaecology. Bethesda: ICRU;1985.

15. Schmid M, Franckena M, Kirchheiner K, Strudza A, Georg P, Dörr W, Pötter R. Distant metastasis in patients with cervical cancer after primary radiotherapy with or without chemotherapy and image guided adaptive brachytherapy. Gynecol Oncol 2014, http://dx.doi.org/10.1016/j.ygyno.2014.02.004

16. Hagen B, Skjeldestad FE, Halvorsen T, Strickert T, Tingulstad S, Lorenz E, Onsrud M. Primary treatment of cervical carcinoma. Acta Obstet Gyn Scan 2000;79:1093-1099.

17. Downinga A, Mikeljevic J, Haward B, Forman D. Variation in the treatment of cervical cancer patients and the effect of consultant workload on survival: a population-based study. Eur J Cancer 2007;15:363-370.

18. Denton A, Bond S, Matthews S, Bentzen SM, Maher EJ; UK Link Gynaecology-Oncology Group. National audit of the management and outcome of carcinoma of the cervix treated with radiotherapy in 1993. Clin Oncol 2000;12:347-353.

19. ICRU. International Commission on Radiation Units and Measurements. ICRU report 50: Prescribing, recording, reporting, photon beam therapy. Washington, DC: 1994.

20. Nomden C, de Leeuw A, Roesink J, Tersteeg R, Moerland M, Witteveen P, Schreuder H, van Dorst E, Jürgenliemk-Schulz I. Clinical outcome and dosimetric parameters of chemo-radiation including MRI guided adaptive brachytherapy with tandem-ovoid applicators for cervical cancer patients: a single institution experience. Radiother Oncol 2013;107:69-74.

21. Wang JZ, Mayr NA, Zhang D, Li K, Grecula JC, Montebello JF, Lo SS, Yuh WT. Sequential magnetic resonance imaging of cervical cancer: the predictive value of

absolute tumour volume and regression ratio measured before, during, and after radiation therapy. Cancer 2010;116:5093-5101.

22. Petereit DG, Pearcey R. Literature analysis of high dose rate brachytherapy fractionation schedules in the treatment of cervical cancer: is there an optimal fractionation schedule? Int J Radiat Oncol Biol Phys 1999;43:359-366.

23. Khosla D, Patel F, Rai B, Chakraborty S, Oinam A, Sharma S, Dose escalation by Intensity-modulated Radiotherapy boost after whole pelvic radiotherapy in postoperative patients of carcinoma cervix with residual disease. Clin Onc 2013;25:e1-6.

24. Kidd EA, Siegel BA, Dehdashti F, Rader JS, Mutic S, Mutch DG, Powell MA, Grigsby PW. Clinical outcomes of definitive intensity modulated radiation therapy with fluorodeoxyglucose-positron emission tomography simulation in patients with locally advanced cervical cancer. Int J Radiat Oncol Biol Phys 2009;77:1085-91.

25. Alevronta E, Lind H, Al-Abany M, Waldenstrom A, Olsson C, Dunberger G, Mavroidis P, Nyberg T, Johansson KA, Åvall-Lundqvist E, Steineck G, Lind BK. Dose response relationships for an atomized symptom of fecal incontinence after gynaecological radiotherapy. Acta Oncol 2013;52:719-26.

26. Tanderup K, Eifel PJ, Yashar CM, Pötter R, Grigsby PW. Curative Radiation Therapy for Locally Advanced Cervical Cancer: Brachytherapy Is NOT Optional. Int J Radiat Oncol Biol Phys 2014;88:537-539

27. Georg D, Kirisits C, Hillbrand M, Dimopoulos J, Pötter R. Image-guided radiotherapy for cervix cancer: High-tech external beam therapy versus high-tech brachytherapy. Int J Radiat Oncol Biol Phys 2008;71:1272–1278.

28. Oh S, Stewart J, Moseley J, Kelly V, Lim K, Xie J, Fyles A, Brock K, Lundin A, Rehbinder H, Milosevic M, Jaffray D, Cho YB. Hybrid adaptive radiotherapy with on-line MRI in cervix cancer IMRT. Radiother Oncol 2014;110:323-328.

29. Hanks G, Kerring D, Kramer S. Patterns of care outcome studies. Results of the national practice in cancer of the cervix. Cancer 1983;51:959-967.

30. Coia L, Won M, Lanciano R, Marcial VA, Martz K, Hanks G. The Patterns of Care Outcome Study for cancer of the uterine cervix. Results of the Second National Practice Survey. Cancer 1990;66:2451-2456.

31. Nag S, Erickson B, Thomadsen B, Orton C, Demanes J, Petereit D. For the American Brachytherapy Society. The American Brachytherapy Society recommendations

for high-dose-rate brachytherapy for carcinoma of the cervix. Int J Radiat Oncol Biol Phys 2000;48:201–211.

32. Chen S, Liang J, Yeh L, Yang S, Shiau A, Lin F. Comparative study of reference points by dosimetric analyses for late complications after uniform external radiotherapy and high-dose-rate brachytherapy for cervical cancer. Int J Radiat Oncol Biol Phys 2004;60:663–671.

33. Dale R, Sinclair J: Radiobiological calculations in routine radiotherapy. In Radiobiological Modelling in Radiation Oncology. Edited by Dale R, Jones B. London: British Institute of Radiology; 2007:158–168.

34. Dale RG. The application of the linear-quadratic dose effect equation to fractional and protracted radiotherapy. Br J Radiol 1985;58:515-528.

35. Jones B. Toxicity after cervical cancer treatment using radiotherapy and chemotherapy. Clin Oncol (R Coll Radiol) 2009;21:56-63.

36. Koh WY, Lim K, Tey J, Lee K, Lim G, Choo B. Outcome of 6 fractions of 5.3 Gray HDR brachytherapy in combination with external beam radiotherapy for treatment of cervical cancer. Gynecol Oncol 2013;131:93–98.

37. Ota T, Takeshima N, Tabata T, Hasumi K, Takizawa K. Treatment of squamous cell carcinoma of the uterine cervix with radiation therapy alone: long-term survival, late complications, and incidence of second cancers. Br J Cancer 2007;97:1058–1062.

38. Serkies K, Dziadziuszko R, Jassem J. Continuous 7-days-a-week external beam irradiation in locally advanced cervical cancer: Final results of the phase I/II study. Int J Radiat Oncol Biol Phys 2012;82:1256–1261.

39. Kim Y, Kim J, Ahn S, Lee S, Shin S, Nam J. High-dose extended-field irradiation and high-dose-rate brachytherapy with concurrent chemotherapy for cervical cancer with positive para-aortic lymph nodes. Int J Radiat Oncol Biol Phys. 2009;74:1522–1528.

40. Hellebust TP, Kristensen GB, Olsen DR. Late effects after radiotherapy for locally advanced cervical cancer: comparison of two brachytherapy schedules and effect of dose delivered weekly. Int J Radiat Oncol Biol Phys. 2010;76:713-718.

41. Katz A, Eifel P. Quantification of intracavitary brachytherapy parameters and correlation with outcome in patients with carcinoma of the cervix. Int J Radiat Oncol Biol Phys 2000;48:1417–1425.

42. Malyapa RS, Mutic S, Low DA, Zoberi I, Bosch WR, Laforest R, Miller TR, Grigsby PW. Physiologic FDG-PET three-dimensional brachytherapy treatment planning for cervical cancer. Int J Radiat Oncol Biol Phys 2002;54:1140-1146

43. Shin KH, Kim TH, Cho JK, et al. CT-guided intracavitary radiotherapy for cervical cancer: Comparison of conventional point A plan with clinical target volume-based three-dimensional plan using dose-volume parameters. Int J Radiat Oncol Biol Phys 2006;64:197-204.

44. Schoeppel SL, LaVigne ML, Martel MK, McShan DL, Fraass BA, Roberts JA. Three dimensional treatment planning of intracavitary gynecologic implants: Analysis of ten cases and implications for dose specification. Int J Radiat Oncol Biol Phys 1994;28:277–283.

45. Van den Bergh F, Meertens H, Moonen L, van Bunningen B, Blom A. The use of a transverse CT image for the estimation of the dose given to the rectum in intracavitary brachytherapy for carcinoma of the cervix. Radiother Oncol 1998;47:85–90.

46. Koom WS, Sohn DK, Kim JY, Kim JW, Shin KH, Yoon SM, Kim DY, Yoon M, Shin D, Park SY, Cho KH. Computed tomography-based high-dose-rate intracavitary brachytherapy for uterine cervical cancer: preliminary demonstration of correlation between dose-volume parameters and rectal mucosal changes observed by flexible sigmoidoscopy. Int J Radiat Oncol Biol Phys 2007;68:1446-1454.

47. Fellner C, Potter R, Knocke TH, Wambersie A. Comparison of radiography- and computed tomography-based treatment planning in cervix cancer in brachytherapy with specific attention to some quality assurance aspects. Radiother Oncol 2001;58:53–62.

48. Wachter-Gerstner N, Wachter S, Reinstadler E, Fellner C, Knocke TH, Wambersie A, Pötter R.Bladder and rectum dose defined from MRI based treatment planning for cervix cancer brachytherapy: Comparison of dose-volume histograms for organ contours and organ wall, comparison with ICRU rectum and bladder reference point. Radiother Oncol 2003;68:269–276.

49. Sun LM, Huang EY, Ko SF, Wang CJ, Leung SW, Lin H, Wu JM, Wu IH, Lee SP. Computer tomography assisted three-dimensional technique to assess rectal and bladder wall dose in intracavitary brachytherapy for uterine cervical cancer. Radiother Oncol 2004;71:333–337.

50. Olszewska A, Saarnak A, de Boer R, van Bunningen B, Steggerda M. Comparison of dose-volume histograms and dose-wall histograms of the rectum of patients treated with intracavitary brachytherapy. Radiother Oncol 2001;61:83-85.

51. Cheng J, Peng L, Chen Y, Huang D, Wu J, Jian J. Unique role of proximal rectal dose in later rectal complications for patients with cervical cancer undergoing high-dose-rate intracavitary brachytherapy. Int J Radiat Oncol Biol Phys 2003;57:1010-1018.

52. Datta N, Basu R, Das K, Rajasekar D, Pandey C, Ayyagari S. Problems in reporting doses and volumes during multiple high-dose-rate intracavitary brachytherapy for carcinoma cervix as per ICRU Report 38: a comparative study using flexible and rigid applicators. Gynecol Oncol 2003;91:285-292.

53. Kim RY, Pareek P. Radiography-based treatment planning compared with computed tomography (CT)-based treatment planning for intracavitary brachytherapy in cancer of the cervix: analysis of dose–volume histograms. Brachytherapy 2003;2:200–206.

54. Kim R, Shen S, Duan J. Image-based three-dimensional treatment planning of intracavitary brachytherapy for cancer of the cervix: Dose-volume histograms of the bladder, rectum, sigmoid colon, and small bowel. Brachytherapy 2007;6:187-194.

55. Jürgenliemk-Schulz I, Tersteeg R, Roesink J, Bijmolt S, Nomden C, Moerland M, de Leeuw A. MRI-guided treatment-planning optimisation in intracavitary or combined intracavitary/interstitial PDR brachytherapy using tandem ovoid applicators in locally advanced cervical cancer. Radiother Oncol 2009;93:322-330.

56. Barillot I, Horiot J, Maingon P, et al. Maximum and mean bladder dose defined from ultrasonography. Comparison with the ICRU reference in gynecological brachytherapy. Radiother Oncol 1994;30:231–238.

57. Davidson M, Yuen J, D'Souza D, Batchelar D. Image-guided cervix high-dose-rate brachytherapy treatment planning: Does custom computed tomography planning for each insertion provide better conformal avoidance of organs at risk? Brachytherapy 2008;7:37-42.

58. Erickson B. The sculpted pear: An unfinished brachytherapy tale. Brachytherapy 2003;2:189–199.

59. Stuecklschweiger GF, Arian-Schad KS, Poier E, Poschauko J, Hackl A. Bladder and rectal dose of gynaecologic high-dose-rate implants: comparison of orthogonal

radiographic measurements with in vivo and CT-assisted measurements. Radiology 1991;181:889-894.

60. Kapp K, Stuecklschweiger GF, Kapp DS, Hackl AG. Dosimetry of intracavitary placements for uterine and cervical carcinoma: Results of orthogonal film, TLD, and CT-assisted techniques. Radiother Oncol 1992;24:137-146.

61. Pelloski C, Palmer M, Chronowski G, Jhingran A, Horton J, Eifel PJ. Comparison between CT-based volumetric calculations and ICRU reference-point estimates of radiation doses delivered to the bladder and rectum during intracavitary brachytherapy for cervical cancer. Int J Radiat Oncol Biol Phys 2005;62:131-137.

62. Gao M, Albuquerque K, Chi A, Rusu I. 3D CT based dose assessment of 2D plans using GEC-ESTRO guidelines for cervical cancer brachytherapy. Brachytherapy 2010;9:55-60.

63. Logsdon MD, Eifel PJ. Figo IIIB squamous cell carcinoma of the cervix: an analysis of prognostic factors emphasizing the balance between external beam and intracavitary radiation therapy. Int J Radiat Oncol Biol Phys 1999;43:763-775.

64. Sood BM, Gorla GR, Garg M, Anderson PS, Fields AL, Runowicz CD, Goldberg GL, Vikram B. Extended-field radiotherapy and high-dose-rate brachytherapy in carcinoma of the uterine cervix: clinical experience with and without concomitant chemotherapy. Cancer 2003;97:1781-1788.

65. Tanderup K , Georg D , Pötter R , Kirisits C , Grau C, Lindegaard JC . Adaptive management of cervical cancer radiotherapy. Sem Radiat Oncol 2010;20:121–129.

66. Taylor A, Powell M. Conformal and Intensity-modulated Radiotherapy for Cervical Cancer. Clin Oncol 2008;20:417-425.

67. Stroom JC, de Boer HC, Huizenga H, Visser AG. Inclusion of geometrical uncertainties in radiotherapy treatment planning by means of coverage probability. Int J Radiat Oncol Biol Phys. 1999;43:905-919.

68. Kerkhof EM, Raaymakers BW, van der Heide UA, et al: Online MRI guidance for healthy tissue sparing in patients with cervical cancer: An IMRT planning study. Radiother Oncol 2008;88:241-249.

69. Lei X, Qian CY, Qing Y, Zhao KW, Yang ZZ, Dai N, Zhong ZY, Tang C, Li Z, Gu XQ, Zhou Q, Feng Y, Xiong YL, Shan JL, Wang D. Californium-252 brachytherapy combined

with external-beam radiotherapy for cervical cancer: long-term treatment results. Int J Radiat Oncol Biol Phys 2011;81:1264-1270.

70. Gerbaulet A, Pötter R, Haie-Meder C. Cervix Cancer. In: Gerbaulet A, Pötter R, Mazeron JJ et al., editors. GEC ESTRO handbook of brachytherapy. ESTRO Brussels;2002. p. 301–63.

71. Rose P, Bundy B, Watkins E, Thigpen J, Deppe G, Maiman M, et al. Concurrent cisplatin-based radiotherapy and chemotherapy for locally advanced cervical cancer. New Engl J Med 1999;340:1144–1153.

72. Dimopoulos J, Schirl G, Baldinger A, Helbich T, Pötter R. MRI assessment of cervical cancer for adaptive radiotherapy. Strahlenther Onkol 2009;185:282–287.

73. Mayr N, Wang J, Lo S, Zhang D, Grecula J, Lu L, Montebello J, Fowler J, Yuh W. Translating response during therapy into ultimate treatment outcome: A personalized 4-dimensional MRI tumour volumetric regression approach in cervical cancer. Int J Radiat Oncol Biol Phys 2010;76:719–727.

74. Schmid MP, Mansmann B, Federico M, Dimopoulos J, Georg P, Fidarova E, Dörr W, Pötter R. Residual tumour volumes and grey zones after external beam radiotherapy (with or without chemotherapy) in cervical cancer patients. A low-field MRI study. Strahlenther Onkol. 2013;189:238-244.

75. Pötter R. Vienna method. In: Gerbaulet A, Pötter R, Mazeron JJ et al., editors. GEC ESTRO handbook of brachytherapy. ESTRO Brussels;2002. p. 331–338.

76. Haie-Meder C, Pötter R, Van Limbergen E, et al: Recommendations from Gynecological (GYN) GEC-ESTRO Working Group (I): concepts and terms in 3D image based 3D treatment planning in cervix cancer brachytherapy with emphasis on MRI assessment of GTV and CTV. Radiother Oncol 2005;74:235–245.

77. Pötter R, Haie-Meder C, Van Limbergen E, Barillot I, De Brabandere M, Dimopoulos J, Dumas I, Erickson B, Lang S, Nulens A, Petrow P, Rownd J, Kirisits C; GEC ESTRO Working Group. Recommendations from gynaecological (GYN) GEC ESTRO working group (II): Concepts and terms in 3D image-based treatment planning in cervix cancer brachytherapy— 3D dose volume parameters and aspects of 3D image-based anatomy, radiation physics, radiobiology. Radiother Oncol 2006;78:67–77.

78. Pötter R, Dimopoulos J, Georg P, Lang S, Waldhausl C, Wachter-Gerstner N, Weitmann H, Reinthaller A, Knocke TH, Wachter S, Kirisits C Clinical impact of MRI

assisted dose volume adaptation and dose escalation in brachytherapy of locally advanced cervix cancer. Radiother Oncol 2007;83:148–155.

79. Mundt AJ, Lujan AE, Rotmensch J, Waggoner SE, Yamada SD, Fleming G, Roeske JC. Intensity-modulated whole pelvic radiotherapy in women with gynecologic malignancies. Int J Radiat Oncol Biol Phys 2002;52:1330-1337.

80. Brixey CJ, Roeske JC, Lujan AE, Yamada SD, Rotmensch J, Mundt AJ. Impact of intensity-modulated radiotherapy on acute hematologic toxicity in women with gynecologic malignancies. Int J Radiat Oncol Biol Phys 2002;54:1388-1396.

81. Chen MF, Tseng CJ, Tseng CC, Kuo YC, Yu CY, Chen WC. Clinical outcome in posthysterectomy cervical cancer patients treated with concurrent Cisplatin and intensity-modulated pelvic radiotherapy: comparison with conventional radiotherapy. Int J Radiat Oncol Biol Phys 2007;67:1438-1444.

82. Lujan AE, Mundt AJ, Yamada SD, Rotmensch J, Roeske JC. Intensity-modulated radiotherapy as a means of reducing dose to bone marrow in gynecologic patients receiving whole pelvic radiotherapy. Int J Radiat Oncol Biol Phys 2003;57:516-521.

83. Taylor A, Powell ME: An assessment of interfractional uterine and cervical motion: Implications for radiotherapy target volume definition in gynaecological cancer. Radiother Oncol 2008;88:250-257.

84. Beadle BM, Jhingran A, Salehpour M, Sam M, Iyer RB, Eifel PJ. Cervix regression and motion during the course of external beam chemo-radiation for cervical cancer. Int J Radiat Oncol Biol Phys 2009;73:235-241.

85. Chan P, Dinniwell R, Haider MA, Cho YB, Jaffray D, Lockwood G, Levin W, Manchul L, Fyles A, Milosevic M. Inter- and intrafractional tumour and organ movement in patients with cervical cancer undergoing radiotherapy: A cinematic-MRI point-of-interest study. Int J Radiat Oncol Biol Phys 2008;70:1507-1515.

86. Baum C, Alber M, Birkner M, Nüsslin F. Robust treatment planning for intensity modulated radiotherapy of prostate cancer based on coverage probabilities. Radiother Oncol 2006;78:27-35.

87. Hysing LB, Söhn M, Muren LP, Alber M. A coverage probability based method to estimate patient-specific small bowel planning volumes for use in radiotherapy. Radiother Oncol 2011;100:407-411.

88. Grégoire V, Jeraj R, Lee JA, O'Sullivan B. Radiotherapy for head and neck tumours in 2012 and beyond: conformal, tailored, and adaptive? Lancet Oncol 2012;13:e292-300.

89. Schefter T, Kavanagh BD, Wu Q, Tong S, Newman F, McCourt S, Arnfield M, Benedict S, Mohan R. Technical considerations in the application of intensity-modulated radiotherapy as a concomitant integrated boost for locally-advanced cervix cancer. Med Dosim 2002;27:177-184.

90. Laursen L, Elstrøm UV, Vestergaard A, Muren LP, Petersen JB, Lindegaard JC, Grau C, Tanderup K. Residual rotational set-up errors after daily cone-beam CT image guided radiotherapy of locally advanced cervical cancer. Radiother Oncol 2012;105:220-225.

91. Mock U, Dieckmann K, Wolff U, Knocke TH, Pötter R. Portal imaging based definition of the planning target volume during pelvic irradiation for gynecological malignancies. Int J Radiat Oncol Biol Phys 1999;45:227-232.

92. Stroom JC, Olofsen-van Acht MJ, Quint S, Seven M, de Hoog M, Creutzberg CL, de Boer HC, Visser AG. On-line set-up corrections during radiotherapy of patients with gynecologic tumours. Int J Radiat Oncol Biol Phys 2000;46:499-506.

93. Creutzberg CL, Althof VG, de Hoog MD, Visser AG, Huizenga H, Wijnmaalen A, Levendag PC. A quality control study of the accuracy of patient positioning in irradiation of pelvic fields. Int J Radiat Oncol Biol Phys 1996;34:697-708.

94. van de Bunt L, van der Heide UA, Ketelaars M, de Kort GA, Jürgenliemk-Schulz IM. Conventional, conformal, and intensity-modulated radiation therapy treatment planning of external beam radiotherapy for cervical cancer: the impact of tumour regression. Int J Radiat Oncol Biol Phys 2006;64:189-196.

95. Han Y, Shin EH, Huh SJ, Lee JE, Park W. Interfractional dose variation during intensity-modulated radiation therapy for cervical cancer assessed by weekly CT evaluation. Int J Radiat Oncol Biol Phys 2006;65:617-623.

96. Raaymakers BW, Lagendijk JJ, Overweg J, Kok JG, Raaijmakers AJ, Kerkhof EM, van der Put RW, Meijsing I, Crijns SP, Benedosso F, van Vulpen M, de Graaff CH, Allen J, Brown KJ. Integrating a 1.5 T MRI scanner with a 6 MV accelerator: Proof of concept. Phys Med Biol 2009;54:N229-N237.

97. Reducing uncertainties about the effects of chemo-radiotherapy for cervical cancer: individual patient data meta-analysis. Cochrane Database Syst Rev. 2010 Jan 20;(1):CD008285.

98. Witte MG, van der Geer J, Schneider C, Lebesque JV, Alber M, van Herk M. IMRT optimization including random and systematic geometric errors based on the expectation of TCP and NTCP. Med Phys 2007;34:3544-3555.

99. Fokdal L, Tanderup K, Hokland S, Røhl S, Pedersen E, Nielsen S, Paludan M, Lindegaard J. Clinical feasibility of combined intracavitary/interstitial brachytherapy in locally advanced cervical cancer employing MRI with a tandem/ring applicator in situ and virtual preplanning of the interstitial component. Radiother Oncol 2013;107:63–68.

100. Nomden C, De Leeuw A, Moerland M, Roesink J, Tersteeg R, Jürgenliemk-Schulz I. Clinical use of the Utrecht applicator for combined intracavitary/interstitial brachytherapy treatment in locally advanced cervical cancer. Int J Radiat Oncol Biol Phys 2012;82:1424–1430.

101. Jürgenliemk-Schulz I, Tersteeg R, Roesink J, Bijmolt S, Nomden C, Moerland M, De Leeuw A. MRI-guided treatment-planning optimisation in intracavitary or combined intracavitary/interstitial PDR brachytherapy using tandem ovoid applicators in locally advanced cervical cancer. Radiother Oncol 2009;93:322–330.

102. Lee L, Damato A, Viswanathan A. Clinical outcomes of high-dose-rate interstitial gynecologic brachytherapy using real-time CT guidance. Brachytherapy 2013;12:303-310.

103. Tan L, Coles C, Hart C, Tait E. Clinical impact of computed tomography-based image-guided brachytherapy for cervix cancer using the tandem-ring applicator - the Addenbrooke's experience. Clin Oncol (R Coll Radiol) 2009;21:175–82.

104. Lindegaard JC, Tanderup K, Nielsen SK, Haack S, Gelineck J. MRI-guided 3D optimization significantly improves DVH parameters of pulsed-dose-rate brachytherapy in locally advanced cervical cancer. Int J Radiat Oncol Biol Phys 2008;71:756-764.

105. Jamema SV, Mahantshetty U, Tanderup K, Malvankar D, Sharma S, Engineer R, Chopra S, Shrivastava SK, Deshpande DD. Inter-application variation of dose and spatial location of D(2cm^3) volumes of OARs during MR image based cervix brachytherapy. Radiother Oncol 2013;107:58-62.

106. Mohamed S, Nielsen S, Fokdal L, Pedersen E, Lindegaard J, Tanderup K. Feasibility of applying a single treatment plan for both fractions in PDR image guided brachytherapy in cervix cancer. Radiother Oncol 2013;107:32-38.

107. Kirisits C, Lang S, Dimopoulos J, Oechs K, Georg D, Potter R. Uncertainties when using only one MRI-based treatment plan for subsequent high-dose-rate tandem and ring applications in brachytherapy of cervix cancer. Radiother Oncol 2006;81:269–275.

108. Anderson C, Lowe G, Wills R, Inchley D, Beenstock V, Bryant L, Chapman C, Hoskin PJ. Critical structure movement in cervix brachytherapy. Radiother Oncol 2013;107:39-45.

109. De Leeuw AA, Moerland MA, Nomden C, Tersteeg RH, Roesink JM, Jurgenliemk-Schulz IM. Applicator reconstruction and applicator shifts in 3D MR-based PDR brachytherapy of cervical cancer. Radiother Oncol 2009;93:341–346..

110. Hellebust TP, Dale E, Skjonsberg A, Olsen DR. Inter fraction variations in rectum and bladder volumes and dose distributions during high dose rate brachytherapy treatment of the uterine cervix investigated by repetitive CT examinations. Radiother Oncol 2001;60:273–80.

111. Georg P, Potter R, Georg D, et al. Dose effect relationship for late side effects of the rectum and urinary bladder in magnetic resonance image-guided adaptive cervix cancer brachytherapy. Int J Radiat Oncol Biol Phys 2012;82:653–657.

112. Morgia M, Cuartero J, Walsh L, Jezioranski J, Keeler K, Xie J, Massey C, Williamson D, Cho YB, Oh S, Fyles A, Milosevic M. Tumour and normal tissue dosimetry changes during MR-guided pulsed-dose-rate (PDR) brachytherapy for cervical cancer. Radiother Oncol 2013;107:46-51.

113. Dimopoulos J, Lang S, Kirisits C, Fidarova E, Berger D, Georg P, Dörr W, Pötter R. Dose–volume histogram parameters and local tumour control in magnetic resonance image–guided cervical cancer brachytherapy. Int J Radiat Oncol Biol Phys 2009;75:56–63.

114. Dimopoulos J, Pötter R, Lang S, Fidarova E, Georg P, Dörr W, Kirisits C. Dose–effect relationship for local control of cervical cancer by magnetic resonance image-guided brachytherapy. Radiother Oncol 2009;93:311–315.

115. Pötter R. Image-guided brachytherapy sets benchmarks in advanced radiotherapy. Radiother Oncol 2009;91:141-146.

116. Pötter R, Dimopoulos J. Clinical outcome of protocol based image (MRI) guided adaptive brachytherapy combined with 3D conformal radiotherapy with or without chemotherapy in patients with locally advanced cervical cancer. Radiother Oncol 2011;100:116–123.

117. Charra-Brunaud C, Harter V, Delannes M, Haie-Meder C, Quetin P, Kerr C, Castelain B, Thomas L, Peiffert D. Impact of 3D image-based PDR brachytherapy on outcome of patients treated for cervix carcinoma in France: Results of the French STIC prospective study. Radiother Oncol 2012;103:305–313.

118. Tharavichitkul E, Chakrabandhu S, Wanwilairat S, Tippanya D, Nobnop W, Pukanhaphan N, Galalae R, Chitapanarux I. Intermediate-term results of image-guided brachytherapy and high-technology external beam radiotherapy in cervical cancer: Chiang Mai University experience. Gynecol Oncol 2013;130:81–85.

119. Haie-Meder C, Chargari C, Rey A, Dumas I, Morice P, Magne N. MRI-based low dose-rate brachytherapy experience in locally advanced cervical cancer patients initially treated by concomitant chemo-radiotherapy. Radiother Oncol 2010;96:161–165.

120. Chargari C, Magne N, Dumas I, Messai T, Vicenzi L, Gillion N, et al. Physics contributions and clinical outcome with 3D-MRI-based pulsed-dose-rate intracavitary brachytherapy in cervical cancer patients . Int J Radiat Oncol Biol Phys 2009;74:133–139.

121. Wanderas AD, Sundset M, Langdal I, Danielsen S, Frykholm G, Marthinsen A. Adaptive brachytherapy of cervical cancer, comparison of conventional point A and CT based individual treatment planning. Acta Oncol 2012; 51:345–354.

122. Narayan K, van Dyk S, Bernshaw D, Rajasooriyar C, Kondalsamy- Chennakesavan S. Comparative study of LDR (Manchester system) and HDR image-guided conformal brachytherapy of cervical cancer: patterns of failure, late complications, and survival. Int J Radiat Oncol Biol Phys 2009;74:1529–1535.

123. Haie-Meder C, Chargari C, Rey A, Dumas I, Morice P, Magne N. DVH parameters and outcome for patients with early-stage cervical cancer treated with preoperative MRI-based low dose rate brachytherapy followed by surgery. Radiother Oncol 2009;93:316–321.

124. Tanderup K, Nesvacil N, Pötter R, Kirisits C. Uncertainties in image guided adaptive cervix cancer brachytherapy: impact on planning and prescription. Radiother Oncol 2013;107:1-5.

125. Fagundes H, Perez CA, Grigsby PW, Lockett MA. Distant metastases after irradiation alone in carcinoma of the uterine cervix. Int J Radiat Oncol Biol Phys 1992;24:197–204.

126. Sakurai H, Mitsuhashi N, Takahashi M, Akimoto T, Muramatsu H, Ishikawa H Imai R, Yamakawa M, Hasegawa M, Niibe H. Analysis of recurrence of squamous cell carcinoma of the uterine cervix after definitive radiation therapy alone: patterns of recurrence, latent periods, and prognosis. Int J Radiat Oncol Biol Phys 2001;50:1136–1144.

127. Park TK, Kwon JY, Kim SW, Kim SH, Kim SN, Kim GE. Patterns of treatment failure following radiotherapy with combination chemotherapy for patients with high-risk stage IIB cervical carcinoma. Int J Clin Oncol 2004;9:120–124.

128. Perez CA, Grigsby PW, Chao KS, Mutch DG, Lockett MA. Tumour size, irradiation dose, and long-term outcome of carcinoma of uterine cervix. Int J Radiat Oncol Biol Phys 1998;41:307-317.

129. Perez CA, Fox S, Lockett MA, Grigsby PW, Camel HM, Galakatos A, Kao MS, Williamson J. Impact of dose in outcome of irradiation alone in carcinoma of the uterine cervix: analysis of two different methods. Int J Radiat Oncol Biol Phys 1991;21:885-898.

130. Paley PJ, Goff BA, Minudri R, Greer BE, Tamimi HK, Koh WJ. The prognostic significance of radiation dose and residual tumour in the treatment of barrel-shaped endophytic cervical carcinoma. Gynecol Oncol 2000;76:373-379.

131. Potter R, Kirisits C, Fidarova EF, Dimopoulos JC, Berger D, Tanderup K, Lindegaard JC. Present status and future of high precision image guided adaptive brachytherapy for cervix carcinoma. Acta Oncol 2008;47:1325–1336.

132. Lindegaard J.C., Fokdal L, Nielsen SK, Rohl LL, Pedersen EM, Petersen LK, Hansen ES, Tanderup K Outcome of image guided adaptive brachytherapy in locally advanced cervical cancer patients. World congress of brachytherapy, ESTRO 2012, Volume 103 supplement 2, Page S17, OC-39.

133. Beriwal S, Kannan N, Kim H, Houser C, Mogus R, Sukumvanich P, Olawaiye A, Richard S, Kelley JL, Edwards RP, Krivak TC. Three-dimensional high dose rate intracavitary image-guided brachytherapy for the treatment of cervical cancer using a hybrid magnetic resonance imaging/computed tomography approach: feasibility and early results. Clin Oncol (R Coll Radiol) 2011;23:685-690.

134. Mahantshetty U, Swamidas J, Khanna N, Engineer R, Merchant NH, Deshpande DD, Shrivastava S. Reporting and validation of gynaecological Groupe European de Curiethérapie European Society for Therapeutic Radiology and Oncology (ESTRO) brachytherapy recommendations for MR image-based dose volume parameters and clinical outcome with high dose-rate brachytherapy in cervical cancers: a single-institution initial experience. Int J Gynecol Cancer 2011;21:1110-1116.

135. Güth U, Ella WA, Olaitan A, Hadwin RJ, Arora R, McCormack M. Total vaginal necrosis: a representative example of underreporting severe late toxic reaction after concomitant chemoradiation for cervical cancer. Int J Gynecol Cancer 2010;20:54-60.

136. Kirchheiner K, Nout R, Tanderup K, Lindegaard J, Westerveld H, Haie-Meder C, Petrič P, Mahantshetty U, Dörr W, Pötter R. Manifestation Pattern of Early-Late Vaginal Morbidity After Definitive Radiation (Chemo)Therapy and Image-Guided Adaptive Brachytherapy for Locally Advanced Cervical Cancer: An Analysis From the EMBRACE Study. Int J Radiat Oncol Biol Phys 2014;89:88-95.

137. Lei X, Qian CY, Qing Y, Zhao KW, Yang ZZ, Dai N, Zhong ZY, Tang C, Li Z, Gu XQ, Zhou Q, Feng Y, Xiong YL, Shan JL, Wang D. Californium-252 brachytherapy combined with external-beam radiotherapy for cervical cancer: long-term treatment results. Int J Radiat Oncol Biol Phys 2011;81:1264-1270.

138. Gondi V, Bentzen SM, Sklenar KL, Dunn EF, Petereit DG, Tannehill SP, Straub M, Bradley KA. Severe late toxicities following concomitant chemoradiotherapy compared to radiotherapy alone in cervical cancer: an inter-era analysis. Int J Radiat Oncol Biol Phys 2012;84:973-982.

139. Vale C, Tierney JF, Stewart LA, Brady M, Dinshaw K, Jakobsen A et al. Reducing uncertainties about the effects of chemoradiotherapy for cervical cancer: a systematic review and meta-analysis of individual patient data from 18 randomized trials. J Clin Oncol 2008;26:5802-5812.

140. Tanderup K, Nielsen SK, Nyvang GB, Pedersen EM, Røhl L, Aagaard T, Fokdal L, Lindegaard JC. From point A to the sculpted pear: MR image guidance significantly improves tumour dose and sparing of organs at risk in brachytherapy of cervical cancer. Radiother Oncol 2010;94:173-180.

141. Westerveld H, Pötter R, Berger D, Dankulchai D, Dörr W, Sora M, Pötter-Lang S, Kirisits C. Vaginal dose point reporting in cervical cancer patients treated with combined

2D/3D external beam radiotherapy and 2D/3D brachytherapy. Radiother Oncol 2013;107:99–105.

142. Lind H, Waldenström AC, Dunberger G, al-Abany M, Alevronta E, Johansson KA, Olsson C, Nyberg T, Wilderäng U, Steineck G, Åvall-Lundqvist E. Late symptoms in long-term gynaecological cancer survivors after radiation therapy: a population-based cohort study. Br J Cancer 2011;105:737-745.

143. Pinn-Bingham M, Puthawala AA, Syed AM, Sharma A, Disaia P, Berman M, Tewari KS, Randall-Whitis L, Mahmood U, Ramsinghani N, Kuo J, Chen WP, McLaren CE. Outcomes of high-dose-rate interstitial brachytherapy in the treatment of locally advanced cervical cancer: long-term results. Int J Radiat Oncol Biol Phys 2013;85:714-720.

144. Kim TH, Kim JY, Sohn DK, Kim YJ, Lee YS, Moon SH, Kim SS, Kim DY. A prospective observational study with dose volume parameters predicting rectosigmoidoscopic findings and late rectosigmoid bleeding in patients with uterine cervical cancer treated by definitive radiotherapy. Radiat Oncol 2013;8:28.

145. Georg P, Kirisits C, Goldner G, Dörr W, Hammer J, Pötzi R, Berger D, Dimopoulos J, Georg D, Pötter R. Correlation of dose-volume parameters, endoscopic and clinical rectal side effects in cervix cancer patients treated with definitive radiotherapy including MRI-based brachytherapy. Radiother Oncol 2009;91:173-180.

146. Georg P, Lang S, Dimopoulos JC, Dörr W, Sturdza AE, Berger D, Georg D, Kirisits C, Pötter R. Dose-volume histogram parameters and late side effects in magnetic resonance image-guided adaptive cervical cancer brachytherapy. Int J Radiat Oncol Biol Phys 2011;79:356-362.

147. Barker CL, Routledge JA, Farnell DJJ et al. The impact of radiotherapy late effects on quality of life in gynaecological cancer patients. Br J Cancer 2009;100:1558–1565.

148. Kirchheiner K, Nout R, Lindegaard J Petrič P, Limbergen EV, Jürgenliemk-Schulz IM, Haie-Meder C, Pötter R, Dörr W. Do clinicians and patients agree regarding symptoms? A comparison after definitive radiochemotherapy in 223 uterine cervical cancer patients. Strahlenther Onkol 2012;188:933–939.

149. Kirchheiner K, Fidarova E, Nout RA, Schmid MP, Sturdza A, Wiebe E, Kranz A, Polterauer S, Pötter R, Dörr W Radiation-induced morphological changes in the vagina. Strahlenther Onkol 2012;188:1010–1019.

150. Georg P, Boni A, Ghabuous A, Goldner G, Schmid MP, Georg D, Pötter R, Dörr W. Timecourse of late rectal- and urinary bladder side effects after MRI-guided adaptive brachytherapy for cervical cancer. Strahlenther Onkol. 2013;189:535-540.

151. Anker C, Cachoeira C, Boucher K, Rankin J, Gaffney D. Does the entire uterus need to be treated in cancer of the cervix? Role of adaptive brachytherapy. Int J Radiat Oncol Biol Phys 2010;76:704–712.

152. Nesvacil N, Tanderup K, Hellebust T, De Leeuw A, Lang S, Mohamed S, Jamema S, Anderson C, Pötter R, Kirisits C. A multicentre comparison of the dosimetric impact of inter- and intra-fractional anatomical variations in fractionated cervix cancer brachytherapy. Radiother Oncol 2013;107:20-25.

153. Levitchi M, Charra-Brunaud C, Quetin P, et al: Impact of dosimetric and clinical parameters on clinical side effects in cervix cancer patients treated with 3D pulse-dose rate intracavitary brachytherapy. Radiother Oncol 2012;103:314–321.

154. Lyman JT. Complication probability as assessed from dose-volume histograms. Radiat Res Suppl 1985;8:S13-19.

155. Burman C, Kutcher GJ, Emami B, Goitein M. Fitting of normal tissue tolerance data to an analytic function. Int J Radiat Oncol Biol Phys1991;21:123-135.

156. Pollack A, Zagars GK, Starkschall G, et al. Prostate cancer radiation dose response: Results of the M.D. Anderson phase III randomized trial. Int J Radiat Oncol Biol Phys 2002;53:1097-1105.

157. Cheung R, Tucker SL, Ye JS, et al. Characterization of rectal normal tissue complication probability after high-dose external beam radiotherapy for prostate cancer. Int J Radiat Oncol Biol Phys 2004;58:1513-1519.

158. Söhn M, Yan D, Liang J, Meldolesi E, Vargas C, Alber M. Incidence of late rectal bleeding in high-dose conformal radiotherapy of prostate cancer using equivalent uniform dose-based and dose-volume-based normal tissue complication probability models. Int J Radiat Oncol Biol Phys 2007;67:1066-1073.

159. Birkner M, Yan D, Alber M, Liang J, Nüsslin F. Adapting inverse planning to patient and organ geometrical variation: algorithm and implementation. Med Phys 2003;30:2822-2831.

160. McShan DL, Kessler ML, Vineberg K, Fraass BA. Inverse plan optimization accounting for random geometric uncertainties with a multiple instance geometry approximation (MIGA). Med Phys 2006;33:1510-1521.

161. Söhn M, Weinmann M, Alber M. Intensity-modulated radiotherapy optimization in a quasi-periodically deforming patient model. Int J Radiat Oncol Biol Phys 2009;75:906-914.

162. Yan D, Jaffray DA, Wong JW. A model to accumulate fractionated dose in a deforming organ. Int J Radiat Oncol Biol Phys 1999;44:665-75.

163. Trofimov A, Rietzel E, Lu HM, Martin B, Jiang S, Chen GT, Bortfeld T. Temporo-spatial IMRT optimization: concepts, implementation and initial results. Phys Med Biol 2005;50:2779-2798.

164. Andersen E, Muren L, Sørensen T, Noe KO, Thor M, Petersen JB, Høyer M, Bentzen L, Tanderup K. Bladder dose accumulation based on a biomechanical deformable image registration algorithm in volumetric modulated arc therapy for prostate cancer. Phys Med Biol 2012;57:7089–7100.

165. Andersen E, Noe K, Sørensen T, Nielsen SK, Fokdal L, Paludan M, Lindegaard JC, Tanderup K. Simple DVH parameter addition as compared to deformable registration for bladder dose accumulation in cervix cancer brachytherapy. Radiother Oncol 2013;107:52–57.

166. Swamidas J, Mahantshetty U, Tanderup K, Malvankar D, Sharma S, Engineer R, Chopra S, Shrivastava SK, Deshpande DD Inter-application variation of dose and spatial location of D2cm3 volumes of OARs during MR image based cervix brachytherapy. Radiother Oncol 2013;107:58–62.

167. Dimopoulos JC, Schard G, Berger D, Lang S, Goldner G, Helbich T, Pötter R. Systematic evaluation of MRI findings in different stages of treatment of cervical cancer: potential of MRI on delineation of target, pathoanatomic structures, and organs at risk. Int J Radiat Oncol Biol Phys 2006;64:1380-1388.

168. Kirkpatrick JP, Meyer JJ, Marks LB. The linear-quadratic model is inappropriate to model high dose per fraction effects in radiosurgery. Semin Radiat Oncol 2008;18:240-243.

169. Brenner DJ. The linear-quadratic model is an appropriate methodology for determining isoeffective doses at large doses per fraction. Semin Radiat Oncol 2008;18:234-239.

170. Roberts SA, Hendry JH, Swindell R, Wilkinson JM, Hunter RD. Compensation for changes in dose-rate in radical low-dose-rate brachytherapy: a radiobiological analysis of a randomised clinical trial. Radiother Oncol 2004;70:63-74.

171. Lim K, Chan P, Dinniwell R, Fyles A, Haider M, Cho YB, Jaffray D, Manchul L, Levin W, Hill RP, Milosevic M. Cervical cancer regression measured using weekly magnetic resonance imaging during fractionated radiotherapy: radiobiologic modelling and correlation with tumour hypoxia. Int J Radiat Oncol Biol Phys 2008;70:126-133.

172. Huang Z, Mayr NA, Yuh WT, Lo SS, Montebello JF, Grecula JC, Lu L, Li K, Zhang H, Gupta N, Wang JZ. Predicting outcomes in cervical cancer: a kinetic model of tumour regression during radiation therapy. Cancer Res 2010;70:463-70.

173. Gasinska A, Fowler JF, Lind BK, Urbanski K. Influence of overall treatment time and radiobiological parameters on biologically effective doses in cervical cancer patients treated with radiation therapy alone. Acta Oncol 2004;43:657-666.

174. Huang Z, Mayr NA, Gao M, Lo SS, Wang JZ, Jia G, Yuh WT. Onset time of tumour repopulation for cervical cancer: first evidence from clinical data. Int J Radiat Oncol Biol Phys 2012;84:478-484.

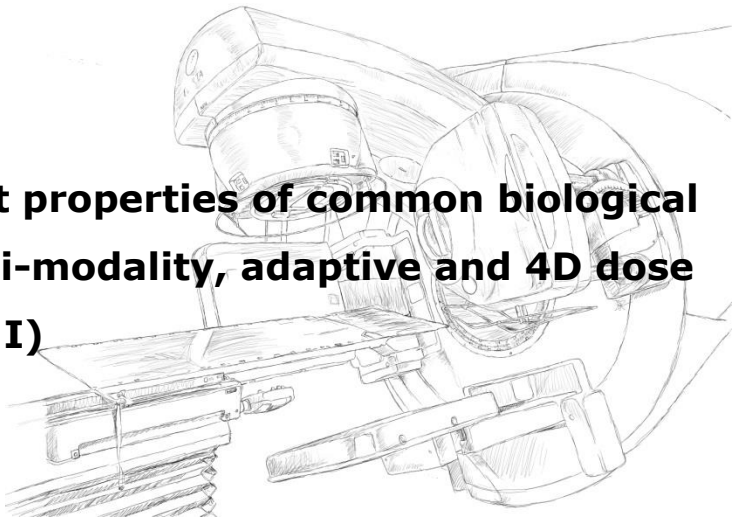

Chapter 2: On expedient properties of common biological score functions for multi-modality, adaptive and 4D dose optimization (Appendix I)

This chapter includes work published by the author – Appendix I (Sobotta et al. Phys Med Biol 2011;56:N123-129)

2.1. Introduction

The need to compute the combined effect of several dose distributions in distinct geometries arises in a number of applications. For example, some approaches to 4D IMRT optimization optimize dose simultaneously on multiple geometries [1-4] by warping the dose in each instance to a reference geometry, thereby realizing optimization in "tissue-eye-view". Also in combined modality treatment, e.g. brachytherapy and external beam therapy, the overall effect has to be computed [5]. Similar problems occur with the dose re-computation in mobile organs, e.g. prostate on daily cone beam CT [6, 7]. Since particle therapy is very sensitive to geometry changes, especially in regions with heterogeneous density, doses have to be computed on several geometries and subsequently combined [8, 9].

All of these methods require a correspondence between the volume elements (voxels) of each geometry instance to add up each dose contribution correctly. In general this requires deformable registration. Given the independently computed doses in each patient geometry, the voxel correspondence is used to warp the individual doses back to some reference geometry. In this reference geometry, the doses are accumulated and evaluated. Unfortunately, there are several issues with this approach. The computation of the deformation fields is fraught with uncertainties and difficult to verify. The computation frequently needs human surveillance and the data set may be incomplete or disturbed by artefacts. Some organs, especially bowel, are difficult to model because of variations in filling and the lack of fiducials. Incomplete knowledge of the extent of movement due to infrequent and sparse imaging may also affect the accuracy of the model. Additionally, special care must be taken to ensure energy conservation during dose warping and accumulation. Dose distributions are frequently analysed with score functions that are a sum over all volume elements of an organ. In contrast to pointwise scores, a lot of the effort that goes into correct dose accumulation is washed out in the

summation. Very often, these score functions are convex, which opens a possibility for very powerful estimations of their true value without going through the process of proper dose accumulation.

This note derives how the mathematical properties of commonly used cost functions, e.g. equivalent uniform dose (EUD) [10], can be exploited to compute boundaries of the combined effect of the dose distributions in different geometries. These boundaries are computed *without* the need for deformable registration. For the target, lower boundaries will be given, and for the critical structures upper boundaries. Thus, a worst case scenario is obtained that may be used for a quick scoring of a treatment plan at only a fraction of the cost of a full analysis. In addition to Sobotta et al [Appendix I] a Monte Carlo simulated treatment plan with simple OAR and target geometrical deformation, as well as a prostate case with interfractional movement and a 4D lung case were simulated to demonstrate the method.

2.2. Methods and Materials

Suppose *F* is a score function and let D_k be the dose distribution of the full treatment applied to the *k*th geometry instance I_k. For dose accumulation, a reference geometry I_0 is chosen. $\widetilde{D}_k$ denotes the warped dose in the reference geometry, i.e. the deformation field from I_k to I_0 applied to dose D_k. Hence, the quantity of main interest, the accumulated dose, is

$$E\left[\widetilde{D}\right] = \frac{1}{N}\sum_{k=0}^{N-1}\widetilde{D}_k \qquad \text{with} \quad \widetilde{D}_0 \equiv D_0 \tag{2.1}$$

Note that the accumulated dose is expressed as an average in (2.1). Average and sum are equivalent because the dose distribution may be rescaled by a constant factor.

Dose warping as well as dose accumulation is a linear operation and therefore the dose integral of D_k over the volume of interest equals that of $\widetilde{D}_k$. This is a direct consequence of energy and volume conservation. By virtue of this, and by way of definition

$$F(D_k) = F\left(\widetilde{D}_k\right) \tag{2.2}$$

If no deformation field is available, the single doses D_k cannot be warped back to the reference geometry, and in other words $\widetilde{D}_k$ is inaccessible. However, by virtue of *Jensen's inequality* [11] for a convex function *F*,

$$F\left(E\left[\widetilde{D}\right]\right) \leq E\left[F\left(\widetilde{D}\right)\right] = E[F(D)] \tag{2.3}$$

can be established. Conversely, for concave functions *F*, (2.3) reverses to

$$F\left(E\left[\tilde{D}\right]\right) \geq E\left[F\left(\tilde{D}\right)\right] = E[F(D)] \qquad (2.4)$$

where $E[F(D)] \equiv 1/N \sum_{k=0}^{N-1} F(D_k)$ is the sum of the score function evaluated for each original geometry instance. The equality relations in (2.3) and (2.4) are due to (2.2).

Convex functions (curved upward) are commonly associated with normal tissues or other dose-limiting objectives. Examples include maximum dose, one-sided dose-limiting quadratic penalty and EUD for serial organs [12], i.e. $f(D) = D^a$, $a \geq 1$. Note that the mean dose is also covered by the inequality because it is synonymous with the serial EUD cost function with $a = 1$. The parallel EUD [12] is an exception because it is neither convex nor concave; however, it can still be handled within the proposed framework, see below. A commonly used cost function for the target volume, the Poisson cell kill EUD [10, 12], is concave.

In practice, this means that in the case of normal tissue the score function value of the accumulated dose $\left(F\left(E\left[\tilde{D}\right]\right)\right)$ is always smaller than the sum of the score functions of the instance doses $(E[F(D)])$ (3). For the target, the EUD of the accumulated dose is always larger than the sum of the EUDs of the instance doses (2.4). Hence, using Jensen's inequality, worst case boundaries for the score function of the accumulated dose can be derived without the need for a deformable registration model.

Note that EUD and other cost functions are volume averages and are therefore insensitive to changes of the absolute volume of some organ or tumour. Still, uncertainties in delineation or volume shrinkage can introduce errors into the above inequalities. In order to maintain the validity of the inequality, it is sufficient to formulate a worst case. The EUD for OARs should be calculated using the organ wall only. The above approximations only hold if the organ volume does not change. While the EUD is typically calculated relative to the entire volume of an organ, it can also be defined relative to a reference volume. For normal tissue this translates to computing the EUD relative to the volume of a geometry instance to maintain the validity of the inequality. It is equivalent to using the smallest volume of the organ of interest in any geometry instance to normalize EUD in each instance.

In case of tumour shrinkage, it is helpful to resort to the mechanistic basis of the model and it is also possible to use a common reference volume for EUD computations. Tumour EUD is derived from the initial number of clonogenic cells, which can be expressed as the mean cell density times the tumour volume. Under the assumption that no clonogenic cells are lost from the initial population by effects other than those caused by radiation,

the primary quantity cell number is preserved despite volume loss. A volume reduction then results in an increase of clonogenic cell density. For the purpose of inequality, the EUDs of different geometry instances may be added although they pertain to differently sized volumes since EUD is independent of cell density. However, if the quantity of interest were the expected number of surviving clonogens instead, the increase in cell density would have to be considered.

The parallel complication function $f(D) = (1 + (D_{tol}/D)^b)^{-1}$ is convex for doses below the dose D_{tol} and concave for doses above, i.e. it has a point of inflection at $D = D_{tol}$. In consequence, the above reasoning cannot be directly applied. However, typical prescriptions demand that large parts of the organ are kept intact; hence, most of the organ volume is irradiated with doses below D_{tol}. For this fraction of the volume, (2.3) applies, i.e. the damage is overestimated. To account for the entire volume of the parallel organ, the cost function can be convexified by linear extrapolation at the point of inflection, see figure 2.1.

Note that the above relation (2.3) is *not* valid for dose-volume constraints. Table 2.1contains an overview of the properties of commonly used score functions.

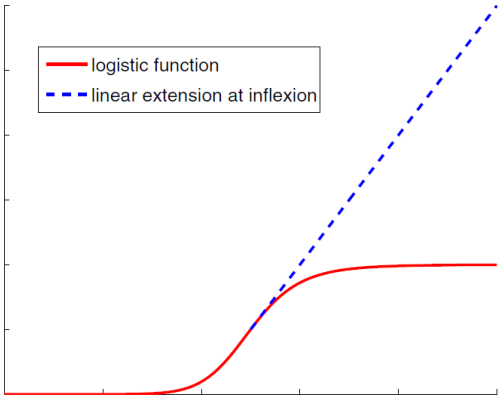

Figure 2.1. The parallel complication cost function (logistic function) is linearly extended at the inflection point to be convex on its entire support.

Table 2.1. Properties of various cost functions.

Cost function	Property
Poisson cell kill EUD	Concave
Parallel EUD	-
Generalized EUD a≥1 (Serial EUD)	Convex
Generalized EUD a≤1	Concave
Average Dose	Convex and concave
DVH Constraints	-
Maximum Dose	Convex
Quadratic Deviation Penalty	Convex

2.2.1. Monte Carlo Simulation

To test the method of determining a worst case scenario as a safe upper boundary for normal tissue and a safe lower boundary for tumours, a simple Monte Carlo simulation was performed on a square water equivalent phantom. A structure of interest (SOI) with a box shape was contoured inside the phantom. A dose distribution of a four-field box treatment plan was simulated with the DOSXYZnrc Monte Carlo code [13]. The field size was 5x5 cm^2 for all four fields and the isocenter was located in the centre of the phantom, and so was the centre of gravity of the SOI as well as the ICRU reference point to which the dose was normalized.

Figure 2.2 displays the phantom, the SOI and the isodose distributions. These isodoses were obtained by simulating 800 000 histories per beam angle of an Elekta Precise 6MV linear accelerator source model. The effect of organ motion was simulated by changing the geometry and position of the SOI through deformation, positional shifts and volume shrinkage. Since the dose per voxel and the position of each deformed/shifted SOI's corresponding voxels can be identified in the resultant DOSXYZnrc .3ddose file of the simulation, the total dose of each voxel in the SOI could be computed for various instances of deformation, shifts and shrinkage.

The SOI was deformed geometrically by dragging the original square geometry to that of a trapezium in two stages. The first stage was a small deformation and the second a larger deformation. The deformed geometry in figure 2.2c was especially selected to produce a steep dose gradient across the structure of interest, and 2.2b to a lesser extent. Considering the size

of the voxels (5 x 5 x 5 mm^3) and the volume of homogeneous dose distribution, the shape of the DVH in this instance represents a very steep change in dose per volume element which could very well be similar to the dose gradients found in brachytherapy.

Positional shifts were performed by moving the centre of gravity of the SOI in various directions. Fig 2.2 (b-h) shows these variations in SOI geometry and position. For comparison with typical cervix cancer EBRT treatment, the plan consisted of 25 fractions of 2 Gy per fraction and each of the geometries was applied over a preselected number of fractions. The SOI was considered as an OAR and a target to test the method for both convex and concave functions of dose. Where the SOI was regarded as an OAR, the dose was calculated as serial EUD with a = 8. Table 2.2 gives a summary of the number of fractions associated with each of the shape or position changes for several different combinations. The SOI was treated as a target as well by calculating the Poisson cell kill EUD (α = 0.4) for positional shifts and tumour shrinkage.

For the purpose of this study, the EUD for the OAR was calculated properly by summing the dose over all treatment fractions to the original OAR geometry. In the worst case estimate the sum of the EUDs of each treatment fraction was calculated without warping the dose per voxel back to the reference geometry. The same was done for the target.

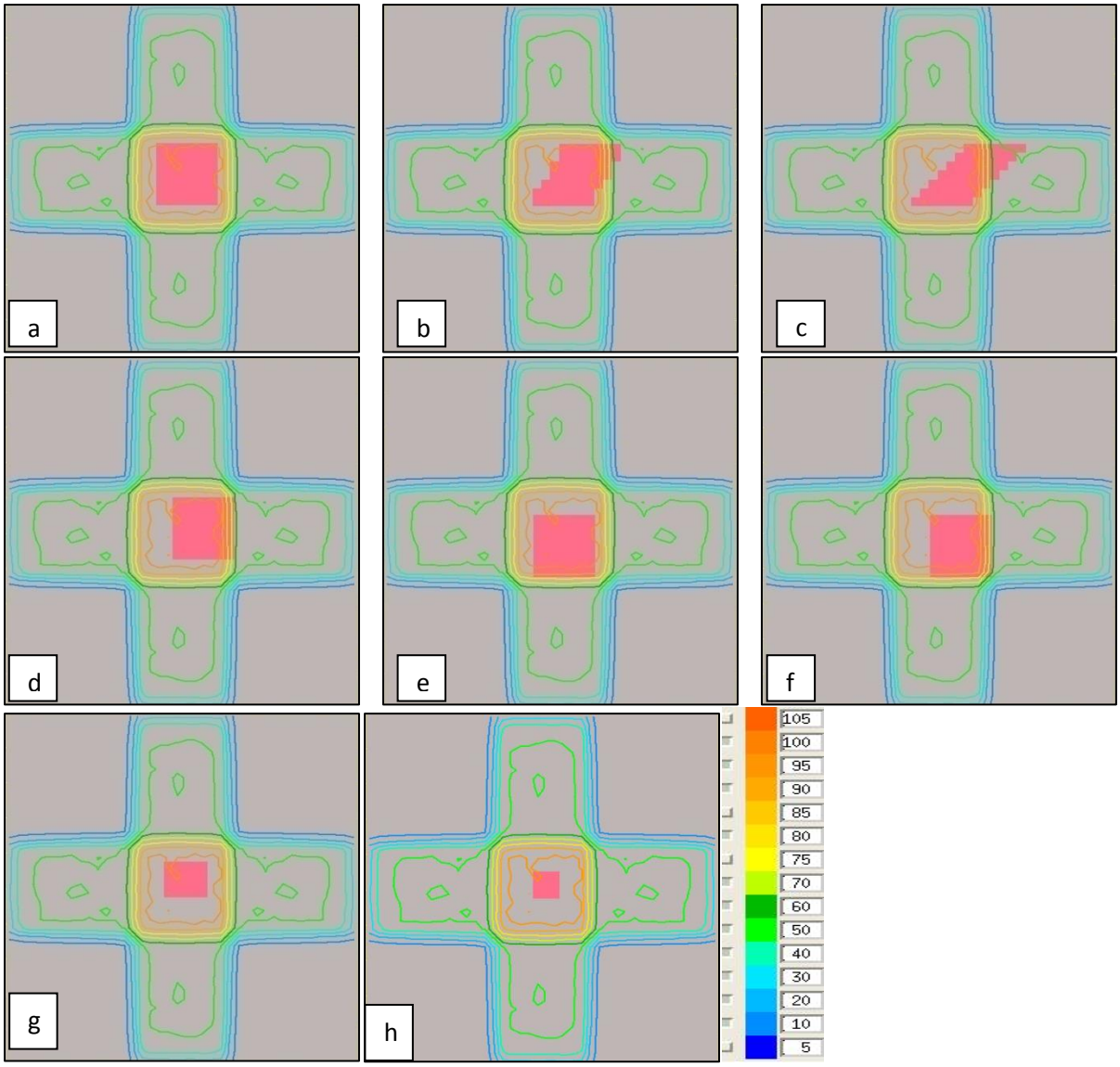

Figure 2.2: The DOSXYZnrc phantom with a square SOI in the high dose region. The deformation of the OAR was achieved by geometrical manipulation and positional changes of the SOI. The dose distribution was kept constant in all instances. The SOI variations were a) original geometry, b) small deformation, c) large deformation, d) right shift, e) downward shift, f) right + downward shift, g) small regression and h) large regression.

Table 2.2: Summary of the fractions corresponding to each SOI geometric and positional change in DOSXYZnrc.

Deformation	Example 1	Example 2	Example 3	Example 4/7	Example 5/8	Example 6/9	Example 10	Example 11	Example 12
SOI type	OAR	OAR	OAR	OAR/Target	OAR/Target	OAR/Target	Target	Target	Target
Original	8 x a	10 x a	3 x a	6 x a	9 x a	3 x a	8 x a	10 x a	3 x a
Small Deformation	8 x b	10 x b	4 x b						
Large Deformation	9 x c	5 x c	18 x c						
Sideway shift				6 x d	9 x d	4 x d			
Downward shift				6 x e	3 x e	7 x e			
Combined shift				7 x f	4 x f	11 x f			
Small Regression							8 x g	10 x g	4 x g
Large Regression							9 x h	5 x h	18 x h

2.2.2. Clinical Simulation

To illustrate this application on a clinical plan, the method was applied to a prostate cancer case. Target, bladder and rectum (wall) EUDs were evaluated in 18 geometries and their averages computed. The biomechanical model, which is the basis of the deformation field for the dose accumulation, is based on Yan et al. (1999). Figure 2.3 illustrates some instances of geometry veriations of the prostate, rectum and bladder in this prostate cancer case, corresponding to the results in table 2.4. The prescribed dose to the prostate was 72 Gy in 36 fractions with a PTV of a 7mm margin around the planning CT prostate gland. The required dose to the PTV was 68.4 Gy (95% of the prescribed dose). The constraints to the OARs was 60 Gy and 61 Gy EUD to the rectum and bladder respectively.

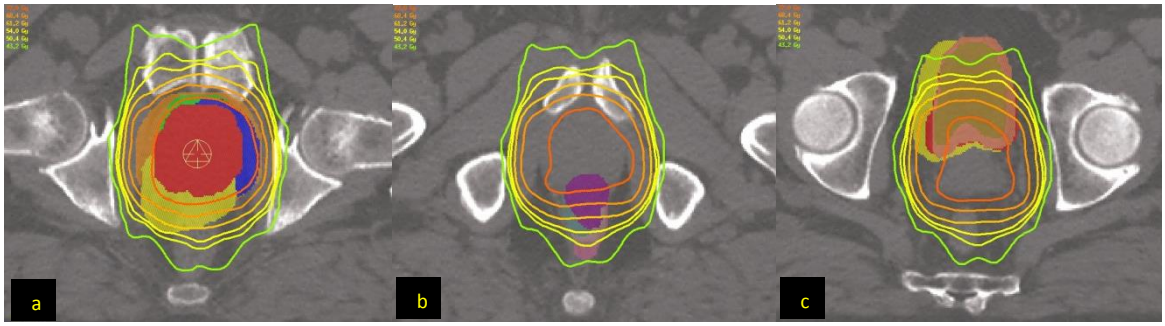

Figure 2.3: A collection of some geometries of the a) prostate, b) rectum and c) bladder in the prostate clinical simulation. In a) the red prostate contour corresponds to CT# 1, yellow to CT# 3, blue to CT# 5, and green to CT# 10. The orange contour is that of the PTV. In b) the pink rectal contour corresponds to CT# 3, grey-blue to CT# 9 and purple to CT# 10. In c) the brown contour corresponds to CT# 1, red to CT# 3, the flesh colour to CT# 7 and the yellow contour to CT# 15.

To illustrate another application, the method was employed for a 4D lung cancer case. The EUDs for the gross tumour volume (GTV) (Poisson cell kill) and the lung (mean dose) were investigated. The basis was eight 4D CT scan instances taken during a breathing cycle. Each of these instances is associated with an instance weight that was computed from the breathing probability density function (PDF). It reflects the relative fraction of a breathing cycle that is represented by a given instance. During dose accumulation, the doses of the respective instances were also weighted. For details, please refer to Söhn et al. (2009).

2.3. Results and discussion

The presented method is valuable because it provides a safe upper boundary on normal tissue doses and effects, and a safe lower boundary for tumour EUD. It is applicable even if deformation fields are not available or tumour shrinkage makes warping and accumulation difficult.

2.3.1. Monte Carlo Simulation

Table 2.3 shows the results obtained in the Monte Carlo simulation of the SOI as an OAR and a tumour. The boundary estimate for the OAR is always larger or equal to the actual accumulated dose in examples 1 - 6. On the other hand, as expected, the tumour estimated dose in examples 7 – 12 is always smaller or equal than the properly accumulated dose in the tumour.

Table 2.3. Comparison of properly accumulated EUDs for OARs and targets with worst case estimates of the total EUD.

Example	Accumulated dose (EUD in Gy)	Worst Case Estimate (EUD in Gy)
1	46.44	46.93
2	46.80	47.23
3	45.95	46.26
4	46.14	47.37
5	46.21	47.43
6	45.65	47.25
7	46.14	45.08
8	46.21	45.15
9	45.65	44.60
10	48.14	48.07
11	48.10	48.05
12	48.20	48.13

2.3.2. Clinical Simulation

Table 2.4 shows the results obtained for the prostate cancer case. The EUD computations based on the accumulated dose and the estimated boundaries yielded 71.60 Gy (> 70.31 Gy) for the prostate, 59.90 Gy (< 61.28 Gy) for the bladder and 56.68 Gy (< 57.80 Gy) for the rectal wall. As predicted, for the target the average EUD in table 2.4.is lower than the EUD of the average dose. The contrary is the case for the organs at risk. Resultantly, a useful worst case approximation of the EUDs was obtained without dose accumulation.

Table 2.4. EUDs for 18 patient geometries and their average.

	Prostate	Bladder	Rectum
	Poisson EUD (Gy)	Serial EUD (Gy)	Serial EUD (Gy)
CT#	α = 0.4	a = 8	a = 12
1	71.73	59.24	63.7
2	70.81	58.61	49.56
3	55.28	62.62	42.41
4	71.7	57.21	57.35
5	70.68	62.80	48.75
6	71.7	60.07	60.9
7	71.63	62.49	54.89
8	64.18	63.97	58.16
9	71.76	60.43	59.44
10	71.5	58.14	64.41
11	71.87	63.72	58.39
12	71.79	60.96	61.16
13	71.63	61.04	62.23
14	71.95	63.76	58.08
15	71.88	64.43	59.16
16	71.67	61.48	58.12
17	71.87	61.65	62.31
18	71.88	60.38	61.46
	70.31	61.28	57.80

Table 2.5 shows the results for the 4D lung case. The EUD of the accumulated dose is 49.84 Gy (> 48.75 Gy) for the GTV and 4.50 Gy (≤ 4.50 Gy) for the lung. Again the prediction in table 2.5.proves to be a worst case estimate. Note that the EUDs for the lung are equal for both methods by necessity, reflecting energy and volume conservation. This is due to the fact that the mean dose score function is linear, hence concave and convex at the same time.

Table 2.5. Instance weights and EUDs for GTV and lung from a breathing cycle (inhale (In) exhale (Ex) respiratory levels in the range 0-100) and the weighted sum of the EUD.

		GTV EUD	Weighted GTV EUD	Lung EUD	Weighted lung EUD
Breathing phase	Weight	Poisson EUD (Gy)α = 0.4	Poisson EUD (Gy)α = 0.4	Serial EUD (Gy)a = 1	Serial EUD (Gy)a = 1
0 In	0.402	48.029	19.312	4.66	1.874
25 In	0.088	48.127	4.229	4.48	0.394
50 In	0.077	49.656	3.800	4.37	0.334
75 In	0.084	49.661	4.190	4.24	0.358
100 Ex	0.117	48.250	5.629	4.29	0.501
75 Ex	0.033	50.718	1.682	4.38	0.145
50 Ex	0.048	49.851	2.379	4.43	0.211
25 Ex	0.152	49.661	7.528	4.51	0.684
		48.749		4.501	

Further applications of this relation have been outlined in the introduction, whereby the combination of brachytherapy and teletherapy is of particular usefulness in practice. Here,

$$EUD(D_{EBT} + D_{BT}) \leq EUD(D_{EBT}) + EUD(D_{BT}) \tag{2.5}$$

for normal tissues and

$$EUD(D_{EBT} + D_{BT}) \geq EUD(D_{EBT}) + EUD(D_{BT}) \tag{2.6}$$

for targets. This work also lays the foundation for robust optimization schemes that require no deformation fields [15]. The application of Jensen's inequality to the optimization of doses for variable patient geometries is the subject of future work.

2.4. Conclusions

A method to derive boundaries on the score function of the accumulated dose of multiple patient geometries was presented. By virtue of Jensen's inequality and the mathematical nature of commonly used score functions, in particular EUD and other biological score functions, it is possible to compute a worst case approximation on the combined effect of doses applied to variable geometries. Because the approach circumvents the

computation of the accumulated doses by means of deformation fields, it eliminates the need for deformable registration and dose warping.

2.5. References

1. Birkner M, Yan D, Alber M, Liang J and Nüsslin F. Adapting inverse planning to patient and organ geometrical variation: algorithm and implementation Med Phys 2003;30:2822–2831.

2. McShan D L, Kessler M L, Vineberg K and Fraass B A. Inverse plan optimization accounting for random geometric uncertainties with a multiple instance geometry approximation (MIGA). Med Phys 2006;33:1510–1521.

3. Söhn M, Weinmann M and Alber M. Intensity-modulated radiotherapy optimization in a quasi-periodically deforming patient model. Int J Radiat Oncol Biol Phys 2009;75:906–914.

4. Trofimov A, Rietzel E, Lu H M, Martin B, Jiang S, Chen G T Y and Bortfeld T. Temporo-spatial IMRT optimization: concepts, implementation and initial results. Phys Med Biol 2005;50:2779–2798.

5. Osorio E M V, Hoogeman M S, Teguh D N, Al Mamgani A, Kolkman-Deurloo I K K, Bondar L, Levendag P C, Heijmen B J. Three-dimensional dose addition of external beam radiotherapy and brachytherapy for oropharyngeal patients using non-rigid registration. Int J Radiat Oncol Biol Phys 2011;80:1268-77

6. Morin O, Gillis A, Chen J, Aubin M, Bucci M K, Roach M and Pouliot J. Megavoltage cone-beam CT: system description and clinical applications. Med Dosim 2006;31:51–61.

7. Rong Y, Smilowitz J, Tewatia D, Tom W A and Paliwal B. Dose calculation on KV cone beam CT images: an investigation of the Hu-density conversion stability and dose accuracy using the site-specific calibration. Med Dosim 2010;35:195–207.

8. Soukup M, Söhn M, Yan D, Liang J and Alber M. Study of robustness of IMPT and IMRT for prostate cancer against organ movement. Int J Radiat Oncol Biol Phys 2009;75:941–9.

9. Knopf A et al. Special report: workshop on 4D-treatment planning in actively scanned particle therapy—Recommendations, technical challenges, and future research directions. Med Phys 2010;37:4608–4614.

10. Niemierko A. Reporting and analyzing dose distributions: a concept of equivalent uniform dose. Med Phys 1997;24:103–110

11. Jensen J: Sur les fonctions convexes et les inegalites entre les valeurs moyennes. Acta Math 1906;30:175–93.

12. Alber M and Nüsslin F. An objective function for radiation treatment optimization based on local biological measures. Phys Med Biol 1999;44:479–93.

13. Kawrakow I. Accurate condensed history Monte Carlo simulation of electron transport I. EGSnrc, the new EGS4 version. Med Phys 2000;27:485–498.

14. Yan D, Jaffray D and Wong J. A model to accumulate fractionated dose in a deforming organ. Int J Radiat Oncol Biol Phys 1999;44:665–675.

15. Sobotta B, Söhn M and Alber M. Robust optimization based upon statistical theory Med Phys 2010;37:4019–4028.

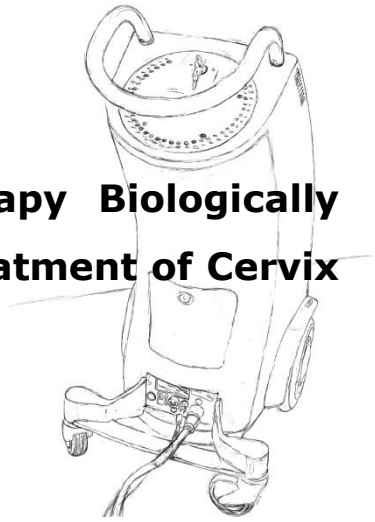

Chapter 3: A Solution for Brachytherapy Biologically Guided Dose Individualisation in the Treatment of Cervix Cancer (Appendix II)

This chapter includes work published by the author – Appendix II (Shaw et al. IFMBE Proceedings 2012;39: 2276-2279)

3.1. Introduction

Brachytherapy (BT) is a well known technique used in the treatment of cervical cancer and there have been many attempts to derive suitable treatment fractionation schedules for combination with external beam radiation treatment. BT treatment has the advantage that doses to organs at risk (OARs) can be quite effectively minimized when delivering very high, though non-uniform doses, to the tumour volume. Recently there have been very useful guidelines set by the GYN GEC-ESTRO working group [1] for achieving curative doses when external beam radiotherapy (EBRT) and BT are combined. However, although these recommendations can probably be easily followed at modern treatment facilities, this is not necessarily the case in most developing countries. In such countries many patients from rural areas are treated at distant hospital complexes where treatment protocols often consider the fact that late OAR toxicities must be kept to an absolute minimum as the management of such toxicities in these patient groups may be critical to overall patient management. Regular access to 3D imaging devices for BT planning is also limited and treatment protocols are usually derived from older 2D treatment planning techniques.

The clinical treatment protocol at our department of Radiation Oncology, Universitas Hospital Annex (Bloemfontein, South Africa) involves the normalization of the brachytherapy dose to a single rectal point. This point lies on the anterior rectal wall that receives the highest dose according to a standard loading and dose distribution pattern and may not receive more than 2 Gy per fraction. In such conservative protocols the net result might be under-dosage of the tumour as a result of the rectum being too close to the applicators during some treatment fractions. This method explicitly ignores the fact that the rectal dose normalization point will most probably vary in spatial position during subsequent treatment fractions. Understandably, the total accumulated rectal dose would be overestimated when such a treatment protocol is followed. This technique has

several other drawbacks, for instance, when the rectum is too close to the applicator or the organ geometry limits dose to the tumour, the treatment may be cancelled and another attempt made at a later time. Such delays will result in prolonged treatment times that negatively impact curative probability or will simply lower tumour doses if treatment time cannot be extended any further [2]. Whatever the decision, these protocols unfortunately limit the use of BT and under exploit the biological advantages and optimization possibilities for effective BT treatment.

These problems can be addressed to some extent by making use of biological models of tumour and normal tissue responses and implementing guidelines for fixed treatment endpoints to maximize tumour dose safely. The variability of organ geometries during the treatment period can sometimes be an advantage, as will be shown in this study.

3.2. Methods and materials

In our radiotherapy department, where a large percentage of patients from rural areas are treated, a conservative approach in the treatment of cervix cancer with brachytherapy is followed. The total number of cervix cancer patients that are treated with curative intent varies between 250 and 400 patients per year on a single high dose rate (HDR) remote afterloading system, resulting in a very high workload. Due to budgetary constraints and logistical reasons, follow-up and management of treatment related toxicity is especially difficult in our patient population.

3.2.1. Treatment and patient data

EBRT treatment consists of 50 Gy delivered in 25 fractions using a standard 4-field box technique. Patients receive an additional 5 concomitant fractions of HDR BT on a 40-channel Flexitron afterloading unit. BT treatment commences after ten EBRT fractions have been delivered, but BT and EBRT are given on the same day. Concurrent Cisplatin-based chemotherapy of 5 – 6 x 25 mg/m^2 body surface area is also administered during the course of treatment. We have selected 10 sequential patients who received treatment during the period of 2007 and 2008 for this study. They were all classified as FIGO stage IIIB locally advanced squamous cell carcinoma of the cervix.

3.2.2. Conventional treatment planning

BT treatment plans were produced on the Isodose Control® Flexiplan treatment planning system making use of CT datasets for each treatment fraction with the applicators already implanted under conscious sedation. Treatment plans are based on the well-known pear-shaped dose distribution achieved using a standard ring and intra-uterine

applicator combination. The dose to the highest rectal dose point of the day was normalized to 2 Gy. The dose to point A was recorded as representative of the gross tumour volume dose in our department. The protocol did not make provision to record and calculate the cumulative dose to the ICRU rectum and bladder dose points [3].

We have retrospectively contoured a High Risk Clinical Target Volume (HR-CTV) [1] as suggested by the Gyn GEC-ESTRO WG. However, a standard loading pattern was still used for treatment planning and the position of the rectal dose normalization point alone influenced the achievable dose to Point A and HR-CTV. The HR-CTV dose was recorded as the minimum dose to 90% of the HR-CTV volume, D90. These tumour representative doses varied as a function of rectal position and geometry. For the purposes of this study we have recorded the full dose volume histograms (DVHs) of the rectum, bladder and HR-CTV. We refer to this treatment planning protocol as the conservative method due to the attempted conservation of low toxicity outcomes.

3.2.3. Biologically guided treatment planning

It is understandable that this conservative treatment protocol might sometimes lead to unacceptably low tumour doses as the highest rectum dose point might be in close proximity to the applicators. Sometimes situations occur when the dose to point A might be even lower than the highest rectal dose point of 2 Gy, resulting in the forfeiture of the treatment. However, by exploiting the effects of fractionation, 3D volumetric treatment planning and biological response models, one can individualize these plans so that each patient's anatomic geometry can be used to optimize, through expansion, the pear-shaped dose distribution to boundaries of normal tissue dose response and at the same time maximise the dose to the tumour.

To test the biologically guided probability of tumour dose escalation, the treatment plans of all 10 patients were re-planned. For this purpose, the use of a single rectal dose point constraint was replaced by a rectum equivalent uniform dose (EUD) [4] constraint based on a 2% probability of developing grade II late rectal bleeding [5] and in addition a 10% probability for a variety of grade II bladder complications. The OAR EUD constraints were chosen as 14.5 Gy and 16 Gy in 2 Gy per fraction equivalent dose for the rectum and bladder respectively and exclude the contribution from EBRT. Since the dose distributions in the OARs and HR-CTV are extremely non-uniform in BT, the EUD has an important role to play as it specifically addresses this issue to simplify DVH interpretation.

3.2.4. EUD calculation and biological parameters

To be able to compare the total dose between fractions of different sized doses, a conversion of dose to the 2 Gy per fraction dose equivalent had to be performed. This was done using the linear quadratic (LQ) model [6]. This model was also incorporated in all EUD calculations. A computer code was developed in Interactive Data Language (IDL) for EUD calculations using the tumour and OAR DVHs as input and a Mann-Whitney-Wilcoxon statistical test was performed on the same IDL platform to test for significant differences in the location of the frequency distributions of data at the p=0.05 or 95% confidence level. The EUD calculation for tumours utilised the cell survival fraction (S_{Tumour}) (3.1 and 3.2), while the generalized EUD was calculated for normal tissues (3.3).

$$S_{Tumour} = e^{(-\{n(\alpha d+\beta d^2)-(\gamma(T_e-T_{del}))\})} \quad (3.1)$$

$$EUD_{Tumour} = \frac{-log(S_{Tumour})}{\left(\alpha+\beta d-\left(\gamma/_d(T_e-T_{del})\right)\right)} \quad (3.2)$$

$$EUD_{OAR} = (\sum_i v_i D_i^a)^{\frac{1}{a}} \quad (3.3)$$

LQ parameters for cervical cancer and the OARs, as well as for the EUD calculation were based on well known values from literature [2, 5]. This way, the EUD concept is extended to account for non-standard fractionation schemes, whereby the current combination of dose distributions and fractionation size at a given isodose level can be equated to a uniform dose for a standard fractionation size. This is particularly important for BT treatments which may utilise large variations in fraction size and show dramatic dose gradients.

Firstly, the EUDs were calculated for all these volumes utilizing the concepts of biological equivalent doses (BED) and equivalent dose in 2 Gy per fraction (EQD2) to allow the usage of comparable published late toxicity data. To bring the EUD of different doses per fraction into consideration, the EQD2 had to be calculated from the BED for each fraction as the late toxicity endpoints used in the optimization of the dose distributions are based on a 2 Gy fractionation schedule.

Secondly, once the rectal, bladder and HR-CTV EUDs according to the conservative protocol were available, the treatment plans were adjusted by simply maximizing the dose to the upper boundaries of the OARs (still using the standard pear-shaped dose distribution according the fixed dwell position ring applicator setup) which has a simultaneous tumour dose escalation effect.

3.2.5. Dose accumulation

It is virtually impossible to sum the doses from different treatment fractions of EBRT when dealing with geometrically changing and deforming tumour and OAR volumes, unless the dose distribution is uniform across the volume of interest or methods of dose warping or deformable image registration is employed. This problem is even greater when doses from different treatment modalities are summed and particularly so in the case of intensity modulated radiotherapy (IMRT) and brachytherapy. However, the use of EUDs allows the determination of a lower or upper dose boundary (Chapter 2), referred to herein as a worst case scenario for dose estimation [7]. This method of a worst case accumulated dose estimate provides a solution for adding sequential EBRT and BT doses and for the comparison of different treatment plans and fractionation.

3.3. Results

To show the potential improvement in tumour dose when using biologically guided dose individualisation, the conservative and biological treatment planning methods were compared. The comparison is made in terms of the delivered dose per BT fraction, as well as the total dose to each volume of interest after 5 brachytherapy fractions, excluding any EBRT dose component.

3.3.1. OAR D2cc and EUD

Recent studies [8–13] described the advantages of using D2cc as a planning and reporting parameter and found large differences when comparing this parameter to the ICRU rectal point. We observed significant deviations in the values of D2cc of the rectum when planning conservatively and comparing these values to a 2Gy rectal normalization point (Figure 3.1). D2cc values are on average between 75 and 80% of that of the normalization dose value (2 Gy). The total rectum D2cc achieved for this group of patients at our treatment facility with the conservative method is significantly lower than those reported in literature that are associated with manageable toxicity rates [9, 14]. Total rectal D2cc in the biological planning method are overall higher than the conservative method, but still lower than those found in other studies. Figure 3.4 gives a correlation between the D2cc and EUD values in the conservative and biological planning methods. The biological method shows a much better correlation than the conservative method.

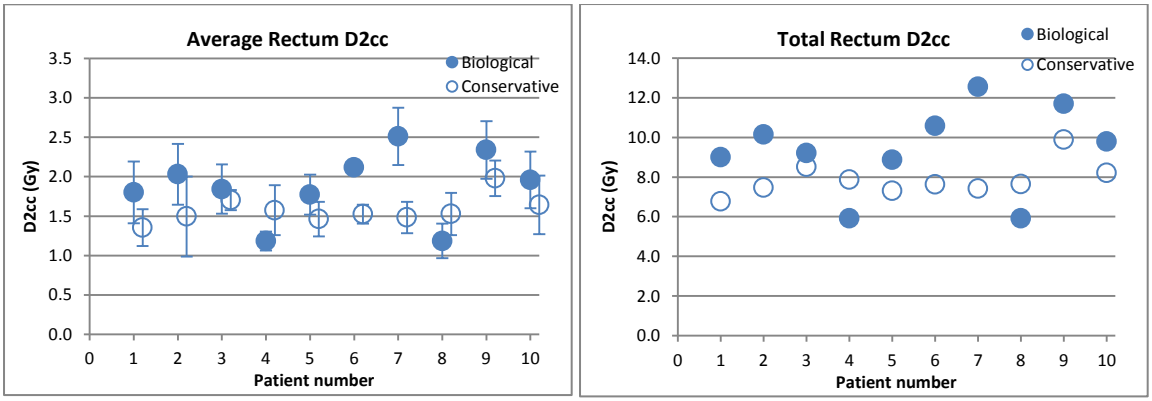

Figure 3.1: Variation in average dose per fraction (and one standard deviation) and total dose (after 5 BT treatment fractions) to the 2cc volume receiving the highest rectal dose for the conservative and biological planning methods.

Figure 3.2 displays the variation in the rectal EUD for both treatment planning methods, as well as the bladder EUDs. From figure 3.1 and 3.2 the biological method results in more rectal dose variations than what is seen in the conservative method. However, the bladder EUD results show a very consistent upper dose value across the population and this is due to the fact that the bladder was dose limiting in 88% of the treatment plans. The conservative method resulted in lower bladder doses overall compared to the biological method, although some outlier patients with much higher bladder doses were found due to the protocol not restricting bladder doses.

3.3.2. Point A and HR-CTV D90

The recommendation from the ABS for point A dose to achieve suitable control rates was 80 – 90 Gy EQD2 which translates to 30 – 40 Gy in our clinic for BT [15]. Our results show that the conservative method produces point A doses that are much lower than this required level (figure 3). The same applies to HR-CTV D90 values that are much lower than recommended by the GEC-ESTRO-based studies [16]. The biological method does result in increased total dose for the majority of the patients in the study, but the average population dose is still below recommended values for both point A and D90.

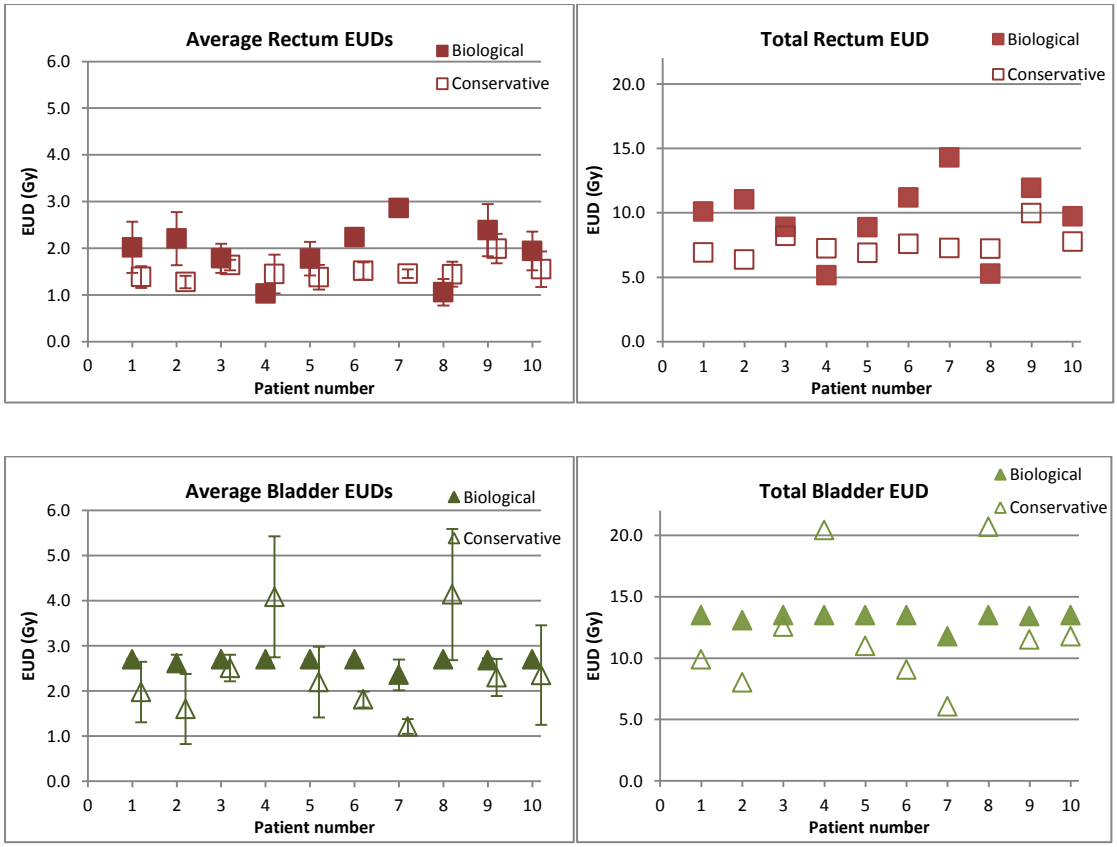

Figure 3.2: Variation in average EUD per fraction (and one standard deviation) and total EUD (after 5 BT treatment fractions) for the rectum and bladder when planning with the conservative and biological methods.

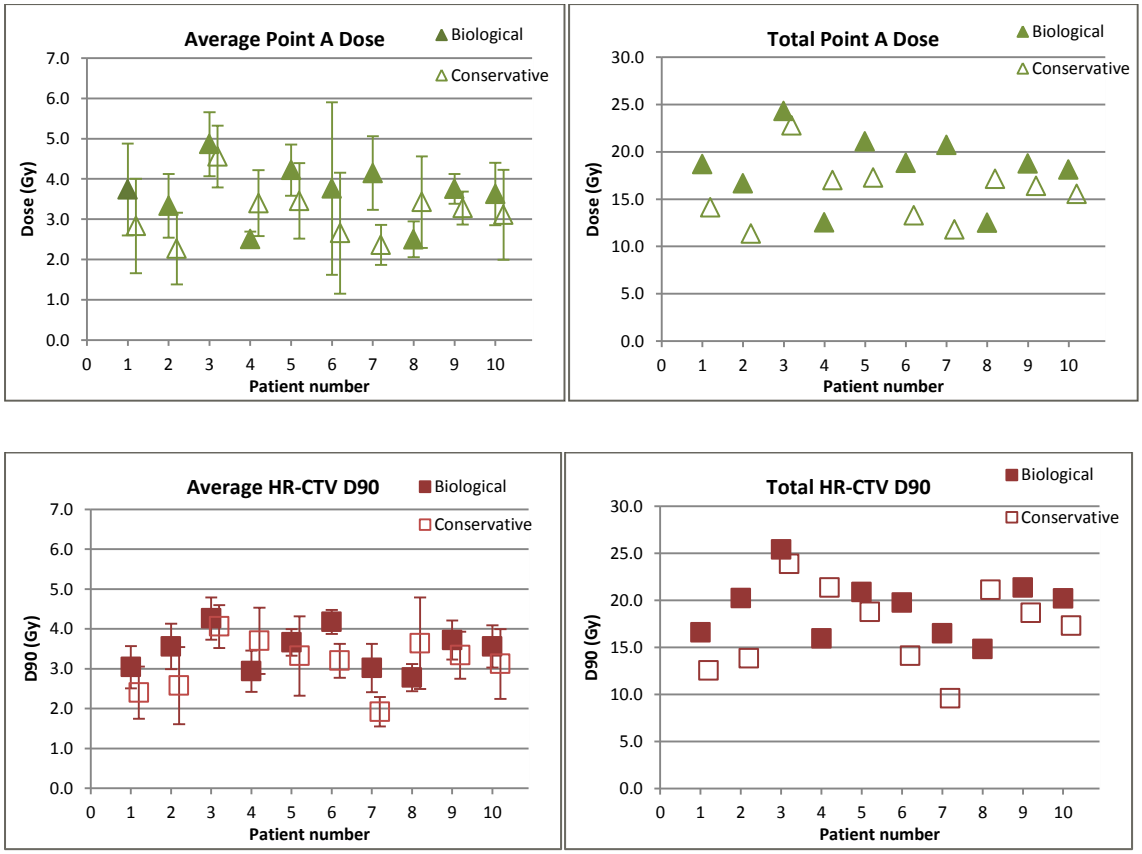

Figure 3.3: Variation in average point A and D90 dose per fraction (and one standard deviation) and total point A dose and D90 (after 5 BT treatment fractions) of the HR-CTV when planning with the conservative and biological methods.

The biologically guided treatment planning method shows potential to safely increase tumour dose considering each patient's individual anatomic organ geometry at the time of each treatment fraction. Considering all the treatment plans included in this study, it was found that larger tumour doses could potentially have been delivered in 80% of the 50 treatment plans if the biologically guided method was used. Table 3.1 gives a summary of the average EUDs after 5 treatment fractions for the 10 patients. In 20% of treatment fractions the rectum limited the achievable tumour dose, while the bladder was limiting in the rest.

Table 3.1: Comparison of the total dose parameters (Gy ± one standard deviation) for 10 patients after 5 fractions produced by the conservative protocol and the biologically guided planning solution in 50 planned treatment fractions

Parameter of interest	Conservative Method	Biological Method	p-value
Rectum EUD	7.54 ± 0.99	9.65 ± 2.82	0.0125
Bladder EUD	12.10 ± 4.86	13.28 ± 0.54	0.0266
HR-CTV D90	17.1 ± 4.7	19.17± 3.19	0.0398
HR-CTV EUD	29.67 ± 2.68	37.57 ± 8.32	0.0098
Point A	15.66 ± 3.32	18.22 ± 3.65	0.0125
Rectal D2cc	7.87 ± 0.86	9.37 ± 2.16	0.0125

As the bladder was the dose limiting organ in 80% of the cases, one would expect the variation in bladder EUD to be less than that of the rectum, as seen from the above results.

When comparing the population average per-fraction EUDs over all 50 planned fractions investigated in the study, the rectum EUDs were escalated from 1.51± 0.24 Gy to 1.93 ± 0.34 Gy, the bladder EUD from 2.42 ± 2.21 Gy to 2.66 ± 0.16 Gy and the HR-CTV D90 and EUDs from 3.42 ± 1.14 Gy to 3.83 ± 0.85 Gy and 5.93 ± 0.47 Gy to 7.51 ± 1.59 Gy in individual treatment fractions. These results differ slightly from the study of Shaw et al. [Appendix II] that were based on 10 patients with early stage disease. The study by Shaw et al. was performed on a group of patients of which the data was inaccessible after a software upgrade of the treatment planning system. In both these sets of results the increase in HR-CTV EUD was more than 25%, while OAR EUDs were in the same dose range.

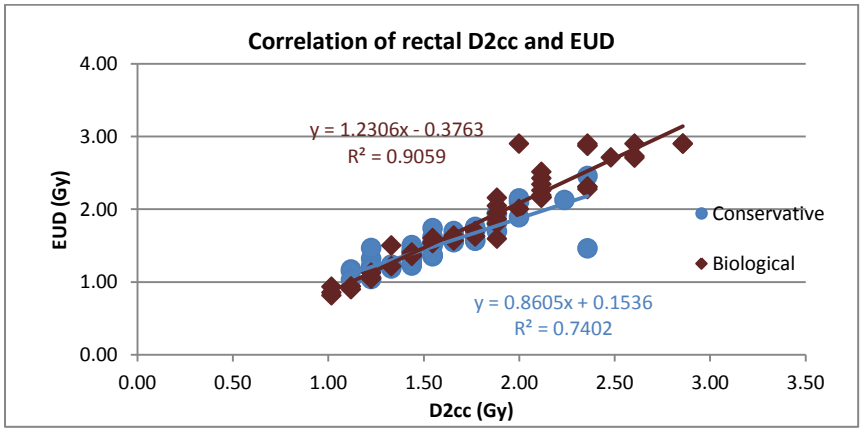

Figure 3.4.: Correlation between the rectum EUD and D2cc values for the conservative and biological planning methods

3.4. Discussion

The use of a spatially variant rectal dose point can probably be considered an improvement compared to the use of a single applicator defined ICRU dose point [3] since the actual area of higher rectal dose is used for dose accumulation and treatment planning. Both these concepts stem from earlier brachytherapy techniques based on 2D radiography based imaging and planning. However, the use of such points is extremely dose limiting if the constraint value is too low and prevents meaningful optimization of the total dose distribution by not considering the rectum volume (and the same holds for the bladder) comprehensively. Such point dose planning parameters do not fit the profile of most organs, like the rectum, that exhibit dose-volume effects. Single dose point constraint parameters also limit dose distribution optimization solutions.

Comprehensive consideration of the OAR DVHs via EUD highlighted larger variations in average and total dose compared to the dose to a rectal volume (Fig. 3.1). But, even the use of a more meaningful single dose volume, namely D2cc, does not result in consistent dose parameters when the OAR is evaluated comprehensively (Fig 3.4) as this dose volume translates to a point on a DVH. In fact, the conservative approach results in a worse correlation between EUD and D2cc of the rectum than when the biological planning method is used.

The low point A dose and HR-CTV D90 values are a result of firstly, the use of a rectal normalization point of which the constraint value is simply too low. Comparison of the associated D2cc values in the conservative planning technique creates the impression that the probability of finding any late rectal complications in this population is extremely small. What is more alarming is that the dose to point A is very low compared to recommended dose for local tumour control [15]. Since point A has been shown to not be a surrogate for the GTV and CTV [17], the inclusion of HR-CTV D90 stresses the fact that the tumour dose achieved with the conservative planning technique is not large enough for adequate rates of local control.

The biological planning method shows promise to escalate tumour dose by using a reliable worst case estimate of OAR dose so that normal tissue total dose constraints would not be violated when accumulating dose from different treatment modalities and in regions, like the pelvis, where organ motion is accentuated. This method could be used in combination with dose distribution optimization to the tumour volume to further potentially escalate the point A and HR-CTV D90 dose to recommended values and beyond. Such optimization should also aim at reducing the volume of OARs included in high dose regions without compromising tumour coverage.

The OAR EUD dose constraints used in this study allowed higher OAR dose compared to the conservative method, but were still too dose limiting at for instance 2% probability of grade 2 rectal bleeding. Since brachytherapy dose distributions have extreme dose gradients compared to EBRT, a small increase in this complication rate projection can most probably result in large tumour dose increases. The bladder in particular was mostly dose limiting and a suitable EUD constraint should be determined for this organ. Further tumour dose escalation can be achieved by performing dose optimization to the target volume and adaptive planning throughout the whole treatment process, especially in combination with interstitial brachytherapy. Suitable OAR EUD parameters should thus be determined for this purpose, especially if future treatments will rely on dose distributions that differ from the historical pear-shaped dose distribution to more conformal image guided dose distributions. Both planning techniques show variation in HR-CTV and point A dose indicating that for a fixed normal tissue endpoint in a patient population, BT treatment could be further improved if treatment plans are individualized to produce maximal tumour dose.

Much of the attention in our department has been focussed on rectal dose and the limitation of rectal complications, but from the results it can be seen that the bladder was mostly dose limiting. The fact that the bladder dose was included in this study resulted in large rectal dose variations and a more constant bladder dose distribution throughout the population of patients, with both OARs still within the dose constraints. The important realization is that the bladder should be considered in the planning process in future. Other organs like the sigmoid, small bowel and vagina should also receive attention if dose adaptation and escalation is pursued.

The conservative planning method delivered fairly "constant" D2cc total rectal dose in the population of patients, but the values were much lower than those associated with 10% grade II rectal toxicity in other studies. Even the EUDs in the biological method were not comparable to 2% toxicity rates due to the bladder dose limitations. However, the biological method does not result in OAR over-dosage when compared to D2cc data.

The EUD is a useful endpoint in the evaluation of treatment plans with non-uniform dose distributions in three dimensional conformal, intensity modulated and brachytherapy radiotherapy treatment planning. When optimizing treatment plans the EUD can very effectively be used in a centre where fixed endpoints for normal tissue effects are to be achieved, as required in our institution where many patients from outlying rural areas are treated. Our results show that all treatment plans deliver the same maximum EUD to the OAR that reaches its limit first. Thus variability in terms of bladder or rectal complications of a certain predetermined degree is limited. Tumour control may vary

between patients, but the maximal permissible dose without unacceptable late toxicity would in most cases be delivered. This is in contrast to the conservative protocol where rectal, bladder and tumour response will vary throughout the whole population. This method could possibly be extended in a similar way to treat all tumours to the same EUD, but this was not considered here.

3.5. Conclusion

In this study we applied an EUD-based dose escalation strategy to obtain maximal tumour dose. This is achieved by individualizing the treatment plans of each patient in the study such that a clinical normal tissue complication probability endpoint would be achieved for the population of patients. However, the deforming OAR volumes in each treatment fraction are allowed to receive their maximal permissible dose or EUD through the worst case scenario approach.

The general conclusion from this investigation is that the EUD-based method of plan optimization is much more efficient in terms of safety boundaries for normal tissue toxicity, even if the volumes and geometries of OARs vary over sequential treatment fractions. It is also a suitable solution for safe escalation of tumour doses at the same time, specifically enabling maximization of tumour dose when considering individual OAR geometries.

This method can be seen as an adaptive fixed endpoint strategy that is extremely useful when summing doses from different treatment modalities. It ensures that all patients treated in this way receive the maximal benefit without detriment, instead of a treatment protocol where only a limited number of patients will reap the benefit of the treatment technique. Single dose points, even those of higher planning value than the ICRU point that does not vary with OAR variations, are not suitable for treatment planning as it limits optimization solutions and CTV dose, or for reporting of treatment.

Lastly, the combination of the rectum and bladder EUD constraints in this study is somewhat arbitrary. Since the total rectal D2cc was so low on average in the biological planning results, an equivalent dose constraint to those of the Gyn GEC-ESTRO WG II [14, 18] should be investigated if EUD-based planning is to be performed in future.

3.6. References

1. Haie-Meder C, Pötter R, Van Limbergen E, et al: Recommendations from Gynecological (GYN) GEC-ESTRO Working Group (I): concepts and terms in 3D image based 3D treatment planning in cervix cancer brachytherapy with emphasis on MRI assessment of GTV and CTV. Radiother Oncol 2005;74:235–245.

2. Wyatt R, Beddoe A, Dale R. The effects of delays in radiotherapy treatment on tumour control. Phys Med Biol 2003;48:139-155.

3. ICRU. International Commission on Radiation Units and Measurements. ICRU report 38: Dose and volume specification for reporting intracavitary therapy in gynaecology. Bethesda: ICRU;1985.

4. Niemierko A. Reporting and analyzing dose distributions: A concept of equivalent uniform dose. Med Phys 1997;24:103-109.

5. Söhn M, Yan D, Liang J, Meldolesi E, Vargas C, Alber M. Incidence of late rectal bleeding in high-dose conformal radiotherapy of prostate cancer using equivalent uniform dose-based and dose-volume-based normal tissue complication probability models. Int J Radiat Oncol Biol Phys 2007;67:1066-1073.

6. Dale R, Jones B (2007) Radiobiological Modelling in Radiation Oncology. British Institute of Radiology, 36 Portland Place, London, W1B 1AT, UK

7. Sobotta RB, Söhn M, Shaw W, Alber M. On expedient properties of common biological score functions for multi-modality, adaptive and 4D optimization. Phys Med Biol 2011;56:N123-N129

8. Shin KH, Kim TH, Cho JK, et al. CT-guided intracavitary radiotherapy for cervical cancer: Comparison of conventional point A plan with clinical target volume-based three-dimensional plan using dose-volume parameters. Int J Radiat Oncol Biol Phys 2006:64:197-204.

9. Schoeppel SL, LaVigne ML, Martel MK, et al. Three-dimensional treatment planning of intracavitary gynecologic implants: Analysis of ten cases and implications for dose specification. Int J Radiat Oncol Biol Phys 1994;28:277–283.

10. Van den Bergh F, Meertens H, Moonen L, et al. The use of a transverse CT image for the estimation of the dose given to the rectum in intracavitary brachytherapy for carcinoma of the cervix. Radiother Oncol 1998;47:85–90.

11. Koom WS, Sohn DK, Kim JY, Kim JW, Shin KH, Yoon SM, Kim DY, Yoon M, Shin D, Park SY, Cho KH. Computed tomography-based high-dose-rate intracavitary brachytherapy for uterine cervical cancer: preliminary demonstration of correlation between dose-volume parameters and rectal mucosal changes observed by flexible sigmoidoscopy. Int J Radiat Oncol Biol Phys 2007;68:1446-1454.

12. Fellner C, Potter R, Knocke TH, et al. Comparison of radiography- and computed tomography-based treatment planning in cervix cancer in brachytherapy with specific attention to some quality assurance aspects. Radiother Oncol 2001;58:53–62.

13. Wachter-Gerstner N, Wachter S, Reinstadler E, et al. Bladder and rectum dose defined from MRI based treatment planning for cervix cancer brachytherapy: Comparison of dose-volume histograms for organ contours and organ wall, comparison with ICRU rectum and bladder reference point. Radiother Oncol 2003;68:269–276.

14. Georg P, Kirisits C, Goldner G, Dörr W, Hammer J, Pötzi R, Berger D, Dimopoulos J, Georg D, Pötter R. Correlation of dose-volume parameters, endoscopic and clinical rectal side effects in cervix cancer patients treated with definitive radiotherapy including MRI-based brachytherapy. Radiother Oncol 2009;91:173-180.

15. Nag S, Erickson B, Thomadsen B, Orton C, Demanes J, Petereit D. For the American Brachytherapy Society. The American Brachytherapy Society recommendations for high-dose-rate brachytherapy for carcinoma of the cervix. Int J Radiat Oncol Biol Phys 2000;48:201–211.

16. Dimopoulos J, Lang S, Kirisits C, Fidarova E, Berger D, Georg P, Dörr W, Pötter R. Dose–volume histogram parameters and local tumour control in magnetic resonance image–guided cervical cancer brachytherapy. Int J Radiat Oncol Biol Phys 2009;75:56–63.

17. Kim H, Beriwal S, Houser C, Huq MS. Dosimetric analyses of 3D image-guided HDR brachytherapy planning for the treatment of cervical cancer: Is point A-based dose prescription still valid in image-guided brachytherapy? Med Dosim 2011;36:166-170.

18. Pötter R, Haie-Meder C, Van Limbergen E, et al: Recommendations from Gynecological (GYN) GEC ESTRO working group (II): Concepts and terms in 3D image-based treatment planning in cervix cancer brachytherapy— 3D dose volume parameters and aspects of 3D image-based anatomy, radiation physics, radiobiology. Radiother Oncol 2006;78:67–77.

Chapter 4: Equivalence of Gyn GEC-ESTRO guidelines for image guided cervical brachytherapy with EUD-based dose prescription (Appendix III)

This chapter includes work published by the author – Appendix III (Shaw et al. Radiation Oncology 2013, 8:266)

4.1. Introduction

Recently, the treatment of cervical cancer has been advanced through the use of image guided brachytherapy (IGBT) [1-4]. The Groupe Européen de Curiethérapie (GEC) and the European SocieTy for Radiotherapy & Oncology (ESTRO) working group (Gyn GEC-ESTRO WG, GGE) presented guidelines that comprise imaging and organ segmentation for planning of every treatment fraction [5,6]; subsequently, limited imaging approaches have been derived [7,8]. Such an approach adapts for organ motion and tumour shape changes by conforming the prescribed dose to the target volume of the day, and thereby increases the chance of applying effective IGBT doses in successive fractions. This image- and volume-based planning strategy allows for a per-fraction analysis of dose distributions and dose volume histograms (DVHs). Further, the total delivered dose up to and including the last treatment fraction can be estimated for clinical target volumes (CTV) and organs at risk (OAR). This constitutes a risk-controlled dose prescription method with DVH criteria for tumour and normal tissue volumes. The relevance of these criteria has been demonstrated by linking them to toxicity [9-11] and local control [11-14]. However, contouring and organ motion are the major contributors of uncertainties in IGBT [15].

The GGE technique requires MRI for tumour and OAR delineation with applicators in-situ. Unfortunately many clinics have limited availability of MRI. One alternative is CT imaging, but due to the lower contrast, CT based planning results in increased OAR volumes, CTV delineation uncertainty and consequently unnecessarily large CTVs, as one tends to plan conservatively [16-19]. These uncertainties can produce lower CTV doses [3, 16] if normal tissue DVH criteria are adhered to. At the same time, contour uncertainty leads to uncertainty of derived DVH criteria for toxicity scoring or tumour control and an uncertainty in the addition of OAR and tumour DVHs for obtaining worst-case estimates of the accumulated dose [6, 15, 20, 21]. Furthermore, with the increased

use of more conformal external beam radiotherapy (EBRT) techniques such as intensity modulated radiotherapy (IMRT), the addition of DVH parameters for such worst case estimates can become unreliable.

This raises the question whether a volume-based treatment plan metric such as the equivalent uniform dose (EUD) [22] could be more robust against contouring and imaging uncertainties than DVH. In EBRT planning, the generalized EUD (gEUD) is well established [23-25] and is mathematically equivalent to the DVH reduction scheme of the Lyman-Kutcher-Burman (LKB) normal tissue complication probability (NTCP) model [26-29]. It is our intention to establish a gEUD-based prescription method for IGBT that can replace the original GGE prescription in terms of dose-volume criteria, but offers advantages in terms of safety and robustness against uncertainties. Further, EUD sports favourable mathematical properties that allow a reliable worst-case estimate of the accumulated dose.

We investigate this question with a three-stage planning study of fractionated IGBT. In stage 1, we record the EUD values of OARs achieved with plans obtained from the dose-volume constrained GGE guidelines. From this, we establish corresponding EUD criteria. In stage 2, the treatments are planned according to these EUD constraints, and their safety is assessed according to the GGE DVH criteria. Finally, in stage 3, the full treatments (EBRT + 5 fractions IGBT) of both strategies are compared by both metrics.

4.2. Methods

4.2.1. Patient selection, imaging and contouring

Ethical approval (ETOVS NR 214/09) was received for this study. Twenty patients who had been treated with high dose rate (HDR) IGBT for carcinoma of the cervix between October 2009 and January 2011 were randomly selected (Table 1). All patients received EBRT consisting of 25 fractions of 2 Gy via a 4-field box technique without midline shielding, and 5 concomitant IGBT treatment fractions of 4.7 Gy (± 0.8 Gy) to the High Risk CTV (HR-CTV; discussed below) with a standard magnetic resonance imaging compatible tandem-ring (Nucletron®). Intra-uterine source positions were located at 1 cm intervals from the ring to the tip, while the length of the intra-uterine applicator was adapted to tumour extent. Source positions in the ring were fixed for all treatments. Our centre's high workload requires that implantations be done under conscious sedation without vaginal packing. Treatment plans were produced on axial CT images for lack of MRI facilities.

Table 4.1. Patient, volume and treatment characteristics

Characteristic	*No of patients and/or value(s)*
Total nr of patients	*20*
Total EBRT dose	*50 Gy*
Total nr of EBRT fractions	*25*
Total nr of IGBT fractions	*5*
Total IGBT dose (Mean ± SD)	*4.7 ± 0.8 Gy*
Total nr of CT datasets in study	*100*
FIGO stage (n)	
II	*5*
III	*12*
IVa	*3*
Volume in cc (Mean ± SD)	
HR-CTV @ 1stIGBT treatment	*49.0 ± 21.0*
IR-CTV @ 1stIGBT treatment	*119.0 ± 43.0*
Rectum	*94.8 ± 32.6*
Bladder	*108.0 ± 91.6*
Dose objectives/constraints	
HR-CTV D90	*≥85 Gy*
IR-CTV D90	*≥60 Gy*
Rectum D2cc	*≤70 Gy*
Bladder D2cc	*≤80 Gy*

Abbreviations: *SD* standard deviation, *cc* cubic centimetres.

Contouring was based on clinical examination and CT images, using the GGE guidelines for the HR-CTV, Intermediate Risk CTV (IR-CTV) and the rectum and bladder walls. The GTV had to be omitted as it cannot be identified on CT images. The HR-CTV consisted of the whole cervix and macroscopic extent of the disease at the time of imaging for IGBT. The IR-CTV encompassed the HR-CTV plus a variable margin depending on the initial extent of the disease, considering tumour regression in response to treatment. The OAR walls and outline with content were delineated according to the same set of recommendations.

4.2.2. Fractionation and dose evaluation parameters

According to the GGE recommendations we recorded the following parameters for purposes of comparison: Minimal dose received in 0.1, 1, and 2 cc of the maximal dose

regions of the OARs (D0.1, 1, 2 cc; outer wall plus content), dose to 90% (D_{90}) of the HR- and IR-CTVs, as well as the EUDs of OAR walls and CTVs.

Full DVHs of each treatment fraction were available in the Flexiplan (Nucletron®) treatment planning system and dose was converted to a 2Gy equivalent dose (EQD2) [30]. According to GGE, the linear quadratic (LQ) model parameters of α/β being 3 Gy for OARs and 10 Gy for tumours (α being 0.3 Gy^{-1}) were applied. Since the treatment was concomitant HDR brachytherapy, repair half-times and repopulation were neglected.

The EUD for target volumes was calculated relative to the EBRT dose delivered in 2 Gy fractions (d = 2 Gy) from the surviving fraction as:

$$EUD = \frac{-Log(S)}{\alpha+\beta d} \quad (4.1)$$

To consider the heterogeneity in dose distributions, the differential DVH of tumours was used to calculate the surviving fraction for each treatment:

$$S = \Sigma_k v_k S(D_k) \quad (4.2)$$

S is calculated from D_k, the dose bin for the v_{k-th} fractional tumour volume.

The gEUD calculation was used for OARs [28, 31], again considering a reference dose of 2 Gy per fraction and is given by

$$gEUD = (\Sigma_k v_k {D_k}^a)^{\frac{1}{a}} \quad (4.3)$$

Where D_k is the EQD2 for the v_{k-th} fractional OAR volume and *a* is the volume effect parameter. The gEUD for rectum and bladder walls was calculated using volume effect parameters (*a*) of 12 for the rectum and 8 for the bladder [23, 32, and 33].

For simplicity we refer to the EUD based, adaptive IGBT planning strategy as the comprehensive volume technique (CV), emphasizing the fact that EUD considers the entire organ volume.

4.2.3. Study 1: prescription constraints

One possibility to establish the gEUD prescription constraints for IGBT treatment planning is to collect them from literature, another by a planning study. From Söhn et al. (2007), we can choose the gEUD upper limit for the rectum to be 67.8 Gy (3.55 Gy EUD per IGBT fraction), at approximately 10% NTCP for grade II (G2) rectal bleeding. However, in the following this gEUD is verified against a rectum D2cc constraint of 70 Gy EQD2 [9, 10] by the planning study. Bladder NTCP model data are scarce and uncertain

[34] due to unaccounted variations in filling. Consequently, the bladder gEUD constraint is determined by the planning study. There are bladder dose guidelines based on the GGE work that show more than 5 - 10% late complication rates when the D2cc is in the order of 70–100 Gy EQD2 [9,10,19,35,36].

To derive the bladder wall gEUD dose constraints, the GGE planning strategy was followed to achieve at least 7.0 Gy per fraction (85 Gy EQD2 from EBRT and IGBT) to the HR-CTV D90. Treatment plans were produced for each treatment fraction on the 100 CT datasets. Each plan started from the standard loading pattern and was manually or graphically optimized until the HR-CTV dose objective was reached, or until one of the two OAR constraints in question prevented any further CTV dose escalation (Table 4.1). *Bladder EUD constraints:* HR-CTV dose was further increased beyond the CTV objective until the bladder D2cc criterion was reached. This constraint was chosen as 80 Gy total dose from EBRT and IGBT, resulting in 6 Gy EQD2 per IGBT fraction. The procedure was repeated on all plans and for each the associated bladder wall gEUD was computed. Consequently, the bladder wall gEUD is solely determined by the D2cc of the bladder and is not influenced by any other OAR criterion or the CTV doses. *Rectum EUD constraints:* To verify the chosen gEUD of 67.8 Gy for an upper rectal limit, we repeated this constraint derivation procedure for the rectal wall by limiting the total rectum D2cc EQD2 to 70 Gy (4.0 Gy EQD2 per fraction).

All 100 "bladder-limited" plans are maximized to the bladder constraint of 6.0 Gy D2cc per fraction and the corresponding bladder wall gEUDs were recorded and all 100 "rectum-limited" plans are maximized to the rectum dose constraint of 4.0 Gy D2cc and the associated rectum wall gEUDs were recorded. From these data, the variation in bladder and rectal wall gEUD at fixed DVH criteria could be found and the EUD criteria could be derived or verified from these gEUD frequency distributions.

4.2.4. Study 2: safety of EUD constraints in terms of GGE constraints

To test the safety of the CV technique, we investigated the appropriateness of the bladder- and rectum wall EUD constraints in terms of the GGE dose volume criteria. Here we maximized the same dose distribution as in study 1 for each treatment plan, but to the point where the bladder wall gEUD constraint was reached instead of the D2cc constraint. At this point we recorded the corresponding D2cc (and other DVH parameters). This procedure was repeated for the rectal wall by maximizing dose to the rectum gEUD constraint. Thus a single plan was optimized against each of the organs at risk separately.

4.2.5. Study 3: comparison of GGE and CV planning strategies for the entire treatment

Once the robustness of the CV technique in each fraction has been established, the two planning strategies can be compared in terms of OAR and CTV dose for a full treatment. The GGE based plans for each patient and each fraction adhered to the two OAR D2cc constraints (Table 1) per fraction, whichever was met first. The HR-CTV D90 was targeted to be at least 85 Gy in total. No upper CTV constraints were set and dose was maximized until an OAR D2cc constraint was reached. The total dose from IGBT and EBRT was calculated. For the CV technique the OAR EUD constraints were employed that were found earlier. Finally, the two strategies could be compared in terms of D90, D2cc and EUD.

4.3. Results

4.3.1. Prescription constraints

The frequency distributions of the OAR wall EUDs for bladder-limited and rectum-limited plans are displayed in Figure 4.1. Table 4.2 provides a summary of the statistics. The spread of EUDs results from the fact that the gEUD is calculated from the full OAR DVH while D2cc is limited to a small volume. Furthermore, the D2cc volume may often include organ contents and this volume is accepted to be contiguous. Notice further some extreme outliers, which are a consequence of an unfavourable organ location in some fractions that brings large parts of the organ close to the high dose range, but below the D2cc criterion.

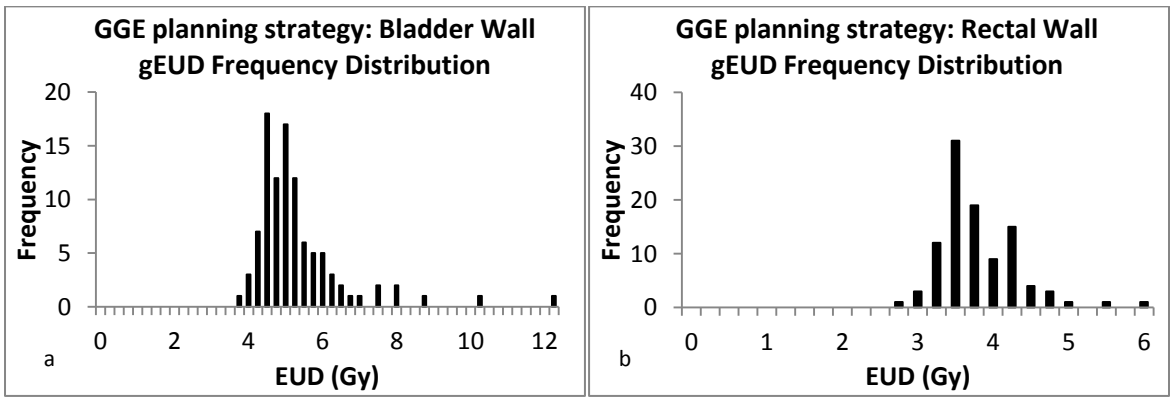

Figure 4.1. GGE planning strategy: Bladder and rectal wall EUD frequency distributions. Frequency distributions of bladder (a) and rectum (b) wall EUDs when dose is maximized to 6 Gy D2cc for bladder and 4 Gy D2cc for rectum.

Table 4.2. Summary of the statistical parameters of the gEUD variations with D2cc and EUD criteria

Statistical measure	*Dose (Gy) GGE strategy*	*Dose (Gy) CV strategy*
Bladder D2cc/gEUD constraint *(planning)*	*6.00*	*5.19*
Bladder Wall gEUD/D2cc		
Mean	*5.19/6.00*	*5.19/6.25*
SD	*1.25/0.00*	*0.00/1.01*
Bladder D0.1 cc		
Mean		*9.97*
SD		*0.85*
Bladder D1cc		
Mean		*7.21*
SD		*0.98*
Rectum D2cc/gEUD constraint *(planning)*	*4.00*	*3.55*
Rectum Wall gEUD/D2cc		
Mean	*3.67/4.00*	*3.55/3.96*
SD	*0.53/0.00*	*0.00/0.49*
Rectum D0.1 cc		
Mean		*5.80*
SD		*0.29*
Rectum D1cc		
Mean		*4.46*
SD		*0.44*

Abbreviations: *SD* standard deviation.

The average gEUD of the rectal wall at a D2cc constraint of 4.0 Gy was 3.67 Gy (±0.53 Gy) which is comparable to the 3.55 Gy from our external beam rectum EUD constraint choice. If this average gEUD was reached in all of the 5 fractions, the NTCP would be ranking at approximately 11%. The average bladder gEUD at a D2cc constraint of 6.0 Gy was 5.19 Gy (±1.25 Gy). The values: rectum wall gEUD ≤ 3.55 Gy and bladder wall gEUD ≤ 5.19 Gy were established as the upper limits for the CV technique. Thus, the total EUD constraint for the bladder wall equals 75.95 Gy.

4.3.2. Safety of EUD criteria in terms of GGE criteria

The safety of these EUD criteria was verified by comparing the D2cc values of CV plans with those obtained from the GGE strategy. Figure 4.2 shows the distribution of D2cc for the OARs with the EUD criteria as determined in the previous section, while Table 4.2

compares the D2cc statistics of the frequency distributions. Figure 4.2 shows that the D2cc distributions are skewed towards lower values and show no outliers towards high doses. The mean of the D2cc distributions closely resembles the GGE criteria, see Table 4.2. For a fractionated treatment, the EUD criteria can thus be considered safe, because even in the worst case (the same organ is dose-limiting in all fractions) the sum of the D2cc of n fractions is likely to be smaller or equal to n times the mean D2cc of the distributions, due to their left-skew. Since the choice of EUD criteria is somewhat arbitrary, we identified those levels, gEUD(x), that result in no more than x% of the 100 treatment plans exceeding the associated GGE criterion, see Table 3.

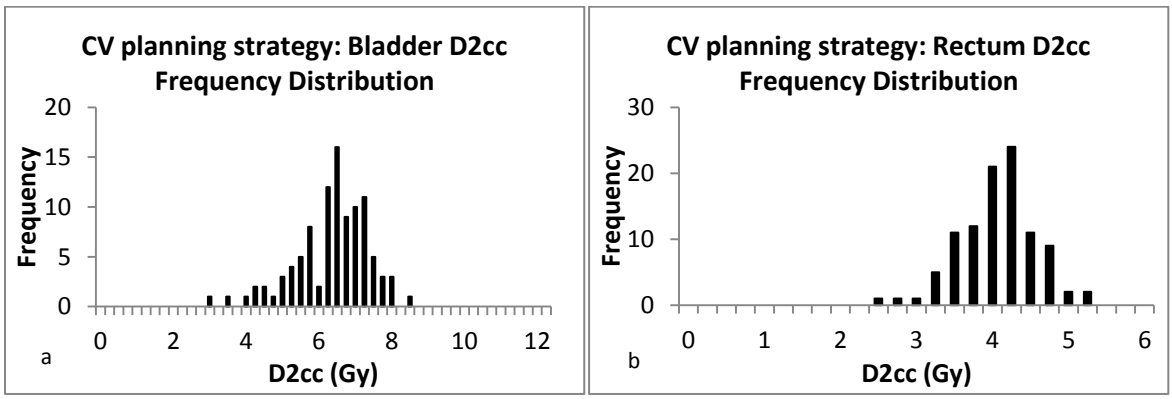

Figure 4.2 CV planning strategy: Bladder and rectal D2cc frequency distributions. Frequency distributions of the bladder (a) and rectum (b) D2ccs when expanding the dose distribution to 5.19Gy EUD for bladder and 3.55Gy EUD for rectum.

Table 4.3 Different gEUD(x) levels resulting in percentage x of treatment fractions with D2cc larger than the GGE constraint and mean and standard deviations of the resulting distributions

x% of treatment fractions	*Rectum gEUD(x) (Gy)*	*Rectum Mean D2cc ± SD (Gy)*	*Bladder gEUD(x) (Gy)*	*Bladder Mean D2cc ± SD (Gy)*
10	*3.12*	*3.49 ± 0.43*	*4.22*	*5.11 ± 0.81*
25	*3.35*	*3.74 ± 0.46*	*4.48*	*5.42 ± 0.86*
48	*3.55*	*3.96 ± 0.49*		
50	*3.58*	*3.99 ± 0.50*	*4.86*	*5.87 ± 0.94*
70			*5.19*	*6.25 ± 1.01*

Abbreviations: *SD* standard deviation.

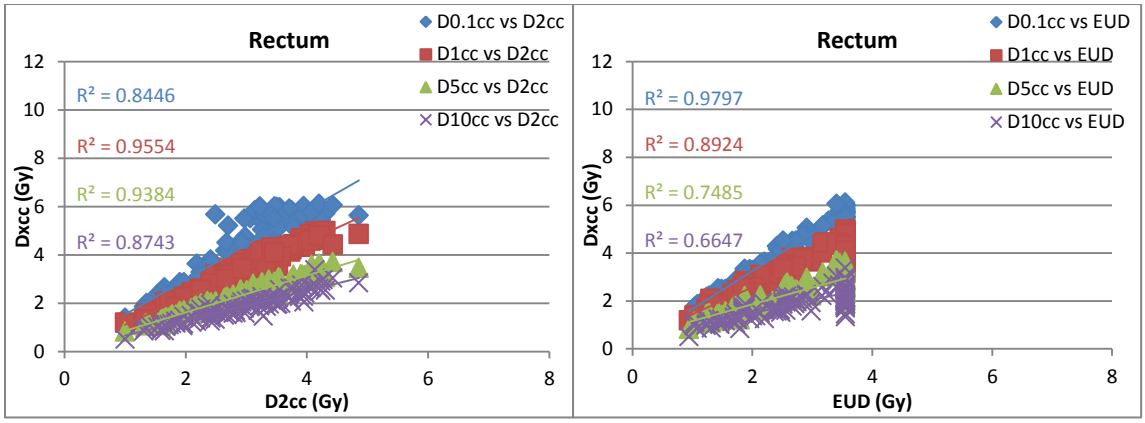

Figure 4.3: Correlation plots of rectal D0.1, 1, 5 and 10cc against D2cc and EUD.

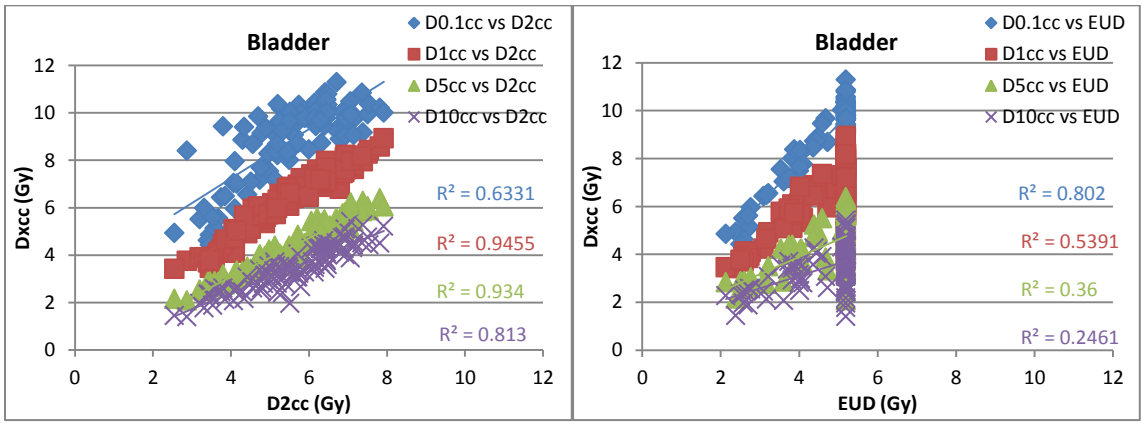

Figure 4.4: Correlation plots of bladder D0.1, 1, 5 and 10cc against D2cc and EUD.

We have also found very good correlations (fig 4.3) between D0.1 cc and D2cc for the rectum (R^2 = 0.84), as well as excellent correlation between D1cc and D2cc for the rectum (R^2 = 0.96). For D5cc and D2cc the correlation was again very good (R^2 = 0.94) and similarly for D10cc and D2cc (R^2 = 0.87). This means that if D2cc can be controlled via the use of the EUD, ulcerations, fistulas and rectal bleeding will also be controlled in terms of small volumes, while dose to larger volumes can also be controlled at the same time with the additional option of a second EUD with a smaller *a* value for complications like constriction and fecal incontinence. Rectal and bladder Dxcc is correlated to EUD in figures 4.3 and 4.4 respectively, and it is seen that D0.1 and D1cc correlates very well with the EUD. Since the volume effect parameter value of *a* was 12 for the rectum it expresses a small volume effect and thus the correlation with larger volumes like D5 and D10cc will become progressively worse. Similarly (fig 4.4), we have found excellent correlation between bladder D1cc and D5cc with D2cc (R^2 = 0.95 and R^2 = 0.93 respectively) as well as D10cc (R^2 = 0.81), but not between D0.1 cc and D2cc (R^2 = 0.63).

The weaker correlation between D0.1cc and D2cc means that maximal bladder doses are not correlated well with D2cc. The most probable reason is the very steep dose gradients that are associated with BT dose distributions, as well as the bladder mostly "folding" around the HR-CTV volume. The consequence is that when D2cc is well controlled, D0.1cc or the maximum dose is not necessarily controlled to the same extent. On the other hand, when comparing D0.1cc with the bladder EUD, excellent correlation is found due to the EUD considering all of the dose points on the DVH from intermediate dose ranges to maximal doses collectively with a volume-effect parameter of a = 8.

The other bladder Dxccs do not correlate as well with the EUD, but this is mostly a result of the bladder EUD constraint that limited further dose increases in most of the treatment fractions. When this dose constraint was reached, it could to some extent have been due to a very high Dx_1 on the one hand and a low Dx_2 on the other, or vice-versa.

4.3.3. Comparison of GGE and CV planning strategies

The two planning approaches were compared in terms of total dose from all 5 IGBT fractions plus the EBRT component for the patients in the study. Very similar total dose parameters for the two techniques were found. Figure 4.5 displays the total dose in the two planning techniques for rectum and bladder D2cc, and HR- and IR-CTV D90. Figure 4.6 displays the rectal and bladder wall gEUDs, and the HR- and IR-CTV EUDs. Table 4 provides the average and standard deviations of their frequency distributions, indicating very similar means.

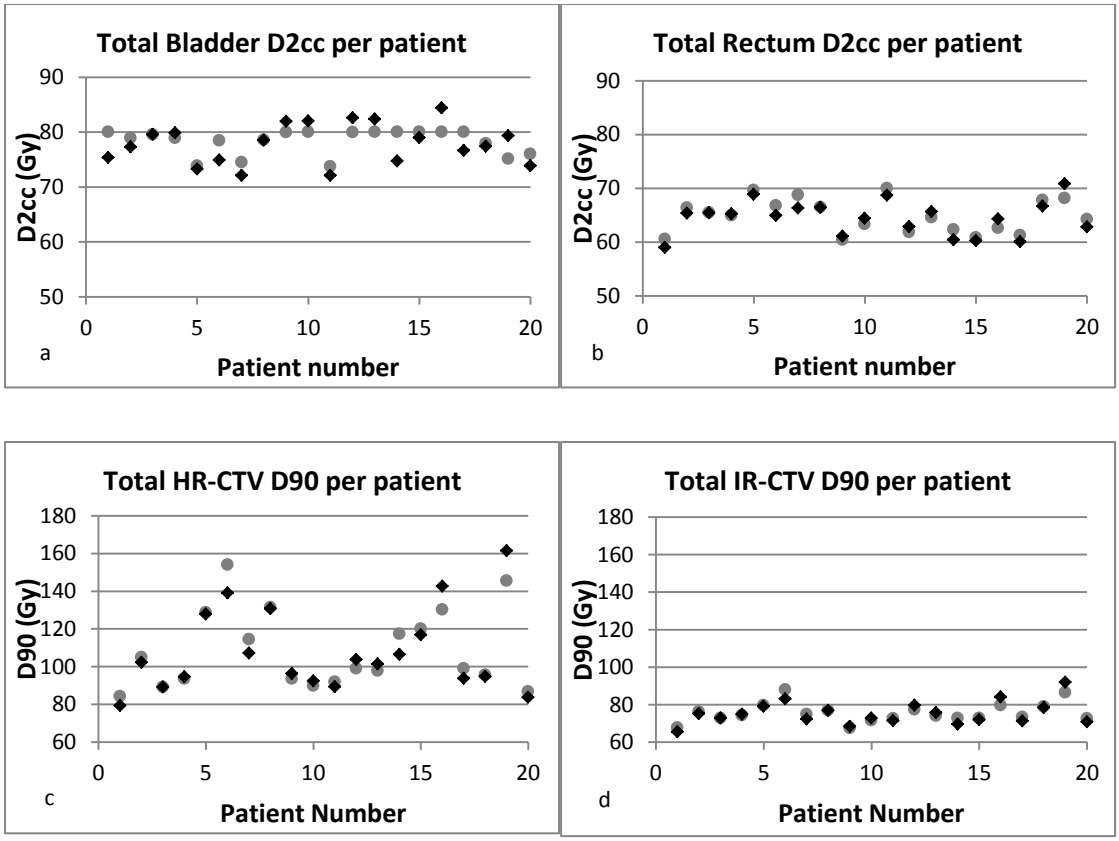

Figure 4.5 Total DVH parameters per patient. Total EQD2 for bladder (a) and rectum (b), and D90 for the HR- (c) and IR-CTV (d). Data are shown for the GGE technique (circles) and the CV technique (diamonds).

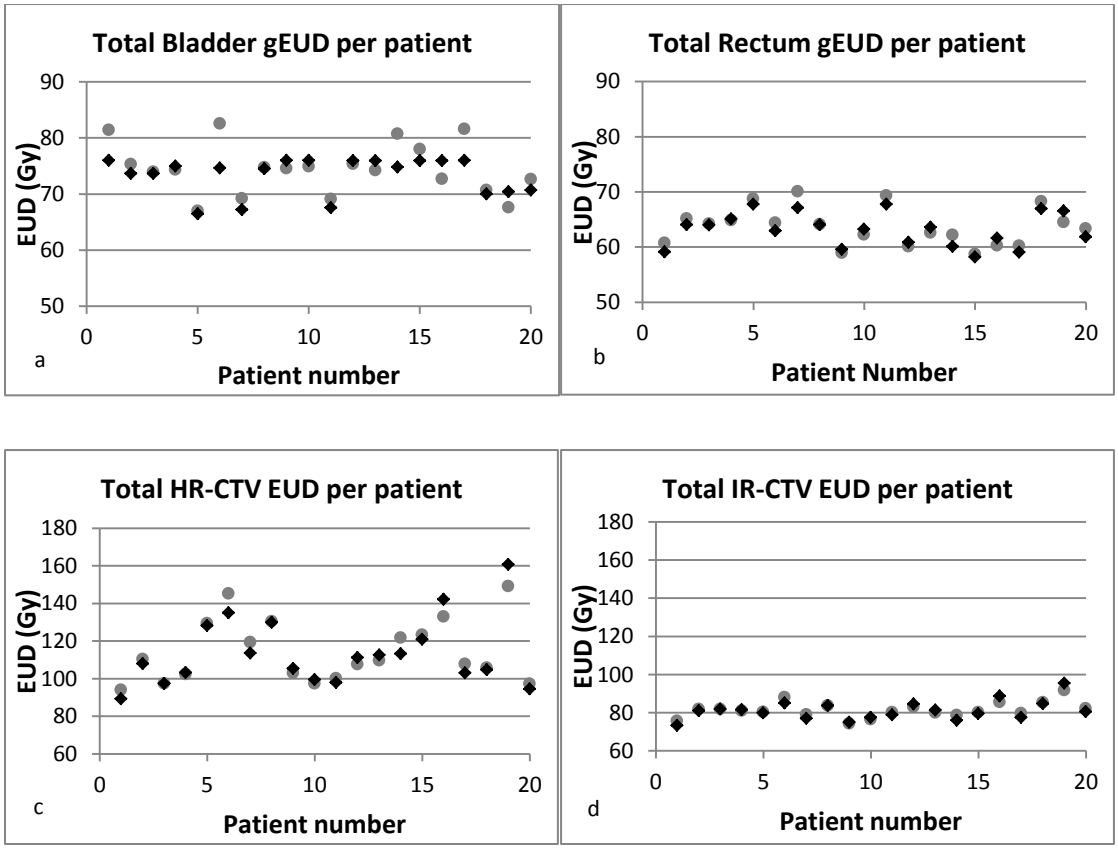

Figure 4.6 Total EUD per patient. Total EUD for bladder (a) and rectal wall (b), HR- (c) and IR-CTV (d). Data are shown for the GGE technique (circles) and the CV technique (diamonds).

Table 4.4 Summary of the statistical variations of the DVH parameters and EUD variations over the full treatment course

Statistical measure	*Technique*	*Rectum*	*Bladder*	*HR-CTV*	*IR-CTV*
		D2cc	***D2cc***	***D90***	***D90***
Mean (Gy)	*GGE*	*64.85*	*78.29*	*108.49*	*75.85*
SD		*3.10*	*2.29*	*20.59*	*5.22*
Mean (Gy)	*CV*	*64.51*	*77.87*	*107.77*	*75.36*
SD		*3.20*	*3.70*	*21.95*	*6.16*
		gEUD	***gEUD***	***EUD***	***EUD***
Mean (Gy)	*GGE*	*63.66*	*74.53*	*114.28*	*81.51*
SD		*3.42*	*4.58*	*16.40*	*4.12*
Mean (Gy)	*CV*	*63.18*	*73.32*	*113.58*	*81.19*
SD		*3.07*	*3.31*	*17.90*	*5.07*

All values in Gy.

Abbreviations: *SD* standard deviation.

4.4. Discussion

We have established OAR gEUD criteria for IGBT treatments that are very comparable to those obtained from the GEC-ESTRO guidelines. EUD constraints can thus be considered a safe and efficient alternative to D2cc criteria.

Compared to a D2cc constraint, which considers an isolated small volume, gEUD has the advantage to consider the dose distribution in the OAR comprehensively and still give high doses a large weight, especially if the volume effect parameter a is significantly greater than 1. For the same reason, it is also less sensitive to contouring and may therefore be a more robust choice if MRI is not available for IGBT planning. To see this, assume that contouring errors lead to errors in the volume of the dose bins of the DVH. Applying the laws of error propagation, we find that the error in D2cc is proportional to the inverse slope of the DVH at D2cc (which tends to be shallow in BT) and proportional to the volume error at that dose bin. In contrast, the error in gEUD is both proportional to the weighted root-mean-square of the volume errors in the dose bins (thus less dependent on a single bin) and smaller by a factor 1/a. This ties in with the intuition, that any kind of average over a number of uncertain quantities (such as EUD) is less uncertain than any single one of these quantities.

It is acknowledged that when the contouring uncertainties affect the maximum dose volume, both D2cc and the gEUD will be impacted. However, the correlation between D2cc and gEUD does not determine the magnitude of the effect. Both gEUD and D2cc will be affected by the contour error in the same direction, but the amplitude of change will be much greater in D2cc, meaning D2cc is much more sensitive. This difference in the amplitude of change will also be more pronounced in the bladder than the rectum due to the smaller bladder volume effect parameter.

The derived EUD criteria depend on the reference D2cc criteria and the volume effect parameter *a*. Since gEUD is a power-law function of dose, it scales with the same factor as D2cc. Small deviations from this law are caused by the EQD2 correction. Within reason, our criteria can therefore be calibrated to different fractionation schemes, i.e. scaled by the ratio of the desired D2cc versus the value used here.

The volume effect parameters (a = 8 for bladder, a = 12 for rectum) are derived from the literature. They do express a very small volume effect of the complications in question, which is also the implicit rationale behind the D2cc criterion. We confirm that the influence of the choice of *a* on our results is small, although safer when $a \geq 8$, since D2cc becomes increasingly smaller with a large *a* at fixed constraint levels; see *a* value

variance in figure 4.7 and table 4.5. In this figure and table, the EUD values were kept constant at 3.55 and 5.19 Gy for rectum and bladder respectively, but the a-value used to calculate the EUD was varied between 8 and 16. It is thus considered safe to err towards large *a* values, i.e. smaller volume effect, when the exact value is not known.

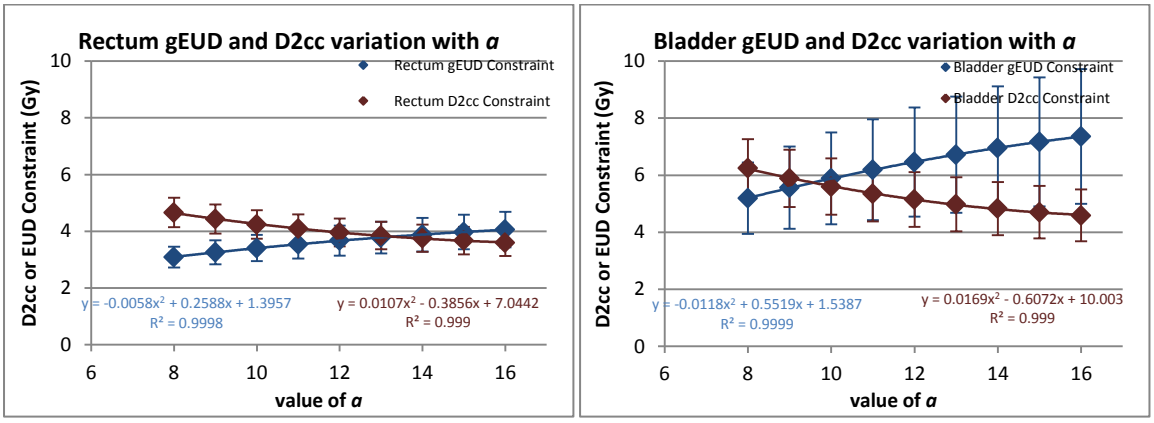

Figure 4.7: Variation in the values of resulting gEUDs for a fixed D2cc constraint in GGE planning as a function of volume effect parameter (a), and resulting D2ccs for a fixed EUD constraint in CV planning as a function of the volume effect parameter for both OARs.

Table 4.5 Variation of gEUD and D2cc for different values of the gEUD volume parameter

Volume parameter (a)	*Rectum gEUD constraint (Gy)**	*Rectum D2cc (Gy)#*	*Bladder gEUD constraint (Gy)***	*Bladder D2cc (Gy)##*
8	*3.09 ± 0.37*	*4.66 ± 0.52*	*5.19 ± 1.25*	*6.25 ± 1.01*
9	*3.26 ± 0.42*	*4.43 ± 0.51*	*5.56 ± 1.44*	*5.89 ± 1.00*
10	*3.41 ± 0.46*	*4.24 ± 0.50*	*5.89 ± 1.61*	*5.60 ± 0.99*
11	*3.54 ± 0.50*	*4.09 ± 0.50*	*6.19 ± 1.77*	*5.35 ± 0.97*
12	*3.67 ± 0.53*	*3.96 ± 0.49*	*6.46 ± 1.91*	*5.15 ± 0.96*
13	*3.78 ± 0.56*	*3.85 ± 0.49*	*6.72 ± 2.04*	*4.98 ± 0.95*
14	*3.88 ± 0.59*	*3.75 ± 0.48*	*6.95 ± 2.16*	*4.83 ± 0.93*
15	*3.97 ± 0.61*	*3.67 ± 0.48*	*7.17 ± 2.26*	*4.70 ± 0.92*
16	*4.06 ± 0.63*	*3.60 ± 0.47*	*7.36 ± 2.36*	*4.59 ± 0.91*

*Calculated with a 4.0Gy rectum D2cc constraint.

** Calculated with a 6.0Gy bladder D2cc constraint.

#Calculated with a 3.55Gy (a = 12) rectum gEUD constraint.

Calculated with a 5.19Gy (a = 8) bladder gEUD constraint.

Occasionally, the use of EUD criteria for IGBT is safer than D2cc. Observe the outliers in Figure 4.1 which are caused by rare unfavourable organ geometries that bring a lot of the organ volume close to the high dose region. In contrast, EUD criteria do not produce excessive D2cc values because of their mathematical construction, which gives very high weights to sub-volumes with a high dose. From Table 4.2, the average D2cc for the OARs, when dose is maximized to each OAR's gEUD constraint, is virtually the same as the GGE-D2cc that was used to derive the EUD criteria. Although there is some dispersion of D2ccs around this average, none of the D2ccs were found to be unacceptably high. If the EUD constraints are reduced, as shown in Table 4.3, to decrease D2cc constraint violations, small changes in EUD result in large reductions in D2cc and a smaller variance of D2cc. Our results suggests that a 6 to 8% reduction in OAR gEUDs produce more than 25% fewer treatment plans that could violate a D2cc constraint. Since we know that D0.1 cc and D1cc also correlates well with D2cc, CV plans that control D2cc would subsequently control the resultant D0.1 cc and D1cc DVH parameters as well.

The D2ccs of the CV technique are evaluated against data from other studies in Table 4.6, which includes D0.1 and D1cc endpoints. The comparison shows that maximizing OAR dose to the EUD constraints does not result in OAR over-dosage. The total average bladder and rectal D0.1, D1 and D2cc when OAR dose is maximized to the EUD constraints falls in a lower range than those presented by Georg et al. for LENT/SOMA

scores of 1–4 and VRS scores of 3–5 [9]. The population averages in their studies [9, 10] are comparable to the dose levels in this study. We have also found that especially the rectal doses in this study are in the lower range of toxicity rates for G2-4 side effects. Based on the Georg et al. studies [9, 10, 35], our criteria relate to a probability of finding G2-G4 side effects in the range of 5-10%.

Table 4.6. Summary of the average DVH parameters in total dose (Gy) of the CV treatment technique, compared to other published values

DVH parameter	***CV***	***Georg et al.*** [9]	***Georg et al.*** [10]	***Levitchi et al.*** [33]	***Jürgenliemk-Schulz et al.*** [38]	***Jürgenliemk-Schulz et al.*** [39]	***Nesvacil et al.*** [40]	***Lindegaard et al.*** [41]
Method	*HDR*	*HDR*	*HDR*	*PDR*	*PDR*	*HDR/PDR*	*HDR*	*PDR*
Rectum								
D0.1 cc	*79 ± 1*	*88 ± 10**	*83 - 132[a]*	*83[b]*				
		*81 ± 13***	*86 ± 27***	*65 ± 15***				*74 ± 9***
D1cc	*72 ± 2*	*76 ± 7**	*71 - 87[a]*					
		*70 ± 9***	*69 ± 14***					*69 ± 6***
D2cc	*70 ± 2*	*72 ± 6**	*67 - 78[a]*	*68[b]*				
		*66 ± 8***	*65 ± 12***	*57 ± 8***	*66 ± 6***	*54 ± 2**[c]*	*57 ± 6***	*67 ± 6***
						*69 ± 2**[d]*		
Bladder								
D0.1 cc	*100 ± 3*		*61 - 178[a]*	*109[b]*				
			*162 ± 75***	*78 ± 22***				*86 ± 12***
D1cc	*86 ± 3*		*71 - 116[a]*					
			*108 ± 31***					*77 ± 8***
D2cc	*81 ± 3*		*70 – 101[a]*	*72[b]*	*81 ± 6***	*53 ± 2**[c]*	*76 ± 9***	
			*95 ± 22***	*64 ± 11***		*101 ± 11**[d]*		*73 ± 6***

Abbreviations: *SD* standard deviation, *HDR* high dose rate, *PDR* pulsed dose rate.

*Clinical symptoms (LENT/SOMA) score 1–4 and Rectoscopic changes (VRS) score 3–5. **Population average; no interstitial needles.

[a]5% - 10% probability of G2-G4 side effects (dose range not shown). [b]Approximately 10% probability of G2-G4 toxicity (dose range not shown).

[c]Small volume tumour. [d]Large volume tumour.

These dose endpoints are also very comparable with studies where large HR-CTV volumes were investigated and no interstitial needles were used. As shown in the study of Jürgenliemk-Schulz et al. [36], we expect that interstitial needles would decrease the EUD of OARs in large tumour volume cases as well. For bladder, we found good correspondence with the results of Levitchi et al. [37], Jürgenliemk-Schulz et al. [36, 38], Nesvacil et al. [39] and Lindegaard et al. [40]. Since there were no upper dose boundaries for the CTV, the CTV dose is expected to spread widely, driven solely by the OAR geometries and relative positions. From Figures 4.5 and 4.6 it is clear that the CV technique does not result in under-dosage of the CTVs.

An important aspect of gEUD is, that it allows an easy worst-case estimate of the gEUD of the total accumulated treatment dose by virtue of Jensen's inequality [41, 42]. The sum of EUDs of each treatment fraction is always greater or equal (for OARs; smaller or equal for targets) to the EUD of the sum of the fraction doses:

$$EUD\left(E\left[\tilde{D}\right]\right) \leq E\left[EUD\left(\tilde{D}\right)\right] = E[EUD(D)] \qquad (4.4)$$

where $E[]$ is the sum over all fractions, $\tilde{D}$ is the dose of each fraction, warped to reference geometry, and D the dose as computed for the patient geometry of the particular fraction. Hence, the left hand side is the EUD of the properly accumulated total dose, while the right hand side is the sum of the EUDs as computed for each fraction individually. For target volumes, the inequality reverses. This estimate is of particular importance for pelvic radiotherapy, where deformable registration of images is difficult to perform reliably. Hence, EUD addition gives a worst case scenario for OARs and CTV without the need for deformable image registration and dose warping [42].

Andersen et al. (2013) described the differences between a D2cc worst case estimate for the bladder and when deformable image registration was used to calculate the total accumulated dose. They reported dose difference ranges of -1.5 to 7.9% and 0.3 to 20% with medians of 1.1% and 4.4% for D2cc and D0.1cc, respectively. Their mean dose deviation was 1.5 ± 1.8% and 5.2 ± 4.2% for D2cc and D0.1cc, respectively. Deviations greater than 5% relative to DIR was found in 2% and 38% of the patients at the D2cc and D0.1cc levels, respectively. Our results in chapter 2 where the average/total EUD was compared to the properly warped doses, amount to a dose difference range of -3.5 to 2.3% with a median of -0.5%. Our mean dose deviation was -0.3 ± 2.0%. This accuracy in the worst case estimate establishes a safety mechanism in dose accumulation and can be performed quickly and easily.

D2cc is not a convex function of dose and is not additive in a strict sense, so that further assumptions about the dose distribution have to be made. Jensen's inequality also applies to maximum and minimum dose, so that, if D2cc and D90 have a strong correlation to the former, the inequality holds for the latter approximately "by proxy". The versatility of EUD summation as worst case estimate extends to the addition of very heterogeneous OAR EBRT doses, for example lymph node boosts. Finally, because there is a variability in reported dose-volume cut-offs for OARs in IGBT [9,35,37,43] and these also differ from cut-offs in EBRT, EUD is helpful in combining the experience in both areas and relating it to the LKB model [44]. Conversely, documented brachytherapy toxicity rates can be useful for focused dose escalation in EBRT, for example dose painting.

4.5. Conclusions

Concluding, a GEC-ESTRO-like IGBT plan adaption is feasible with EUD criteria, instead of D2cc criteria. Because of the mathematical construction of gEUD, and the fact that it considers the organ volume comprehensively, it is inherently more robust against contouring uncertainties. This could make gEUD a better choice than D2cc if IGBT has to be performed on CT, instead of MR, images. The summation of EUDs per treatment fraction gives a reliable worst case estimate of the total treatment dose, which opens possibilities for safe dose escalation in IGBT or simultaneous integrated boost in EBRT.

4.6. References

1. Kirisits C, Pötter R, Lang S, Dimopoulos J, Wachter-Gerstner N, Georg D: Dose and volume parameters for MRI-based treatment planning in intracavitary brachytherapy for cervical cancer. Int J Radiat Oncol Biol Phys 2005;62:901–911.

2. Barillot I, Reynaud-Bougnoux A: The use of MRI in planning radiotherapy for gynaecological tumours. Cancer Imaging 2006;6:100–106.

3. Pötter R, Kirisits C, Fidarova E, et al: Present status and future of high-precision image guided adaptive brachytherapy for cervix carcinoma. Acta Oncol 2008;47:1325–1336.

4. Viswanathan A, Erickson B: Three-dimensional imaging in gynecologic brachytherapy: a survey of the American Brachytherapy Society. Int J Radiat Oncol Biol Phys 2010;76:104–109.

5. Haie-Meder C, Pötter R, Van Limbergen E, et al: Recommendations from Gynecological (GYN) GEC-ESTRO Working Group (I): Concepts and terms in 3D image based 3D treatment planning in cervix cancer brachytherapy with emphasis on MRI assessment of GTV and CTV. Radiother Oncol 2005;74:235–245.

6. Pötter R, Haie-Meder C, Van Limbergen E, et al: Recommendations from Gynecological (GYN) GEC ESTRO working group (II): Concepts and terms in 3D image-based treatment planning in cervix cancer brachytherapy—3D dose volume parameters and aspects of 3D image-based anatomy, radiation physics, radiobiology. Radiother Oncol 2006;78:67–77.

7. Lang S, Nesvacil N, Kirisits C, et al: Uncertainty analysis for 3D image-based cervix cancer brachytherapy by repetitive MR imaging: Assessment of DVH-variations between two HDR fractions within one applicator insertion and their clinical relevance. Radiother Oncol 2013;107:26–31.

8. Mohamed S, Nielsen S, Fokdal L, Pedersen EM, Lindegaard JC, Tanderup K: Feasibility of applying a single treatment plan for both fractions in PDR image guided brachytherapy in cervix cancer. Radiother Oncol 2013;107:32–38.

9. Georg P, Kirisits C, Goldner G, et al: Correlation of dose-volume parameters, endoscopic and clinical rectal side effects in cervix cancer patients treated with definitive radiotherapy including MRI-based brachytherapy. Radiother Oncol 2009;91:173–180.

10. Georg P, Pötter R, Georg D, et al: Dose effect relationship for late side effects of the rectum and urinary bladder in magnetic resonance image-guided adaptive cervix cancer brachytherapy. Int J Radiat Oncol Biol Phys 2012;82:653–657.

11. Pötter R, Georg P, Dimopoulos J, et al: Clinical outcome of protocol based image (MRI) guided adaptive brachytherapy combined with 3D conformal radiotherapy with or without chemotherapy in patients with locally advanced cervical cancer. Radiother Oncol 2011;100:116–123.

12. Dimopoulos J, Lang S, Kirisits C, et al: Dose–volume histogram parameters and local tumour control in Magnetic Resonance Image–Guided cervical cancer brachytherapy. Int J Radiat Oncol Biol Phys 2009;75:56–63.

13. Dimopoulos J, Pötter R, Lang S, et al: Dose–effect relationship for local control of cervical cancer by magnetic resonance image-guided brachytherapy. Radiother Oncol 2009;93:311–315.

14. Lee L, Damato A, Viswanathan A: Clinical outcomes of high-dose-rate interstitial gynecologic brachytherapy using real-time CT guidance. Brachytherapy 2013;12:303–310.

15. Tanderup K, Nesvacil N, Pötter R, Kirisits C: Uncertainties in image guided adaptive cervix cancer brachytherapy: Impact on planning and prescription. Radiother Oncol 2013;107:1–5.

16. Viswanathan A, Dimopoulos J, Kirisits C, Berger D, Pötter R: Computed tomography versus magnetic resonance imaging based contouring in cervical cancer brachytherapy: Results of a prospective trial and preliminary guidelines for standardized contours. Int J Radiat Oncol Biol Phys 2007;68:491–498.

17. Charra-Brunaud C, Harter V, Delannes M, et al: Impact of 3D image-based PDR brachytherapy on outcome of patients treated for cervix carcinoma in France: Results of the French STIC prospective study. Radiother Oncol 2012;103:305–313.

18. Eskander RN, Scanderbeg D, Saenz C, Yashar C, Brown M: Comparison of computed tomography and magnetic resonance imaging in cervical cancer brachytherapy target and normal tissue contouring. Int J Gynecol Cancer 2010;20:47–53.

19. Hegazy H, Pötter R, Kirisits C, Berger D, Federico M, Sturdza A, Nesvacil N: High-risk clinical target volume delineation in CT-guided cervical cancer brachytherapy:

Impact of information from FIGO stage with or without systematic inclusion of 3D documentation of clinical gynecological examination. Acta Oncol 2013;52:1345–1352.

20. Andersen E, Muren L, Sørensen T, et al: Bladder dose accumulation based on a biomechanical deformable image registration algorithm in volumetric modulated arc therapy for prostate cancer. Phys Med Biol 2012;57:7089–7100.

21. Andersen E, Noe K, Sørensen T, et al: Simple DVH parameter addition as compared to deformable registration for bladder dose accumulation in cervix cancer brachytherapy. Radiother Oncol 2013;107:52–57.

22. Niemierko A: Reporting and analyzing dose distributions: A concept of equivalent uniform dose. Med Phys 1997;24:103–110.

23. Söhn M, Yan D, Liang J, Meldolesi E, Vargas C, Alber M: Incidence of late rectal bleeding in high-dose conformal radiotherapy of prostate cancer using equivalent uniform dose–based and dose–volume–based normal tissue complication probability models. Int J Radiat Oncol Biol Phys 2007;67:1066–1073.

24. Wu Q, Mohan R, Niemierko A, Schmidt-Ullrich R: Optimization of intensity-modulated radiotherapy plans based on the equivalent uniform dose. Int J Radiat Oncol Biol Phys 2002;52:224–235.

25. Schwarz M, Lebesque J, Mijnheer B, Damen E: Sensitivity of treatment plan optimization for prostate cancer using the equivalent uniform dose (EUD) with respect to the rectal wall volume parameter. Radiother Oncol 2004;73:209–218.

26. Lyman J: Complication probability as assessed from dose–volume histograms. Radiat Res 1985;104:S13–19.

27. Burman C, Kutcher G, Emami B, Goitein M: Fitting of normal tissue tolerance data to an analytic function. Int J Radiat Oncol Biol Phys 1991;21:123–135.

28. Mohan R, Mageras GS, Baldwin B, et al: Clinically relevant optimization of 3-D conformal treatments. Med Phys 1992;19:933–944.

29. Alber M, Belka C: A normal tissue dose response model of dynamic repair processes. Phys Med Biol 2006;51:153–172.

30. Dale R, Sinclair J: Radiobiological calculations in routine radiotherapy. In Radiobiological Modelling in Radiation Oncology. Edited by Dale R, Jones B. London: British Institute of Radiology;2007:158–168.

31. Niemierko A: A generalized concept of equivalent uniform dose [Abstract]. Med Phys 1999;26:1100.

32. Soukup M, Söhn M, Yan D, Liang J, Alber M: Study of robustness of IMPT and IMRT for prostate cancer against organ movement. Int J Radiat Oncol Biol Phys 2009;75:941–949.

33. Bolstad-Hysing L, Skorpen T, Alber M, Fjellsbø LB, Helle SI, Muren LP: Influence of organ motion on Conformal vs. Intensity-modulated pelvic radiotherapy for prostate cancer. Int J Radiat Oncol Biol Phys 2008;71:1496–1503.

34. Viswanathan A, Yorke E, Marks L, Eifel PJ, Shipley WU: Radiation dose–volume effects of the urinary bladder. Int J Radiat Oncol Biol Phys 2010;76:S116–S122.

35. Georg P, Lang S, Dimopoulos J, et al: Dose–volume histogram parameters and late side effects in magnetic resonance image–guided adaptive cervical cancer brachytherapy. Int J Radiat Oncol Biol Phys 2011;79:356–362.

36. Jürgenliemk-Schulz I, Tersteeg R, Roesink J, et al: MRI-guided treatment-planning optimization in intracavitary or combined intracavitary/interstitial PDR brachytherapy using tandem ovoid applicators in locally advanced cervical cancer. Radiother Oncol 2009;93:322–330.

37. Levitchi M, Charra-Brunaud C, Quetin P, et al: Impact of dosimetric and clinical parameters on clinical side effects in cervix cancer patients treated with 3D pulse-dose rate intracavitary brachytherapy. Radiother Oncol 2012;103:314–321.

38. Jürgenliemk-Schulz I, Lang S, Tanderup K, et al: Variation of treatment planning parameters (D90 HR-CTV, D2cc for OAR) for cervical cancer tandem ring brachytherapy in a multicentre setting: Comparison of standard planning and 3D image guided optimization based on a joint protocol for dose–volume constraints. Radiother Oncol 2010;94:339–345.

39. Nesvacil N, Pötter R, Sturdza A, Hegazy N, Federico M, Kirisits C: Adaptive image guided brachytherapy for cervical cancer: A combined MRI-/CT-planning technique with MRI only at first fraction. Radiother Oncol 2013;107:75–81.

40. Lindegaard J, Tanderup K, Nielsen S, Haack S, Gelineck J: MRI-guided 3D optimization significantly improves DVH parameters of pulsed-dose-rate brachytherapy in locally advanced cervical cancer. Int J Radiat Oncol Biol Phys 2008;71:756–764.

41. Jensen J: Sur les fonctions convexes et les inegalites entre les valeurs moyennes. Acta Math 1906;30:175–93.

42. Sobotta B, Söhn M, Shaw W, Alber M: On expedient properties of common biological score functions for multi-modality, adaptive and 4D dose optimization. Phys Med Biol 2011;56:N123–129.

43. Thibault I, Lavallée M, Aubin S, Laflamme N, Vigneault E: Inverse-planned gynecologic high-dose-rate interstitial brachytherapy: Clinical outcomes and dose volume histogram analysis. Brachytherapy 2012;11:181–191.

44. Michalski J, Gay H, Jackson A, Tucker S, Deasy J: Radiation dose-volume effects in radiation-induced rectal injury. Int J Radiat Oncol Biol Phys 2010;76:S123–129.

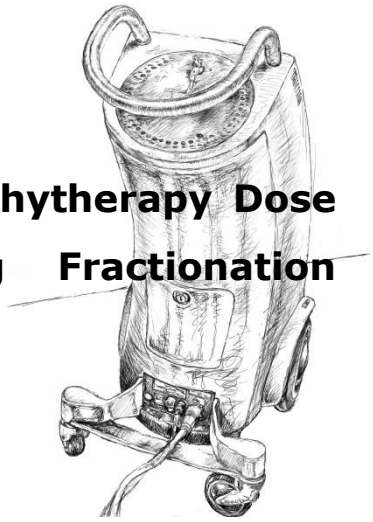

Chapter 5: Image Guided Adaptive Brachytherapy Dose Escalation for Cervix Cancer using Fractionation Compensation

This chapter includes work by the author that was submitted for consideration for publication in the Radiotherapy and Oncology (Green) Journal

5.1. Introduction

Image guided adaptive brachytherapy (IGABT) considers normal organ positional and geometrical variations, captured by daily magnetic resonance imaging [1-4], computed tomography or ultrasound imaging [5-7]. The adaptation results in improvements in both tumour control and normal tissue complication [1-3, 8-11]. The lower toxicity achieved by IGABT allows escalation of CTV dose with suitable Dose Volume Histogram (DVH) constraints for organs at risk (OARs) [12-13]. For the same purpose, Equivalent Uniform Dose (EUD) constraints have been established [14]. Dose escalation studies demonstrate local control rates above 85%, even for advanced disease, and might also favourably impact cancer specific survival and overall survival [1, 2, 8]. Doses of more than 90 Gy to 90% of the High Risk-CTV (HR-CTV D90) [15] result in better tumour control for long periods after treatment while significantly influencing distant metastasis free survival at acceptable low treatment related morbidity.

At its core, IGABT relinquishes constant fraction sizes to seize the opportunity of a favourable organ geometry for dose escalation. This tendency towards higher doses is customarily kept in check by strict per-fraction constraints for OARs. However, especially in the case of several (3-5) IGABT fractions, an alternative to constant per-fraction constraints are constraints on the total delivered dose, which allow that OARs may receive higher than average dose in one fraction, if that can be compensated in other fractions. Such compensation in combination with total dose constraints requires keeping record of the delivered dose, and a prediction about the dose that can be delivered in the remaining fractions. Therefore, a number of schemes are possible, depending on the assumptions behind the prediction. One such concept was proposed by Lang et al. (2007) who suggested that the difference between the total dose constraint and the already delivered dose be equally split between the remaining fractions and become the new per-fraction dose constraint. In terms of dose compensation, this is a relatively

conservative approach because it hedges the bets on a favourable geometry at the future fractions, instead of reaping the maximum benefit at the current fraction. This thinking originates from the observation that geometry changes are predominantly due to long term time trends rather than randomness, and therefore the scheme can afford to be optimistic and modest. In this manuscript, we employ the scheme suggested by Lang et al. to a population of 20 cervix patients to explore its benefits compared to constant per-fraction constraints of various natures. Less optimistic and therefore greedier schemes can be imagined and will be discussed briefly. Naturally, the efficacy of the compensation scheme depends on the number of IGABT fractions. For this reason, fractionation compensation schemes with between 2 to 5 fractions were evaluated.

One fundamental difficulty of combined external beam radiotherapy (EBRT) and IGABT is the correct addition of dose distributions, which has immediate implications for dose compensation. Per-fraction constraints are obviously independent of the delivered dose, but fractionation compensation schemes ideally require, that the delivered dose be computed in each patient geometry and accumulated via deformable image registration to a reference geometry (dose warping). In addition, intensity modulated radiotherapy (IMRT) is being used more frequently [17-19], complicating the addition of EBRT and IGABT dose in OARs due to more irregular dose distributions. Dose warping for OARs in the pelvis and a shrinking target volume is a largely unsolved problem and currently associated with substantial uncertainties. For the typical high-dose/small-volume DVH constraints employed in IGABT, it has been suggested that doses at a given volume of e.g. 2cc, say, are simply added for EBRT and all fractions of IGABT [20-23]**.** However, this can only be an approximation and can err on both sides; both total dose constraint violations and diminished compensation potential could be the consequences. In contrast, it has been shown [14, 24] that gEUD (for a >= 1) has the advantageous mathematical property to afford a rigorous worst-case estimate for the gEUD of the warped and accumulated dose, computed as the sum of the gEUD of the fraction doses. Hence, in the present planning study, we employ EUD in two roles: as a safeguard for dose compensation performed with DVH constraints, and as an alternative to DVH constraints for the fractionation compensation.

5.2. Methods and Materials

We used the image datasets of 20 patients treated with CT-based IGBT for carcinoma of the cervix in this retrospective planning study. Treatment consisted of 25 fractions EBRT of 2 Gy via a 4-field box technique without midline shielding, prescribed to the ICRU reference point. Five concomitant high dose rate (HDR) IGBT treatment fractions were given, starting in the third week of EBRT. Overall treatment time was less than 44 days.

The average delivered dose was 4.7 ± 0.8 Gy to D90 of the HR-CTV. IGBT was delivered using a standard magnetic resonance imaging compatible tandem-ring applicator (Nucletron®) and the implantations were done under conscious sedation without vaginal packing. Treatment plans were generated for each fraction. The distribution of FIGO Stage Classification for local tumour stage was IIB = 5, IIIB = 12 and IVa = 3 patients. Concomitant weekly Cisplatin-based chemotherapy (5 – 6 x 25 mg/m^2 body surface area) was also administered during this time. The average HR-CTV volume at the first brachytherapy treatment was 49.0 ± 21.0 cc and shrunk on average by 33.8% over the full course of treatment.

5.2.1. Contouring and dose constraints

Tumour and organ at risk (OAR) contours were generated for each treatment based on the Gyn GEC-ESTRO WG I guidelines [15]. They included HR-CTV and IR-CTV for tumour, and rectum and bladder outer walls plus content as OARs. The HR-CTV consisted of the whole cervix and macroscopic extent of the disease at the time of IGBT. The initial disease extent at diagnosis determined the IR-CTV which encompassed the HR-CTV. The same set of recommendations was followed for the OAR walls plus content and the walls without content were contoured additionally.

Dose constraints were based on DVH points [20] of minimum dose received in 2cc of the maximum dose regions of the OAR outer wall plus content (D2cc) and additional D0.1cc and D1cc. Dose to 90% (D90) of the HR-CTV was also recorded. Full DVHs of each treatment plan was available for analysis and the EUD [25] of the HR-CTV was calculated, as was the gEUD [25, 26] of the OAR *walls*. We have previously established that gEUD dose constraints are equivalent to DVH-based constraints of D2cc for IGABT [14]. The same OAR total gEUD constraints of 67.8 Gy (3.55 Gy per fraction) and 75.95 Gy (5.19 Gy per fraction), for rectum and bladder respectively, were used in this study and all doses were converted to the 2 Gy equivalent dose (EQD2) [20, 27]. All dose values are given in 2 Gy equivalents unless otherwise stated.

5.2.3. Dose prescription and IGABT treatment planning

The conventional, constant per-fraction constrained, IGABT treatment plans were hand-optimized to attain a total goal dose of 90 Gy to the HR-CTV D90. It consisted of 50 Gy from the EBRT component plus an IGABT goal of 40 Gy. Planning started from a standard plan dose distribution in each fraction and performing dose optimization to the HR-CTV constraint dose, while considering the optimal OAR dose per fraction (discussed below). Graphical optimization by isodose line dragging was performed for each CT and

contour combination of the day, thus adapting dose to a shrinking HR-CTV and minimizing OAR dose by as much as possible.

5.2.4. Choosing the optimal OAR dose per fraction

The concept of IGABT is to generate a plan of the day using OAR constraints per fraction. One or more of the fractional OAR constraints could restrict the tumour dose, while other OAR constraints might not have been reached in the same treatment fraction. Alternatively, the tumour dose constraint could be reached without the OARs being at their constraints, or conversely only at the expense of one or more OAR constraint violations. The scenario might change in a subsequent fraction. Since OARs exhibit different levels of mobility, have different geometrical configurations and vary in spatial position from day to day in relation to the tumour volume, there exists the possibility of adjusting OAR constraints over the course of treatment to reach a total treatment constraint, which we define as "fractionation compensation".

We briefly repeat the scheme of Lang et al. (2007) to introduce the notation used here. We distinguish between the dose distribution per fraction d_i, which is evaluated by a dose metric (E.g. D2cc, EUD, gEUD) to yield m_i. Each constraint c_i is expressed in the corresponding metric. Sums over multiple fractions are expressed like this:

$$\sum_{i=1}^{n} d_i = D_n \qquad (5.1a)$$

$$\sum_{i=1}^{n} m_i = M_n \qquad (5.1b)$$

$$\sum_{i=1}^{n} c_i = C_n \qquad (5.1c)$$

where we explicitly assume idealized dose warping, conversion to 2 Gy equivalence and accumulation with respect to the dose distribution (5.1a), and simple summation of numbers for metrics and constraints (5.1b,c). Given j treatment fractions have been delivered, we determine c_{j+1} such that after n fractions M_n equals the total dose constraint $\boldsymbol{C_n}$:

$$\boldsymbol{C_n} = M_j + (n-j)c_{j+1} \quad , \qquad (5.2)$$

therefore

$$c_{j+1} = \frac{\boldsymbol{C_n} - M_j}{n-j} \quad . \qquad (5.3)$$

Constraints for OARs and the CTV D90 may not be achievable simultaneously. In this case, the target constraint always has priority, i.e. the plan will violate some OAR constraints. These constraint violations may be

compensated for in later fractions, so that they do not necessarily result in a violation of the total constraint. Figure 1 displays a flow chart of the compensation scheme employed here.

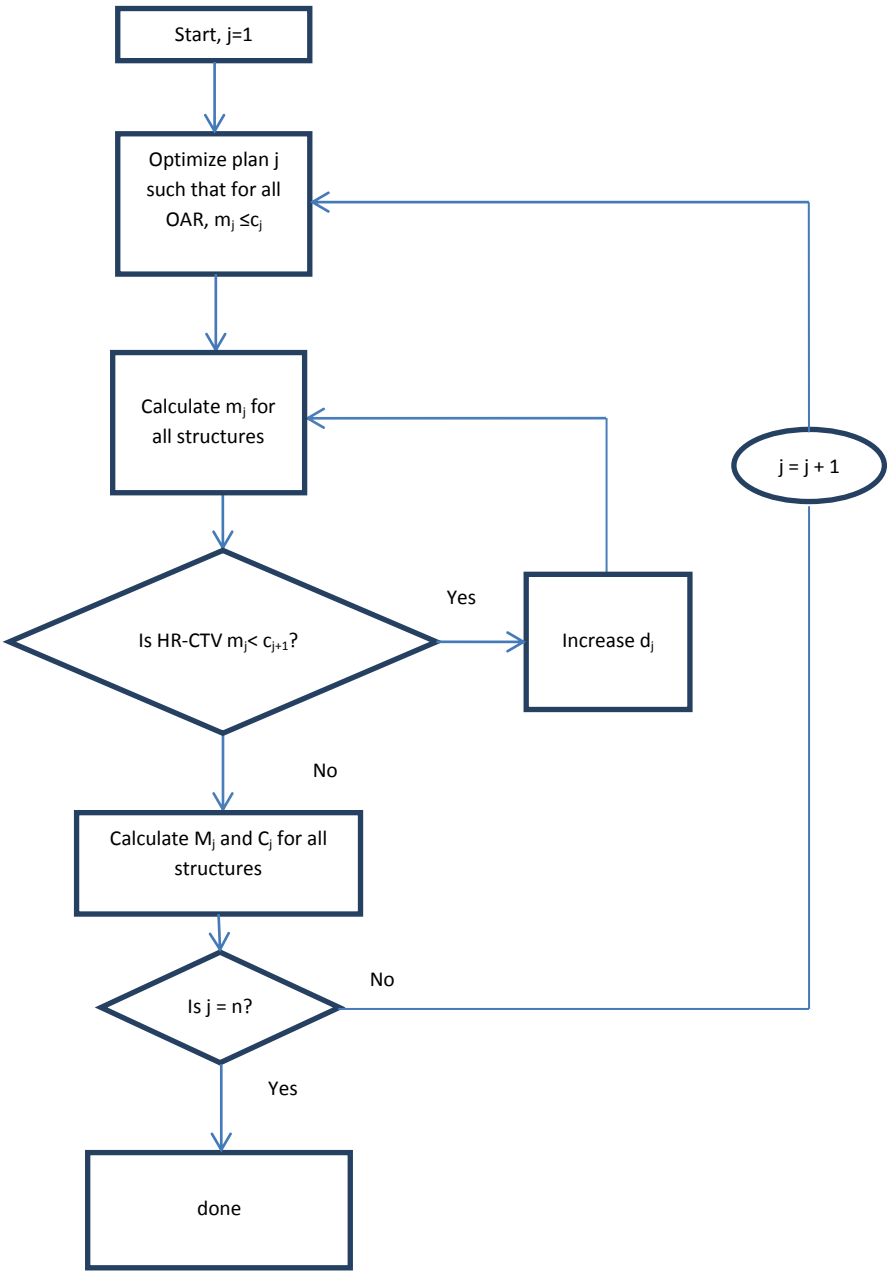

Figure 1: A Flow chart representing the algorithm for the fractionation compensation planning strategy.

To investigate the effect of the number of treatment fractions on the efficacy of fractionation compensation, several fractionation schedules were investigated that are commonly used in the brachytherapy community [28], based on the corresponding fraction's image datasets. These schedules are detailed in table1.

Table 5.1: Per-fraction IGABT OAR and HR-CTV constraints for various treatment fraction numbers. Dose values are EQD2.

Volume of interest	Per-fraction Dose Constraints (Gy)				
	Metric type	2 fractions	3 fractions	4 fractions	5 fractions
Rectum	D2cc	10	6.7	5	4
	gEUD	8.9	5.9	4.4	3.6
Bladder	D2cc	15	10	7.5	6
	gEUD	13.0	8.7	6.5	5.2
HR-CTV	D90	20	13.3	10	8
	Total Dose Constraints (Gy)				
	Metric type	All Fractionation Schedules			
Rectum	D2cc	20.0			
	gEUD	17.8			
Bladder	D2cc	30.0			
	gEUD	26.0			
HR-CTV	D90	40.0			

The precise accumulation of delivered doses is currently too cumbersome to be performed routinely. In general, one finds that

$$M(D_j) \neq \sum m_j = M_j \tag{5.4}$$

The suggested work-around is to use eq. 1b, especially for DVH constraints, which requires some assumptions about the size and location of normal tissue hot spots to be viable. However, for a convex metric like gEUD (a≥1), one finds by virtue of Jensen's inequality [14, 24, 29] strictly:

$$M(D_j) \leq \sum m_j = M_j \tag{5.5}$$

Conversely, for tumours the EUD is a concave function of dose meaning the sum of the EUDs of each treatment fraction is always smaller or equal to the EUD of warped and accumulated instance doses. The EUD/gEUD thus ensures a reliable worst case estimate of the metrics of the total treatment dose without the need for dose warping. If the actual dose optimization is performed with non-convex metrics like D2cc, gEUD can still

be used to catch cases where the simple addition of metrics errs on the unsafe side. We also test the effectiveness of fractionation compensation for gEUD dose constraints with the expectation that it offers more flexibility than "worst-case-DVH-addition and D2cc".

5.2.5. Dose planning criteria

We investigated the effect of fractionation compensation (COMP) on HR-CTV D90 by performing COMP for each fractionation schedule and compared it to constant per-fraction constraints (CONST). This was done for a D90 constraint of at least 40 Gy, irrespective of the OAR dose. Table 1 provides a summary of the per-fraction and total dose constraints used in this study. Two planning methods were compared: One in which the Gyn GEC-ESTRO (GGE) OAR DVH constraint parameters were used as metric (GGE method), and one with dose constraints in terms of EUD (Comprehensive volume (CV) method).

5.2.6. Statistical analysis

To test the significance of the observed differences, the Statistical Analysis Software (SAS v9.4, SAS Institute Inc.) package was used to identify differences in the population dose metrics of the planning techniques. Since the OAR doses are limited by constraints, resulting in a left skew frequency distribution, and minimum CTV constraints result in a right skew frequency distribution, non-parametric univariate analysis was applied with the Wilcoxon Signed Rank Test to identify statistically significant differences between dose metrics at the 95% or p=0.05 confidence level.

5.3. Results

5.3.1. Effect of the number of fractions on fractionation compensation

Using the per-fraction metric addition eq. (5.1b), a comparison was made between the distributions of total metrics for all twenty patients. There was no significant difference in the spread of the values when COMP was compared to CONST in all four fractionation schedules using the GGE planning method, see figure 5.2.

For HR-CTV dose metrics of both COMP and CONST, we saw a significant increase in D90 and the EUD with an increasing number of fractions. At the same time, the OAR dose metrics showed slight reductions. The increase in the average and median HR-CTV metrics per extra treatment fraction are shown in figure 5.3a and b. The average total D90 in 2 fractions was 52.9 Gy for CONST and 53.0 Gy for COMP, while their median doses were 42.4 Gy and 40.0 Gy respectively. Even though CONST sometimes creates a

higher dose in a single fraction than COMP, the COMP total dose metric in the HR-CTV is naturally always equal or higher.

Because fractionation compensation only takes effect if different organs are dose limiting, patients for which the same OAR was always limiting were excluded in a second analysis of the same study. For the remaining cohort of patients that benefit most from fractionation compensation, the average total D90 in 2 fractions using the GGE planning method was 65.6 Gy for CONST and 70.8 Gy for COMP, while their median doses were 61.3 Gy and 65.2 Gy respectively. The increase in the average and median doses per extra treatment fraction are also shown in figure 5.3c and d. To clarify this data, it is important to consider the fact that only 4 patients could be classified as benefiters when two treatment fractions were planned. This number increased to 6 in three fractions, 8 in four fractions and 10 in five fractions. Due to this increase from two to three planned fractions the average and mean HR-CTV D90 decreased as a result of the inclusion of patients with significantly lower target doses, though still benefiters, along with the existing benefiters in two treatment fractions. The same applies to fractions three and four, and four and five.

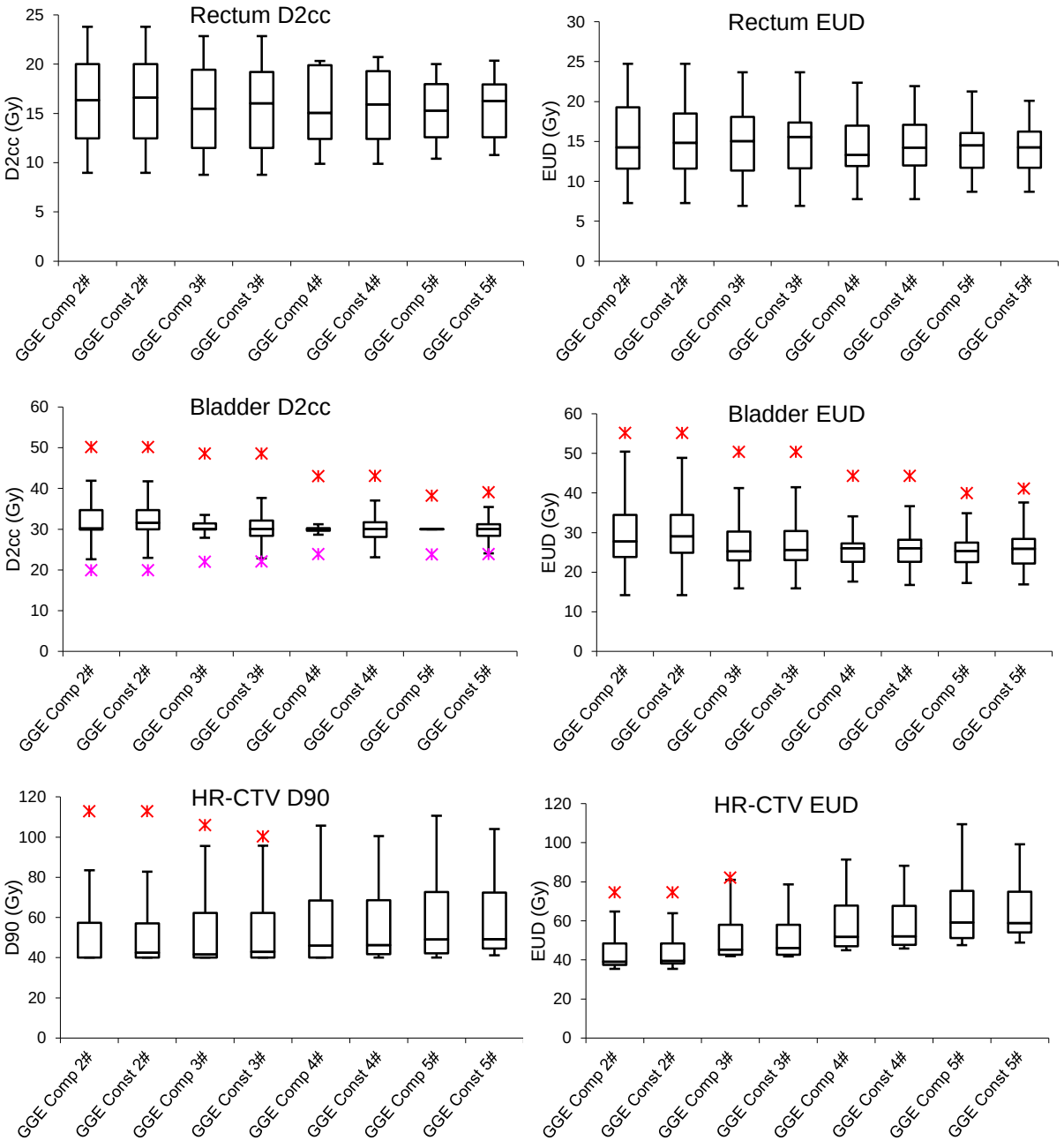

Figure 5.2: Box-whiskers plots comparing the frequency distributions of the 20 patients in this study of all dose metrics for the GGE COMP and CONST planning techniques. Data comprises results of 2 to 5 treatment fractions (#). Red and pink asterisks represent outliers in the frequency distribution.

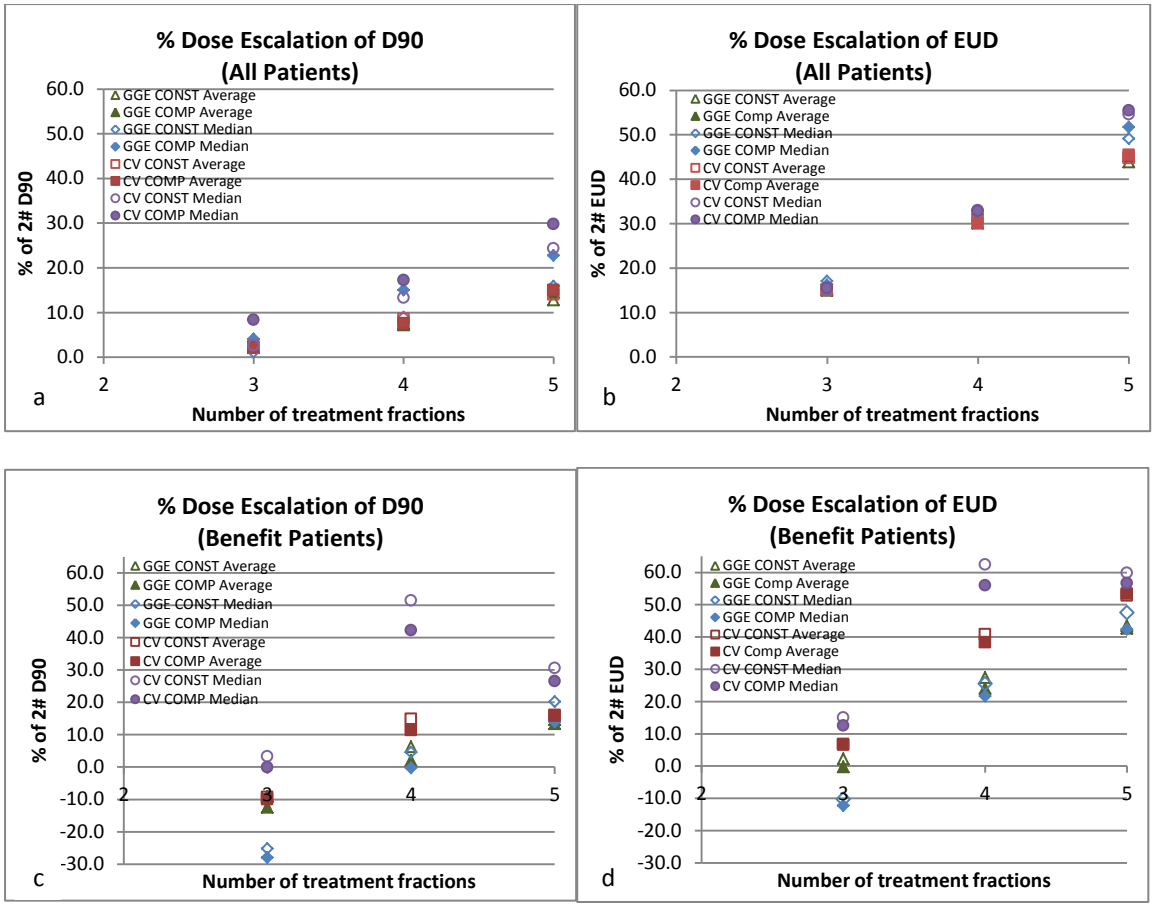

Figure 5.3: The increase in the average and median dose metrics per extra treatment fraction relative to 2 fractions for a) HR-CTV D90 and b) HR-CTV EUD in the total patient population and c) HR-CTV D90 and d) HR-CTV EUD in patients that had changing dose limiting OARs and therefore maximum benefit from fractionation compensation. The increase is expressed as the percentage dose metric increase relative to the value found for 2 fractions (#).

For this selected cohort of patients who benefitted from fractionation compensation, the differences between CONST and COMP were found to be not significant for all dose metrics when 2 to 5 fractions were planned. Table 5.2 contains the percentage difference between CONST and COMP for averages, medians and their respective p-values for the distribution of total dose metrics. Additionally, table 5.3 shows the same results that would be achieved if OAR dose was maximized in the same way, but without an HR-CTV D90 constraint of 40 Gy. Table 5.3 illustrates the power of compensation at fixed toxicity levels resulting in meaningful differences in dose metrics for 2 to 5 fractions. As for the total population of patients, the HR-CTV D90 increased on average by 7 – 8% in population average dose and 9 – 14 % in population median dose with each additional treatment fraction. This increase was found to be similar in magnitude between fractions 3 and 4, and 4 and 5, being 5.6 – 7 % average dose and 7.0 – 11.0 % median dose (fig.

5.3). All increases in HR-CTV D90 and EUD were significant when increasing the number of treatment fractions from 2 to 3, 3 to 4 and 4 to 5, whether CONST or COMP was performed.

Table 5.2: Percentage difference between CONST and COMP of the average and median doses using the GGE planning method. P-values of the distribution of total dose metrics for 2 to 5 treatment fractions are also supplied. The % difference indicates how much COMP is larger than CONST.

	2 Fractions			3 Fractions			4 Fractions			5 Fractions		
	% Diff			% Diff			% Diff			% Diff		
Metric	Ave	Median	p	Ave	Median	p	Ave	Median	p	Ave	Median	P
Rectum D0.1cc	4.3	6.0	0.0125	3.0	3.0	0.0215	1.2	3.0	0.0266	3.9	3.3	0.0362
Rectum D1cc	4.1	5.7	0.0125	3.0	2.9	0.0215	1.3	1.0	0.0266	4.2	3.2	0.0362
Rectum D2cc	6.0	6.0	0.0125	2.9	1.0	0.0215	2.2	3.2	0.0266	4.8	4.5	0.0098
Rectum EUD	5.9	5.9	0.0125	3.0	3.9	0.0215	1.9	0.7	0.0266	4.5	0.0	0.0098
Bladder D0.1cc	7.2	6.1	0.0125	3.2	4.5	0.0215	1.2	2.8	0.0266	4.5	6.1	0.0362
Bladder D1cc	6.3	5.9	0.0125	3.1	0.9	0.0215	1.3	2.1	0.0266	4.3	6.2	0.0362
Bladder D2cc	8.0	8.0	0.0125	4.0	6.9	0.0215	3.1	3.3	0.0266	6.4	7.0	0.0098
Bladder EUD	7.4	7.4	0.0125	4.1	1.0	0.0215	2.8	1.7	0.0266	6.3	6.5	0.0098
HR-CTV D90	7.9	7.9	0.0125	3.9	3.9	0.0215	3.6	2.8	0.0266	6.6	2.2	0.0098
HR-CTV EUD	5.2	5.2	0.0125	2.7	2.8	0.0215	2.5	2.0	0.0266	4.6	1.6	0.0098

Table 5.3: Percentage difference between CONST and COMP of the average and median doses using the GGE planning method when OAR doses are maximized to fixed dose constraints in the absence of an HR-CTV constraint. P-values of the distribution of total dose metrics for 2 to 5 treatment fractions are also supplied. The % difference indicates how much COMP is larger than CONST.

	2 Fractions			3 Fractions			4 Fractions			5 Fractions		
	% Diff			% Diff			% Diff			% Diff		
Metric	Ave	Median	p	Ave	Median	p	Ave	Median	p	Ave	Median	P
Rectum D0.1cc	3.2	2.9	0.0125	2.5	2.3	0.0215	1.3	2.7	0.0266	3.4	3.1	0.0362
Rectum D1cc	3.2	3.1	0.0125	2.5	2.2	0.0215	1.3	1.1	0.0266	4.0	2.7	0.0362
Rectum D2cc	4.6	4.3	0.0125	1.9	0.6	0.0215	1.4	2.3	0.0266	4.2	4.0	0.0098
Rectum EUD	4.1	4.0	0.0125	2.2	2.1	0.0215	1.8	0.9	0.0266	3.9	0.4	0.0098
Bladder D0.1cc	5.6	4.1	0.0125	2.3	2.7	0.0215	1.0	1.6	0.0266	4.0	5.2	0.0362
Bladder D1cc	4.0	3.8	0.0125	2.1	1.0	0.0215	1.0	0.9	0.0266	3.4	4.8	0.0362
Bladder D2cc	5.9	5.8	0.0125	2.2	3.9	0.0215	3.0	3.0	0.0266	5.0	5.6	0.0098
Bladder EUD	5.1	5.1	0.0125	2.4	1.0	0.0215	2.8	1.8	0.0266	4.6	4.3	0.0098
HR-CTV D90	8.9	8.9	0.0125	4.7	5.0	0.0215	4.3	4.4	0.0266	7.9	8.1	0.0098
HR-CTV EUD	7.0	7.0	0.0125	4.2	4.2	0.0215	4.1	4.0	0.0266	7.3	7.6	0.0098

5.3.2. Effectiveness of fractionation compensation when using EUD-based dose prescription

This section repeats the study of the previous section, but treatment planning was performed with EUD-based planning constraints. As in Shaw et al. (2013), we refer to EUD based treatment planning as the comprehensive volume (CV) technique. Firstly, the distribution of total doses for all twenty patients is compared for all dose metrics. Like in the GGE planning outcomes, there was no significant difference in the frequency distributions of the values when COMP was compared to CONST in all four fractionation schedules.

The mean/median of HR-CTV D90 and EUD values for the 20 patients was again significantly increased with each additional treatment fraction added to the treatment schedule, while the OAR doses decreased. The increase in the average and median doses using the CV planning method are also shown in figure 5.3. The average D90 from 2 fractions was 52.4 Gy for CONST and 52.4 Gy for COMP, while their median doses were 42.8 Gy and 40.0 Gy respectively. Similarly, for the whole patient population and benefiter cohort, the COMP D90 values were always larger than CONST dose values., unless an individual obtained a larger than constraint D90 in the first fraction in CONST, but failed to obtain this constraint in the second fraction, ultimately leading to large OAR constraint violations. The results for the benefiters with alternatingly dose limiting OARs are also included in figure 5.3. Their average D90 from 2 fractions was 61.3 Gy for CONST and 65.2 Gy for COMP, while their median doses were 45.4 and 47.6 Gy respectively. Though we could not find a statistical difference between the GGE and CV total dose metrics, the average and median GGE HR-CTV D90 and EUD was consistently larger than the corresponding average and median CV dose metrics.

5.3.3. Verification of DVH parameter total dose computation against EUD

We compare the distributions of total dose metrics in the GGE method with those of the CV method to verify that the GGE DVH-constraint addition is in line with the EUD-based planning results. Figure 5.4 provides box-whiskers plots of the frequency distributions of these two techniques for the whole patient population. Fractionation schedules of 2 to 5 fractions are shown. Figure 5.5 provides equivalent box-whiskers plots of the frequency distributions of these two techniques for the patients in which fractionation compensation could be applied with benefit. In both figures 5.4 and 5.5 we found no significant differences in the tumour dose between the GGE and CV techniques after adjusting the significance level for multiple testing with the Bonferroni method. However,

in figure 5.5 of the benefiters group, we found statistically significant lower OAR doses where the CV technique was applied.

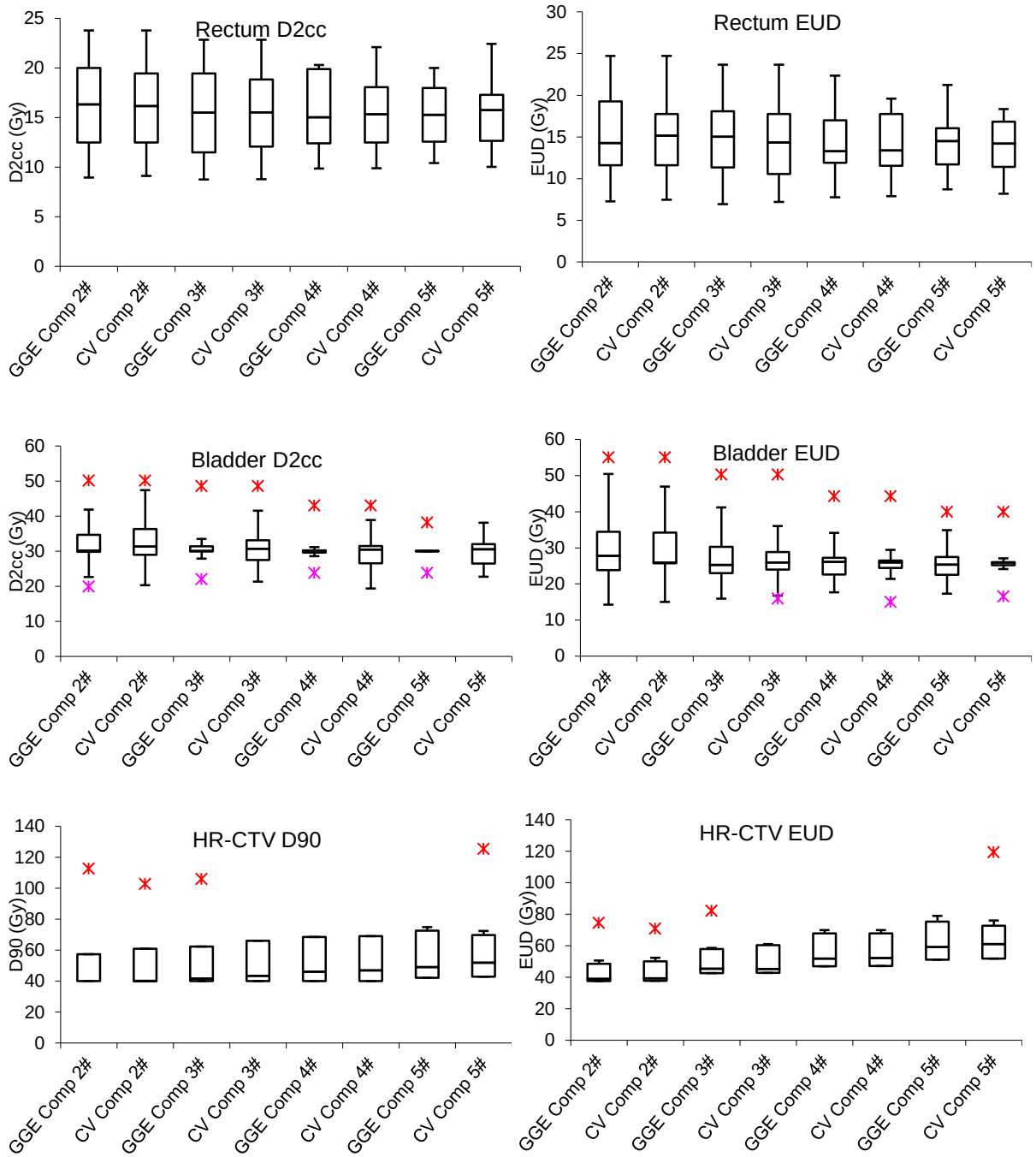

Figure 5.4: Box-whiskers plots of the frequency distributions of all dose metrics for the GGE and CV planning techniques with fractionation compensation. Data comprises results of 2 to 5 treatment fractions (#). Red and pink asterisks represent outliers in the frequency distribution.

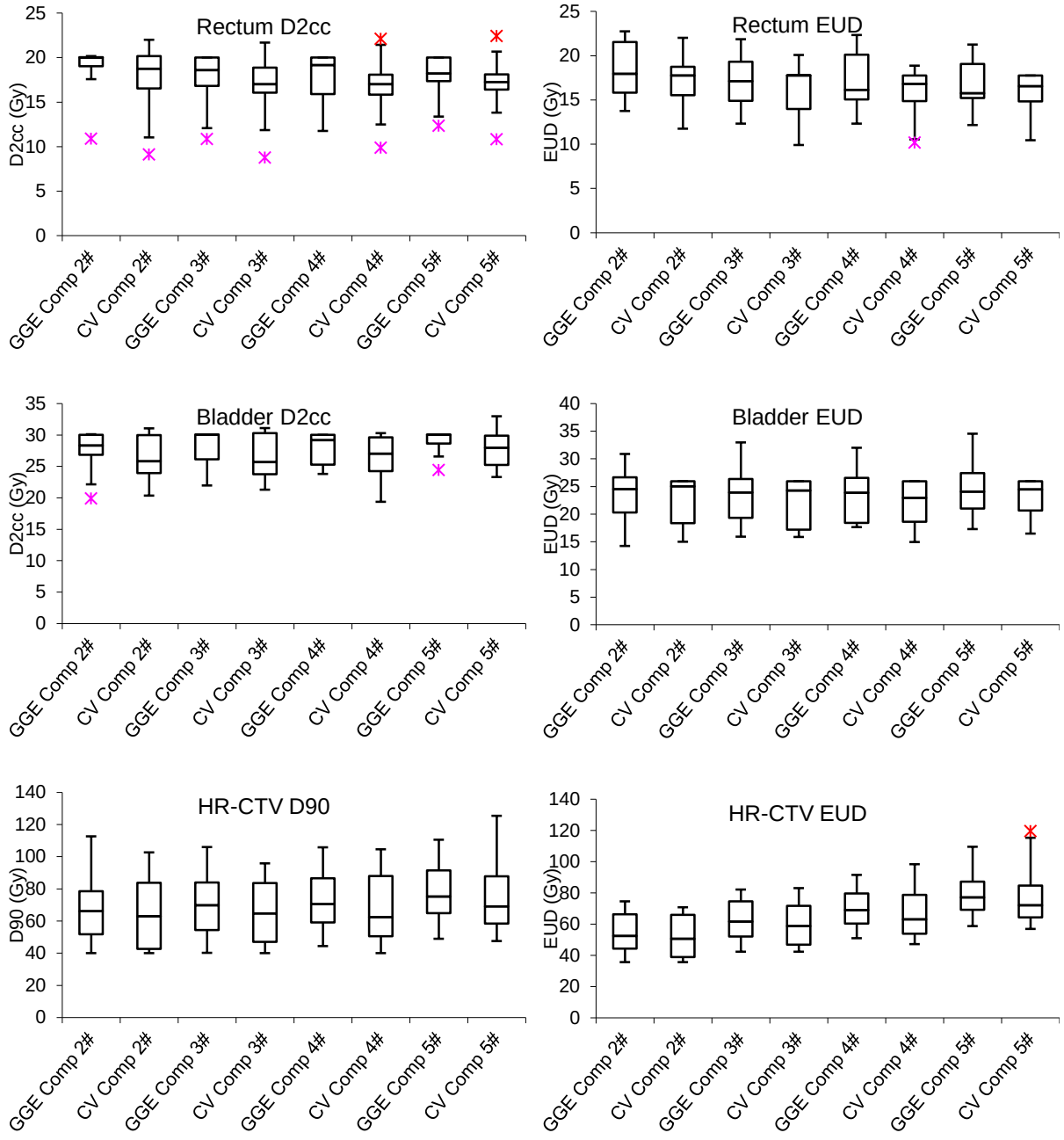

Figure 5.5: Box-whiskers plots of the frequency distributions of all dose metrics for the GGE and CV planning techniques with fractionation compensation in the patient cohort for which fractionation compensation was beneficial. Data comprises results of 2 to 5 treatment fractions (#) and two planning metrics (GGE and CV). Red and pink asterisks represent outliers in the frequency distribution.

5.3.4. Effectiveness of total OAR dose compensation when per-fraction constraints can be violated

By setting a minimum total HR-CTV D90 of 40 Gy as the highest planning priority, the effectiveness of OAR total dose compensation could be investigated. Whenever a

constant per fraction OAR constraint is violated during the course of treatment, COMP ensures OAR dose reduction to equal or below the total dose constraint if favourable future geometries allow. If no such favourable geometries arise, at least one of the OAR total dose constraints will be violated. Figure 5.5 contains a summary of all the constant per-fraction constraint violations and total dose constraint violations for the GGE and CV planning techniques with COMP. It demonstrates that fractionation compensation is more effective when more treatment fractions are planned as the number of total dose constraint violations decrease with increasing fraction numbers.

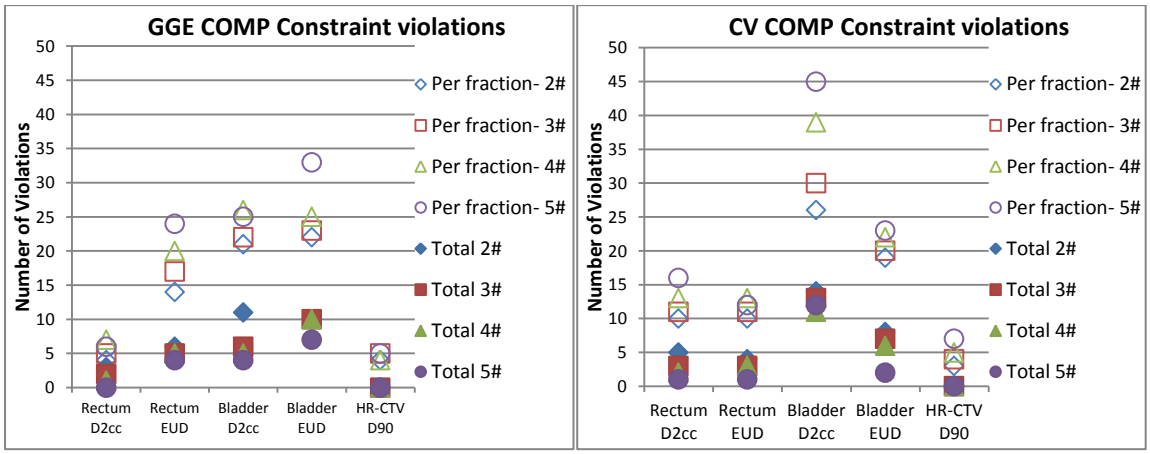

Figure 5.5: Per-fraction constant- and total dose constraint violations for GGE and CV planning. Empty markers represent the number of constraint violations in the population of patients on a per-fraction basis for each fractionation schedule (#), while filled markers represent the total dose constraint violations for each fractionation (#) schedule.

5.5. Discussion

When considering the total patient population in this study, we found no statistically significant differences between CONST and COMP using the GynGEC-ESTRO treatment planning recommendations. However, the investigation shows that the subgroup of patients with alternatingly dose limiting OARs obtain significant dose escalation with COMP.Although population average OAR doses are elevated towards the dose constraint, the HR-CTV dose escalation can be achieved without violation of the initial OAR dose constraint in all patients. It must be kept in mind though that by setting a minimum HR-CTV D90 constraint some OAR dose constraint violations can be expected if more favourable organ geometries do not arise during throughout the total treatment course. Nevertheless, COMP has the ability to still minimize those violations.

Regarding the GGE planning method across all fractionation schedules, COMP notably impacts the average and median doses of the OARs in this population when compared to CONST. It leads to a slight increase in the OAR dose in the benefiters group. However, this increase is small and mostly influenced by the requirement of the minimum HR-CTV D90 dose constraint and this constraint is the only reason why an OAR total dose constraint may be violated when applying COMP. For the frequency distributions of the HR-CTV, COMP mostly leads to lower median and higher average doses in the population due to the increase in the achievable tumour dose in the benefiters group.

The effect of dose escalation with COMP was most significant in the 2 and 5 fraction schedule with an average benefitersdose increase in the range of 6.6 – 7.9 % compared to CONST. This is the increase for the total benefitersgroup, but may be significantly larger for a particular individual. At the same time, the OAR dose could also be significantly higher than CONST. Hypothetically, these relative dose metric increases do not translate to asimple re-scaling of the dose distribution, because biologically, the slope of the TCP and NTCP curve at the dose range of 70-80 Gy for OARs and 90-100 Gy for tumours are not the same (Georg et al. 2011, Dimopoulos et al. 2009). Schmidt et al. (2014) and Pötter et al. (2011) have indicated that local control increases by more than 1% per Gy in the dose range from 81 to 90 Gy.

The outcomes of the studies of Pötter et al. (2011), Lindegaard et al. (2013) and Schmidt et al. (2014) motivate the selection of a minimum HR-CTV D90 of at least 90 Gy. The HR-CTV fractionation compensation planning procedure outlined in figure 1 ensures that this minimum target dose is always achieved and will sometimes have an associated cost of OAR total dose constraint violations. In combination with OAR fractionation compensation, at least a partial recovery of the OAR damage can be achieved in some patients when more favourable organ geometries arise during later fractions of the treatment. This is particularly evident in the CV technique where the OAR total dose becomes progressively lower with more treatment fractions (fig. 5). Occasionally some patients might require constraint adaptation or an extra treatment fraction if normal organ geometries are continuously too dose limiting.

With an increase in the number of scheduled fractions, more opportunities to adapt the dose distribution to the changing HR-CTV and normal organ geometries arise. This results in an increased number of benefiters with an increased number of treatment fractions and supports the use of more treatment fractions in IGABT. Figure 3 shows that the relative increase in CTV dose with the number of fraction is larger when performing COMP rather than CONST in the median values of the GGE and CV technique, and COMP always has an equal or higher total dose in the total population. In the benefiter’s

cohort, both the average and median gains are larger with CONST, but COMP already leads to higher HR-CTV D90s in 2 fractions. At the same time, the OAR dose metrics in CONST are always higher than in COMP due to the inability of CONST to compensate to lower total OAR doses when the minimum HR-CTV dose is achievable with OAR dose to spare.

When more treatment fractions are planned with the same OAR total dose criteria, the tumour dose can be escalated at no additional OAR dose cost beyond the constraint criteria. In figure 3 it can be seen that the percentage dose increase to the tumour per additional treatment fraction, far outweighs the estimated 1% loss in tumour control due to the added daily tumour repopulation estimate [30, 31]. Furthermore, fractionation compensation results in an average 4.6-6.6 % higher tumour dose compared to constant per-fraction constraints when a total of 5 fractions were planned, with a larger increase possible for a particular individual. Overall, significant differences in tumour dose can be found regardless of the number of treatment fractions that are given and results are more favourable when the total number of treatment fractions is increased. Fewer fractions lead to more and larger OAR constraint violations.

We could only identify significant differences between the GGE and CV techniques in the OAR dose metrics of the benefiter group results. However, CV has the advantage of an accurately calculated worst case accumulated dose estimate. CV leads to safely escalated doses in the lower dose region of the HR-CTV D90 frequency distribution, while the GGE technique results in higher doses in the high dose region of the same frequency distribution, which carries the risk of OAR overdosage. Calculating gEUDs acts as a sentinel in cases where addition of D2cc underestimates the total dose and the application of Jensen's Inequality ensures that fractionation compensation does not lead to over-dosage of OARs.

Figures 5.4 and 5.5 demonstrate that CV is somewhat more conservative than GGE in terms of OAR doses, but HR-CTV doses are comparable. D2cc constraint parameters do sometimes lead to higher OAR dose outliers for individuals, particularly in the case of the bladder, being the more frequent dose limiting organ in this study population. Overall, the OAR doses are slightly higher in the GGE approach, particularly for small numbers of fractions. Our conclusion is that any of these two planning approaches can be used for plan optimization and evaluation, but the EUD calculations retains the advantage in that it considers the DVH comprehensively and is reproducible in the calculation of accumulated dose. The D2cc dose addition sometimes leads to significant total dose EUD constraint violations (see rectum and bladder EUDs in figure 5.5). This can become

important when heterogeneous dose distributions from IGART are combined with brachytherapy dose.

The fractionation compensation scheme explored here is optimistic and conservative: it amounts to the assumption that the current situation is a good predictor of the future fractions. If a trend towards more favourable patient geometries is present because of tumour shrinkage, this assumption has a good chance of becoming true. More pessimistic and aggressive schemes would aim to exploit any chance of compensation and not hope for better chances. The appropriate formula can be derived by assuming that the already delivered fractions, including the current one, are the best predictors for future ones. The fractional constraint of fraction j+1 is then:

$$c_{j+1} = \left(\frac{j+1}{n}\right)\boldsymbol{C} - M_j \qquad (5.5)$$

In other words, it aims to perform the entire compensation in the current fraction, while the conservative approach distributes it over all undelivered fractions. Comparing the fractionation compensation approaches of equations 4 and 5, we could not find any statistically significant differences in their respective dose metrics. This can be a consequence of the observed time trend of a shrinking HR-CTV. We expect that eq. 5.5 will be more beneficial when there are no clear time trends of tumour shrinkage and brachytherapy is applied at/after the end of the EBRT schedule, when tumour shrinkage has already taken place. It might also be more effective when dose distributions with more degrees of freedom are planned, like in the use of interstitial needles. Because our primary concern was safety of the implicit dose escalation, we chose to place the conservative approach into the centre of our presentation. Our results show that COMP is a robust planning strategy since both conservative and aggressive dose escalation schemes deliver results that are comparable to CONST.

The quantitative results of this study depend on the study population, in particular the mix of patients with alternatingly dose-limiting OARs and one constantly dose-limiting OAR. This mix is likely to be very variable between institutions and countries and we can therefore not make any statements about the population efficacy of this technique. Independent of these factors, we stress that COMP will never perform worse than CONST. Further, more treatment fractions increase the efficacy of fractionation compensation in terms of CTV dose escalation without OAR constraint violations. However, there could be a chance of higher toxicity in a population since more individuals will indeed exhaust the OAR constraints in exchange for an individual dose escalation.

Dose was manually optimized by graphical tools. Following the EBRT experience,where EUD has been used in inverse biological optimization of the planned dose distributions [32, 33], it is expected that such inverse biologically optimized IGABT treatment plans will be superior to current inverse optimization based on DVH parameters or manually optimized plans. Also, if interstitial needles are used in combination with intracavitary applicators, OAR dose will be further reduced making the proposed planning method/approach of tumour dose maximization more effective. We would like to point out, that the DVH-constraint addition is likely to suffer from greater uncertainties when the dose distributions are optimized with more degrees of freedom, making the use of EUD more appealing in this context.

Several other limitations exist concerning this study. They include the fact that only the bladder and rectum were used as OARs. More organs, like the vagina, sigmoid and small bowel could have limited the HR-CTV dose and resulted in more alterations between dose limiting organs. This would have increased the effect of COMP. Furthermore, the patients included in this study received 5 brachytherapy treatment fractions during their actual treatment, with their first fraction in week 3 when tumour shrinkage is at a maximum. As a consequence, there is a bias towards 4-5 fraction schedules and the optimistic compensation scheme.

5.6. Conclusion

Fractionation compensation is an approach to take the concept of image-guided adaptive brachytherapy one step further by not only creating a plan-of-the-day, but also taking into account the delivered BT fractions and a prediction about the future course of the treatment. The present study demonstrates its effectiveness in particular for a sub-group of the study population who present with a scenario where different organs can become dose-limiting in each fraction. The concept can be enhanced by the use of equivalent-dose constraints that offer a mathematically sound estimate of the total delivered dose.

5.7. References

1. Pötter R, Georg P, Dimopoulos J, et al: Clinical outcome of protocol based image (MRI) guided adaptive brachytherapy combined with 3D conformal radiotherapy with or without chemotherapy in patients with locally advanced cervical cancer. Radiother Oncol 2011, 100:116–123.

2. Lindegaard JC, Fokdal LU, Nielsen SK, Juul-Christensen J, Tanderup K, MRI-guided adaptive radiotherapy in locally advanced cervical cancer from a Nordic perspective, Acta Oncol 2013;52:1510-1519

3. Nesvacil N, Pötter R, Sturdza A, Hegazy N, Federico M, Kirisits C. Adaptive image guided brachytherapy for cervical cancer: a combined MRI-/CT-planning technique with MRI only at first fraction. Radiother Oncol. 2013;107:75-81.

4. Jamema SV, Mahantshetty U, Tanderup K, Malvankar D, Sharma S, Engineer R, Chopra S, Shrivastava SK, Deshpande DD. Inter-application variation of dose and spatial location of D(2cm(3)) volumes of OARs during MR image based cervix brachytherapy. Radiother Oncol. 2013;107:58-62.

5. Viswanathan A, Dimopoulos J, Kirisits C, Berger D, Pötter R: Computed tomography versus magnetic resonance imaging based contouring in cervical cancer brachytherapy: results of a prospective trial and preliminary guidelines for standardized contours. Int J Radiat Oncol Biol Phys 2007;68:491–498.

6. Schmid MP, Pötter R, Brader P, Kratochwil A, Goldner G, Kirchheiner K, Sturdza A, Kirisits C, Feasibility of transrectal ultrasonography for assessment of cervical cancer, Strahlenther Onkol 2013;189:123-8.

7. Duane FK, Langan B, Gillham C, Walsh L, Rangaswamy G, Lyons C, Dunne M, Walker C, McArdle O, Impact of delineation uncertainties on dose to organs at risk in CT-guided intracavitary brachytherapy. Brachytherapy 2014;13:210-218.

8. Schmid MP, Franckena M, Kirchheiner K, Strudza, Georg P. Dörr W, Pötter R, Distant metastasis in patients with cervical cancer after primary radiotherapy with or without chemotherapy and image guided adaptive brachytherapy. Gynecol Oncol 2014, http://dx.doi.org/10.1016/j.ygyno.2014.02.004

9. Pötter R, Dimopoulos J, Georg P, Clinical Impact of MRI assisted dose volume adaptation and dose escalation in brachytherapy of locally advanced cervix cancer. Radiother Oncol 2007;83:148-55.

10. Dimopoulos J, Pötter R, Lang S, et al: Dose–effect relationship for local control of cervical cancer by magnetic resonance image-guided brachytherapy. Radiother Oncol 2009;93:311–315.

11. Georg P, Boni A, Ghabuous A, Goldner G, Schmid MP, Georg D, Pötter R, Dörr W. Timecourse of late rectal- and urinary bladder side effects after MRI-guided adaptive brachytherapy for cervical cancer. Strahlenther Onkol. 2013;189:535-540.

12. Georg P, Kirisits C, Goldner G, et al: Correlation of dose-volume parameters, endoscopic and clinical rectal side effects in cervix cancer patients treated with definitive radiotherapy including MRI-based brachytherapy. Radiother Oncol 2009;91:173–180.

13. Georg P, Pötter R, Georg D, et al: Dose effect relationship for late side effects of the rectum and urinary bladder in magnetic resonance image guided adaptive cervix cancer brachytherapy. Int J Radiat Oncol Biol Phys 2012;82:653–657.

14. Shaw W, Rae W, Alber M, Equivalence of Gyn GEC-ESTRO guidelines for image guided cervical brachytherapy with EUD-based dose prescription, Radiat Oncol 2013;8:266.

15. Haie-Meder C, Pötter R, Van Limbergen E, et al: Recommendations from Gynecological (GYN) GEC-ESTRO Working Group (I): concepts and terms in 3D image based 3D treatment planning in cervix cancer brachytherapy with emphasis on MRI assessment of GTV and CTV. Radiother Oncol 2005;74:235–245.

16. Lang S, Kirisits C, Dimopoulos J, Georg D, Pötter R, Treatment planning for MRI assisted brachytherapy of gynecologic malignancies based on total dose constraints, Int J Radiat Oncol Biol Phys 2007;69:619–627.

17. Taylor A, Powell M. Conformal and Intensity-modulated Radiotherapy for cervical cancer. Clin Oncol 2008;20:417-425

18. Chen CC, Lin JC, Jan JS, Ho SC, Wang L. Definitive intensity-modulated radiation therapy with concurrent chemotherapy for patients with locally advanced cervical cancer. Gynecol Oncol 2011l;122:9-13.

19. Gandhi AK, Sharma DN, Rath GK, Julka PK, Subramani V, Sharma S, Manigandan D, Laviraj MA, Kumar S, Thulkar S. Early clinical outcomes and toxicity of intensity modulated versus conventional pelvic radiation therapy for locally advanced cervix carcinoma: a prospective randomized study. Int J Radiat Oncol Biol Phys 2013;87:542-8.

20. Pötter R, Haie-Meder C, Van Limbergen E, et al: Recommendations from Gynecological (GYN) GEC ESTRO working group (II): Concepts and terms in 3D image-based treatment planning in cervix cancer brachytherapy— 3D dose volume parameters and aspects of 3D image-based anatomy, radiation physics, radiobiology. Radiother Oncol 2006;78:67–77.

21. Tanderup K, Nesvacil N, Pötter R, Kirisits C. Uncertainties in image guided adaptive cervix cancer brachytherapy: impact on planning and prescription. Radiother Oncol 2013;107:1-5.

22. Andersen E, Muren L, Sørensen T, et al: Bladder dose accumulation based on a biomechanical deformable image registration algorithm in volumetric modulated arc therapy for prostate cancer. Phys Med Biol 2012;57:7089–7100.

23. Andersen E, Noe K, Sørensen T, et al: Simple DVH parameter addition as compared to deformable registration for bladder dose accumulation in cervix cancer brachytherapy. Radiother Oncol 2013;107:52–57.

24. Sobotta RB, Söhn M, Shaw W, Alber M. On expedient properties of common biological score functions for multi-modality, adaptive and 4D optimization. Phys Med Biol 2011;56:N123-N129.

25. Niemierko A: Reporting and analyzing dose distributions: a concept of equivalent uniform dose. Med Phys 1997;24:103–110.

26. Niemierko A: A generalized concept of equivalent uniform dose [Abstract]. Med Phys 1999;26:1100.

27. Dale RG. The application of the linear–quadratic dose–effect equation to fractionated and protracted radiotherapy. Br J Radiol 1985;58:515–28.

28. Jürgenliemk-Schulz I, Lang S, Tanderup K, et al: Variation of treatment planning parameters (D90 HR-CTV, D2cc for OAR) for cervical cancer tandem ring brachytherapy in a multicentre setting: Comparison of standard planning and 3D image guided optimisation based on a joint protocol for dose–volume constraints. Radiother Oncol 2010;94:339–345.

29. Jensen J: Sur les fonctions convexes et les inegalites entre les valeurs moyennes. Acta Math 1906;30:175–93.

30. Dimopoulos JC, Lang S , Kirisits C, Fidarova EF, Berger D, Georg P, et al . Dose-volume histogram parameters and local tumour control in magnetic resonance image-guided cervical cancer brachytherapy. Int J Radiat Oncol Biol Phys 2009;75:56–63.

31. Lanciano RM, Pajak TF, Martz K, Hanks GE. The influence of treatment time on outcome for squamous cell cancer of the uterine cervix treated with radiation: a patterns-of-care study. Int J Radiat Oncol Biol Phys 1993;25:391-397.

32. Dale RG, Hendry JH, Jones B, Robertson AG, Deehan C, Sinclair JA. Practical methods for compensating for missed treatment days in radiotherapy, with particular reference to head and neck schedules. Clin Oncol (R Coll Radiol) 2002;14:382-393.

33. Wu Q, Mohan R, Niemierko A, Schmidt-Ullrich R: Optimization of intensity-modulated radiotherapy plans based on the equivalent uniform dose. Int J Radiat Oncol Biol Phys 2002;52:224-235.

34. Schwarz M, Lebesque J, Mijnheer B, Damen E: Sensitivity of treatment plan optimization for prostate cancer using the equivalent uniform dose (EUD) with respect to the rectal wall volume parameter. Radiother Oncol 2004;73:209-218.

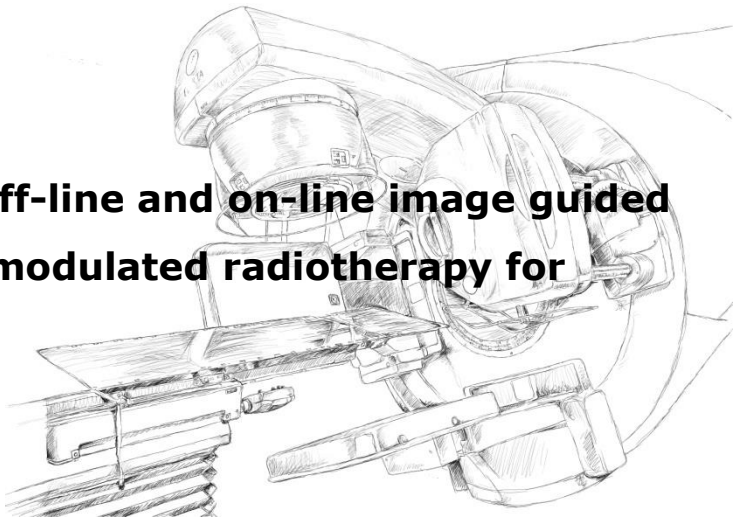

Chapter 6: EUD-based off-line and on-line image guided adaptation in intensity modulated radiotherapy for cervical cancer

6.1. Introduction

In conformal external beam radiotherapy, optimal treatment planning margins ensure that adequate tumour dose can be delivered considering acceptable normal tissue dose [1-4]. This margin, usually referred to as the planning target volume (PTV), encompasses the clinical target volume (CTV) and must consider various structural and positional deviations from the original volumes of interest that were delineated on a single snapshot planning CT of the patient in the treatment position. Typical deviations in cervix cancer treatment are due to tumour shrinkage, normal organ motion, setup deviations and treatment related weight loss [5-8]. Several methods to compensate for these deviations have been discussed for other treatment sites [9-12], as well as the cervix and surrounding tissues [13-17]. Although several of these proposed techniques can be used to compensate for deviations, in general there exist considerable uncertainties about the total dose accumulated in a conformal external beam radiotherapy (EBRT) treatment, like intensity modulated radiotherapy (IMRT) or volumetric modulated arc therapy (VMAT). To ensure recommended dose prescription metrics [18] are achieved, margin size "recipes" have been derived to minimize geographical misses and they can consider the dosimetric effects of setup variations and organ motion [19]. Organ motion compensation sometimes requires very large margins for treatment planning, often including large volumes of normal tissue in the PTV. Resultantly, the level of normal tissue sparing becomes smaller when margins are large and the gain in IMRT normal tissue sparing diminishes with increasing margin size.

It may well be that the dosimetric effect of setup errors and organ motion and deformation might not be as pronounced as the geometrical effect they allude to [10, 20, 21]. If that is the case, there exists a window of opportunity to achieve the desired tumour doses with adaptive image guided radiotherapy with minimal intervention during the treatment course by record keeping of accumulated dose and intervening only when projected tumour doses are below a certain threshold dose, or higher than this dose in the case of normal tissues. Ahmad et al. (2014) illustrated that a margin of the day concept utilizing a library of treatment plans reduce the workload of an image-guided

adaptive treatment protocol compared to on-line daily adaptation and plan re-calculation. However, in both these techniques dose accumulation remains problematic in the pelvis region, leading to possible overestimation of the required margin size. IMRT and VMAT have important roles to play in the treatment of cervical cancer since they have the capability to reduce normal tissue dose which drastically reduce acute side effects of radiation treatment [22-24]. These techniques also lead to reduced late morbidity compared to conventional techniques [25]. For this reason we investigate the dosimetric effects of typical setup correction procedures for minimum imaging protocols utilizing the favourable properties of dose metrics like the equivalent uniform dose (EUD) [26-27]. We apply the same evaluation metric to test reduced workload on-line and off-line adaptive treatment strategies for cervix IMRT to minimize normal tissue dose without tumour under-dosage.

6.2. Methods and Materials

6.2.1 Patient population and conventional treatment planning

During the first half of 2010 we have determined setup variations for 21 patients in this study who received 25 fractions of external beam radiotherapy (EBRT) to the whole pelvis with a 4-field box planning technique and 15MV x-rays. The clinical target volume included the cervical tumour, uterus, parametrium, at least the upper third of the vagina, and the pelvic lymph nodes. Of these patients, 5 were classified as FIGO stage IIB and the rest stage IIIB. Patients received concurrent Cisplatin-based chemotherapy of 5–6 x of 25 mg/m^2 body surface area during the course of treatment. Treatment plans were produced on 3D CT data of which the imaging was done in the week before treatment commenced. Patients also received 5 concomitant high dose rate brachytherapy (BT) treatments.

6.2.2. Contouring

Contouring for the actual treatment received via 4 field box technique consisted of the outer rectum and bladder walls as OARs and a box which included the primary tumour and cervix, parametrium and nodal regions. The box stretches from the junction of the anterior third and posterior two thirds of the symphysis to the junction of S2-S3 in the anterior-posterior direction. The superior edge of the volume starts at the superior border of the L5 vertebral body and stretches inferiorly to the inferior edge of the obturator foramen, or lower if clinically indicated due to vaginal extension of the tumour. Understandably these box-type volumes include very large small bowel volumes and almost whole bladder and rectal structures. Lateral borders of this PTV are 1cm lateral to

the pelvic brim. For the purpose of this planning study, contours for the production of IMRT treatment plans were produced retrospectively. Since imaging was CT based, the Gross Tumour Volume could not be identified. The following ROI's were contoured: The primary CTV which included the entire uterus, at least the upper one third of the vagina, and the parametrial tissue; in case of vaginal involvement, at least 9 mm below the most caudal extent of the tumour was included. The left and right nodal CTVs were delineated for the external, internal and the common iliac nodes. The internal iliac nodes included the obturator nodes, while the common iliac contours included the sub-aortic pre-sacral nodes. The nodal volumes are denoted as RII for right internal iliac, RCI for right common iliac, REI for right external iliac and similarly for the left nodal CTVs. Vessels were used to define the nodal regions up to the level of the L5-S1 interspace. Critical organs were contoured including the outer walls of the bladder, rectum (from the anus to the recto-sigmoid flexure), and bowel (both small and large intestines up to the level of L5-S1).

6.2.3. Imaging

To determine systematic and random geometrical setup variations for this patient population, daily electronic portal images (EPIs) were produced with the Elekta Iview GT 2D planar imaging module on an Elekta Precise linear accelerator with 6MV photons that provides the best imaging contrast, compared to 15MV. 2D electronic portal images (EPIs) were matched to the original planning CT digitally reconstructed radiographs (DRRs) by bony landmark matching on a combination of anterior-posterior and lateral beam angles. EPIs were produced for each treatment fraction with the patient in the treatment position for the first setup of the day without any adjustments made unless a gross setup error was identified, being larger than a 10 mm deviation. 9 planning equivalent CT datasets for each patient were also produced using the same scan setup as for the original planning CT on a 16 slice Toshiba Acquilion CT scanner with 3mm slice thicknesses, resulting in 10 CT datasets in total (including the planning CT). Patients were imaged 4 times during the first week of treatment and once a week in subsequent treatment weeks until completion of the EBRT phase of treatment. 3D image registration with the original planning CT dataset was performed with bony matching. The number of imaging datasets amounted to 25 fractions x 21 patients = 1050 sets of EPIs and 10 imaging days x 21 patients = 210 sets of 3D CT datasets.

6.2.4. Setup correction protocols

It has been shown that the extended no-action level (eNAL) setup correction protocol (SCP) [28] is a very effective protocol for reducing systematic errors in patient setup.

We compared the dosimetric effects of this protocol with treatment where no corrections for setup deviations were made. The advantage of this protocol over most others is that it corrects for time trends in setup deviation. This evaluation was done using the data obtained from the 2D and 3D image datasets.

6.2.5. Treatment planning and margin evaluation

To define a suitable planning margin for setup deviations we evaluated different magnitudes of CTV-PTV margins. Taylor and Powell [5, 7] stated that margins for this purpose are usually in the range of 5 – 7 mm in cervix cancer treatment. Kerkhof et al. [4] showed that even smaller margins can be used if on-line MRI guided treatment can be performed, including the effects of organ motion. In our study, we wanted to discriminate between the required margins to address setup deviations and organ motion, particularly because nodal CTV positions are usually quite stable during the treatment period, while the primary tumour volumes vary in position and geometry due to several reasons.

We used an equally spaced 9 beam configuration of step-and-shoot IMRT delivery for treatment planning on the HYPERION (University of Tübingen, Germany) treatment planning system for the margin size evaluation. Dose was slightly escalated compared to the conventional 4-field box technique, to 54-56 Gy in 2Gy fractions to both the primary and nodal CTVs so as to create very steep dose gradients in the vicinity of the CTVs. Biologically optimized plans were produced for 14 of the original 21 patients in this study using 10MV x-rays for the IMRT plans. Higher energy IMRT treatments are contaminated with neutrons and thus we refrained from using 15MV beams. The dose prescription and constraint criteria were based on equivalent uniform dose (EUD) and this parameter was used for dose evaluation purposes as well (table 6.1). The decision of using a volume effect parameter of 12 for the bladder was simply from a dose optimization perspective to enforce a larger restriction on the high dose regions of the bladder than by using a value of 8. The difference is simply in terms of the optimization: The high doses volumes are reduced and the EUD is more sensitive to changes in the dose distribution for optimization. EUDs were calculated for treatments delivered without the utilization of an SCP, as well as with the implementation of the eNAL SCP. Evaluation of the PTV-CTV margins could be done with the EUD dose metric as a tool for calculating a worst case dose estimate based on its favourable underlying mathematical properties, described in chapters 2, 4 and 5.

IMRT treatment plans were produced for constant OAR and CTV volumes, but with increasing PTV margin sizes. These margin sizes included 1 – 12 mm, 15 mm, 20 mm and 25 mm. Each patient therefore had 15 different treatment plans, optimized with the

same optimization criteria, although some constraint values had to be relaxed as PTV margins were increased. Table 1 summarizes the most important constraints in the optimization criteria used.

Table 6.1: Standard optimization criteria for the 9-field beam arrangement.

VOI	Objective/Constraint	Prescription/Threshold dose	Iso-constraint
Primary CTV	Poisson Cell Kill	56 Gy	
Primary CTV	Quadratic overdose	59 Gy	0.05
Nodal CTVs	Poisson Cell Kill	56 Gy	
Nodal CTVs	Quadratic overdose	59 Gy	0.03
PTV	Poisson Cell Kill	56 Gy	
PTV	Quadratic overdose	59 Gy	0.05
PTV	Quadratic under-dose (only for evaluation)	53.5 Gy	Variable
Rectum Total Volume	Serial EUD (a = 12)		51 Gy
Rectum Non-overlapping Volume	Serial EUD (a = 8)		44 Gy
Sigmoid Total Volume	Serial EUD (a = 12)		51 Gy
Sigmoid Non-overlapping Volume	Serial EUD (a = 8)		44 Gy
Bladder Total Volume	Serial EUD (a = 12)		50 Gy
Bladder Non-overlapping Volume	Serial EUD (a = 8)		43 Gy
Small Intestine Total Volume	Serial EUD (a = 12)	50 Gy	50 Gy
Small Intestine Total Volume	Overdose DVH	40 Gy	50 %

6.2.6. Setup variation simulation

The impact of the CTV-PTV margin size was investigated by simulating the treatment on the original planning CT dataset of each patient. For each of the PTV margins sizes, 28 treatment fractions were simulated by shifting the isocenter according to the fraction setup error and re-calculating the dose distributions with the isocenter position of the

day for both uncorrected setup errors (RAW) and eNAL corrected setup errors. We simulated the treatment plans of the 14 patients above in 28 fractions of 2 Gy per fraction. This amounted to 14 x 28 x 2 x 15 = 11 760 dose matrices.

6.2.7. Adaptive treatment simulation

The ideal solution for the irradiation of a mobile tumour in a mobile surrounding is daily imaging and treatment plan adaptation based on each imaging dataset. In this scenario both setup corrections and organ motion is corrected for in one process. However, this workflow is impractical on a daily basis with current technology and would require almost instantaneous imaging and fast automated segmentation, structure positional and shape evaluation, re-planning and dose accumulation before treatment is performed. Such resources do not exist in a complete clinical package yet. To overcome some of these limitations, we investigated the following hybrid off-line and on-line adaptation methods:

6.2.7.1. On-line re-planning and fractionation adaptation

We investigated one patient of which 10 CT datasets were available for evaluation with an on-line re-planning strategy. Although one patient cannot be regarded as representative of a population of cervix cancer patients, our intension was not to perform a "proof-by-numbers", but rather an application of the concept.

A seven field 10MV IMRT plan was produced on CT1 (planning CT) with a 50 Gy EUD dose prescription to the primary and nodal CTVs. We found that this seven field plan gave similar results to a nine field plan. The ICRU 83 (2010) recommendations of 95% of the prescribed dose to 99% of the PTV was followed, using a 5mm planning margin to compensate for intra-fraction volumetric deviations of the tumour. Table 6.2 provides a summary of the total volume EUD constraints for the OARs and was also used for dose evaluation of the adaptation process. CT2-10 were regarded as on-line CT images of the patient in the treatment position and all the primary-CTV volumes were compared, by visual inspection, with the original plan's primary PTV contour. When significant deviations of the current CTV with respect to the original CTV were found, on-line re-planning was performed. Where the deviation was accepted to be small and still within the PTV contour, the dose distribution was re-calculated off-line to determine the EUDs of all the volumes of interest up to and including the current fraction. We regard the dose calculation process as an off-line dose calculation, unless an on-line recalculation was warranted due to excessive organ motion. Dose accumulation was done by summing the EUDs for all relevant structures for each treatment fraction. The total dose without any re-planning adaptation was compared to the case where on-line re-planning was performed.

Table 6.2: EUD constraints used in the optimization of the treatment plan for on-line and off-line adaptation. These constraints were set for the total OAR volumes.

Organ at Risk	Total EUD constraint (Gy)	Volume effect parameter (a)
Rectum	45	12
Bladder	47	12
Sigmoid	50	12
Small Bowel	45	12

6.2.7.2. Off-line dose accumulation and fractionation compensation

For this section of the study, we applied a similar method as in 6.2.7.1. by re-calculating the dose of each fraction off-line, but never performing on-line re-planning if major structure deviations were found. Instead, using equation 5.6 of chapter 5, we determined by how much the OAR constraints could be relaxed or tightened for a future treatment fraction to compensate for the under-dosage of the tumour and possible over-dosage of the OARs based on total dose constraints. Off-line re-planning was performed for future fractions using a slightly larger margin size to still limit normal tissue involvement, but at a higher dose level. Each time a new plan was required and produced, the plan was placed in the patient's library for future use when necessary. Dose accumulation was again done by EUD summation and the total dose without any re-planning adaptation could be compared to the case where off-line re-planning was performed. The same optimization- and evaluation criteria as in table 6.2 were used for OARs.

6.3. Results

6.3.1. Imaging and setup deviations

We have calculated similar systematic and random errors for the EPI and CT datasets. When compared to the RAW setup errors, the eNAL protocol reduces the overall systematic error significantly. Reduction of the random errors is not an explicit function of the eNAL protocol or any off-line SCP for that matter. In principle, only on-line setup corrections reduce the random setup errors. eNAL required 7 EPIs per patient throughout the course of 25 treatment fractions. Table 6.3 provides a summary of the maximum deviations found in each direction for RAW setup errors and when eNAL was utilized. Figure 6.1 shows 2D distributions of setup deviations in all three dimensions as recorded on the anterior-posterior and lateral EPIs. Table 6.4 is a summary of the resultant RAW

systematic and random errors, as well as the same data in the case of eNAL implementation. The table contains the errors for both the EPI and CT datasets.

Table 6.3 Maximum deviations found with and without the application of the eNAL SCP.

Direction	No SCP Applied	eNAL SCP applied
Sup – Inf	-15.0 mm	-13.0 mm
Lat (L-R)	-19.5 mm	-16.3 mm
Ant - Post	-16.3 mm	-12.2 mm

Abbreviations: Sup – superior, Inf – inferior, Lat – lateral Left (L) or Right (R), Ant – anterior, Post - posterior

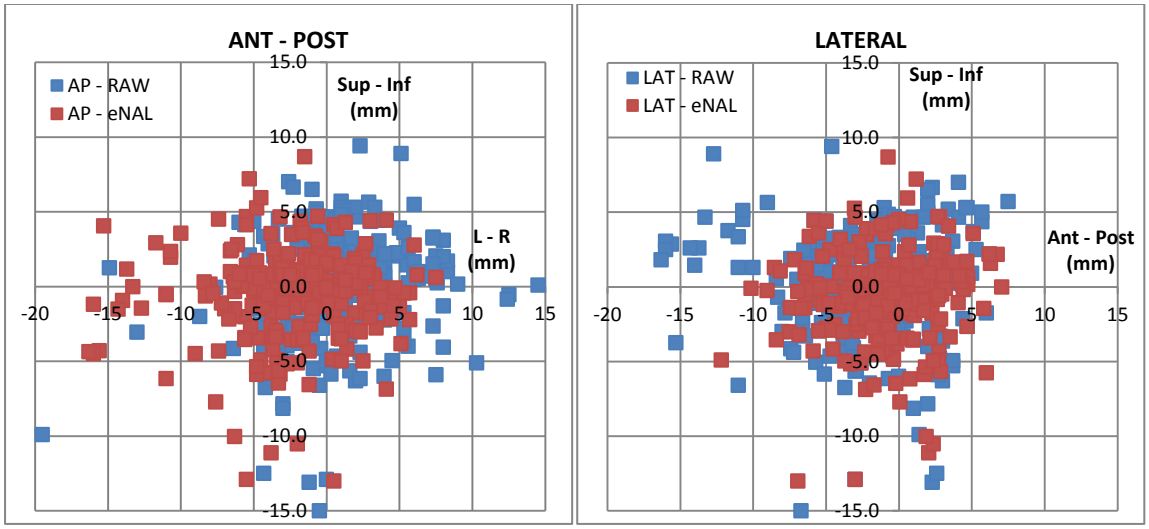

Figure 6.1: Setup deviation plots on anterior–posterior (ant-post) and lateral EPIs showing deviations in ant-post, superior-inferior (sup-inf) and left-right (L-R) directions. The setup errors without correction are RAW errors and blue in colour, while the red errors are the eNAL generated results.

Table 6.4 Systematic (Σ) and random (σ) errors resulting from the evaluation of the RAW EPI and CT image analyses, as well as the eNAL results. Additionally, the recommended margin size for treatment planning is also included. All values are in mm.

Σ	**SUP-INF**	**LAT**	**ANT-POST**	**σ**	**SUP-INF**	**LAT**	**ANT-POST**
EPID RAW	2.2	2.4	3.2	EPID RAW	2.5	3.6	3.1
EPID eNAL	0.7	1.1	1.2	EPID eNAL	2.9	3.7	3.5
CT RAW	1.6	2.4	4.5	CT RAW	2.5	4.0	3.2
CT eNAL	1.1	1.2	1.9	CT eNAL	2.6	4.6	4.0
Margin Size	**SUP-INF**	**LAT**	**ANT-POST**				
EPID RAW	7	9	10				
EPID eNAL	4	5	6				
CT RAW	6	9	14				
CT eNAL	5	6	8				

The recommended margin size that results in 90% probability that the minimum actual absorbed dose in the CTV is equal to the minimum dose in the PTV, i.e., 95% of 50 Gy, was calculated with the 'Van Herk margin recipe' [19]. These results are also displayed in table 6.4. The random errors have a much smaller impact on the calculated margin size than the syustematic errors have. However, the random errors here are reasonably large (fig 6.1) and could be attributed to the fact that the majority of patients included in this study had BMI values in the obese range and actual treatment was based on large volume 4-field box plans, possibly resulting in diminished accuracy and circumspection during setup.

6.3.2. EUD-based determination of the margin size

Using the distribution of setup errors found in 6.3.1., setup variations were randomly simulated and dose distributions were re-calculated with the isocenter of the day to determine the total dose in the RAW and eNAL corrected datasets. Figure 6.2 shows the resultant EUDs of the initial optimized treatment plans of the 14 patients in the study, each with 15 different margin sizes used in the optimization process. Note that the target EUDs that were achieved are stable over the first 6 mm of increasing margin size. As the margins increase further, larger volumes of overlapping PTV and OARs are found and these subsequently reduce the achievable PTV and CTV EUD with the optimization constraints in table 6.1. It could thus be expected that similar correlations of target EUD and margin size would be found when the simulation of setup errors was carried out.

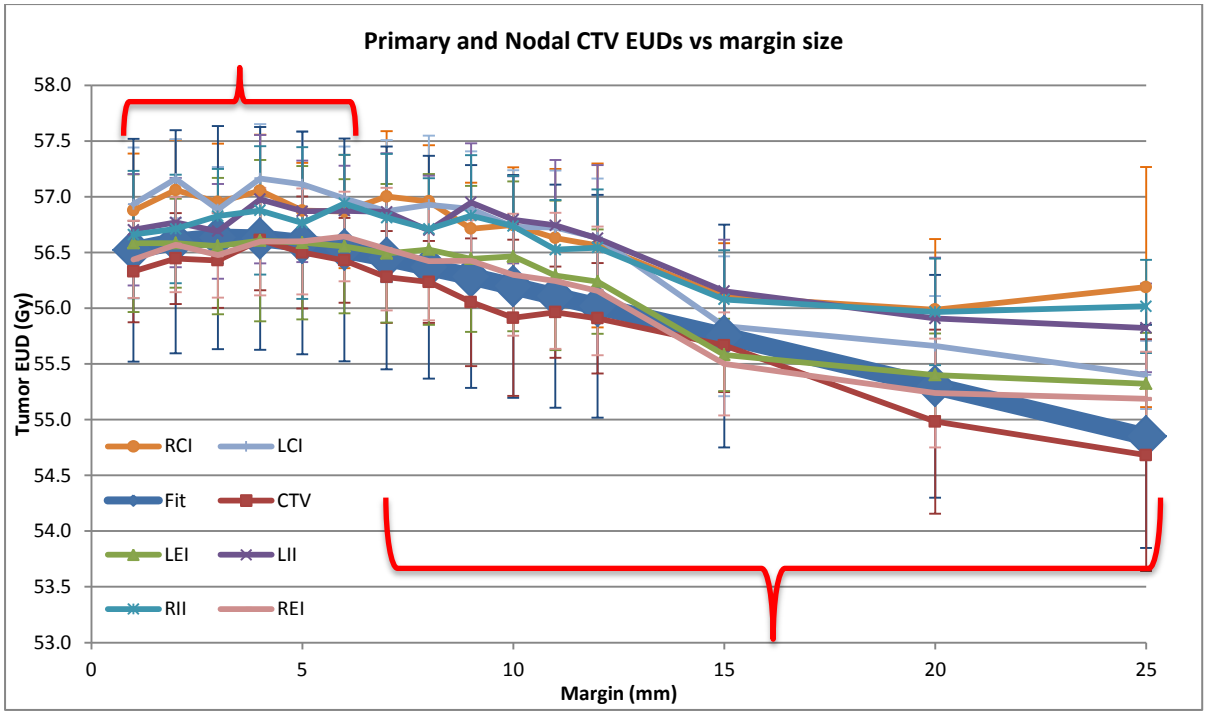

Figure 6.2: Target EUD variations of initial optimized treatment plans when the PTV margin size is increased. An average fit to the data is included in dark blue with large markers. CTV is the primary CTV and as before, RCI = right common iliac, LCI = left common iliac, REI = right external iliac, LEI = left external iliac, RII = right internal iliac and LII = left internal iliac.

Figure 6.3 a-g shows the resultant total target EUDs of the primary CTV and individual nodal CTVs for the RAW and eNAL simulations. A double exponential curve was fitted to the results and excellent agreement was found between the target EUD data points and the mathematical fit (correlation coefficients > 0.98 for all curves). Figure 6.3 h is a fit to the average of all target EUDs associated with different margin sizes. The target EUD fit has the form of:

$$y = x_0 + a\left(1 - e^{\frac{-x}{b}}\right) + cx + e^{\frac{-x}{d}} \qquad (6.1)$$

Table 6.5 contains the values of the fit parameters used in the equation. From figure 6.3 h the most suitable target margins range between 5 to 12 mm, and the dose increase achieved with the eNAL protocol over no use of a setup protocol ranges between 0.5 to 1 Gy total EUD and is statistically significant at the 95% confidence level (two-tailed student's t-test). The EUD fit in equation 6.1 results in at least 87% of patients in this study receiving at least an average EUD to each of the CTV volumes of 55.2Gy with a margin of 4-5 mm and larger with the eNAL correction applied. Without the correction, this margin needs to be larger than 9mm with an associated loss in CTV EUDs due to PTV and OAR overlap.

Table 6.5: Parameters for a mathematical fit to the EUD variations with increasing margin size.

	Parameters				
Correction	x_0	a	b	c	d
RAW	52.13	4.13	3.54	-0.08	0.10
eNAL	53.16	3.71	3.46	-0.09	0.10

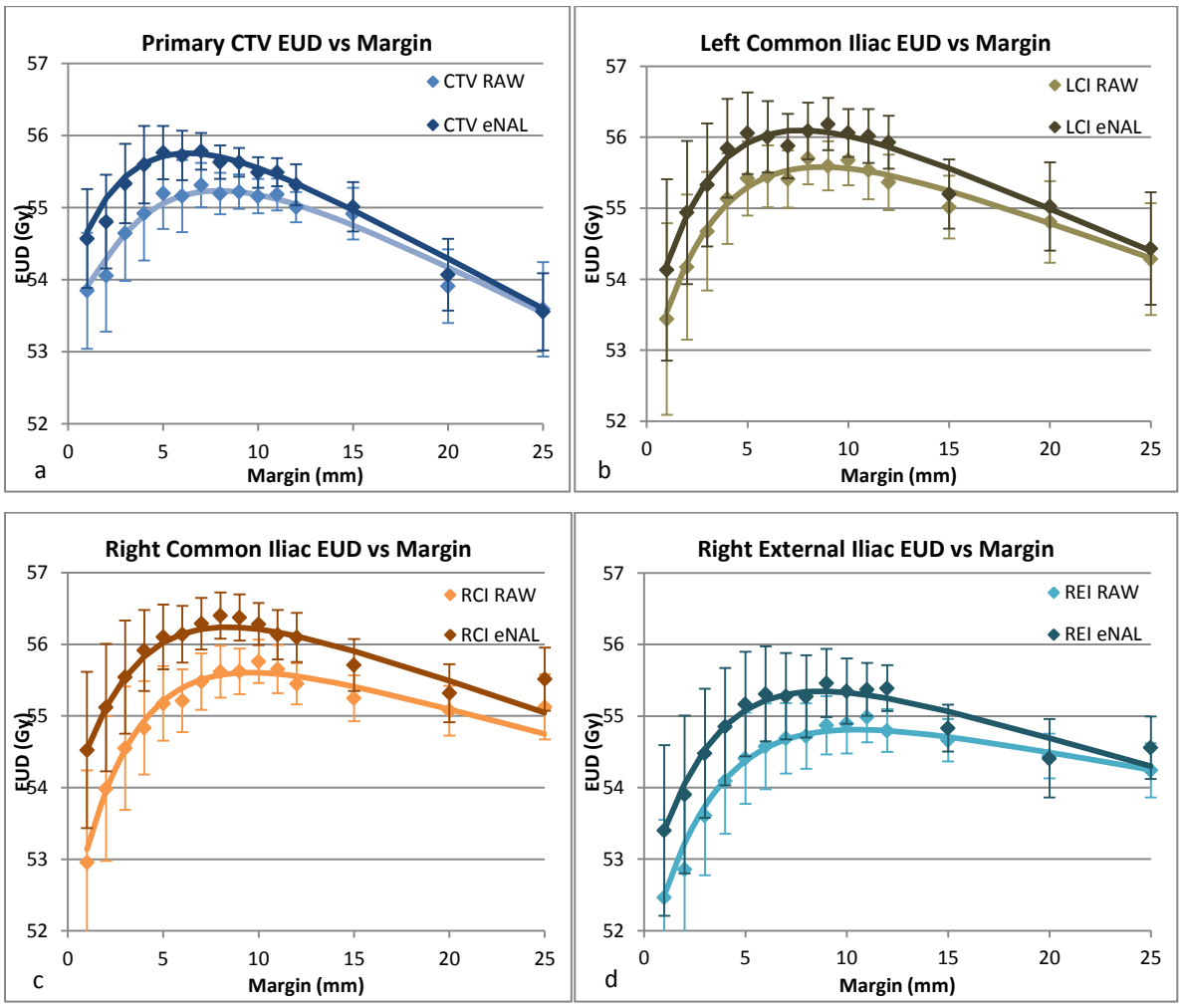

Figure 6.3. a) Primary CTV (CTV), b) Left Common Iliac (LCI), c) Right Common Iliac (RCI) and d) Right External Iliac (REI) EUD variations for 14 patients over 28 simulated treatment fractions with increasing PTV margin size. Data is shown for the RAW setup errors without any corrections and the eNAL corrected data.

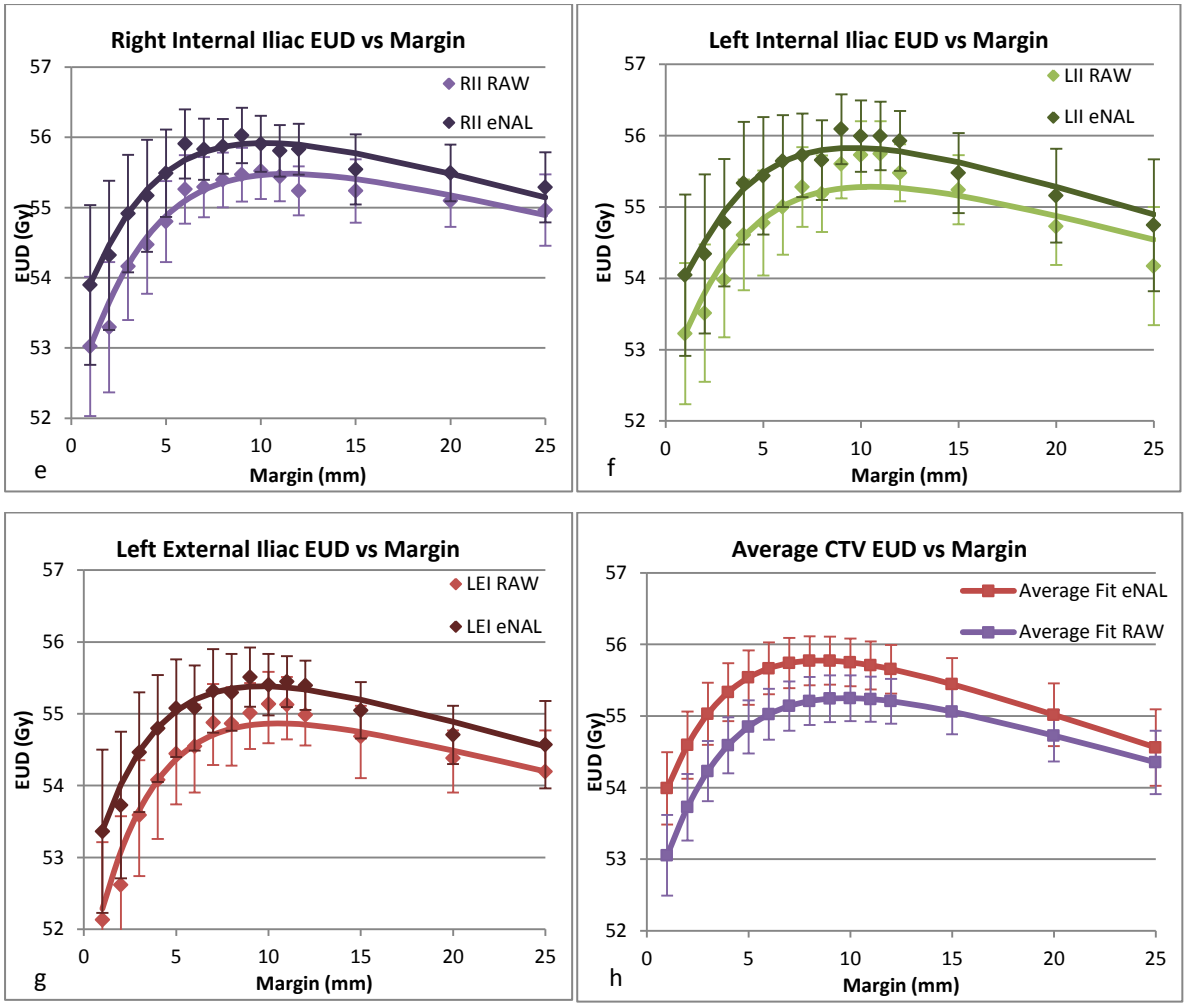

Figure 6.3. e) Right Internal Iliac (RII), f) Left Internal Iliac (LII), g) Left External Iliac (LEI) and h) average CTV EUD variations for 14 patients over 28 simulated treatment fractions with increasing PTV margin size. Data is shown for the RAW setup errors without any corrections and the eNAL corrected data.

6.3.4. Effect of margin size on PTV and OAR dose

Figures 6.4, 6.5 and 6.6 shows similar results to 6.3, only for the PTV and OARs. Each OAR plot has a solid red line that indicates the plan optimization constraint values that were used during the planning process. Figure 6.4 a and b are the results of the PTV EUD that decreases almost linearly with increasing margin due to the dose constraints of the overlapping OARs, while fig.6.5b is the root-mean-square (rms) under-dosage of the PTV that increases with larger OAR overlap.

The correlation of OAR EUDs and volumes receiving x Gy or more (V_x) in figures 6.5 and 6.6 respectively, have been fitted with second degree polynomial functions. From these OAR graphs the constraint criteria were never violated when margins of up to 15mm were used. The decrease in PTV EUD is thus a requirement to obey the constraint criteria

used here, although the CTV EUDs were still adequate in most cases. Table 6.6 illustrates how a margin size can be selected for a required CTV dose level (±1 standard deviation) in terms of EUD, based on equation 6.1. The corresponding PTV EUDs are also shown.

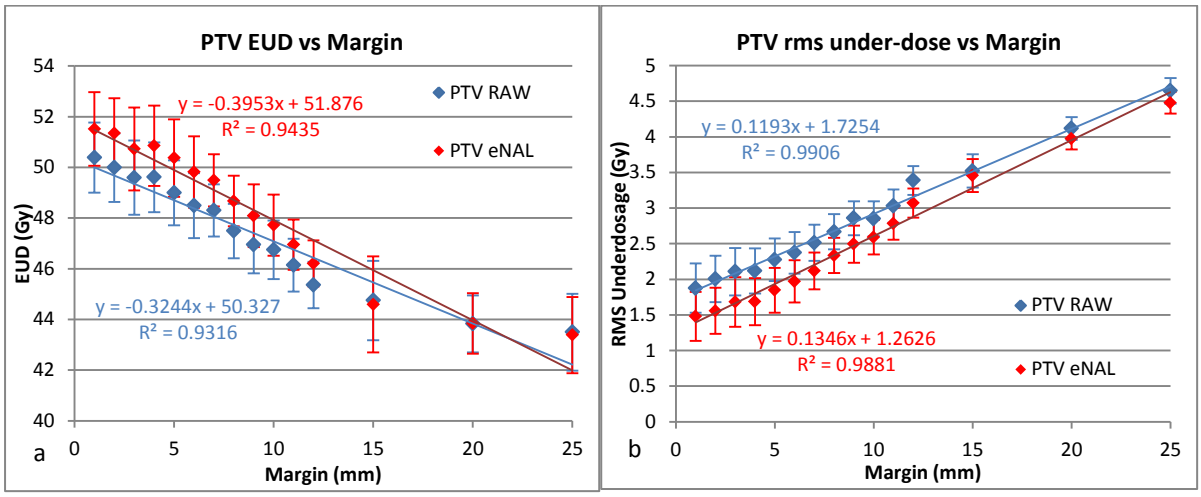

Figure 6.4 Variations of the a) Planning target volume (PTV) EUD and b) root-mean square under-dosage of the PTV for the 14 patients over 28 simulated treatment fractions with increasing PTV margin size. Data is shown for the RAW setup errors without any corrections and the eNAL corrected data.

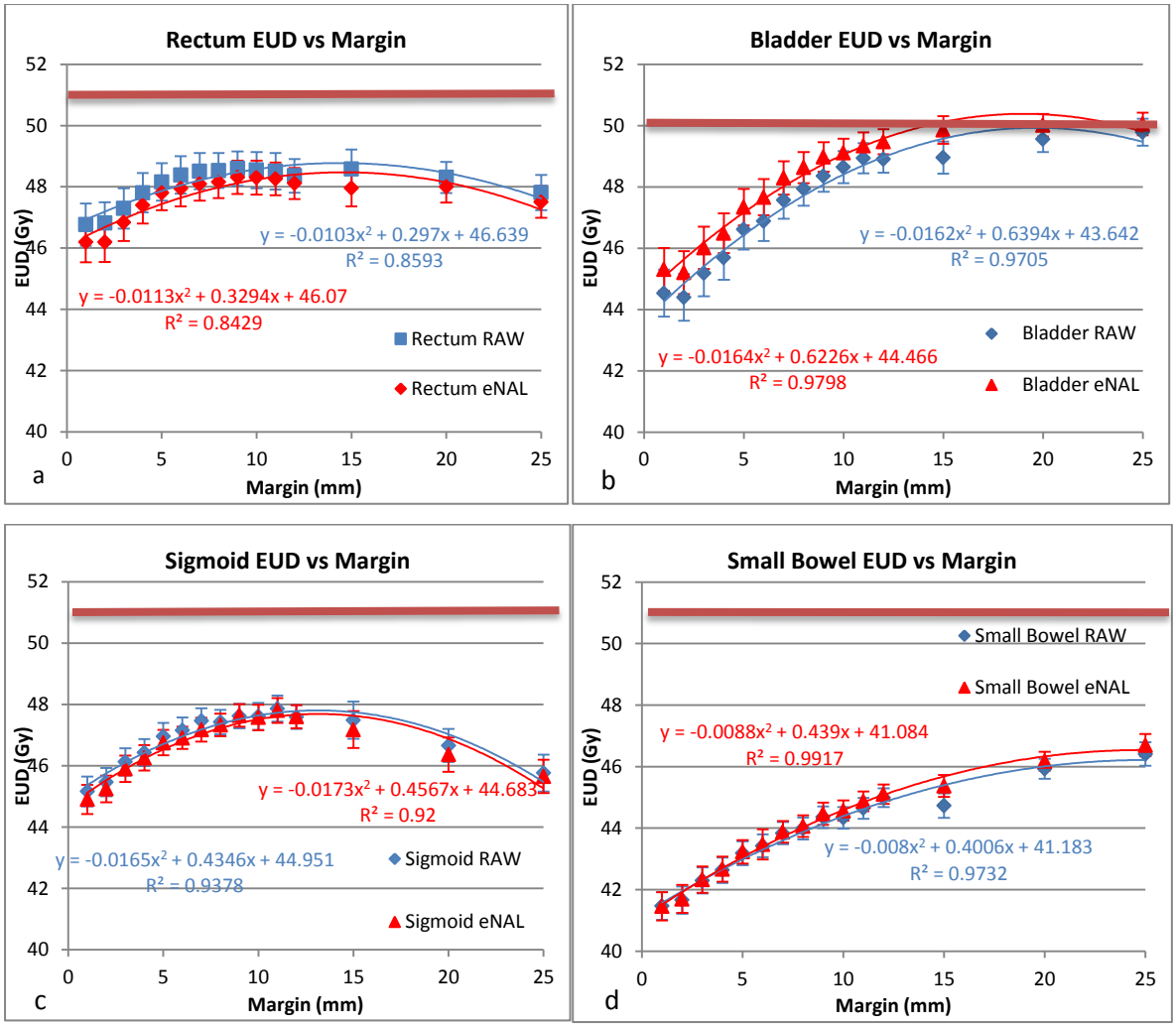

Figure 6.5 EUD variations of the a) Rectum, b) Bladder, c) Sigmoid and d) Small Bowel for the 14 patients over 28 simulated treatment fractions with increasing PTV margin size. Data is shown for the RAW setup errors without any corrections and the eNAL corrected data. Solid red lines represent the values of the plan optimization constraints.

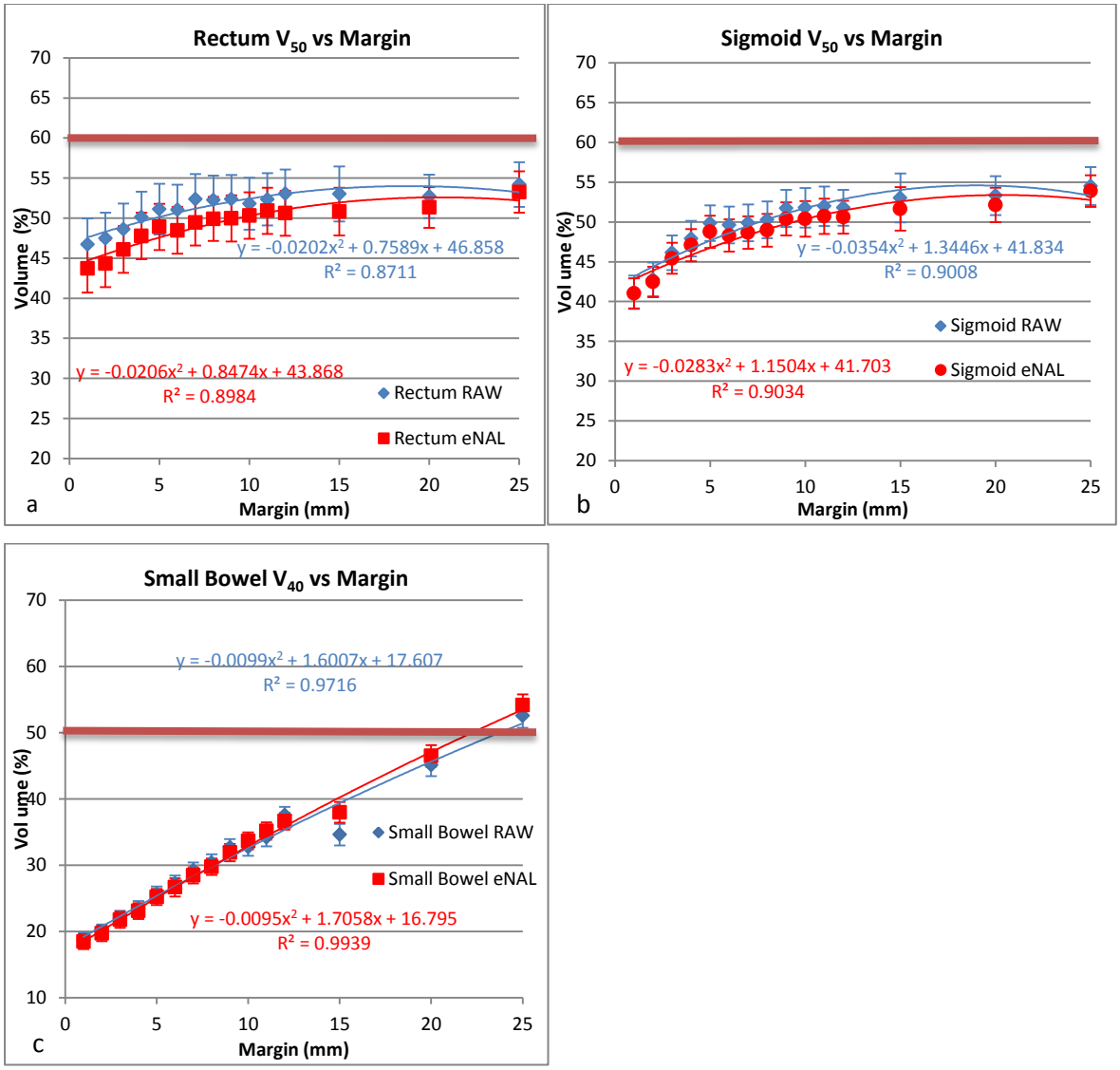

Figure 6.6 V_x (volume receiving x Gy and more) variations of the a) Rectum, b) Sigmoid and c) Small Bowel for the 14 patients over 28 simulated treatment fractions with increasing PTV margin size. Data is shown for the RAW setup errors without any corrections and the eNAL corrected data. Solid red lines represent the values of the plan optimization constraints.

Table 6.6: CTV margin requirements per EUD dose level. Minimum PTV EUDs are also indicated for each CTV EUD level.

	No SCP		eNAL SCP	
CTV EUD (Gy)	Margin(mm) ± EUD SD	PTV EUD (Gy)	Margin (mm) ± EUD SD	PTV EUD (Gy)
53.0	1 (± 1.5 Gy)	50.0	-	-
54.0	3 (± 1.5 Gy)	49.4	1 (± 1.0 Gy)	51.5
55.0	6 (± 1.5 Gy)	48.4	3 (± 1.0 Gy)	50.7
55.2	9 (± 1.5 Gy)	47.4	4 (± 1.0 Gy)	50.3
55.5	-	-	5 (± 1.0 Gy)	50.0
55.8	-	-	9 (± 1.0 Gy)	48.3

SD = standard deviation

6.3.5. Adaptive treatment simulation

An axial image with primary CTV contours of the planning CT, fractions 4, 8 and 23 is illustrated in figure 6.7a. Figure 6.7b is a sagittal view of the same patient and the 95% and prescribed dose (50 Gy) isodose lines are displayed in figure 6.7c. The CTV contours differ significantly between the initial planning CT and fractions 4 and 8 due to bladder and rectal filling, while the 23rd fraction's contour differs mostly due to major tumour shrinkage. Clearly, such motion and shrinkage does not only result in tumor under-dosage, but could result in OAR over-dosage (specifically small bowel in fraction 23) as well.

6.3.5.1. On-line re-planning

Figure 6.8a shows the simulation results of the primary CTV EUDs for the 9 CT images over which dose could be accumulated. The data represents an extract of only the imaged days to characterize motion progression over the full treatment course. Both the EUDs without adaptation and with on-line adaptation are shown. In fractions 4, 8 and 23 it is evident that the CTV was under-dosed. Superimposed on these results are the adaptive strategy results showing the corresponding adapted CTV dose. The associated OAR EUDs are shown in figure 6.8b-e. Figure 6.8a displays the minimum dose in 99% of the CTV volume (D99) of the respective instances throughout the total treatment, similar to the ICRU 83 (2010) D_{98} parameter (we chose D_{99} in accordance with Ahmad et al (2013)). The on-line adaptation manages to adjust all D_{99} values of the CTV above 1.90 Gy per fraction, which is 95% of the prescribed dose (2 Gy per fraction). Table 6.7 is a summary of the average EUDs to the CTV and OARs found in the on-line adaptive strategy. These dose values serve as a worst case estimate of the total dose.

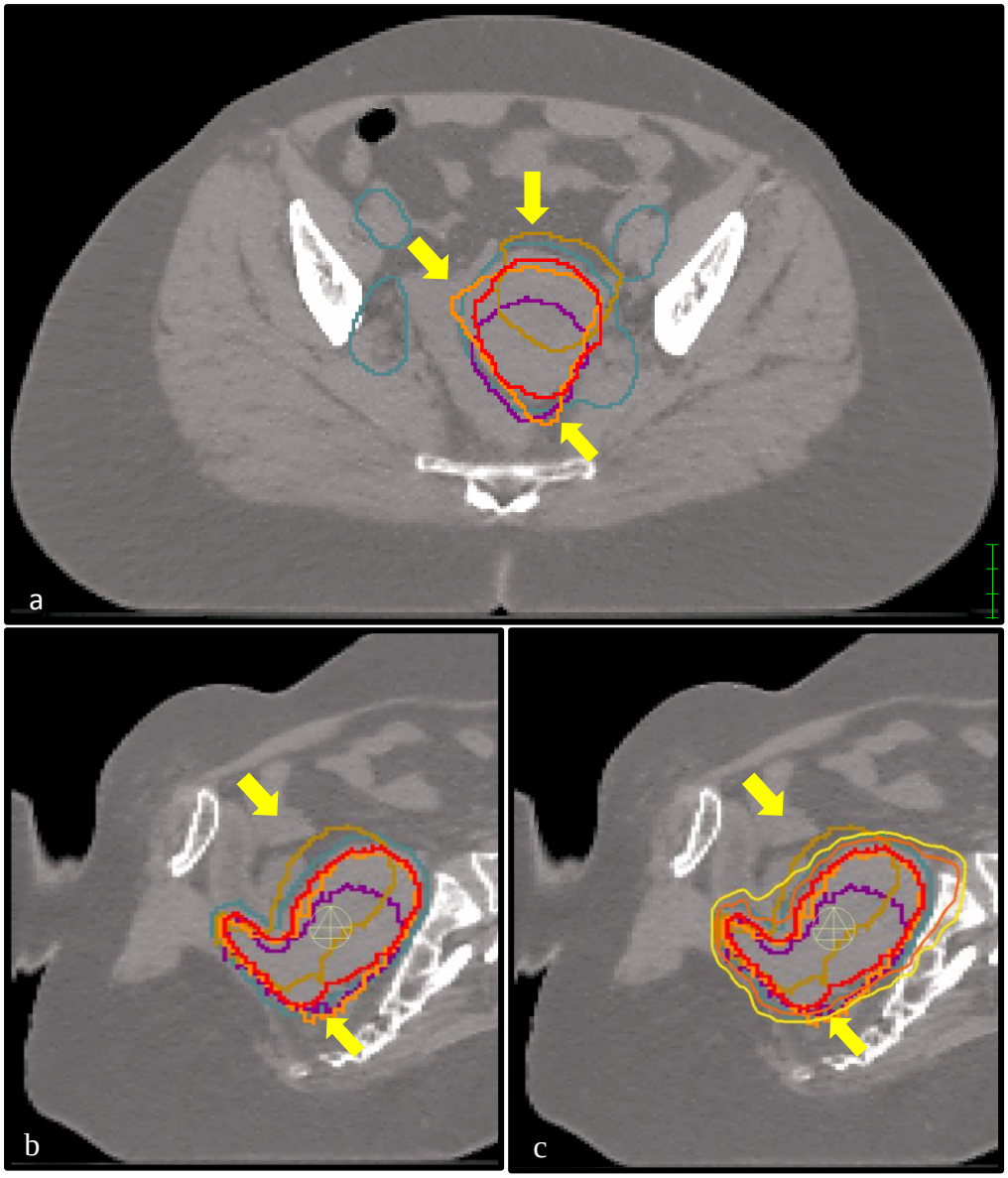

Figure 6.7. a) Axial, b) sagittal and c) sagittal plus isodose-lines CT images of the patient in this example. The blue contour is the planning 5mm PTV, red is the planning primary CTV, orange is the primary CTV of treatment fraction 4, brown is the CTV of fraction 8 and purple is the CTV of fraction 23. The isodose-lines represent 47.5 Gy (yellow) and 50 Gy (orange). The yellow pointers indicate regions of major motion/deformation and possible tumour under-dosage.

Table 6.7: Comparison of projected total EUDs of the primary CTV and OARs of the original treatment plan, on-line and off-line adaptive strategies.

Planning strategy:	Original	On-line adaptation	Off-line adaptation
Volume of interest	EUD (Gy)	EUD (Gy)	EUD (Gy)
Primary CTV	48.3	50.7	50.3
Rectum	45.3	44.5	45.1
Bladder	45.6	44.2	45.3
Sigmoid	48.7	48.0	48.8
Small Bowel	48.7	39.1	40.9

Figure 6.9b-e shows the minimum dose in the highest dose regions of the OARs. The volumes receiving these dose levels and more were chosen as 5% and 15% of the rectum, sigmoid and small bowel, and 5% and 25% of the bladder. For each of the three on-line adapted treatment fractions, the original and adapted doses differ from each other and the adapted doses are always lower than the original doses. The trends seen in table 6.7 are supported by the D_x data in figure 6.9.

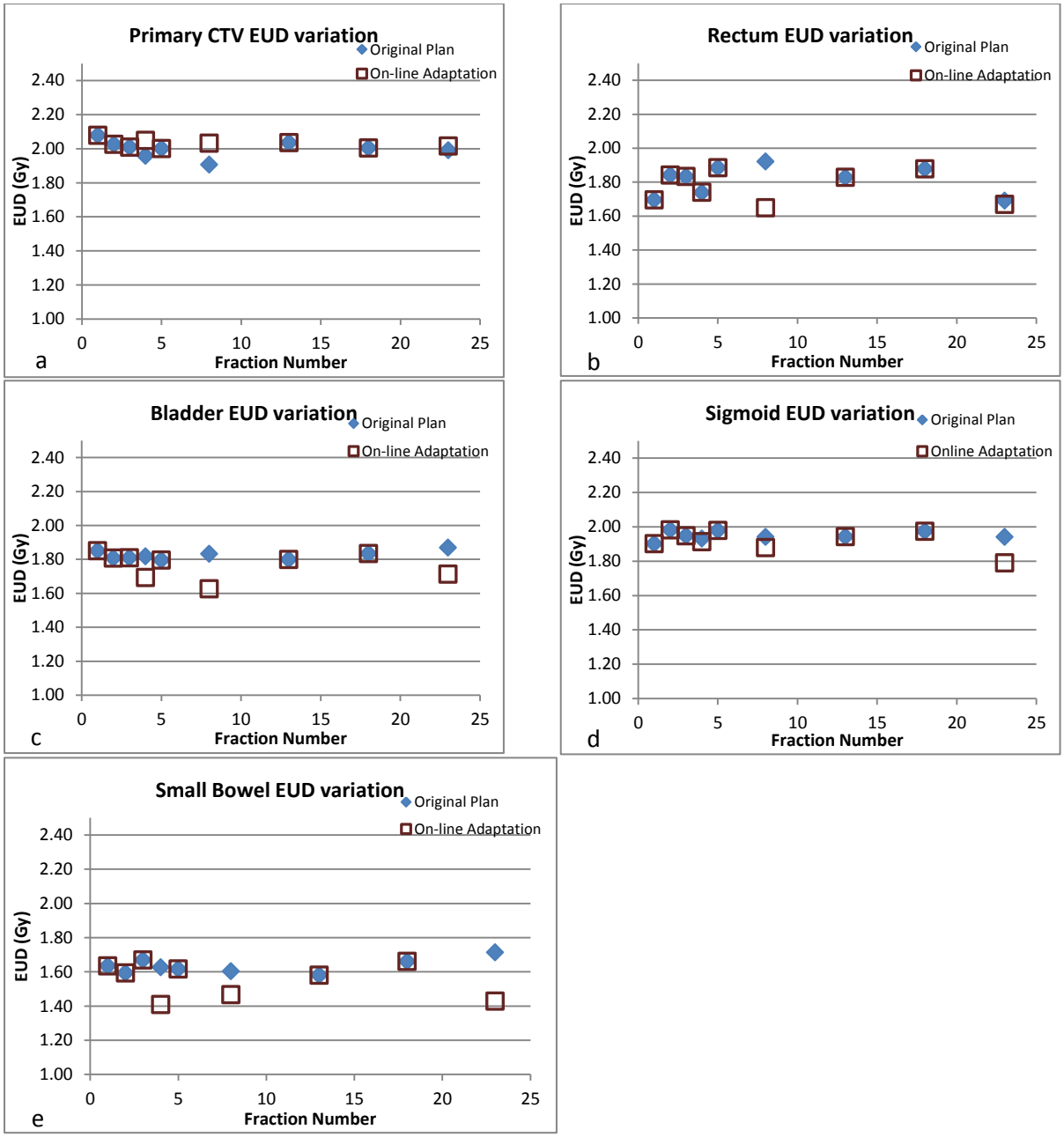

Figure 6.8. Comparison of a) CTV and OAR EUDs (b–e) of the original treatment plan without any adaptation during the treatment, and on-line adaptation performed during the course of the treatment.

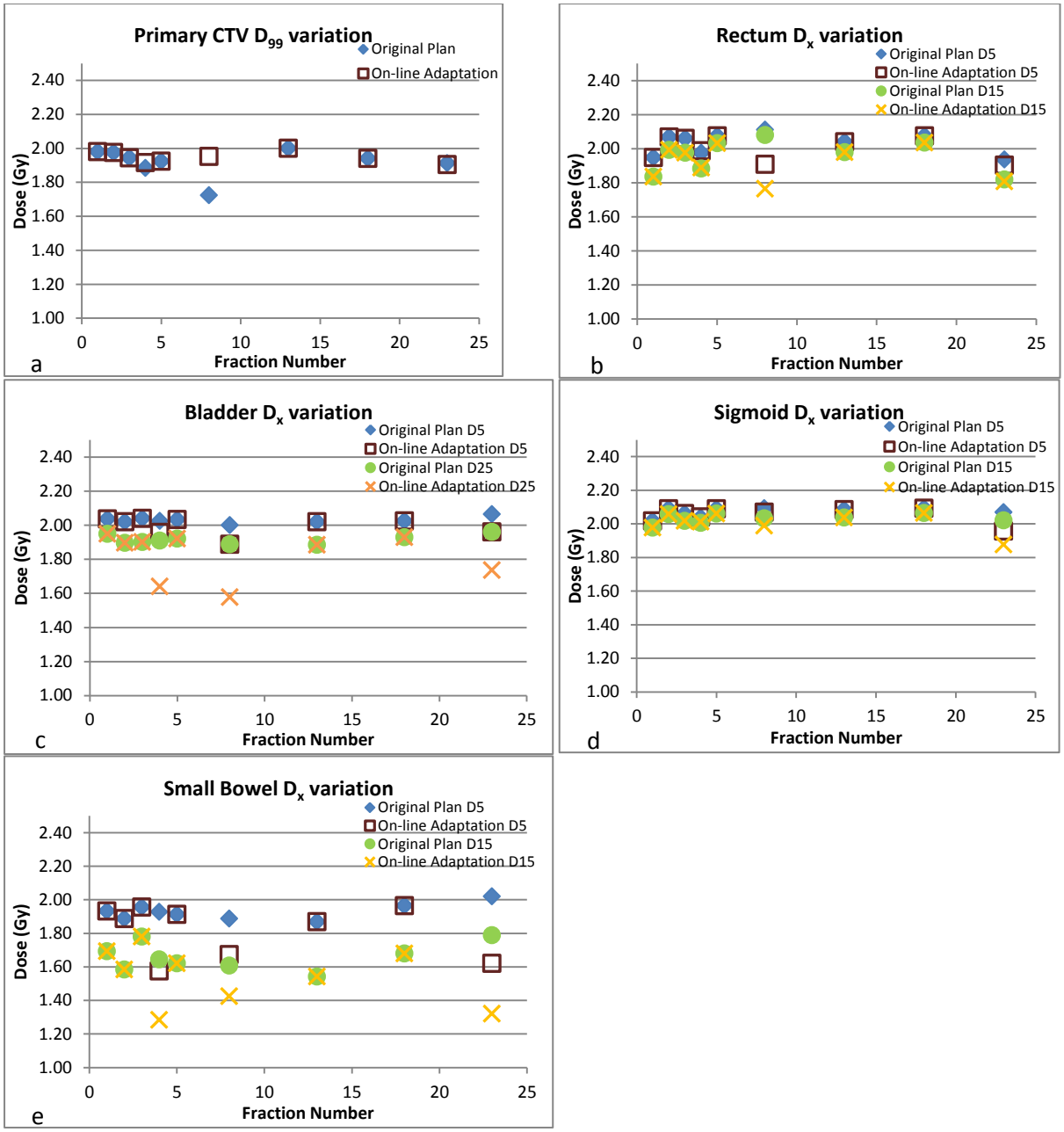

Figure 6.9. Comparison of a) CTV and OAR D_x (b–e) of the original treatment plan without any adaptation during the treatment, and on-line adaptation performed during the course of the treatment. The volumes, x, were 99% for the CTV, 5 and 15% for the rectum, sigmoid and small bowel, and 5 and 25% for the bladder.

6.3.5.2. Off-line dose accumulation and adaptation

In figure 6.10a the simulation results of the off-line technique is displayed for the primary CTV on the 9 CT datasets. As before, EUDs with and without adaptation is shown. The D_{99} values for the CTV are displayed in figure 6.11a and the OAR EUDs in fig.6.10b–e. The Dx values for the OARs are shown in fig. 6.11b–e. As in fig6.8a, the off-line strategy manages to increase the CTV dose with off-line adaptation by increasing the

OAR constraints based on past treatment fraction results. The average EUD for a whole treatment with off-line adaptation was projected 50.3 Gy EUD versus 48.3 Gy without adaptation. Table 6.7 summarizes the projected doses.

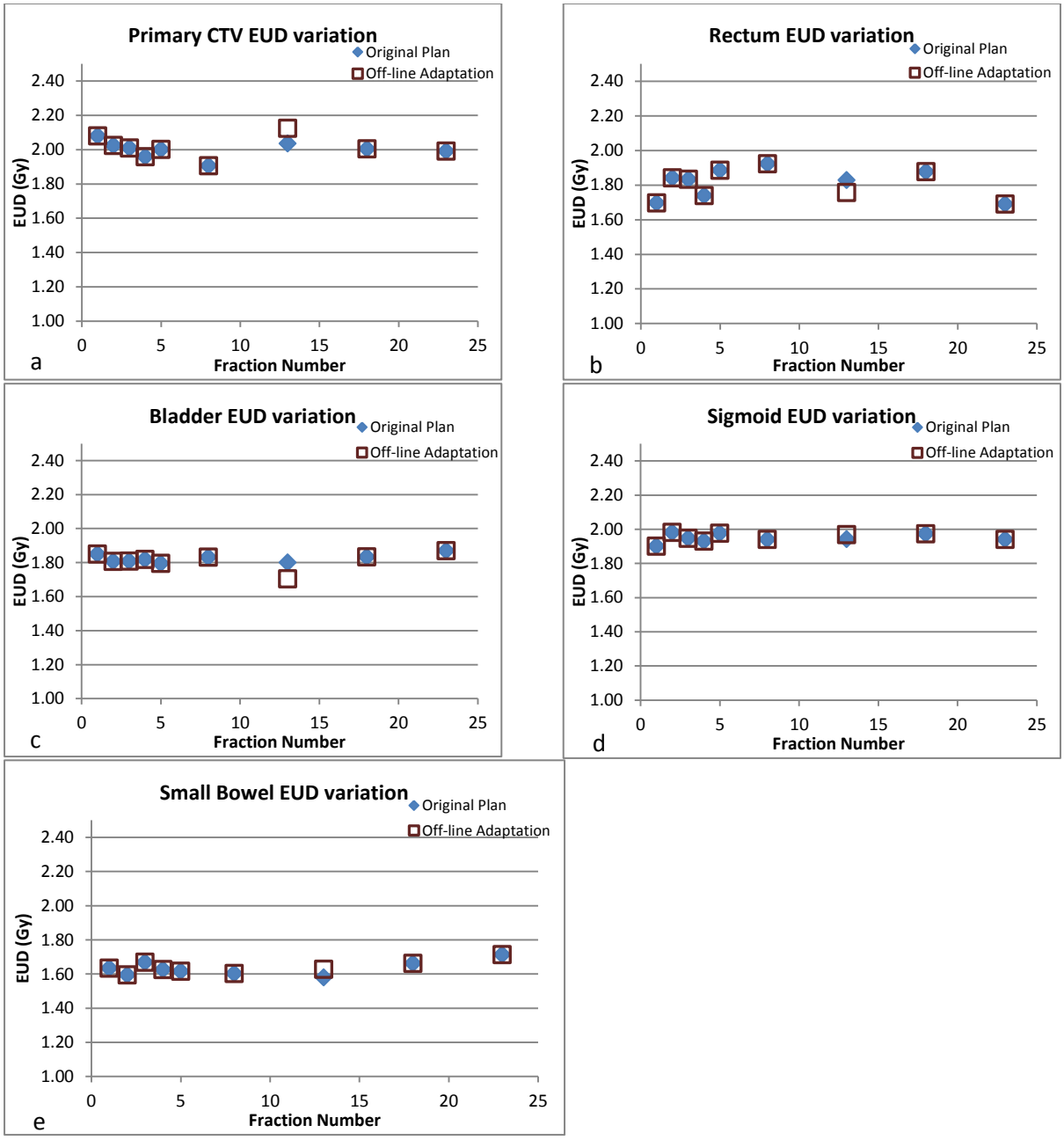

Figure 6.10. Comparison of a) CTV and OAR EUDs (b–e) of the original treatment plan without any adaptation during the treatment, and off-line adaptation performed during the course of the treatment.

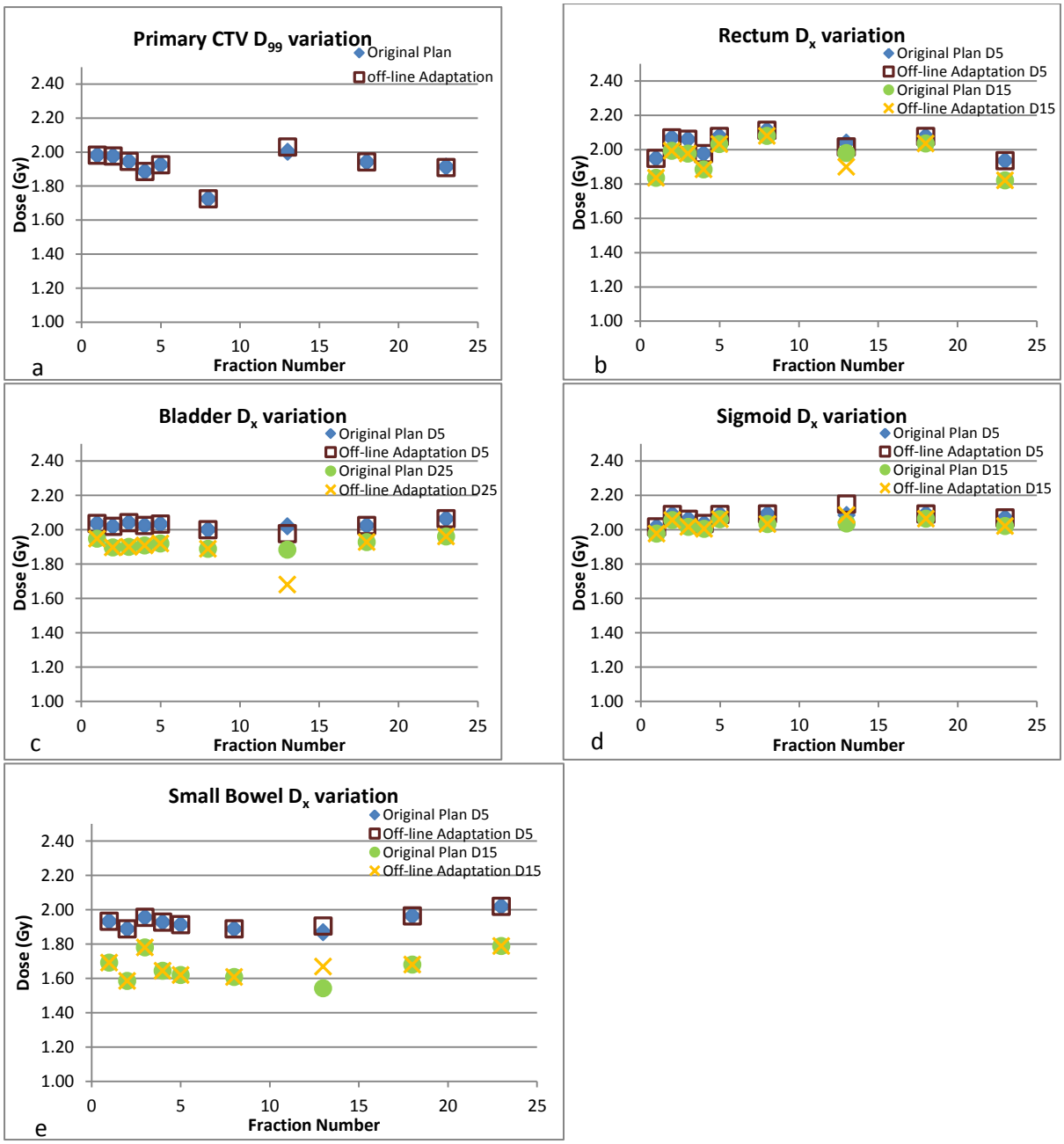

Figure 6.11. Comparison of a) CTV and OAR D_x (b–e) of the original treatment plan without any adaptation during the treatment, and off-line adaptation performed during the course of the treatment. The volumes, x, were 99% for the CTV, 5 and 15% for the rectum, sigmoid and small bowel, and 5 and 25% for the bladder.

6.4. Discussion

As a starting point, treatment planning margins ensure that adequate tumour dose can be planned for the CTV. Since normal tissue sparing is also an important aspect of treatment planning, these margins are kept as small as what target coverage would allow, based on patient population characteristics, anatomical site and treatment execution. The size of the margin can further be influenced by the type of image

guidance used for treatment and whether the images provide a means to perform 2D geometrical or positional adaptations during the setup procedure, or 3D geometrical and dosimetrical adaptations combined during all aspects of the treatment procedure.

6.4.1. Geometric and dosimetric margin assessment

In the geometric and dosimetric margin assessment results of this study there is a general observation that off-line setup corrections, particularly the use of the eNAL SCP, impacts geometric target coverage. This selection of patients could well benefit from such a minimum imaging protocol as the systematic errors for the population was almost halved. Dosimetrically it was evident that tumour dose is increased with the application of the eNAL protocol, while rectal and sigmoid doses were decreased. Bladder dose increased when the SCP was invoked due to the larger errors being in the Ant-Post direction. Small bowel dose was very similar for the two cases. The biggest impact could be seen in bladder dose, but the differences between RAW and eNAL results for OARs were overall small and almost no OAR constraint violations were found with and without the SCP invoked.

A major impact of the SCP was seen in the EUDs of the tumour volumes. The largest effect was on tumour volumes with small margins, typically 1 – 4 mm, and more so for smaller tumour volumes (nodes) than larger volumes (primary CTV). Both the margin recipe employed here, as well as the EUD dosimetric evaluation showed that margins can be drastically decreased with the use of the eNAL SCP, resulting in major OAR sparing.

Current geometric margin recipes that do not consider site specific physical dose distributions or biological effects of radiation might sometimes overestimate the required margin size as seen here. Such methods assume that the lower dose outside the 95% isodose line has no impact on cell kill in the tumour, but from a biological perspective this is an oversimplification. The dose gradients outside the CTV, inside the PTV, does add to significant cell kill (see table 6.6). This is an advantage of in-plane penumbra smoothing due to the use of co-planar beam angles or arcs and the resultant tumour exit dose. However, caution should be taken not to overestimate the cell kill capability of very low tumour dose, especially if the associated volume of low dose becomes large. The use of the EUD in this way of margin determination is quite valuable due to its sub-additive properties, which cannot be said for D_x (x being the volume receiving dose D).

The calculated margin requirements might only be applicable to cervix cancer and cannot simply be used elsewhere where the impact may be different, like the spinal cord. Furthermore, utilizing off-line SCPs will probably not be so useful in the treatment of cervix cancer with IMRT or VMAT since on-line imaging is preferable due to the excessive

motion of tumours and OARs in the female pelvic area. The use of off-line SCPs clearly prove to be advantages in maintaining planned doses and would be recommended where online protocols are not used. Considering the probability of achieving the same estimated biological effect of 95% of the prescribed dose for 90% of patients, 5mm margins are required to compensate for SCP corrected setup errors. Larger margins might be required for smaller (thinner) target volumes found in isolation or requiring very steep dose gradients due to serial-type organs in close proximity.

The use of the EUD as a dosimetric evaluation metric demonstrates that PTV margins are in a sense only "planning tools" and their under-dosage does not necessarily translate to tumour under-dosage because the dose is not zero outside the tumour volume. It would be useful to build the dose-gradient-margin-effect into the optimization procedure, rather than to optimize plans based on a fixed geometrical requirement in future. Gordon and Siebers (2008) have taken some steps in this direction.

6.4.2. Geographic and dosimetric adaptive treatment simulation

In the adaptive treatment simulation part of this study it was demonstrated that substantial tumour shrinkage and organ motion can significantly influence target coverage in cervix cancer treatment (fig 6.7). Several adaption strategies have been proposed, of which the on-line image-based strategies prove to be effective. Soft tissue dose matrix matching [14] has potentially better coverage results than bone-to-bone matching for the primary CTV, but since nodal CTVs are stable in relation to the pelvic bones, adaptation based only on soft tissue matching might result in nodal geographic miss.

In this limited study, sufficient target coverage can be achieved using either on-line and off-line re-planning. Although the concept seems executable, the study has to be extended to a larger number of patients over a wide spectrum of disease stage. In this single example, as was observed in other studies [14, 15], target movements and deformations are not predictable and bladder and rectal volume management protocols do not adequately control organ motion in a predictable way [28]. The PTV margin size for off-line re-planning must be large enough to include potential protrusion of the CTV outside the original prescribed dose region during the treatment excecution. As shown by Ahmad et al. (2013), several very large margins might be required to achieve a D_{99} of 95% of the prescribed dose to the CTV over the whole treatment course. From figure 6.7a a single large, non-adaptive margin could typically result in OAR over-dosage (fraction 23) and too small margins may result in tumour under-dosage (fractions 4 and 8).

In this example OAR doses were fairly constant throughout the simulated treatment course, except for the small bowel in fraction 23. The OAR dosimetric effects were less pronounced in fractions where large CTV motion was observed, but the impact of tumour shrinkage closer to the end of the treatment schedule resulted in major small bowel dose increases. In neither of the two strategies were OAR total dose violations seen. This is partly a consequence of the steep IMRT dose gradients that only influence the EUD of the non-overlapping section of the OARs, and that high dose regions of the OARs followed the movement of the CTV in mobile fractions. The unpredictability of movement may cause dose escalation in the OARs, or even dose reduction for some patients. Whatever the result, this will be patient specific.

It is expected that with the advances in computing power, auto-segmentation, imaging time reduction and automated re-planning, on-line and off-line re-planning will become less time consuming and more practical. One of the major concerns in both these approaches is the accumulation of dose over the course of treatment and is the driving factor behind the necessity to re-plan and adapt, or not. It was our explicit aim to show that costly dose accumulation with deformable image registration can be avoided using the EUD as a worst case dose estimate, supported by the D_x results. This procedure is repeatable, robust and straight forward to execute. Dose adaptation can thus be done safely, even if there is a requirement to escalate dose at some stage of the treatment to compensate for earlier under-dosages.

We recognise the limitations of this study. Patient geometry updates were weekly in the last 4 weeks and not daily in the adaptive section, only CT images were used in both parts of this study and clinical effects have only been correlated to the EUD for a few organs so far. Most importantly, we showed an example of only one patient. However, despite these limitations, the procedure has elements very similar to other studies based on larger patient groups, but more importantly we demonstrate the usefulness of on- and off-line dose adaptation using the EUD as a metric for worst case dose estimates, supported by D_x values for tumours and OARs.

6.5. Conclusion

Setup deviations, organ motion and deformation degrade the conformity of the planned dose distribution. The absorbed dose can in some instances differ significantly from the original planned dose distribution. Adaptations for these deviations are thus required to ensure curable treatment without the detriment of normal tissue over-dosage. The EUD proved to be a useful tool in determining the required margin sizes for this population-based sample of setup errors and shows reasonable similarities with published margin

recipes, but has the added advantage of evaluating the dose distribution comprehensively. EUD derived margins hint that margin recipes might overestimate the required margin size to compensate for setup errors.

In regions like the female pelvis where organ motion and deformation may be very large, off-line setup correction protocols may reduce target under-dosage, but organ motion can only be addressed with large PTV margins, resulting in reduced OAR sparing. A higher workload daily image guided protocol is more fitting for the treatment of these patients where off-line and on-line treatment adaptation are suitable techniques to achieve adequate target conformity throughout the treatment course. However, in both cases of image guided radiotherapy a reliable method for a cumulative dose estimate is required for ultimate decision making, i.e., to adapt the treatment plan/procedure or not. The EUD is such a reliable and robust estimate and can be implemented with ease, even in extremely mobile surroundings, like the female pelvis, and it has the potential to refine off-line and on-line adaptive treatment strategies. Further tests should be performed to evaluate the effectivity of the EUD in both these techniques and with the advent of using MRlinacs clinically, which provide excellent soft tissue contrast for accurate tumour delineation, the EUD could be a very usefull tool to assess planning margin sizes by combining superior soft tissue constrast and accurate tumour delineation with an accurate worst case scenario dose determination.

6.6. References

1. ICRU. International Commission on Radiation Units and Measurements. Prescribing, recording and reporting photon beam therapy. ICRU Report 50. Oxford University Press, Oxford, United Kingdom (1993)

2. ICRU. International Commission on Radiation Units and Measurements. Prescribing, recording and reporting photon beam therapy (Supplement to ICRU Report 50). ICRU Report 62. Oxford University Press, Oxford, United Kingdom (1999)

3. Van de Bunt L, van der Heide UA, Ketelaars M, et al. Conventional, conformal, and intensity-modulated radiation therapy treatment planning of external beam radiotherapy for cervical cancer: the impact of tumour regression. Int J Radiat Oncol Biol Phys 2006;64:189-196.

4. Kerkhof EM, Raaymakers BW, van der Heide UA, et al: Online MRI guidance for healthy tissue sparing in patients with cervical cancer: An IMRT planning study. Radiother Oncol 2008;88:241-249.

5. Taylor A, Powell ME: An assessment of interfractional uterine and cervical motion: Implications for radiotherapy target volume definition in gynaecological cancer. Radiother Oncol 2008;88:250-257.

6. Beadle BM, Jhingran A, Salehpour M, et al: Cervix regression and motion during the course of external beam chemoradiation for cervical cancer. Int J Radiat Oncol Biol Phys 2009;73:235-241.

7. Taylor A, Powell M. Conformal and Intensity-modulated Radiotherapy for cervical cancer. Clin Oncol 2008;20:417-425.

8. Chan P, Dinniwell R, Haider MA, et al: Inter- and intrafractional tumour and organ movement in patients with cervical cancer undergoing radiotherapy: A cinematic-MRI point-of-interest study. Int J Radiat Oncol Biol Phys 2008;70:1507-1515.

9. Stroom JC, Heijmen BJ. Geometrical uncertainties, radiotherapy planning margins, and the ICRU-62 report. Radiother Oncol 2002;64:75-83.

10. Witte MG, van der Geer J, Schneider C, Lebesque JV, Alber M, van Herk M. IMRT optimization including random and systematic geometric errors based on the expectation of TCP and NTCP. Med Phys 2007;34:3544-55.

11. Gordon JJ, Siebers JV. Evaluation of dosimetric margins in prostate IMRT treatment plans. Med Phys 2008;35:569-75.

12. Moore JA, Gordon JJ, Anscher M, Silva J, Siebers JV. Comparisons of treatment optimization directly incorporating systematic patient setup uncertainty with a margin-based approach. Med Phys 2012;39:1102-11.

13. Lim K, Small W Jr, Portelance L, Creutzberg C, Jürgenliemk-Schulz I, Mundt A, et al. Consensus guidelines for delineation of clinical target volume for intensity modulated pelvic radiotherapy for the definitive treatment of cervix cancer . Int J Radiat Oncol Biol Phys 2011;79:348–55.

14. Oh S, Stewart J, Moseley J, Kelly V, Lim K, Xie J, Fyles A, Brock KK, Lundin A, Rehbinder H, Milosevic M, Jaffray D, Cho YB. Hybrid adaptive radiotherapy with on-line MRI in cervix cancer IMRT. Radiother Oncol 2014;110:323-8.

15. Ahmad R, Bondar L, Voet P, Mens J, Quint S, Dhawtal G, Heijmen B, Hoogeman M. A margin-of-the-day online adaptive intensity-modulated radiotherapy strategy for cervical cancer provides superior treatment accuracy compared to clinically recommended margins: A dosimetric evaluation. Acta Oncol 2013;52:1430–1436.

16. Bondar M, Hoogeman M, Mens J, Quint S, Ahmad R, Dhawtal G, et al. Individualized nonadaptive and online adaptive IMRT strategies for cervical cancer patients based on pretreatment acquired variable bladder filling CT-scans. Int J Radiat Oncol Biol Phys 2012;83:1617–23.

17. Tyagi N, Lewis J, Yashar C, Vo D, Jiang S, Mundt A, et al . Daily online cone beam computed tomography to assess interfractional motion in patients with intact cervical cancer. Int J Radiat Oncol Biol Phys 2011;80:273–80.

18. ICRU. International Commission on Radiation Units and Measurements. Prescribing, recording, and reporting photon-beam intensity-modulated radiation therapy (IMRT). ICRU Report 83. J ICRU 2010;10:1–106.

19. Van Herk M, Remeijer P, Rasch C, Lebesque J, The probability of correct target dosage: dose-population histograms for deriving treatment margins in radiotherapy. Int J Radiat Oncol Biol Phys 2000;47:1121–1135.

20. Gordon JJ, Weiss E, Abayomi OK, Siebers JV, Dogan N. The effect of uterine motion and uterine margins on target and normal tissue doses in intensity modulated radiation therapy of cervical cancer. Phys Med Biol 2011;56:2887-901.

21. Xu H, Gordon JJ, Siebers JV. Sensitivity of postplanning target and OAR coverage estimates to dosimetric margin distribution sampling parameters. Med Phys 2011;38:1018-27.

22. Brixey CJ, Roeske JC, Lujan AE, et al: Impact of intensity-modulated radiotherapy on acute hematologic toxicity in women with gynecologic malignancies. Int J Radiat Oncol Biol Phys 2002;54:1388-1396.

23. Chen MF, Tseng CJ, Tseng CC, et al: Clinical outcome in post hysterectomy cervical cancer patients treated with concurrent Cisplatin and intensity-modulated pelvic radiotherapy: Comparison with conventional radiotherapy. Int J Radiat Oncol Biol Phys 2007;67:1438-1444.

24. Cozzi L, Dinshaw K, Shrivastava S, Mahantshetty U, Engineer R, Deshpande D, Jamema S, Vanetti E, Clivio A, Nicolini G, Fogliata A. A treatment planning study comparing volumetric arc modulation with RapidArc and fixed field IMRT for cervix uteri radiotherapy Radiother Oncol 2008;89:180–191.

25. Verma J, Sulman E, Jhingran A, Tucker S, Rauch G, Eifel P, Klopp A. Dosimetric Predictors of Duodenal Toxicity After Intensity Modulated Radiation Therapy for Treatment of the Para-aortic Nodes in Gynecologic Cancer. Int J Radiat Oncol Biol Phys 2014;88:357-362.

26. Niemierko A. Reporting and analysing dose distributions: a concept of equivalent uniform dose. Med Phys 1997;24:103–110.

27. Niemierko A: A generalized concept of equivalent uniform dose [Abstract]. Med Phys 1999;26:1100.

28. De Boer J, Heijmen B. A new approach to off-line setup corrections: combining safety with minimum workload. Med Phys 2002;29:1998-2012.

29. Ahmad R , Hoogeman MS , Quint S, Mens JW, de Pree I, Heijmen BJM . Inter-fraction bladder filling variations and time trends for cervical cancer patients assessed with a portable 3-dimensional ultrasound bladder scanner. Radiother Oncol 2008;89:172–179.

Chapter 7: Conclusion

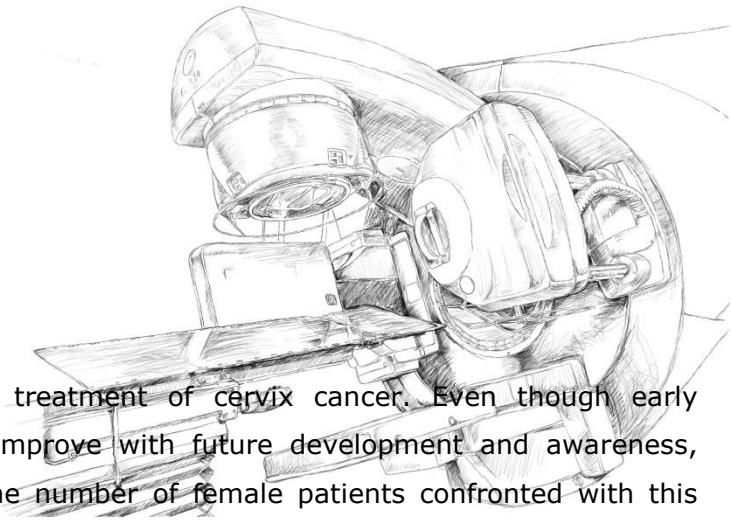

Radiotherapy has no equal in the treatment of cervix cancer. Even though early detection of the disease is set to improve with future development and awareness, recent statistics indicate a rise in the number of female patients confronted with this disease. Vaccination programs might reduce the incidence of cervix cancer in developed countries, but it is expected that developing countries will still be confronted with high incidence, mortality and prevalence rates for the next few decades.

Since radiotherapy consists of mostly two different treatment modalities, being external beam radiotherapy and brachytherapy, there is a need to be able to combine the dose delivered from each modality into a total dose value that can be correlated with treatment outcome.

7.1. Cumulative dose

In this study the EUD concept was applied to the cervix cancer radiation treatment planning problem of calculating the cumulative dose over multiple geometry instances in external beam radiotherapy (EBRT) and brachytherapy (BT), as well as the combination thereof.

Over the many years these two modalities have been used in several different combinations, a reliable dose accumulation method has not been developed that can be implemented clinically and used routinely in the combination of EBRT and BT. That said, this problem exists for each of these single modality treatments on their own. Some methods have been developed for this purpose based on warping dose back to a reference geometry, but they are fraught with uncertainties and difficult to verify. Their limitations and need for human intervention make them impractical for routine implementation.

The need for reliable total dose calculation is at an all time high. Recent developments in cervix cancer brachytherapy has transformed this procedure to individualised dose distributions for each patient in each treatment fraction, based on the high risk clinical target volume (HR-CTV) and organs at risk (OARs) geometrical configurations at the time of treatment. This image guided adaptive brachytherapy (IGABT) technique forces the dose distribution to follow the pathways of a shrinking tumour volume to deliver higher than before doses, but spares the organs at risk at the same time, and much

more than what was achieved in the past. The radiobiological effects of fractionated treatment are considered in the calculation of each per fraction dose, but total dose accumulation still relies on dose volume histogram (DVH) parameter summation and will typically lead to overestimations of the cumulative dose in these organs.

The same limitations in total dose calculation are applicable to external beam treatment. Since this part of the total treatment is delivered over a large number of fractions, it is simply accepted that the OARs and tumour receive the full prescribed dose in the volumes of interest for cervix cancer treatment, being most importantly the HR-CTV D90 and organ at risk D2ccs. No differentiation is thus made between the spatial location of the high or low dose regions and they are accepted to be contiguous. It is understandable and reasonable that such assumptions should be made, but they become problematic when non-standard treatment like IGABT and image guided adaptive radiotherapy (IGART) are combined to achieve very high and conformal tumour doses and sparing organs at risk at the same time. Then the addition of DVH parameters results in a very vague descriptions of the accumulated dose. Another important limitation when using OAR DVH parameter criteria is that the possible favourable outcomes of the optimization process are limited, whereas the use of EUD in plan optimization results in superior optimized plans.

The female uterus is a classic example of a mobile soft tissue target for which IGART and IGABT is an absolute necessity to achieve the required high dose levels in the target for local control, while sparing the normal tissues adequately. Image guided adaptive treatment has recently become more common practice in both external beam radiotherapy and brachytherapy, necessitating the need to compute the total dose effect accurately.

This study has derived how the mathematical properties of the equivalent uniform dose (EUD) can be exploited to compute a reliable worst case estimate of the combined effect of the dose distributions in multiple different geometries. A worst case scenario is obtained this way and may be used for a quick scoring of a treatment plan at only a fraction of the cost of a full analysis, without the need for deformable registration. The method was tested on several different geometries and various levels of complexity and proved to be accurate, extremely useful and straight forward to implement.

By virtue of Jensen’s inequality for a convex function, like the EUD of an OAR, the sum of the EUDs of each treatment fraction is always larger or equal to the EUD of warped and accumulated instance doses. Conversely, for tumours the EUD is a concave function of dose meaning the sum of the EUDs of each treatment fraction is always smaller or equal

to the EUD of warped and accumulated instance doses. This means that the EUD ensures a reliable worst case estimate of the metrics of the total treatment dose without the need for dose warping.

7.2. Brachytherapy treatment planning

The necessity to compute an accurate total dose effect is important in developing countries where patients often come from rural areas to be treated at radiotherapy facilities in bigger cities. There exists a strong rationale to ensure that these patients do not develop severe late side effects from treatment since the follow-up of the patients and management of late effects are usually done elsewhere, where access to specialized medical facilities could be non-existent. A typical conservative brachytherapy treatment protocol in our centre was tested against an EUD-based method.

While the use of a spatially variable rectal dose point in the conservative protocol considers spatially variable high dose regions, unlike the ICRU 38 recommendation, such point-based planning approaches are extremely dose limiting and prevents meaningful optimization of the treatment plans. These techniques do not consider the OAR volume comprehensively as is done in EBRT. The rationale behind the use of a dose point also disregards the profile of the OARs encountered in cervix cancer treatment that exhibit dose-volume effects.

The low tumour doses found in this study when applying such conservative planning strategies could in actual fact be escalated for all patients, even if a standard loading pattern for brachytherapy treatment was used. But clear guidelines on the values of the EUDs for OARs needed to be set as the constraints used in this study were still very dose limiting, even though the average tumour dose could be escalated. It became apparent in this study that much of the OAR dose sparing was focussed on the rectum, while in retrospect, the bladder was mostly dose limiting and future treatment in this department should prioritise the sparing of the bladder as well. Other organs like the sigmoid, small bowel and vagina should also receive attention if dose adaptation and escalation is pursued. In centres like ours were fixed levels of late normal tissue toxicity is set, the EUD can play a very useful role in treatment planning since an upper boundary of normal tissue dose and effect is achieved.

Since there was motivation to define suitable EUD dose constraints for image guided brachytherapy that do not exist, the subsequent investigation was aimed at defining an equivalent EUD-based dose prescription to that of the Gyn GEC-ESTRO recommendations. This was done in a planning study by deriving EUD constraint criteria

from GEC-ESTRO planning results and testing the criteria against the GEC-ESTRO results. The safety of the EUD method lies in the fact that it was derived from the GEC-ESTRO planning criteria by considering the DVHs of the OARs comprehensively, and the application of Jensen's inequality theorem ensures that the cumulative OAR EUD will always be less than or equal to the real EUD that was delivered over the full course of treatment. The EUD is also more robust against contour uncertainties of which DVH parameters are quite sensitive to and thus limit plan optimization possibilities. The fact that the EUD provides a reliable worst case estimate of cumulative dose also opens possibilities for safe dose escalation in IGBT or simultaneous integrated boosts in EBRT.

The influence of the choice of the volume effect parameter that is used in the determination of the EUD was also tested. The influence was found to be small, although safer when larger than 8. This means that if there is any uncertainty as to the correct value for a given OAR, a larger value should rather be used than a smaller to err on the safe side, without restricting plan optimization solutions too much. It was also seen that the EUD based plans are sometimes safer than the Gyn GEC-ESTRO plans as the latter occasionally produces OAR EUDs that are extremely high. Conversely, the EUD does not produce extreme D2cc values, even if the OAR volumes are unfavourable. Resulting OAR doses from EUD-based plans compared very well with other published Gyn GEC-ESTRO based results.

The most important aspect of this study is that the EUD method results in similar doses for cervix cancer IGBT that is found in GEC-ESTRO, but the dose accumulation method is reliable and safe. Compared to other studies where dose warping was performed to verify DVH parameter based worst case estimates of the cumulative dose, the DVH method may over- and under-estimate the dose, but the EUD will never underestimate the real EUD of the OAR. The use of EUD as a dose metric in IGBT, IGABT and IGART could potentially increase the credibility of dose-response relationships.

7.3. Fractionation compensation

To use the full potential of biological adaptive treatment planning, fractionation effects can be exploited by utilizing the cumulative biological effective dose at the end of every treatment fraction to maximize the tumour dose. It has been shown that doses in the range of 87-90 Gy to the HR-CTV D90 result in very high rates of local control and affects distant metastases and disease free survival as well. The EUD can be employed in two roles for dose escalation of the tumour: as a safeguard for dose compensation performed with DVH constraints, and as an alternative to DVH constraints for the fractionation compensation.

It could be demonstrated that by using more treatment fractions (4-5 fractions), the interplay between different dose limiting OARs on a per-fraction basis can be exploited to increase the tumour dose significantly in many patients without violating total dose constraints. By applying fractionation compensation, patients with favourable organ geometries reap the benefit of more fractions since optimal fractional OAR doses can be used to escalate the tumour dose even further. Fractionation compensation in combination with OAR dose maximization to a safe EUD constraint results in safely increased HR-CTV dose. This comes at no cost larger than that which the initial OAR dose constraints set out to achieve.

As mentioned in chapter 5, a dose escalation in the D90 of the HR-CTV from 81 Gy to 90 Gy has been associated with local control increases of 10%. In this light it might be postulated that even if fractionation compensation only achieves a 5 or 6 % escalation in tumour dose, this escalation could possibly translate into 5-6% increase in local control if the D90 of the HR-CTV can be escalated beyond 81 Gy. It is estimated that the effect of chemotherapy on local control is of the same order. Thus, with a simple planning constraint manipulation, local control can be increased at no additional toxicity cost. However, this type of dose escalation should only be done when accurate cumulative doses can be calculated and thus requires the application of EUD based planning.

7.4. Fast evaluation for adaptive radiotherapy

The versatility of the EUD was shown in the calculation of suitable setup variation margins for external beam IMRT of cervix cancer treatment. Compared to well known margin recipes, the EUD evaluation resulted in margin sizes comparable to theoretically derived margins, but considers the tumour dose comprehensively. Resultantly, the EUD method sometimes allow the use of smaller margins that will still result in adequate tumour dose and better OAR sparing, even if the PTV dose does not conform to typical internationally recommended prescription criteria.

However, setup variations in cervix cancer treatment would best be considered with online correction since the dosimetric effect of organ motion and deformation in the female pelvis is much greater than the effect of setup deviations. Since the EUD is a reliable total dose estimate, we have shown in a simple example that it is useful in keeping track of delivered doses during a course of external beam IMRT and that on-line treatment adaptation can be performed based on the cumulative EUD of the treatment to date, or by performing off-line adaptation when the need arises in a fast and effective way.

7.5. Future development

We believe that this dose metric holds promise to be used in on-line and off-line adaptive treatment strategies because of its ease of implementation and quick results. The safety of this methodology is supported by the application of the Jensen inequality of dose summation and provides a reliable and easily computable worst case dose estimate. It would certainly be worthwhile to further explore the use of the EUD in clinical studies where DVH and EUD dose metrics could be measured against treatment outcome. The ease in the calculation of the EUD and subsequent dose accumulation would require a minimal dosimetric workload for this purpose.

There are several other applications for the EUD in radiotherapy treatment planning. The first of these is the implementation in inverse optimization algorithms for biologically optimized brachytherapy treatment plans. Chapter 3, 4 and 5 alludes to the expansion of brachytherapy treatment planning in this way and it may prove to achieve better optimization results than what was reported here. Manual optimization performed in this study is one of the major limitations of the study. Furthermore, the study can be expanded to include more patients and test more possible scenarios.

Other applications might be the use of the EUD in Quality Assurance for IMRT or VMAT on a per patient basis. Several dosimetry devices and their software modules make use of dose or fluence measurements to recomputed dose distributions on the original planning CT. It is proposed that the EUD can be used as a dose metric to assess the quality of the delivered dose on the planning CT in comparison to the original optimized plan. The sensitivity of the EUD can be tested for this type of application and could potentially lead to the derivation of other similar types of dose metrics.

Summary

Recent advances in the treatment methods for cervical cancer have brought about many concerns of which one is how to calculate the cumulative dose in the extremely mobile pelvic organs and the tumour. This study demonstrates how a worst case estimate of the total dose for normal tissues and the tumour can be calculated without the need for deformation fields and dose warping. The method utilizes the equivalent uniform dose (EUD) concept and it has favourable mathematical properties for this application. This method is very fast in computing the cumulative dose from several treatment fractions and from different treatment modalities in deformable geometries and is straight forward to implement.

This application was used to evaluate conservative brachytherapy treatment planning protocols at our treatment centre and highlighted several limitations of this conservative treatment technique. EUD-based dose constraints could also be derived to perform image guided brachytherapy (IGBT) with these constraints in a way equivalent to the Gyn GEC-ESTRO standard of treatment, but with the added safety assurance of a reliable worst case dose estimate. For the same reason, a dose escalation study to improve local control in the primary cervical tumour with an image guided adaptive brachytherapy technique could be performed. This study showed that more treatment fractions with the same tumour and normal tissue constraints result in significantly higher tumour doses at no cost to normal tissues, and that a method of fractionation compensation could escalate the tumour dose even more for some patients.

The EUD proved to be a useful way of evaluating the required planning target volume margin size for external beam radiotherapy in the form of IMRT as well and the effect of setup correction protocols in the pelvic region could be described dosimetrically. Based on the EUD results, the eNAL setup correction protocol ensures significantly higher tumour doses and lower normal tissue dose compared to the case when there is no effort to correct for treatment setup errors. Since the cervix tumour is extremely mobile and subject to deformation during the course of radiotherapy, the EUD was also investigated as a cumulative dose determinant to assist in decision making during on-line and off-line image guided adaptive radiotherapy. In both on-line and off-line techniques the intended tumour dose could be reached without violating normal tissue dose constraints while severe organ motion and tumour deformation occurred during the treatment course. This was done via a quick update of the delivered dose to date.

Key Words: Equivalent Uniform Dose, Cumulative Dose, Dose Volume Histogram, Treatment Planning, Organ at Risk, Tumour, Worst Case Scenario, IGABT, IGART

Opsomming

Onlangse vooruitgang in die behandelings metodes vir servikale kanker het verskeie bekommernisse uitgelig waarvan een die vraag is hoe om die kumulatiewe dosis in die uiters mobiele bekkenorgane en kanker gewas te bereken. Hierdie studie toon hoe 'n "ergste geval skatting" van die totale dosis vir normale weefsel en die gewas kan bereken word sonder die noodsaaklikheid om van vervormings velde en dosis buiging gebruik te maak. Die metode gebruik die ekwivalent uniforme dosis (EUD) konsep en dit beskik oor gunstige wiskundige eienskappe vir hierdie toepassing. Hierdie metode is baie vinnig in die berekening van die kumulatiewe dosis vanaf verskeie behandelings fraksies en vanaf verskillende behandelingsmodaliteite in vervormbare geometrië en is maklik om te implementeer.

Hierdie toepassing was gebruik om 'n konserwatiewe bragiterapie behandelings beplanning protokol by ons sentrum vir behandeling te evalueer en beklemtoon 'n paar beperkinge van hierdie spesifieke behandelings tegniek. EUD-gebaseerde dosis beperkings was ook afgelei sodat beeld gebaseerde bragiterapie (IGBT) uitgevoer kon word met hierdie beperkings aangewend op 'n manier soortgelyk aan die GYN GEC-ESTRO standaard van behandeling. Die EUD metode beskik egter oor die bykomende versekering van veiligheid deur middel van 'n betroubare "ergste geval" dosis beraming. Vir hierdie selfde rede kon 'n dosis eskalasie studie uitgevoer word om plaaslike beheer in die primêre servikale gewas te verbeter met 'n aangepaste beeld begeleidings bragiterapie tegniek. Hierdie studie het getoon dat meer behandelings fraksies, met dieselfde gewas en normale weefsel dosis beperkings, lei tot aansienlik hoër gewas dosisse sonder om normale weefsel dosis te verhoog. Deur verder fraksionerings kompensasie toe te pas kan die gewas dosis selfs verder verhoog word vir sommige pasiënte.

Die EUD is bewys as 'n nuttige manier om die vereiste beplannings teiken volume marge grootte mee te evalueer vir eksterne bundel bestraling in die vorm van IMRT, sowel as die uitwerking van opstellings korreksie protokolle vir die bekken area in vergelyking met geen korreksie protokol nie. Gebaseer op die EUD resultate lewer die eNAL opstellings korreksie protokol verseker aansienlik hoër dosisse aan die gewas en laer dosisse aan die normale weefsel in vergelyking met wanneer daar geen poging vir korreksies uitgevoer word nie. Aangesien die serviks gewas uiters beweeglik en onderhewig aan vervorming is deur die loop van bestraling, was die EUD ook ondersoek as 'n kumulatiewe dosis determinant om te help met besluitneming tydens aktiewe en dormante aangepaste beeld begeleide bestraling. In beide die aktiewe en dormante tegnieke kon die beoogde gewas dosis bereik word sonder die oortreding van die

normale weefsel dosis beperkings, terwyl erge orgaan beweging en gewas vervorming plaasgevind het tydens die behandelings kursus. Hierdie prosedure kon baie spoedig uitgevoer word deur eenvoudig die gegewe dosis tot op hede op te dateer met die EUD.

Sleutel Woorde: Ekwivalente Uniforme Dosis, Kumulatiewe Dosis, Dosis Volume Histogram, Behandelings Beplannning, Kritieke Orgaan, Tumor, Ergste Geval Skatting, IGABT, IGART

Acknowledgements

It is always risky to acknowledge people who contributed and supported one in completing a thesis as the chance of forgetting someone is real, but of course not intentional. Consequently I would like to thank everyone that have contributed, in whichever way, to the successful completion of this thesis. Above all I am grateful towards my Heavenly Father for this opportunity and the strength I received to complete this work.

I have learnt so much during this voyage, both work related and not related at all! I have met so many interesting and talented people that have enriched my life in several ways.

To my promoter, Prof. William Rae, for your willingness to have taken on this project with me. Thank you for your support and input in this manuscript. I trust that this journey was learnsome to you as well, and it was a pleasure sharing ideas and thoughts with you during this time. Thank you for your encouragement, positive attitude and contribution to this work and my professional career.

Prof. Markus Alber, my co-promoter, I have no words to describe my gratitude towards you. Without your input in my career reaching over almost a decade now, I would probably not have reached this milestone. Thank you for all the discussions, visits to your department, Skype sessions, telephone conversations and emails. You have always been available to answer even my most modest questions. What I have learnt from you in our discussions is immeasurable and has no equal. Thank you for always making time for me and urging me to complete this study. I appreciate your commitment and encouragement, for being a tough sparring partner, and for your endorsement to work on Hyperion.

I would like to thank the examiners who scrutinized this thesis for your positive contributions to the standard of the document. Thank you for your willingness to have acted as examiners and the constructive critique you have so carefully formulated. Your positive commentary has made me realize that it was all worth it.

Dr. Uulke van der Heide for your positive attitude towards this project and the interest that you took in it. I have had very constructive discussions with you and Prof. Ben Mijnheer while I visited you overseas. Thank you both for giving me the perspective that led to a meaningful investigation. Also Dr. Matthias Söhn for the fruitful discussions we had and your willingness to assist me with anything.

I would like to acknowledge the patients who participated in this study. Without your consent and the use of your data, this would not have been possible.

I sincerely thank my colleagues at work for your support, especially in the last couple of weeks when you took over many more tasks in my absence. Thank you Dedri, Cobus, Lourens, Itumeleng, Freek and especially Omer, for your constant inquisition on my progress.

To my family, that is extended family, for your continued love, support and motivation. Even though we as a family have had so many setbacks during this period, not once have you hesitated or forgotten to express your support, offered some kind of assistance

or neglected a pep-talk. Thank you for supporting Lerie during this time when the boys needed their mother more than usual due to their father's absence. Thanks also, Ouboet, for taking the time to produce the cover design and those in the chapters.

To my wife goes my sincerest gratitude. Dankie Lief, dat ek uiteindelik kon klaarmaak hiermee, selfs in die moeilike tyd na Neil se geboorte. Dankie vir jou geduld met my, ondersteuning en geloof dat hierdie saak tot 'n suksesvolle einde sou kom. Jou kapasiteit vir my en my dinge is groter as wat ek ooit besef het. Ek is nou klaar en jy het jou man terug. Liampie en Neiltjie, Pappa is nou 100% beskikbaar en nou het ons weer 'n nuwe, beter normaal. Ek is baie lief vir julle almal.

Lastly, I thank the Medical Research Council (MRC) of South Africa for providing me with funding that could be utilized for the completion this project.

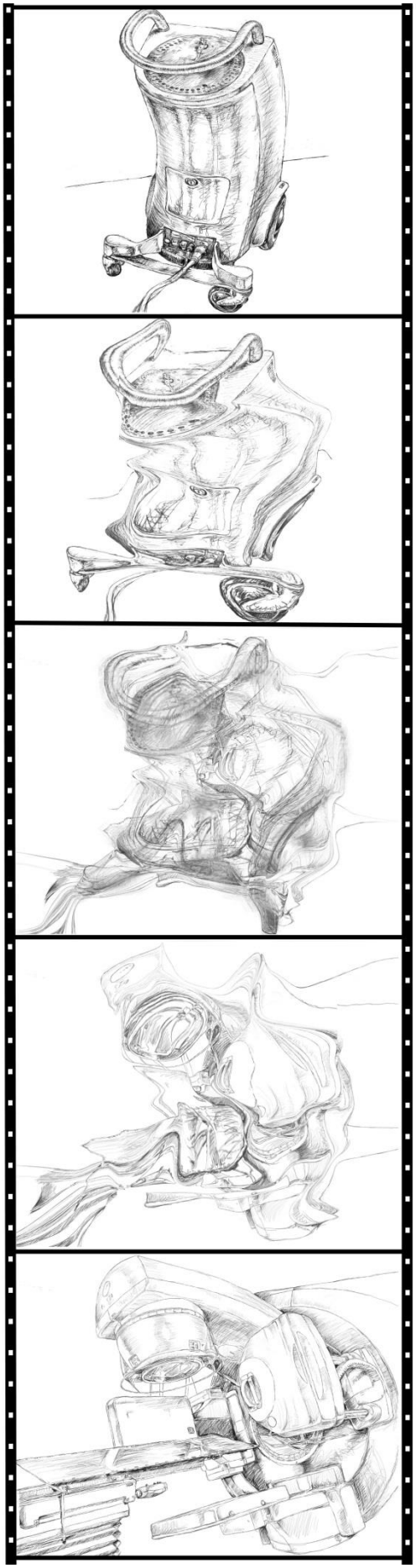

Appendixes

Appendix I: Sobotta B, Söhn M, Shaw W and Alber M. On expedient properties of common biological score functions for multi-modality, adaptive and 4D dose optimization. Phys Med Biol 2011;56:N123–N129

Appendix II: Shaw W, Rae W and Alber M. A Solution for brachytherapy biologically guided dose individualisation in the treatment of cervix cancer. World Congress on Medical Physics and Biomedical Engineering, IFMBE Proceedings 2012;39: 2276–2279.

Appendix III: Shaw W, Rae W and Alber M. Equivalence of Gyn GEC-ESTRO guidelines for image guided cervical brachytherapy with EUD-based dose prescription. Radiat Oncol 2013;8:266.

Phys. Med. Biol. **56** (2011) N123–N129 doi:10.1088/0031-9155/56/10/N01

NOTE

On expedient properties of common biological score functions for multi-modality, adaptive and 4D dose optimization

B Sobotta[1], M Söhn[2], W Shaw[3] and M Alber[1]

[1] Section for Biomedical Physics, Radioonkologische Uniklinik, Universität Tübingen, 72076 Tübingen, Germany
[2] Department of Radiation Oncology, University Hospital Grosshadern, LMU München, 81377 München, Germany
[3] Department of Medical Physics, Faculty of Health Sciences, University of the Free State, PO Box 339, Bloemfontein 9300, South Africa

E-mail: benjamin.sobotta@med.uni-tuebingen.de

Received 1 January 2011, in final form 9 March 2011
Published 13 April 2011
Online at stacks.iop.org/PMB/56/N123

Abstract
Frequently, radiotherapy treatments are comprised of several dose distributions computed or optimized in different patient geometries. Therefore, the need arises to compute the comprehensive biological effect or physical figure of merit of the combined dose of a number of distinct geometry instances. For that purpose the dose is typically accumulated in a reference geometry through deformation fields obtained from deformable image registration. However, it is difficult to establish precise voxel-by-voxel relationships between different anatomical images in many cases. In this work, the mathematical properties of commonly used score functions are exploited to derive an upper boundary for the maximum effect for normal tissue and a lower boundary for the minimum effect for the target of accumulated doses on multiple geometry instances.

(Some figures in this article are in colour only in the electronic version)

1. Introduction

The need to compute the combined effect of several dose distributions in distinct geometries arises in a number of applications. For example, some approaches to 4D IMRT optimization optimize dose simultaneously on multiple geometries (Birkner *et al* 2003, McShan *et al* 2006, Söhn *et al* 2009, Trofimov *et al* 2005) by warping the dose in each instance to a reference geometry, thereby realizing optimization in 'tissue-eye-view'. Also in combined modality treatment, e.g. brachytherapy and external beam therapy, the overall effect has to be computed (Osorio *et al* 2010). Similar problems occur with the dose recomputation in mobile organs,

e.g. prostate on daily cone beam CT (Morin *et al* 2006, Rong *et al* 2010). Since particle therapy is very sensitive to geometry changes, especially in regions with heterogeneous density, doses have to be computed on several geometries and subsequently combined (Soukup *et al* 2009, Knopf *et al* 2010).

All of these methods require a correspondence between the volume elements (voxels) of each geometry instance to add up each dose contribution correctly. In general this requires deformable registration. Given the independently computed doses in each patient geometry, the voxel correspondence is used to warp the individual doses back to some reference geometry. In this reference geometry, the doses are accumulated and evaluated. Unfortunately, there are several issues with this approach. The computation of the deformation fields is fraught with uncertainties and difficult to verify. The computation frequently needs human surveillance and the data set may be incomplete or disturbed by artifacts. Some organs, especially bowel, are difficult to model because of variations in filling and the lack of fiducials. Incomplete knowledge of the extent of movement due to infrequent and sparse imaging may also affect the accuracy of the model. Additionally, special care must be taken to ensure energy conservation during dose warping and accumulation. Dose distributions are frequently analyzed with score functions that are a sum over all volume elements of an organ. In contrast to pointwise scores, a lot of the effort that goes into correct dose accumulation is washed out in the summation. Very often, these score functions are convex, which opens a possibility for very powerful estimations of their true value without going through the process of proper dose accumulation.

This note derives how the mathematical properties of commonly used cost functions, e.g. equivalent uniform dose (EUD) (Niemierko 1997), can be exploited to compute boundaries of the combined effect of the dose distributions in different geometries. These boundaries are computed *without* the need for deformable registration. For the target, lower boundaries will be given, and for the critical structures upper boundaries. Thus, a worst case scenario is obtained that may be used for a quick scoring of a treatment plan at only a fraction of the cost of a full analysis. The method is demonstrated on a prostate case with interfractional movement and a 4D lung case.

2. Methods and materials

Suppose F is a score function and let D_k be the dose distribution of the full treatment applied to the kth geometry instance I_k. For dose accumulation, a reference geometry I_0 is chosen. $\tilde{D}_k$ denotes the warped dose in the reference geometry, i.e. the deformation field from I_k to I_0 applied to dose D_k. Hence, the quantity of main interest, the accumulated dose, is

$$\mathrm{E}[\tilde{D}] = \frac{1}{N}\sum_{k=0}^{N-1}\tilde{D}_k \qquad \text{with} \quad \tilde{D}_0 \equiv D_0. \tag{1}$$

Note that the accumulated dose is expressed as an average in (1). Average and sum are equivalent because the dose distribution may be rescaled by a constant factor.

Dose warping as well as dose accumulation is a linear operation and therefore the dose integral of D_k over the volume of interest equals that of $\tilde{D}_k$. This is a direct consequence of energy and volume conservation. By virtue of this, and by way of definition

$$F(D_k) = F(\tilde{D}_k). \tag{2}$$

If no deformation field is available, the single doses D_k cannot be warped back to the reference geometry, and in other words $\tilde{D}_k$ is inaccessible. However, by virtue of *Jensen's inequality* (Jensen 1906) for a convex function F,

$$F(\mathrm{E}[\tilde{D}]) \leqslant \mathrm{E}[F(\tilde{D})] = \mathrm{E}[F(D)] \tag{3}$$

can be established. Conversely, for concave functions F, (3) reverses to

$$F(\mathrm{E}[\tilde{D}]) \geqslant \mathrm{E}[F(\tilde{D})] = \mathrm{E}[F(D)], \tag{4}$$

where $\mathrm{E}[F(D)] \equiv 1/N \sum_{k=0}^{N-1} F(D_k)$ is the sum of the score function evaluated for each original geometry instance. The equality relations in (3) and (4) are due to (2).

Convex functions (curved upward) are commonly associated with normal tissues or other dose-limiting objectives. Examples include maximum dose, one-sided dose-limiting quadratic penalty and EUD for serial organs (Alber and Nüsslin 1999), i.e. $f(D) = D^a$, $a \geqslant 1$. Note that the mean dose is also covered by the inequality because it is synonymous with the serial EUD cost function with $a = 1$. The parallel EUD (Alber and Nüsslin 1999) is an exception because it is neither convex nor concave; however, it can still be handled within the proposed framework, see below. A commonly used cost function for the target volume, the Poisson cell kill EUD (Niemierko 1997, Alber and Nüsslin 1999), is concave.

In practice, this means that in the case of normal tissue the score function value of the accumulated dose ($F(\mathrm{E}[\tilde{D}])$) is always smaller than the sum of the score functions of the instance doses ($\mathrm{E}[F(D)]$) (3). For the target, the EUD of the accumulated dose is always larger than the sum of the EUDs of the instance doses (4). Hence, using Jensen's inequality, worst case boundaries for the score function of the accumulated dose can be derived without the need for a deformable registration model.

Note that EUD and other cost functions are volume averages and are therefore insensitive to changes of the absolute volume of some organ or tumor. Still, uncertainties in delineation or volume shrinkage can introduce errors into the above inequalities. In order to maintain the validity of the inequality, it is sufficient to formulate a worst case. For normal tissue, this would be equivalent to using the smallest volume of the organ of interest in any geometry instance to normalize EUD in each instance. In case of tumor shrinkage, it is helpful to resort to the mechanistic basis of the model. Tumor EUD is derived from the initial number of clonogenic cells, which can be expressed as the mean cell density times the tumor volume. Under the assumption that no clonogenic cells are lost from the initial population by effects other than those caused by radiation, the primary quantity cell number is preserved despite volume loss. A volume reduction then results in an increase of clonogenic cell density. For the purpose of inequality, the EUDs of different geometry instances may be added although they pertain to differently sized volumes since EUD is independent of cell density. However, if the quantity of interest were the expected number of surviving clonogens instead, the increase in cell density would have to be considered.

The parallel complication function $f(D) = (1 + (D_{\mathrm{tol}}/D)^b)^{-1}$ is convex for doses below the dose D_{tol} and concave for doses above, i.e. it has a point of inflection at $D = D_{\mathrm{tol}}$. In consequence, the above reasoning cannot be directly applied. However, typical prescriptions demand that large parts of the organ are kept intact; hence, most of the organ volume is irradiated with doses below D_{tol}. For this fraction of the volume, (3) applies, i.e. the damage is overestimated. To account for the entire volume of the parallel organ, the cost function can be convexified by linear extrapolation at the point of inflection, see figure 1.

Note that the above relation (3) is *not* valid for dose–volume constraints. Table 1 contains an overview of the properties of commonly used score functions.

3. Results and discussion

The presented method is valuable because it provides a safe upper boundary on normal tissue doses and effects, and a safe lower boundary for tumor EUD. It is applicable even if deformation fields are not available or tumor shrinkage makes warping and accumulation difficult.

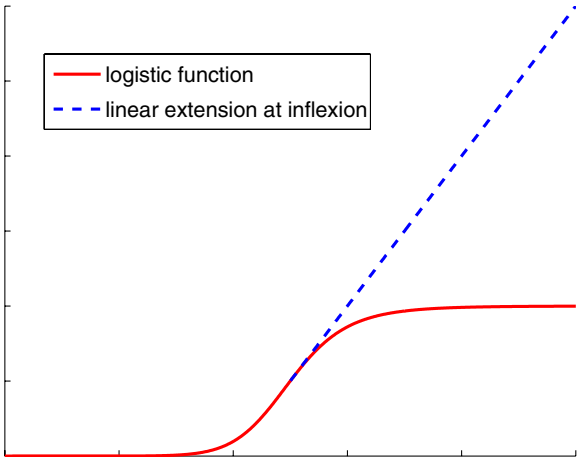

Figure 1. The parallel complication cost function (logistic function) is linearly extended at the inflection point to be convex on its entire support.

Table 1. Properties of various cost functions.

Cost function	Property
Poisson cell kill EUD	Concave
Parallel EUD	–
Generalized EUD $k \geqslant 1$ (Serial EUD)	Convex
Generalized EUD $k \leqslant 1$	Concave
Average dose	Convex *and* concave
DVH constraints	–
Maximum dose	Convex
Quadratic deviation penalty	Convex

To illustrate one possible application, the method was applied to a prostate cancer case. Target, bladder and rectum (wall) EUDs were evaluated in 18 geometries and their averages computed, table 2. The biomechanical model, which is the basis of the deformation field for the dose accumulation, is based on Yan *et al* (1999). The EUD computations based on the accumulated dose and the estimated boundaries yielded 71.601 Gy ($>$ 70.31 Gy) for the prostate, 59.897 Gy ($<$ 61.28 Gy) for the bladder and 56.675 Gy ($<$ 57.8 Gy) for the rectal wall. As predicted, for the target the average EUD in table 2 is lower than the EUD of the average dose. The contrary is the case for the organs at risk. Resultingly, a useful worst case approximation of the EUDs was obtained without dose accumulation.

To illustrate another application, the method was employed for a 4D lung cancer case. The EUDs for the gross tumor volume (GTV) (Poisson cell kill) and the lung (mean dose) were investigated. The basis were eight 4D CT scan instances taken during a breathing cycle. Each of these instances is associated with an instance weight that was computed from the breathing PDF. It reflects the relative fraction of a breathing cycle that is represented by a given instance. During dose accumulation, the doses of the respective instances were also

Table 2. EUDs for 18 patient geometries and their average.

CT #	Prostate Poisson EUD (Gy) $\alpha = 0.4$	Bladder Serial EUD (Gy) $a = 8$	Rectum Serial EUD (Gy) $a = 12$
1	71.73	59.24	63.7
2	70.81	58.61	49.56
3	55.28	62.62	42.41
4	71.7	57.21	57.35
5	70.68	62.80	48.75
6	71.7	60.07	60.9
7	71.63	62.49	54.89
8	64.18	63.97	58.16
9	71.76	60.43	59.44
10	71.5	58.14	64.41
11	71.87	63.72	58.39
12	71.79	60.96	61.16
13	71.63	61.04	62.23
14	71.95	63.76	58.08
15	71.88	64.43	59.16
16	71.67	61.48	58.12
17	71.87	61.65	62.31
18	71.88	60.38	61.46
	70.31	61.28	57.80

Table 3. Instance weights and EUDs for GTV and lung from a breathing cycle (inhale (In) exhale (Ex) respiratory levels in the range 0–100) and the weighted sum of the EUD.

Breathing phase	Weight	GTV EUD Poisson EUD (Gy) $\alpha = 0.4$	Weighted GTV EUD Poisson EUD (Gy) $\alpha = 0.4$	Lung EUD Serial EUD (Gy) $a = 1$	weighted lung EUD Serial EUD (Gy) $a = 1$
0 In	0.402	48.029	19.312	4.66	1.874
25 In	0.088	48.127	4.229	4.48	0.394
50 In	0.077	49.656	3.800	4.37	0.334
75 In	0.084	49.661	4.190	4.24	0.358
100 Ex	0.117	48.250	5.629	4.29	0.501
75 Ex	0.033	50.718	1.682	4.38	0.145
50 Ex	0.048	49.851	2.379	4.43	0.211
25 Ex	0.152	49.661	7.528	4.51	0.684
			48.749		4.501

weighted. For details, please refer to Söhn *et al* (2009). The EUD of the accumulated dose is 49.835 Gy ($>$ 48.749 Gy) for the GTV and 4.501 Gy ($\leqslant$ 4.501 Gy) for the lung. Again the prediction in table 3 proves to be a worst case estimate. Note that the EUDs for the lung are equal for both methods by necessity, reflecting energy and volume conservation. This is due

to the fact that the mean dose score function is linear, hence concave and convex at the same time.

Further applications of this relation have been outlined in the introduction, whereby the combination of brachytherapy and teletherapy is of particular usefulness in practice. Here,

$$\mathrm{EUD}(D_{\mathrm{EBT}} + D_{\mathrm{BT}}) \leqslant \mathrm{EUD}(D_{\mathrm{EBT}}) + \mathrm{EUD}(D_{\mathrm{BT}}) \tag{5}$$

for normal tissues and

$$\mathrm{EUD}(D_{\mathrm{EBT}} + D_{\mathrm{BT}}) \geqslant \mathrm{EUD}(D_{\mathrm{EBT}}) + \mathrm{EUD}(D_{\mathrm{BT}}) \tag{6}$$

for targets. This work also lays the foundation for robust optimization schemes that require no deformation fields (Sobotta *et al* 2010). The application of Jensen's inequality to the optimization of doses for variable patient geometries is the subject of future work.

4. Conclusions

A method to derive boundaries on the score function of the accumulated dose of multiple patient geometries was presented. By virtue of Jensen's inequality and the mathematical nature of commonly used score functions, in particular EUD and other biological score functions, it is possible to compute a worst case approximation on the combined effect of doses applied to variable geometries. Because the approach circumvents the computation of the accumulated doses by means of deformation fields, it eliminates the need for deformable registration and dose warping.

Acknowledgment

We would like to thank D Yan and J Liang from Beaumont Hospital, Royal Oak, MI, USA, for providing the sample prostate cancer patient and the corresponding deformation fields.

References

Alber M and Nüsslin F 1999 An objective function for radiation treatment optimization based on local biological measures *Phys. Med. Biol.* **44** 479–93

Birkner M, Yan D, Alber M, Liang J and Nüsslin F 2003 Adapting inverse planning to patient and organ geometrical variation: algorithm and implementation *Med. Phys.* **30** 2822–31

Jensen J L W V 1906 Sur les fonctions convexes et les inégalités entre les valeurs moyennes *Acta Math.* **30** 175–93

Knopf A *et al* 2010 Special report: workshop on 4D-treatment planning in actively scanned particle therapy—Recommendations, technical challenges, and future research directions *Med. Phys.* **37** 4608–14

McShan D L, Kessler M L, Vineberg K and Fraass B A 2006 Inverse plan optimization accounting for random geometric uncertainties with a multiple instance geometry approximation (MIGA) *Med. Phys.* **33** 1510–21

Morin O, Gillis A, Chen J, Aubin M, Bucci M K, Roach M and Pouliot J 2006 Megavoltage cone-beam CT: system description and clinical applications *Med. Dosim.* **31** 51–61

Niemierko A 1997 Reporting and analyzing dose distributions: a concept of equivalent uniform dose *Med. Phys.* **24** 103–10

Osorio E M V, Hoogeman M S, Teguh D N, Al Mamgani A, Kolkman-Deurloo I K K, Bondar L, Levendag P C and Heijmen B J 2010 Three-dimensional dose addition of external beam radiotherapy and brachytherapy for oropharyngeal patients using nonrigid registration *Int. J. Radiat. Oncol. Biol. Phys.* at press

Rong Y, Smilowitz J, Tewatia D, Tom W A and Paliwal B 2010 Dose calculation on KV cone beam CT images: an investigation of the Hu-density conversion stability and dose accuracy using the site-specific calibration *Med. Dosim.* **35** 195–207

Sobotta B, Söhn M and Alber M 2010 Robust optimization based upon statistical theory *Med. Phys.* **37** 4019–28

Söhn M, Weinmann M and Alber M 2009 Intensity-modulated radiotherapy optimization in a quasi-periodically deforming patient model *Int. J. Radiat. Oncol. Biol. Phys.* **75** 906–14

Soukup M, Söhn M, Yan D, Liang J and Alber M 2009 Study of robustness of IMPT and IMRT for prostate cancer against organ movement *Int. J. Radiat. Oncol. Biol. Phys.* **75** 941–9

Trofimov A, Rietzel E, Lu H M, Martin B, Jiang S, Chen G T Y and Bortfeld T 2005 Temporo-spatial IMRT optimization: concepts, implementation and initial results *Phys. Med. Biol.* **50** 2779–98

Yan D, Jaffray D and Wong J 1999 A model to accumulate fractionated dose in a deforming organ *Int. J. Radiat. Oncol. Biol. Phys.* **44** 665–75

A Solution for Brachytherapy Biologically Guided Dose Individualisation in the Treatment of Cervix Cancer

W. Shaw[1], W.I.D. Rae[1] and M. Alber[2]

[1] Department of Medical Physics, University of the Free State, Bloemfontein, South Africa
[2] Section for Biomedical Physics, Radioonkologische Uniklinik, Universität Tübingen, Germany

Abstract— Inadequate resources for the management and follow-up of patients in developing countries results in very conservative cervix brachytherapy treatment protocols. Conservative treatment approaches may result in under-utilization of this treatment technique, thus masking its favourable attributes. A biological model-based brachytherapy planning method for cervix cancer is used to demonstrate how fixed normal tissue complication endpoints and sufficient tumour doses can effectively be achieved. Treatment plans for ten cervix cancer patients each receiving 5 fractions of conservative CT-based brachytherapy were compared to biologically optimized plans. The conservative protocol requires 2 Gy normalized dose to the highest rectal dose point per fraction, most probably leading to tumour under dosage. Individualized planning based on population normal tissue endpoints and maximal tumour dose may potentially solve this problem. Treatment plans were retrospectively optimized with respect to the tolerance rectum and bladder equivalent uniform doses (EUDs), and taking into consideration the effects of fractionation and non-standard doses. Organ deformation and tumour shrinkage was considered by doing treatment imaging per fraction and considering dose boundaries (worst case scenarios) for maximum normal tissue and minimum target effects which could be calculated for each fractional EUD. Biologically guided treatment plans showed potential to safely increase tumour doses considering the patients' anatomic organ geometries at the time of treatment in 88% of the treatment plans. Average high-risk CTV EUDs were escalated from 18.0Gy (SD=4.1Gy) in 5 fractions to 25.9Gy (SD=5.5Gy). The EUDs to the rectum and bladder were safely escalated from 6.5Gy (SD=1.0Gy) to 11.0Gy (SD=3.0Gy) and 10.8Gy (SD=4.8Gy) to 16.1Gy (SD=1.7Gy) respectively. This method shows potential for major improvement in terms of local control at acceptable toxicity levels and is particularly useful where an upper limit for normal tissue complication should not be contravened. The method is interactive and applicable to any dose fractionation schedule.

Keywords— **brachytherapy, cervix cancer, optimisation, individualisation, equivalent uniform dose.**

I. Introduction

Brachytherapy (BT) is a well known technique used in the treatment of cervical cancer and there have been many attempts to derive suitable treatment fractionation schedules for combination with external beam radiation treatment. BT treatment has the advantage that doses to organs at risk (OARs) can be quite effectively minimized when delivering very high, though non-uniform doses, to the tumour volume. Recently there have been very useful guidelines set by the (GYN) GEC-ESTRO working group[1] for achieving curative doses when external beam radiotherapy (EBRT) and BT are combined. However, although these recommendations can probably be easily followed at modern treatment facilities, this is not necessarily the case in most developing countries. In such countries many patients from rural areas are treated at distant hospital complexes where treatment protocols often consider the fact that late OAR toxicities must be kept to an absolute minimum as the management of such toxicities in these patient groups may be critical to patient management.

One such protocol involves the normalization of the brachytherapy dose to a single rectal point which receives the highest dose according to the standard dose distribution pattern. However, in such cases the net result might be under dosage of the tumour as a result of the rectum being too close to the applicators during some treatment fractions. This method explicitly ignores the fact that this dose point will most probably vary in position during subsequent treatment fractions. Thus the maximum overall rectal dose would be overestimated when such a treatment protocol is followed. This technique has several other drawbacks, for instance, when the rectum is too close to the applicator or the organ geometry limits dose to the tumour, the treatment may be cancelled and another attempt made at a later time. Such delays will result in prolonged treatment times that negatively impact curative probability or will simply lower tumour doses if treatment time cannot be extended any further[2]. Whatever the decision, these protocols unfortunately limit the use of BT and underutilise exploitation of the biological advantages and optimization possibilities for effective BT treatment.

These problems can be addressed by making use of biological models of tumour and normal tissue responses and using guidelines for fixed treatment endpoints to maximize tumour dose safely. The variability of organ geometries during the treatment

M. Long (Ed.): World Congress on Medical Physics and Biomedical Engineering, IFMBE Proceedings 39, pp. 2276–2279, 2012.
www.springerlink.com

period can sometimes be an advantage, as will be shown in this study.

II. Methods and materials

In our hospital complex, where a large percentage of patients from rural areas are treated, a conservative approach in the treatment of cervix cancer with brachytherapy is followed. Patients are treated to 50 Gy in 25 fractions EBRT using a standard 4-field box technique. They receive an additional 5 fractions of high dose rate (HDR) BT afterloading on a 40-channel Flexitron afterloading unit commencing after ten EBRT fractions have been delivered. BT treatment plans are developed on the Nucletron Flexiplan treatment planning system making use of CT datasets for each treatment fraction with the applicators already implanted under conscious sedation. Treatment plans are based on the well-known pear-shaped dose distribution volume achieved using a standard ring and intra-uterine applicator combination. The dose to the highest rectal dose point is normalized to 2 Gy. Doses to point A and the High Risk Clinical Target Volume (HR-CTV)[1] are recorded and vary as a function of rectal position and geometry. Dose volume histograms of the rectum, bladder and HR-CTV are calculated.

It is understandable that this treatment protocol might sometimes lead to unacceptably low tumour doses as the highest rectum dose point might be in close proximity to the applicators. This often results in situations where the dose to point A might even be lower than the highest rectal dose point of 2 Gy, resulting in the forfeiture of the treatment. However, by exploiting the effects of fractionation, 3D volumetric treatment planning and biological response models one can individually optimize these plans so that each patient's anatomic geometry can be used to optimize, through expansion, the pear-shaped dose distribution to boundaries of normal tissue dose response and at the same time maximise the dose to the tumour.

Using the linear quadratic (LQ) model[3], a biological optimization treatment planning method for cervical cancer brachytherapy was developed and compared to the conservative treatment planning method used in our institution by means of the equivalent uniform dose (EUD)[4]. A computer code was developed in Interactive Data Language (IDL) for this purpose which utilised the cell survival fraction (S_{TUMOR}) and subsequently the EUD for tumours (eq. 1 and 2), while the generalized EUD was calculated for normal tissues (eq. 3).

$$S_{TUMOR} = \exp(-\{n(\alpha d+\beta d^2)-(\gamma(T_e-T_{del})\}) \quad (1)$$

$$EUD_{TUMOR} = -log(S_{TUMOR})/(\alpha+\beta d-(\gamma/d(T_e-T_{del})) \quad (2)$$

$$EUD_{OAR} = (\sum_i v_i D_i^{\alpha})^{1/\alpha} \quad (3)$$

LQ parameters for cervical cancer and the OARs, as well as for the EUD calculation were based on well known values from literature[2,3].

The EUD concept is extended to account for non-standard fractionation schemes, whereby the current combination of dose distributions and fractionation size at a given isodose level can be equated to a uniform dose for a standard fractionation size. This is particularly important for BT treatments which may utilise large variations in fraction size and show dramatic dose gradients.

The datasets of ten patients treated with 5 fractions of HDR BT according to our conservative treatment protocol were used retrospectively in this study to show the potential enhancement in tumour dose when using biologically guided dose individualisation. Contours were delineated for the rectum, bladder and HR-CTV.

Firstly, the equivalent uniform doses (EUDs) were calculated for all these volumes utilizing the concepts of biological equivalent doses (BED) and equivalent dose in 2 Gy per fraction (EQD_2) to allow the usage of comparable published late toxicity data. To bring the EUD of different doses per fraction into consideration, the EQD_2 had to be calculated from the BED for each fraction as the late toxicity endpoints used in the optimization of the dose distributions are based on a 2 Gy fractionation schedule.

Secondly, once the rectal, bladder and HR-CTV EUDs according to the conservative protocol were available, the treatment plans were re-optimized by simply maximizing the dose to the upper boundaries of the OARs (still using the standard pear-shaped dose distribution according the fixed dwell position ring applicator setup) which has a simultaneous tumour dose escalation effect.

It is virtually impossible to sum the doses from different treatment fractions of EBRT when dealing with geometrically changing and deforming tumour and OAR volumes. This problem is even greater when doses from different treatment modalities are summed and requires complex models of dose warping. However, the use of EUDs allows the determination of a lower or upper dose boundary, referred to herein as a worst case scenario for determining dose[5]. This method of worst case scenario provides a solution for adding sequential EBRT and BT doses and for the comparison of different treatment plans and fractionation.

Pre- and post-optimized doses where compared to evaluate the potential for safely escalating dose in the tumour without exceeding acceptable normal tissue toxicity levels. These levels are defined at a 2% probability of grade II late rectal bleeding and 10% probability for a variety of grade II bladder complications. They amount to EUDs of 64.5 Gy at 2 Gy per fraction and 66 Gy at 2 Gy per fraction for the rectum and bladder respectively.

III. Results

The biologically guided treatment plans showed potential to safely increase tumour doses considering each patient's individual anatomic organ geometry at the time of each treatment fraction. Considering all the treatment plans included in this study, it was found that larger tumour doses could potentially have been delivered in 88% of the 50 treatment plans if the biologically guided method was used. Table 1 gives a summary of the average EUDs after 5 treatment fractions for the 10 patients. In 20% of treatment fractions the rectum limited the achievable tumour dose, while the bladder was limiting in the rest.

Table 1 Comparison of the average EUDs (Gy ± one standard deviation) for 10 patients after 5 fractions produced by the conservative protocol and the biologically guided planning solution in 50 planned treatment fractions

	Conservative Method	Biological Method
Rectum	6.5 ± 1.0	11.0 ± 3.0
Bladder	10.8 ± 4.8	16.1 ± 1.7
HR-CTV	18.0 ± 4.1	25.9 ± 5.5

When comparing the population average EUDs over all 50 planned fractions investigated in the study, the rectum EUDs were escalated from 1.3±0.3 Gy to 2.3±0.7 Gy, the bladder EUD from 2.2±1.2 Gy to 3.3±0.4 Gy and the HR-CTV EUDs from 3.7±1.2 Gy to 5.3±1.4 Gy in individual treatment fractions. As the bladder was the dose limiting organ in 88% of the cases, one would expect the variation in bladder EUD to be less than that of the rectum, as seen from the above results.

IV. Discussion

The EUD is a useful endpoint in the evaluation of treatment plans with non-uniform dose distributions in three dimensional conformal, intensity modulated and brachytherapy radiotherapy treatment planning. When optimizing treatment plans the EUD can very effectively be used in a centre where fixed endpoints for normal tissue effects are to be achieved, as required in our institution where many patients from outlying rural areas are treated. From our results it is clear that all treatment plans deliver the same maximum EUD to the OAR that reaches its limit first. Thus variability in terms of bladder or rectal complications of a certain predetermined degree is limited. Tumour control may vary between patients, but the maximal permissible dose without unacceptable late toxicity would in most cases be delivered. This is in contrast to the conservative protocol where rectal, bladder and tumour response vary throughout the whole population. This method could possibly be extended in a similar was to treat all tumours to the same EUD, but this was not considered here.

V. Conclusion

In this study we applied an EUD-based optimization strategy to obtain maximal tumour dose. This is achieved by individualizing the treatment plans of each patient in the study such that a clinical normal tissue complication probability endpoint would be achieved for the population of patients. However, the deforming OAR volumes in each treatment fraction are allowed to receive their maximal permissible dose or EUD through the worst case scenario approach.

The general conclusion from this investigation is that the EUD-based method of plan optimization is much more efficient in terms of safety boundaries for normal tissue toxicity, even if the volumes and geometries of OARs vary over sequential treatment fractions. It is also a suitable solution for safe escalation of tumour doses at the same time, specifically enabling maximization of tumour dose when considering individual OAR geometries.

This method can be seen as an adaptive fixed endpoint strategy that is extremely useful when summing doses from different treatment modalities. It ensures that all patients treated in this way receive the maximal benefit without detriment, instead of a treatment protocol where only some patients reap the benefit of the treatment technique.

References

1. Haie-Meder C, et al. (2005) Gynaecological (GYN) GEC-ESTRO Working Group, Recommendations from Gynaecological (GYN) GEC-ESTRO Working Group (I): concepts and terms in 3D image based 3D treatment planning in cervix cancer brachytherapy with emphasis on MRI assessment of GTV and CTV. Rad Onc 74(3), 235-45

2. Wyatt R, Beddoe A, Dale R (2003) The effects of delays in radiotherapy treatment on tumour control. Phys Med Biol 48, 139-155
3. Dale R, Jones B (2007) Radiobiological Modelling in Radiation Oncology. British Institute of Radiology, 36 Portland Place, London, W1B 1AT, UK
4. Niemierko A (1997) Reporting and analyzing dose distributions: A concept of equivalent uniform dose. Med Phys 24, 103-109
5. Sobotta RB, Söhn M, Shaw W, Alber M (2011) On expedient properties of common biological score functions for multi-modality, adaptive and 4D optimization. Phys Med Biol, 56, N123-N129

Author: Prof William I.D. Rae
Institute: Department of Medical Physics (G68)
Faculty of Health Sciences
University of the Free State
Street: Nelson Mandela Drive
City: Bloemfontein
Country: South Africa
Email: raewid@ufs.ac.za

Shaw et al. Radiation Oncology 2013, 8:266
http://www.ro-journal.com/content/8/1/266

RADIATION ONCOLOGY

RESEARCH Open Access

Equivalence of Gyn GEC-ESTRO guidelines for image guided cervical brachytherapy with EUD-based dose prescription

William Shaw[1*], William ID Rae[1] and Markus L Alber[2]

Abstract

Background: To establish a generalized equivalent uniform dose (gEUD) -based prescription method for Image Guided Brachytherapy (IGBT) that reproduces the Gyn GEC-ESTRO WG (GGE) prescription for cervix carcinoma patients on CT images with limited soft tissue resolution.

Methods: The equivalence of two IGBT planning approaches was investigated in 20 patients who received external beam radiotherapy (EBT) and 5 concomitant high dose rate IGBT treatments. The GGE planning strategy based on dose to the most exposed 2 cm^3 (D2cc) was used to derive criteria for the gEUD-based planning of the bladder and rectum. The safety of gEUD constraints in terms of GGE criteria was tested by maximizing dose to the gEUD constraints for individual fractions.

Results: The gEUD constraints of 3.55 Gy for the rectum and 5.19 Gy for the bladder were derived. Rectum and bladder gEUD-maximized plans resulted in D2cc averages very similar to the initial GGE criteria. Average D2ccs and EUDs from the full treatment course were comparable for the two techniques within both sets of normal tissue constraints. The same was found for the tumor doses.

Conclusions: The derived gEUD criteria for normal organs result in GGE-equivalent IGBT treatment plans. The gEUD-based planning considers the entire dose distribution of organs in contrast to a single dose-volume-histogram point.

Keywords: Image guided brachytherapy, Planning study, Equivalent uniform dose, Dose volume constraints, Comprehensive volume, Worst case estimate

Background

Recently, the treatment of cervical cancer has been advanced through the use of image guided brachytherapy (IGBT) [1-4]. The Groupe Européen de Curiethérapie (GEC) and the European SocieTy for Radiotherapy & Oncology (ESTRO) working group (Gyn GEC-ESTRO WG, GGE) presented guidelines that comprise imaging and organ segmentation for planning of every treatment fraction [5,6]; subsequently, limited imaging approaches have been derived [7,8]. Such an approach adapts for organ motion and tumor shape changes by conforming the prescribed dose to the target volume of the day, and thereby increases the chance of applying effective IGBT doses in successive fractions. This image- and volume-based planning strategy allows for a per-fraction analysis of dose distributions and dose volume histograms (DVHs). Further, the total delivered dose up to and including the last treatment fraction can be estimated for clinical target volumes (CTV) and organs at risk (OAR). This constitutes a risk-controlled dose prescription method with DVH criteria for tumor and normal tissue volumes. The relevance of these criteria has been demonstrated by linking them to toxicity [9-11] and local control [11-14]. However, contouring and organ motion are the major contributors of uncertainties in IGBT [15].

The GGE technique requires MRI for tumor and OAR delineation with applicators in-situ. Unfortunately many clinics have limited availability of MRI. One alternative

* Correspondence: shaww@ufs.ac.za
[1]Department of Medical Physics (G68), University of the Free State, Nelson Mandela Drive, Park West, Bloemfontein 9300, South Africa
Full list of author information is available at the end of the article

is CT imaging, but due to the lower contrast, CT based planning results in increased OAR volumes, CTV delineation uncertainty and consequently unnecessarily large CTVs, as one tends to plan conservatively [16-19]. These uncertainties can produce lower CTV doses [3,16] if normal tissue DVH criteria are adhered to. At the same time, contour uncertainty leads to uncertainty of derived DVH criteria for toxicity scoring or tumor control and an uncertainty in the addition of OAR and tumor DVHs for obtaining worst-case estimates of the accumulated dose [6,15,20,21]. Furthermore, with the increased use of more conformal external beam radiotherapy (EBT) techniques such as intensity modulated radiotherapy (IMRT), the addition of DVH parameters for such worst case estimates can become unreliable.

This raises the question whether a volume-based treatment plan metric such as the equivalent uniform dose (EUD) [22] could be more robust against contouring and imaging uncertainties than DVH. In EBT planning, the generalized EUD (gEUD) is well established [23-25] and is mathematically equivalent to the DVH reduction scheme of the Lyman-Kutcher-Burman (LKB) normal tissue complication probability (NTCP) model [26-29]. It is our intention to establish a gEUD-based prescription method for IGBT that can replace the original GGE prescription in terms of dose-volume criteria, but offers advantages in terms of safety and robustness against uncertainties. Further, EUD sports favorable mathematical properties that allow a reliable worst-case estimate of the accumulated dose.

We investigate this question with a three-stage planning study of fractionated IGBT. In stage 1, we record the EUD values of OARs achieved with plans obtained from the dose-volume constrained GGE guidelines. From this, we establish corresponding EUD criteria. In stage 2, the treatments are planned according to these EUD constraints, and their safety is assessed according to the GGE DVH criteria. Finally, in stage 3, the full treatments (EBT + 5 fractions IGBT) of both strategies are compared by both metrics.

Methods

Patient selection, imaging and contouring

Ethical approval (ETOVS NR 214/09) was received for this study. Twenty patients who had been treated with high dose rate (HDR) IGBT for carcinoma of the cervix between October 2009 and January 2011 were randomly selected (Table 1). All patients received EBT consisting of 25 fractions of 2 Gy via a 4-field box technique without midline shielding, and 5 concomitant IGBT treatment fractions of 4.7 Gy (± 0.8 Gy) to the High Risk CTV (HR-CTV; discussed below) with a standard magnetic resonance imaging compatible tandem-ring (Nucletron®). Intra-uterine source positions were located at 1 cm intervals from the ring to the tip, while the length of the intra-uterine applicator was adapted to tumor extent. Source positions in the ring were fixed for all treatments. Our center's high workload requires that implantations be done under conscious sedation without vaginal packing. Treatment plans were produced on axial CT images for lack of MRI facilities.

Table 1 Patient, volume and treatment characteristics

Characteristic	*No of patients and/or value(s)*
Total nr of patients	*20*
Total EBT dose	*50 Gy*
Total nr of EBT fractions	*25*
Total nr of IGBT fractions	*5*
Total IGBT dose (Mean ± SD)	*4.7 ± 0.8 Gy*
Total nr of CT datasets in study	*100*
FIGO stage (n)	
II	*5*
III	*12*
IVa	*3*
Volume in cc (Mean ± SD)	
HR-CTV @ 1st IGBT treatment	*49.0 ± 21.0*
IR-CTV @ 1st IGBT treatment	*119.0 ± 43.0*
Rectum	*94.8 ± 32.6*
Bladder	*108.0 ± 91.6*
Dose objectives/constraints	
HR-CTV D90	*≥ 85 Gy*
IR-CTV D90	*≥ 60 Gy*
Rectum D2cc	*≤ 70 Gy*
Bladder D2cc	*≤ 80 Gy*

Abbreviations: *SD* standard deviation, *cc* cubic centimeters.

Contouring was based on clinical examination and CT images, using the GGE guidelines for the HR-CTV, Intermediate Risk CTV (IR-CTV) and the rectum and bladder walls. The GTV had to be omitted as it cannot be identified on CT images. The HR-CTV consisted of the whole cervix and macroscopic extent of the disease at the time of imaging for IGBT. The IR-CTV encompassed the HR-CTV plus a variable margin depending on the initial extent of the disease, considering tumor regression in response to treatment. The OAR walls and outline with content were delineated according to the same set of recommendations.

Fractionation and dose evaluation parameters

According to the GGE recommendations we recorded the following parameters for purposes of comparison: Minimal dose received in 0.1, 1, and 2 cc of the maximal dose regions of the OARs (D0.1, 1, 2 cc; outer wall plus content), dose to 90% (D_{90}) of the HR- and IR-CTVs, as well as the EUDs of OAR walls and CTVs.

Full DVHs of each treatment fraction were available in the Flexiplan (Nucletron®) treatment planning system and dose was converted to a 2 Gy equivalent dose (EQD2) [30]. According to GGE, the linear quadratic (LQ) model

parameters of α/β being 3 Gy for OARs and 10 Gy for tumors (α being 0.3 Gy^{-1}) were applied. Since the treatment was concomitant HDR brachytherapy, repair half-times and repopulation were neglected.

The EUD for target volumes was calculated relative to the EBT dose delivered in 2 Gy fractions (d = 2 Gy) from the surviving fraction as:

$$EUD = \frac{-Log(S)}{\alpha + \beta d} \quad (1)$$

To consider the heterogeneity in dose distributions, the differential DVH of tumors was used to calculate the surviving fraction for each treatment:

$$S = \Sigma_k v_k S(D_k) \quad (2)$$

S is calculated from D_k, the dose bin for the v_{k-th} fractional tumor volume.

The gEUD calculation was used for OARs [28,31], again considering a reference dose of 2 Gy per fraction and is given by

$$gEUD = (\Sigma_k v_k {D_k}^a)^{\frac{1}{a}} \quad (3)$$

where D_k is the EQD2 for the v_{k-th} fractional OAR volume and a is the volume effect parameter. The gEUD for rectum and bladder walls was calculated using volume effect parameters (a) of 12 for the rectum and 8 for the bladder [23,32,33].

For simplicity we refer to the EUD based, adaptive IGBT planning strategy as the comprehensive volume technique (CV), emphasizing the fact that EUD considers the entire organ volume.

Study 1: prescription constraints

One possibility to establish the gEUD prescription constraints for IGBT treatment planning is to collect them from literature, another by a planning study. From Söhn et al. (2007), we can choose the gEUD upper limit for the rectum to be 67.8 Gy (3.55 Gy EUD per IGBT fraction), at approximately 10% NTCP for grade II (G2) rectal bleeding. However, in the following this gEUD is verified against a rectum D2cc constraint of 70 Gy EQD2 [9,10] by the planning study. Bladder NTCP model data are scarce and uncertain [34] due to unaccounted variations in filling. Consequently, the bladder gEUD constraint is determined by the planning study. There are bladder dose guidelines based on the GGE work that show more than 5 - 10% late complication rates when the D2cc is in the order of 70–100 Gy EQD2 [9,10,19,35,36].

To derive the bladder wall gEUD dose constraints, the GGE planning strategy was followed to achieve at least 7.0 Gy per fraction (85 Gy EQD2 from EBT and IGBT) to the HR-CTV D90. Treatment plans were produced for each treatment fraction on the 100 CT datasets. Each plan started from the standard loading pattern and was manually or graphically optimized until the HR-CTV dose objective was reached, or until one of the two OAR constraints in question prevented any further CTV dose escalation (Table 1). *Bladder EUD constraints:* HR-CTV dose was further increased beyond the CTV objective until the bladder D2cc criterion was reached. This constraint was chosen as 80 Gy total dose from EBT and IGBT, resulting in 6 Gy EQD2 per IGBT fraction. The procedure was repeated on all plans and for each the associated bladder wall gEUD was computed. Consequently, the bladder wall gEUD is solely determined by the D2cc of the bladder and is not influenced by any other OAR criterion or the CTV doses. *Rectum EUD constraints:* To verify the chosen gEUD of 67.8 Gy for an upper rectal limit, we repeated this constraint derivation procedure for the rectal wall by limiting the total rectum D2cc EQD2 to 70 Gy (4.0 Gy EQD2 per fraction).

All 100 "bladder-limited" plans are maximized to the bladder constraint of 6.0 Gy D2cc per fraction and the corresponding bladder wall gEUDs were recorded and all 100 "rectum-limited" plans are maximized to the rectum dose constraint of 4.0 Gy D2cc and the associated rectum wall gEUDs were recorded. From these data, the variation in bladder and rectal wall gEUD at fixed DVH criteria could be found and the EUD criteria could be derived or verified from these gEUD frequency distributions.

Study 2: safety of EUD constraints in terms of GGE constraints

To test the safety of the CV technique, we investigated the appropriateness of the bladder- and rectum wall EUD constraints in terms of the GGE dose volume criteria. Here we maximized the same dose distribution as in study 1 for each treatment plan, but to the point where the bladder wall gEUD constraint was reached instead of the D2cc constraint. At this point we recorded the corresponding D2cc (and other DVH parameters). This procedure was repeated for the rectal wall by maximizing dose to the rectum gEUD constraint. Thus a single plan was optimized against each of the organs at risk separately.

Study 3: comparison of GGE and CV planning strategies for the entire treatment

Once the robustness of the CV technique in each fraction has been established, the two planning strategies can be compared in terms of OAR and CTV dose for a full treatment. The GGE based plans for each patient and each fraction adhered to the two OAR D2cc constraints (Table 1) per fraction, whichever was met first. The HR-CTV D90 was targeted to be at least 85 Gy in total. No upper CTV constraints were set and dose was maximized until an OAR D2cc constraint was reached. The total dose from IGBT and EBT was calculated. For the CV technique the

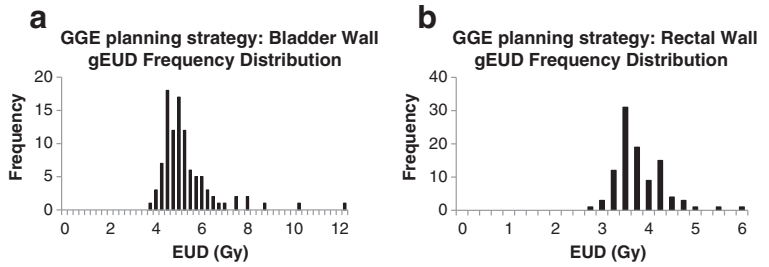

Figure 1 GGE planning strategy: Bladder and rectal wall EUD frequency distributions. Frequency distributions of bladder **(a)** and rectum **(b)** wall EUDs when dose is maximized to 6 Gy D2cc for bladder and 4 Gy D2cc for rectum.

OAR EUD constraints were employed that were found earlier. Finally, the two strategies could be compared in terms of D90, D2cc and EUD.

Results

Prescription constraints

The frequency distributions of the OAR wall EUDs for bladder-limited and rectum-limited plans are displayed in Figure 1. Table 2 provides a summary of the statistics. The spread of EUDs results from the fact that the gEUD is calculated from the full OAR DVH while D2cc is limited to a small volume. Furthermore, the D2cc volume may often include organ contents. Notice further some extreme outliers, which are a consequence of an unfavorable organ location in some fractions that brings large parts of the organ close to the high dose range, but below the D2cc criterion.

The average gEUD of the rectal wall at a D2cc constraint of 4.0 Gy was 3.67 Gy (±0.53 Gy) which is comparable to the 3.55 Gy from our external beam rectum EUD constraint choice. If this average gEUD was reached in all of the 5 fractions, the NTCP would be ranking at approximately 11%. The average bladder gEUD at a D2cc constraint of 6.0 Gy was 5.19 Gy (±1.25 Gy). The values: rectum wall gEUD ≤ 3.55 Gy and bladder wall gEUD ≤ 5.19 Gy were established as the upper limits for the CV technique. Thus, the total EUD constraint for the bladder wall equals 75.95 Gy.

Safety of EUD criteria in terms of GGE criteria

The safety of these EUD criteria was verified by comparing the D2cc values of CV plans with those obtained from the GGE strategy. Figure 2 shows the distribution of D2cc for the OARs with the EUD criteria as determined in the previous section, while Table 2 compares the D2cc statistics of the frequency distributions. Figure 2 shows that the D2cc distributions are skewed towards lower values and show no outliers towards high doses. The mean of the D2cc distributions closely resembles the GGE criteria, see Table 2. For a fractionated treatment, the EUD criteria can thus be considered safe, because even in the worst case (the same organ is dose-limiting in all fractions) the sum of the D2cc of n fractions is likely to be smaller or equal to n times the mean D2cc of the distributions, due to their left-skew. Since the choice of EUD criteria is somewhat arbitrary, we identified those levels, gEUD(x), that result in no more than x% of the 100 treatment plans exceeding the associated GGE criterion, see Table 3.

We have also found very good correlations between D0.1 cc and D2cc for the rectum ($R^2 = 0.84$), as well as excellent correlation between D1cc and D2cc for the rectum ($R^2 = 0.96$). This means that if D2cc can be controlled via the use of the EUD, ulcerations, fistulas and rectal

Table 2 Summary of the statistical parameters of the gEUD variations with D2cc and EUD criteria

Statistical measure	*Dose (Gy) GGE strategy*	*Dose (Gy) CV strategy*
Bladder D2cc/gEUD constraint *(planning)*	*6.00*	*5.19*
Bladder Wall gEUD/D2cc		
Mean	*5.19/6.00*	*5.19/6.25*
SD	*1.25/0.00*	*0.00/1.01*
Bladder D0.1 cc		
Mean		*9.97*
SD		*0.85*
Bladder D1cc		
Mean		*7.21*
SD		*0.98*
Rectum D2cc/gEUD constraint *(planning)*	*4.00*	*3.55*
Rectum Wall gEUD/D2cc		
Mean	*3.67/4.00*	*3.55/3.96*
SD	*0.53/0.00*	*0.00/0.49*
Rectum D0.1 cc		
Mean		*5.80*
SD		*0.29*
Rectum D1cc		
Mean		*4.46*
SD		*0.44*

Abbreviations: *SD* standard deviation.

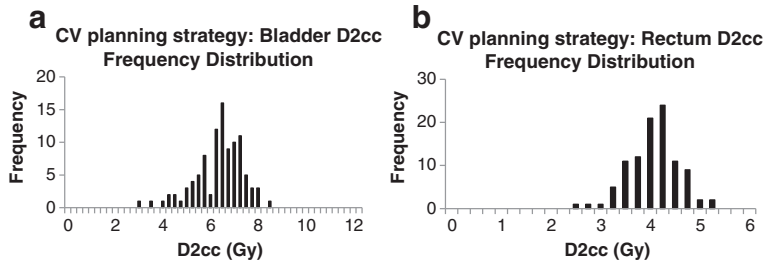

Figure 2 CV planning strategy: Bladder and rectal D2cc frequency distributions. Frequency distributions of the bladder **(a)** and rectum **(b)** D2ccs when expanding the dose distribution to 5.19 Gy EUD for bladder and 3.55 Gy EUD for rectum.

bleeding will also be controlled. Similarly, we have found excellent correlation between bladder D1cc and D5cc with D2cc ($R^2 = 0.95$ and $R^2 = 0.93$ respectively), and a worse correlation between D0.1 cc and D2cc ($R^2 = 0.63$).

Comparison of GGE and CV planning strategies

The two planning approaches were compared in terms of total dose from all 5 IGBT fractions plus the EBT component for the patients in the study. Very similar total dose parameters for the two techniques were found. Figure 3 displays the total dose in the two planning techniques for rectum and bladder D2cc, and HR- and IR-CTV D90. Figure 4 displays the rectal and bladder wall gEUDs, and the HR- and IR-CTV EUDs. Table 4 provides the average and standard deviations of their frequency distributions, indicating very similar means.

Discussion

We have established OAR gEUD criteria for IGBT treatments that are very comparable to those obtained from the GEC-ESTRO guidelines. EUD constraints can thus be considered a safe and efficient alternative to D2cc criteria.

Compared to a D2cc constraint, which considers an isolated small volume, gEUD has the advantage to consider the dose distribution in the OAR comprehensively and still give high doses a large weight, especially if the volume effect parameter a is significantly greater than 1. For the same reason, it is also less sensitive to contouring and may therefore be a more robust choice if MRI is not available for IGBT planning. To see this, assume that contouring errors lead to errors in the volume of the dose bins of the DVH. Applying the laws of error propagation, we find that the error in D2cc is proportional to the inverse slope of the DVH at D2cc (which tends to be shallow in BT) and proportional to the volume error at that dose bin. In contrast, the error in gEUD is both proportional to the weighted root-mean-square of the volume errors in the dose bins (thus less dependent on a single bin) and smaller by a factor 1/a. This ties in with the intuition, that any kind of average over a number of uncertain quantities (such as EUD) is less uncertain than any single one of these quantities.

The derived EUD criteria depend on the reference D2cc criteria and the volume effect parameter a. Since gEUD is a power-law function of dose, it scales with the same factor as D2cc. Small deviations from this law are caused by the EQD2 correction. Within reason, our criteria can therefore be calibrated to different fractionation schemes, i.e. scaled by the ratio of the desired D2cc versus the value used here.

The volume effect parameters (a = 8 for bladder, a = 12 for rectum) are derived from the literature. They do express a very small volume effect of the complications in question, which is also the implicit rationale behind the D2cc criterion. We confirm that the influence of the choice of a on our results is small, although safer when $a \geq 8$, since D2cc becomes increasingly smaller with a large a at fixed constraint levels; see a value variance in Table 5. It is thus considered safe to err towards large a values, i.e. smaller volume effect, when the exact value is not known.

Occasionally, the use of EUD criteria for IGBT is safer than D2cc. Observe the outliers in Figure 1 which are

Table 3 Different gEUD(x) levels resulting in percentage x of treatment fractions with D2cc larger than the GGE constraint and mean and standard deviations of the resulting distributions

x % of treatment fractions	*Rectum gEUD(x) (Gy)*	*Rectum mean D2cc ± SD (Gy)*	*Bladder gEUD(x) (Gy)*	*Bladder mean D2cc ± SD (Gy)*
10	*3.12*	*3.49 ± 0.43*	*4.22*	*5.11 ± 0.81*
25	*3.35*	*3.74 ± 0.46*	*4.48*	*5.42 ± 0.86*
48	*3.55*	*3.96 ± 0.49*		
50	*3.58*	*3.99 ± 0.50*	*4.86*	*5.87 ± 0.94*
70			*5.19*	*6.25 ± 1.01*

Abbreviations: *SD* standard deviation.

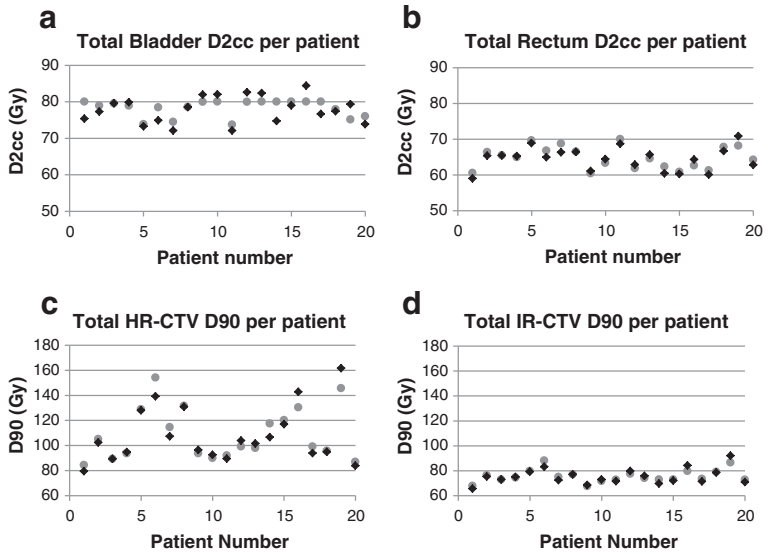

Figure 3 Total DVH parameters per patient. Total EQD2 for bladder **(a)** and rectum **(b)**, and D90 for the HR- **(c)** and IR-CTV **(d)**. Data are shown for the GGE technique (circles) and the CV technique (diamonds).

caused by rare unfavorable organ geometries that bring a lot of the organ volume close to the high dose region. In contrast, EUD criteria do not produce excessive D2cc values because of their mathematical construction, which gives very high weights to sub-volumes with a high dose. From Table 2, the average D2cc for the OARs, when dose is maximized to each OAR's gEUD constraint, is virtually the same as the GGE-D2cc that was used to derive the EUD criteria. Although there is some dispersion of D2ccs around this average, none of the D2ccs were found to be unacceptably high. If the EUD constraints are reduced, as shown in Table 3, to decrease D2cc constraint violations, small changes in EUD result in large reductions in D2cc and a smaller variance of D2cc. Our results suggests that a 6 to 8% reduction in OAR gEUDs produce more than 25% fewer treatment plans that could violate a D2cc constraint. Since we know that D0.1 cc and D1cc also correlates well with D2cc, CV plans that control D2cc would subsequently control the resultant D0.1 cc and D1cc DVH parameters as well.

The D2ccs of the CV technique are evaluated against data from other studies in Table 6, which includes D0.1

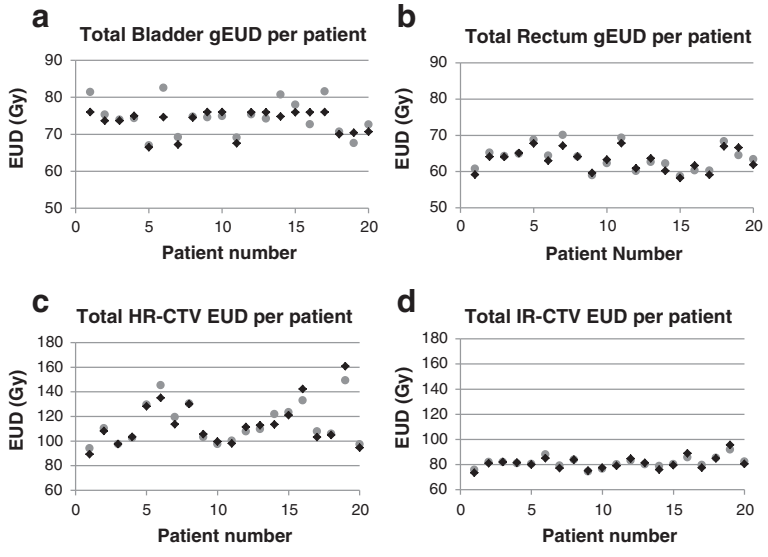

Figure 4 Total EUD per patient. Total EUD for bladder **(a)** and rectal wall **(b)**, HR- **(c)** and IR-CTV **(d)**. Data are shown for the GGE technique (circles) and the CV technique (diamonds).

Table 4 Summary of the statistical variations of the DVH parameters and EUD variations over the full treatment course

Statistical measure	*Technique*	*Rectum*	*Bladder*	*HR-CTV*	*IR-CTV*
		D2cc	***D2cc***	***D90***	***D90***
Mean (Gy)	*GGE*	*64.85*	*78.29*	*108.49*	*75.85*
SD		*3.10*	*2.29*	*20.59*	*5.22*
Mean (Gy)	*CV*	*64.51*	*77.87*	*107.77*	*75.36*
SD		*3.20*	*3.70*	*21.95*	*6.16*
		gEUD	***gEUD***	***EUD***	***EUD***
Mean (Gy)	*GGE*	*63.66*	*74.53*	*114.28*	*81.51*
SD		*3.42*	*4.58*	*16.40*	*4.12*
Mean (Gy)	*CV*	*63.18*	*73.32*	*113.58*	*81.19*
SD		*3.07*	*3.31*	*17.90*	*5.07*

All values in Gy.
Abbreviations: *SD* standard deviation.

and D1cc endpoints. The comparison shows that maximizing OAR dose to the EUD constraints does not result in OAR over-dosage. The total average bladder and rectal D0.1, D1 and D2cc when OAR dose is maximized to the EUD constraints falls in a lower range than those presented by Georg et al. for LENT/SOMA scores of 1–4 and VRS scores of 3–5 [9]. The population averages in their studies [9,10] are comparable to the dose levels in this study. We have also found that especially the rectal doses in this study are in the lower range of toxicity rates for G2-4 side effects. Based on the Georg et al. studies [9,10,35], our criteria relate to a probability of finding G2-G4 side effects in the range of 5-10%.

These dose endpoints are also very comparable with studies where large HR-CTV volumes were investigated and no interstitial needles were used. As shown in the study of Jürgenliemk-Schulz et al. [36], we expect that interstitial needles would decrease the EUD of OARs in large tumor volume cases as well. For bladder, we found good correspondence with the results of Levitchi et al. [37], Jürgenliemk-Schulz et al. [36,38], Nesvacil et al. [39] and Lindegaard et al. [40]. Since there were no upper dose boundaries for the CTV, the CTV dose is expected to spread widely, driven solely by the OAR geometries and relative positions. From Figures 3 and 4 it is clear that the CV technique does not result in underdosage of the CTVs.

An important aspect of gEUD is, that it allows an easy worst-case estimate of the gEUD of the total accumulated treatment dose by virtue of Jensen's inequality [41,42]. The sum of EUDs of each treatment fraction is always greater or equal (for OARs; smaller or equal for targets) to the EUD of the sum of the fraction doses:

$$EUD(E[\tilde{D}]) \leq E[EUD(\tilde{D})] = E[EUD(D)] \quad (4)$$

where E[] is the sum over all fractions, $\tilde{D}$ is the dose of each fraction, warped to reference geometry, and D the dose as computed for the patient geometry of the particular fraction. Hence, the left hand side is the EUD of the properly accumulated total dose, while the right hand side is the sum of the EUDs as computed for each fraction individually. For target volumes, the inequality reverses. This estimate is of particular importance for pelvic radiotherapy, where deformable registration of images is difficult to perform reliably. Hence, EUD addition gives a worst case scenario for OARs and CTV without the need for deformable image registration and dose warping [42].

D2cc is not a convex function of dose and is not additive in a strict sense, so that further assumptions about the dose distribution have to be made. Jensen's inequality also applies to maximum and minimum dose, so that, if D2cc and D90 have a strong correlation to the former, the inequality holds for the latter approximately "by proxy". The versatility of EUD summation as worst case estimate

Table 5 Variation of gEUD and D2cc for different values of the gEUD volume parameter

Volume parameter (a)	*Rectum gEUD constraint (Gy)**	*Rectum D2cc (Gy)#*	*Bladder gEUD constraint (Gy)***	*Bladder D2cc (Gy) ##*
8	*3.09 ± 0.37*	*4.66 ± 0.52*	*5.19 ± 1.25*	*6.25 ± 1.01*
9	*3.26 ± 0.42*	*4.43 ± 0.51*	*5.56 ± 1.44*	*5.89 ± 1.00*
10	*3.41 ± 0.46*	*4.24 ± 0.50*	*5.89 ± 1.61*	*5.60 ± 0.99*
11	*3.54 ± 0.50*	*4.09 ± 0.50*	*6.19 ± 1.77*	*5.35 ± 0.97*
12	*3.67 ± 0.53*	*3.96 ± 0.49*	*6.46 ± 1.91*	*5.15 ± 0.96*
13	*3.78 ± 0.56*	*3.85 ± 0.49*	*6.72 ± 2.04*	*4.98 ± 0.95*
14	*3.88 ± 0.59*	*3.75 ± 0.48*	*6.95 ± 2.16*	*4.83 ± 0.93*
15	*3.97 ± 0.61*	*3.67 ± 0.48*	*7.17 ± 2.26*	*4.70 ± 0.92*
16	*4.06 ± 0.63*	*3.60 ± 0.47*	*7.36 ± 2.36*	*4.59 ± 0.91*

*Calculated with a 4.0 Gy rectum D2cc constraint.
**Calculated with a 6.0 Gy bladder D2cc constraint.
#Calculated with a 3.55 Gy (a = 12) rectum gEUD constraint.
##Calculated with a 5.19 Gy (a = 8) bladder gEUD constraint.

Table 6 Summary of the average DVH parameters in total dose (Gy) of the CV treatment technique, compared to other published values

DVH parameter	*CV*	*Georg et al.* [9]	*Georg et al.* [10]	*Levitchi et al.* [33]	*Jürgenliemk-Schulz et al.* [38]	*Jürgenliemk-Schulz et al.* [39]	*Nesvacil et al.* [40]	*Lindegaard et al.* [41]
Method	*HDR*	*HDR*	*HDR*	*PDR*	*PDR*	*HDR/PDR*	*HDR*	*PDR*
Rectum								
D0.1 cc	*79 ± 1*	*88 ± 10**	*83 - 132* [a]	*83* [b]				
		*81 ± 13***	*86 ± 27***	*65 ± 15***				*74 ± 9***
D1cc	*72 ± 2*	*76 ± 7**	*71 - 87* [a]					
		*70 ± 9***	*69 ± 14***					*69 ± 6***
D2cc	*70 ± 2*	*72 ± 6**	*67 - 78* [a]	*68* [b]				
		*66 ± 8***	*65 ± 12***	*57 ± 8***	*66 ± 6***	*54 ± 2*** [c]	*57 ± 6***	*67 ± 6***
						*69 ± 2*** [d]		
Bladder								
D0.1 cc	*100 ± 3*		*61 - 178* [a]	*109* [b]				
			*162 ± 75***	*78 ± 22***				*86 ± 12***
D1cc	*86 ± 3*		*71 - 116* [a]					
			*108 ± 31***					*77 ± 8***
D2cc	*81 ± 3*		*70 – 101*[a]	*72* [b]	*81 ± 6***	*53 ± 2*** [c]	*76 ± 9***	
			*95 ± 22***	*64 ± 11***		*101 ± 11*** [d]		*73 ± 6***

Abbreviations: *SD* standard deviation, *HDR* high dose rate, *PDR* pulsed dose rate.
*Clinical symptoms (LENT/SOMA) score 1–4 and Rectoscopic changes (VRS) score 3–5.
**Population average; no interstitial needles.
[a]5% - 10% probability of G2-G4 side effects (dose range not shown).
[b]Approximately 10% probability of G2-G4 toxicity (dose range not shown).
[c]Small volume tumor.
[d]Large volume tumor.

extends to the addition of very heterogeneous OAR EBT doses, for example lymph node boosts. Finally, because there is a variability in reported dose-volume cut-offs for OARs in IGBT [9,35,37,43] and these also differ from cut-offs in EBT, EUD is helpful in combining the experience in both areas and relating it to the LKB model [44]. Conversely, documented brachytherapy toxicity rates can be useful for focused dose escalation in EBT, for example dose painting.

Conclusions

Concluding, a GEC-ESTRO-like IGBT plan adaption is feasible with EUD criteria, instead of D2cc criteria. Because of the mathematical construction of gEUD, and the fact that it considers the organ volume comprehensively, it is inherently more robust against contouring uncertainties. This could make gEUD a better choice than D2cc if IGBT has to be performed on CT, instead of MR, images. The summation of EUDs per treatment fraction gives a reliable worst case estimate of the total treatment dose, which opens possibilities for safe dose escalation in IGBT or simultaneous integrated boost in EBT.

Competing interests

The authors declare that they have no competing interests.

Authors' contributions

WS contributed to study design, data acquisition and management, treatment planning, physical evaluation of treatment plans, result analysis and writing the final manuscript. WIDR contributed to result analysis and drafted the manuscript. MLA contributed to the conception of the study, study design and revision of the manuscript. All authors read and approved the final manuscript.

Acknowledgements

The University of the Free State was supported by research grants from the Medical Research Foundation (MRC) of South Africa and the Aarhus University Hospital was supported by CIRRO - The Lundbeck Foundation Center for Interventional Research in Radiation Oncology and The Danish Council for Strategic Research.

Author details

[1]Department of Medical Physics (G68), University of the Free State, Nelson Mandela Drive, Park West, Bloemfontein 9300, South Africa. [2]Department of Oncology, Aarhus University, Nørrebrogade 44/5, Aarhus 8000, Denmark.

Received: 27 September 2013 Accepted: 8 November 2013
Published: 13 November 2013

References

1. Kirisits C, Pötter R, Lang S, Dimopoulos J, Wachter-Gerstner N, Georg D: **Dose and volume parameters for MRI-based treatment planning in intracavitary brachytherapy for cervical cancer.** *Int J Radiat Oncol Biol Phys* 2005, **62:**901–911.
2. Barillot I, Reynaud-Bougnoux A: **The use of MRI in planning radiotherapy for gynaecological tumours.** *Cancer Imaging* 2006, **6:**100–106.
3. Pötter R, Kirisits C, Fidarova E, *et al*: **Present status and future of high-precision image guided adaptive brachytherapy for cervix carcinoma.** *Acta Oncol* 2008, **47:**1325–1336.
4. Viswanathan A, Erickson B: **Three-dimensional imaging in gynecologic brachytherapy: a survey of the American Brachytherapy Society.** *Int J Radiat Oncol Biol Phys* 2010, **76:**104–109.
5. Haie-Meder C, Pötter R, Van Limbergen E, *et al*: **Recommendations from Gynecological (GYN) GEC-ESTRO Working Group (I): concepts and terms in 3D image based 3D treatment planning in cervix cancer brachytherapy with emphasis on MRI assessment of GTV and CTV.** *Radiother Oncol* 2005, **74:**235–245.
6. Pötter R, Haie-Meder C, Van Limbergen E, *et al*: **Recommendations from Gynecological (GYN) GEC ESTRO working group (II): Concepts and terms in 3D image-based treatment planning in cervix cancer brachytherapy—3D dose volume parameters and aspects of 3D image-based anatomy, radiation physics, radiobiology.** *Radiother Oncol* 2006, **78:**67–77.
7. Lang S, Nesvacil N, Kirisits C, *et al*: **Uncertainty analysis for 3D image-based cervix cancer brachytherapy by repetitive MR imaging: assessment of DVH-variations between two HDR fractions within one applicator insertion and their clinical relevance.** *Radiother Oncol* 2013, **107:**26–31.
8. Mohamed S, Nielsen S, Fokdal L, Pedersen EM, Lindegaard JC, Tanderup K: **Feasibility of applying a single treatment plan for both fractions in PDR image guided brachytherapy in cervix cancer.** *Radiother Oncol* 2013, **107:**32–38.
9. Georg P, Kirisits C, Goldner G, *et al*: **Correlation of dose-volume parameters, endoscopic and clinical rectal side effects in cervix cancer patients treated with definitive radiotherapy including MRI-based brachytherapy.** *Radiother Oncol* 2009, **91:**173–180.
10. Georg P, Pötter R, Georg D, *et al*: **Dose effect relationship for late side effects of the rectum and urinary bladder in magnetic resonance image-guided adaptive cervix cancer brachytherapy.** *Int J Radiat Oncol Biol Phys* 2012, **82:**653–657.
11. Pötter R, Georg P, Dimopoulos J, *et al*: **Clinical outcome of protocol based image (MRI) guided adaptive brachytherapy combined with 3D conformal radiotherapy with or without chemotherapy in patients with locally advanced cervical cancer.** *Radiother Oncol* 2011, **100:**116–123.
12. Dimopoulos J, Lang S, Kirisits C, *et al*: **Dose–volume histogram parameters and local tumor control in Magnetic Resonance Image–Guided cervical cancer brachytherapy.** *Int J Radiat Oncol Biol Phys* 2009, **75:**56–63.
13. Dimopoulos J, Pötter R, Lang S, *et al*: **Dose–effect relationship for local control of cervical cancer by magnetic resonance image-guided brachytherapy.** *Radiother Oncol* 2009, **93:**311–315.
14. Lee L, Damato A, Viswanathan A: **Clinical outcomes of high-dose-rate interstitial gynecologic brachytherapy using real-time CT guidance.** *Brachytherapy* 2013, **12:**303–310.
15. Tanderup K, Nesvacil N, Pötter R, Kirisits C: **Uncertainties in image guided adaptive cervix cancer brachytherapy: impact on planning and prescription.** *Radiother Oncol* 2013, **107:**1–5.
16. Viswanathan A, Dimopoulos J, Kirisits C, Berger D, Pötter R: **Computed tomography versus magnetic resonance imaging based contouring in cervical cancer brachytherapy: results of a prospective trial and preliminary guidelines for standardized contours.** *Int J Radiat Oncol Biol Phys* 2007, **68:**491–498.
17. Charra-Brunaud C, Harter V, Delannes M, *et al*: **Impact of 3D image-based PDR brachytherapy on outcome of patients treated for cervix carcinoma in France: results of the French STIC prospective study.** *Radiother Oncol* 2012, **103:**305–313.
18. Eskander RN, Scanderbeg D, Saenz C, Yashar C, Brown M: **Comparison of computed tomography and magnetic resonance imaging in cervical cancer brachytherapy target and normal tissue contouring.** *Int J Gynecol Cancer* 2010, **20:**47–53.
19. Hegazy H, Pötter R, Kirisits C, Berger D, Federico M, Sturdza A, Nesvacil N: **High-risk clinical target volume delineation in CT-guided cervical cancer brachytherapy: Impact of information from FIGO stage with or without systematic inclusion of 3D documentation of clinical gynecological examination.** *Acta Oncol* 2013, **52:**1345–1352.
20. Andersen E, Muren L, Sørensen T, *et al*: **Bladder dose accumulation based on a biomechanical deformable image registration algorithm in volumetric modulated arc therapy for prostate cancer.** *Phys Med Biol* 2012, **57:**7089–7100.
21. Andersen E, Noe K, Sørensen T, *et al*: **Simple DVH parameter addition as compared to deformable registration for bladder dose accumulation in cervix cancer brachytherapy.** *Radiother Oncol* 2013, **107:**52–57.
22. Niemierko A: **Reporting and analyzing dose distributions: a concept of equivalent uniform dose.** *Med Phys* 1997, **24:**103–110.
23. Söhn M, Yan D, Liang J, Meldolesi E, Vargas C, Alber M: **Incidence of late rectal bleeding in high-dose conformal radiotherapy of prostate cancer using equivalent uniform dose–based and dose–volume–based normal tissue complication probability models.** *Int J Radiat Oncol Biol Phys* 2007, **67:**1066–1073.

24. Wu Q, Mohan R, Niemierko A, Schmidt-Ullrich R: **Optimization of intensity-modulated radiotherapy plans based on the equivalent uniform dose.** *Int J Radiat Oncol Biol Phys* 2002, **52:**224–235.
25. Schwarz M, Lebesque J, Mijnheer B, Damen E: **Sensitivity of treatment plan optimization for prostate cancer using the equivalent uniform dose (EUD) with respect to the rectal wall volume parameter.** *Radiother Oncol* 2004, **73:**209–218.
26. Lyman J: **Complication probability as assessed from dose–volume histograms.** *Radiat Res* 1985, **104:**S13–19.
27. Burman C, Kutcher G, Emami B, Goitein M: **Fitting of normal tissue tolerance data to an analytic function.** *Int J Radiat Oncol Biol Phys* 1991, **21:**123–135.
28. Mohan R, Mageras GS, Baldwin B, *et al*: **Clinically relevant optimization of 3-D conformal treatments.** *Med Phys* 1992, **19:**933–944.
29. Alber M, Belka C: **A normal tissue dose response model of dynamic repair processes.** *Phys Med Biol* 2006, **51:**153–172.
30. Dale R, Sinclair J: **Radiobiological calculations in routine radiotherapy.** In *Radiobiological Modelling in Radiation Oncology.* Edited by Dale R, Jones B. London: British Institute of Radiology; 2007:158–168.
31. Niemierko A: **A generalized concept of equivalent uniform dose [Abstract].** *Med Phys* 1999, **26:**1100.
32. Soukup M, Söhn M, Yan D, Liang J, Alber M: **Study of robustness of IMPT and IMRT for prostate cancer against organ movement.** *Int J Radiat Oncol Biol Phys* 2009, **75:**941–949.
33. Bolstad-Hysing L, Skorpen T, Alber M, Fjellsbø LB, Helle SI, Muren LP: **Influence of organ motion on Conformal vs. Intensity-modulated pelvic radiotherapy for prostate cancer.** *Int J Radiat Oncol Biol Phys* 2008, **71:**1496–1503.
34. Viswanathan A, Yorke E, Marks L, Eifel PJ, Shipley WU: **Radiation dose–volume effects of the urinary bladder.** *Int J Radiat Oncol Biol Phys* 2010, **76:**S116–S122.
35. Georg P, Lang S, Dimopoulos J, *et al*: **Dose–volume histogram parameters and late side effects in magnetic resonance image–guided adaptive cervical cancer brachytherapy.** *Int J Radiat Oncol Biol Phys* 2011, **79:**356–362.
36. Jürgenliemk-Schulz I, Tersteeg R, Roesink J, *et al*: **MRI-guided treatment-planning optimisation in intracavitary or combined intracavitary/interstitial PDR brachytherapy using tandem ovoid applicators in locally advanced cervical cancer.** *Radiother Oncol* 2009, **93:**322–330.
37. Levitchi M, Charra-Brunaud C, Quetin P, *et al*: **Impact of dosimetric and clinical parameters on clinical side effects in cervix cancer patients treated with 3D pulse-dose rate intracavitary brachytherapy.** *Radiother Oncol* 2012, **103:**314–321.
38. Jürgenliemk-Schulz I, Lang S, Tanderup K, *et al*: **Variation of treatment planning parameters (D90 HR-CTV, D2cc for OAR) for cervical cancer tandem ring brachytherapy in a multicentre setting: Comparison of standard planning and 3D image guided optimisation based on a joint protocol for dose–volume constraints.** *Radiother Oncol* 2010, **94:**339–345.
39. Nesvacil N, Pötter R, Sturdza A, Hegazy N, Federico M, Kirisits C: **Adaptive image guided brachytherapy for cervical cancer: a combined MRI-/CT-planning technique with MRI only at first fraction.** *Radiother Oncol* 2013, **107:**75–81.
40. Lindegaard J, Tanderup K, Nielsen S, Haack S, Gelineck J: **MRI-guided 3D optimization significantly improves DVH parameters of pulsed-dose-rate brachytherapy in locally advanced cervical cancer.** *Int J Radiat Oncol Biol Phys* 2008, **71:**756–764.
41. Jensen J: **Sur les fonctions convexes et les inegalites entre les valeurs moyennes.** *Acta Math* 1906, **30:**175–93.
42. Sobotta B, Söhn M, Shaw W, Alber M: **On expedient properties of common biological score functions for multi-modality, adaptive and 4D dose optimization.** *Phys Med Biol* 2011, **56:**N123–129.
43. Thibault I, Lavallée M, Aubin S, Laflamme N, Vigneault E: **Inverse-planned gynecologic high-dose-rate interstitial brachytherapy: clinical outcomes and dose volume histogram analysis.** *Brachytherapy* 2012, **11:**181–191.
44. Michalski J, Gay H, Jackson A, Tucker S, Deasy J: **Radiation dose-volume effects in radiation-induced rectal injury.** *Int J Radiat Oncol Biol Phys* 2010, **76:**S123–129.

doi:10.1186/1748-717X-8-266
Cite this article as: Shaw *et al.*: Equivalence of Gyn GEC-ESTRO guidelines for image guided cervical brachytherapy with EUD-based dose prescription. *Radiation Oncology* 2013 **8**:266.